Immune response and tissue cytoprotection

Two sides of the same coin in immunopathology

Ivo Marguti

Dissertation presented to obtain the Ph.D degree in Biochemistry

Instituto de Tecnologia Química e Biológica | Universidade Nova de Lisboa

Research work coordinated by:

FUNDAÇÃO CALOUSTE GULBENKIAN
Instituto Gulbenkian de Ciência

Oeiras,
October, 2011

INSTITUTO
DE TECNOLOGIA
QUÍMICA E BIOLÓGICA
/UNL

Knowledge Creation

Ph.D Supervisor: Dr. Thiago Lopes Carvalho

The work presented on this Thesis has been funded by the grant SFHR/BD/33218/2007 from:

FCT Fundação para a Ciência e a Tecnologia
MINISTÉRIO DA EDUCAÇÃO E CIÊNCIA

Index

Acknowledgments

I would like to express my deepest gratitude to Dr. Thiago Lopes Carvalho, who became my supervisor under turbulent circumstances and made everything in his power to ensure the completion of this Thesis in the best possible way. I am also in great debt with Dr. Bruno Silva-Santos and Dr. Lars Jansen, who were caught in the turmoil and were utterly understanding and supportive. The help of the three of you was indispensable for the completion of this Thesis.

My gratitude also extends to the IGC Direction for the opportunity to work at this Institute for four years, and for making sure its students are supported whenever needed.

I would also like to thank my dear friend Dr. Luiz Vicente Rizzo for his constant availability to support and advise a former student. Many times he has offered the right word at the right time, and I feel very fortunate to have him as a friend.

Many thanks to the people that generously spent their time making this Thesis better. A very special thanks to Alê, Lu, Virgínia and Jorge Carneiro.

My appreciation is extended to the co-authors of the published work that made this Thesis possible.

Many thanks to Rui Gardner and Telma Lopes for endless hours spent sorting cells.

Finally, I would like to thank the "*Fundação para a Ciência e a Tecnologia*" for the financial support given through the grant SFHR/BD/33218/2007

Preface

This thesis is organized in 5 Chapters, preceded by an summary written in Portuguese and in English. Chapter 1 consists of a general introduction to the themes discussed throughout the thesis, and includes a published review article. Chapter 2, 3 and 4 consist of experimental work published during the thesis period. Chapter 5 is and extended discussion integrating the published work presented in the previous chapters.

Sumário

O sistema imune é fundamental para a manutenção da viabilidade do hospedeiro em casos de infecção. No entanto, os mecanismos usados pelo sistema imune para controlar infecções podem também causar destruição tecidual, levando ao desenvolvimento de imunopatologia. Para sobreviver a infecções o hospedeiro precisa controlar a proliferação do agente infeccioso e, ao mesmo tempo, evitar os efeitos deletérios da resposta imune em seus tecidos. Para alcançar este objetivo, o hospedeiro utiliza as seguintes estratégias: aumento da capacidade tecidual de suportar danos infligidos pelo sistema imune e/ou controle da ativação exacerbada do sistema imune. Nesta Tese buscou-se aprofundar o conhecimento sobre os mecanismos utilizados pelo hospedeiro para empregar de maneira bem sucedida tais estratégias.

Para estudar o papel de células do sistema imune na regulação da magnitude de respostas imunológicas, analisamos a capacidade das células dendríticas (DC) de expandir células T reguladoras (T_{REG}). Utilizando um sistema de co-cultura de células *in vitro*, demonstrou-se que as DC são capazes de induzir a expanão da população de T_{REG} com capacidade supressora. É de realçar que, a expansão de T_{REG} foi maior quando as DC apresentavam antígenos não-próprios. Estes resultados sugerem que a expansão da população de T_{REG} durante uma resposta imunológica pode servir como um mecanismo regulador da ativação exacerbada do sistema imune. Dessa maneira, interações entre células do sistema imune podem ser suficientes para atenuar o desenvolvimento de uma resposta imune patológica e prevenir o desenvolvimento de imunopatologia.

Os mecanismos envolvidos na prevenção da imunopatologia através do aumento da capacidade tecidual de suportar danos causados pelo sistema imune, foram estudados em dois modelos experimentais de infecção, malária e sepse. Utilizando o modelo experimental de sepse, estudou-se o efeito da enzima heme oxigenase-1 (HO-1) na proteção dos tecidos contra danos causados pela resposta imune. Para tal, foram utilizados ratinhos com o gene da enzima HO-1 intacto (*Hmox1*$^{+/+}$) e ratinhos em que este gene foi inativado (*Hmox1*$^{-/-}$). A indução de sepse em ratinhos *Hmox1*$^{+/+}$ acarretou modesto dano tecidual a orgãos viatis, enquanto o mesmo procedimento em animais *Hmox1*$^{-/-}$ causou severo dano tecidual a orgãos vitais levando à falência dos mesmos. É importante notar que apesar da diferença observada na severidade dos danos aos orgãos vitais, a resposta imune à infecção induzida pela sepse foi muito similar em ambos os genótipos. Esses dados sugerem que na ausência da expressão de HO-1 há um aumento na susceptibilidade dos orgãos a danos causados pelo sistema imune. A maior suscetibilidade observada em animais *Hmox1*$^{-/-}$ ocorre, ao menos parcialmente, devido ao maior nível de heme em circulação nestes animais. É de realçar que, a administração de heme a animais *Hmox1*$^{+/+}$ após a indução de sepse desencadeou severo dano tecidual a orgãos vitais, enquanto a retirada de heme da circulação preveniu o desenvolvimento de sepse severa. Esses resultados reforçam a noção de que o heme atua como uma molécula capaz de potencializar danos teciduais a orgãos vitias em animais com sepse.

Utilizando um modelo experimental de malária cerebral (ECM), demonstrou-se que mutações na hemoglobina conferem proteção contra o desenvolvimento dessa doença. Animais

transgênicos que expressam moléculas de hemoglobina mutadas (Hb^{SAD}), o que acarreta uma forma leve de anemia falciforme, não desenvolvem ECM, enquanto animais com hemoglobina normal (Hb^{WT}) sucumbem à doença. É de realçar que, a proteção conferida pela Hb^{SAD} possui dois componentes: o aumento da capacidade dos tecidos em suportar danos infligidos pelo sistema imune e, o controle da responsta imunológica evitando o desenvolvimento de uma resposta exacerbada. Como observado no modelo experimental de sepse, a expressão de HO-1 em animais com Hb^{SAD} é essencial para manter baixos níveis de heme durante a infecção e, assim, evitar a potencialização dos danos causados pelo sistema imune. Por outro lado, a Hb^{SAD} possui um efeito immunoregulatório, ainda sem mecanismo definido, que é independente da expressão de HO-1. Esse efeito induz uma drástica redução na expansão e ativação de células T $CD8^+$, essenciais para o desenvolvimento da ECM.

Os resultados apresentados sugerem que o desenvolvimento de imunopatologia pode ser evitado por mecanismos que atuam tanto no tecido quanto no sistema imune. A compreensão de que estes dois compartimentos podem ser alvo de intervenções terapêuticas para evitar o desenvolvimento de imunopatologia abre novas possibilidades para o desenvolvimento de terapias para doenças em que grande parte da patologia é reflexo de uma resposta imune exacerbada.

Summary

The immune system is fundamental to maintaining the host's viability upon infection. Nonetheless, the mechanisms used to control pathogens may also cause tissue damage, leading to the development of immunopathology. The host's capacity to survive infections depends on its ability to control the pathogen burden, while avoiding the deleterious effect of immune responses on its own tissues. To achieve this goal, the host may apply the following strategies: increasing tissue resilience to immune-mediated insult and/or controlling exacerbated immune activation. This Thesis sought insight into the mechanisms used by the host to successfully employ both strategies.

To study the role of immune cells in regulating the extent of immune activation, we analyzed the capacity of dendritic cells (DC) to expand regulatory T cells (T_{REG}). By using an *in vitro* co-culture system, it was demonstrated herein that DC can induce the expansion of T_{REG} with suppressive activity. Importantly, T_{REG} expansion is greater when DC are loaded with non-self antigens. These findings suggest that the expansion of the T_{REG} compartment during an immune response might serve as a mechanism to avoid unfettered immune activation that could result in immunopathology. In this way, the interactions among the cells of the immune system might, *per se*, be sufficient to prevent the development of immunopathology.

The mechanisms operating in tissues to prevent immunopathology were investigated in two experimental models of systemic infections, malaria and sepsis. Analysis of wild type (WT) and heme oxygenase-1 deficient (*Hmox1*$^{-/-}$) mice undergoing sepsis, induced by cecal ligation and puncture (CLP), revealed that, while WT animals showed signs of mild tissue

damage and organ failure, *Hmox1*$^{-/-}$ mice suffered from extensive tissue damage leading to multi-organ failure. Importantly, this occurred despite apparently similar overall levels of immune activation in WT and *Hmox1*$^{-/-}$ mice, suggesting that in the absence of HO-1 tissues become less resilient to insults perpetrated by the immune system and, therefore, more prone to immune-mediated damage. The diminished resilience to immune insult is at least partially due to increased heme levels in *Hmox1*$^{-/-}$ mice. In line with the pathological effect of heme in precipitating tissue damage in sepsis, its administration caused mild sepsis to become lethal in WT type animals, while heme scavenging rescued mice from developing severe sepsis.

The action of increased tissue cytoprotection acts together with the control of unfettered immune response to afford protection against experimental cerebral malaria (ECM) by mutations in hemoglobin. Transgenic animals carrying a mutated form of hemoglobin (*Hb*^{SAD}), leading to a mild sickle cell disease phenotype, were protected from ECM development while animals with normal hemoglobin (*Hb*^{WT}) succumbed. The protection afforded by *Hb*^{SAD} derives from a composite effect of increased tissue cytoprotection in addition to immunoregulation. As in sepsis, HO-1 protects against ECM development by decreasing heme levels upon infection, thereby protecting tissues from the highly deleterious effects of combined exposure to pro-inflammatory mediators and heme molecules. On the other hand, the immunoregulatory effect of *Hb*^{SAD} works by a yet unidentified mechanism, independent of HO-1 expression, and leads to the marked suppression of $CD8^+$ T cells proliferation and activation.

Overall, these findings suggest that immunopathology can be counteracted by mechanisms that operate in tissues by

increasing their capacity to bear immune-mediated insult, or within the immune system, by limiting unfettered activation. The realization that both tissues and the immune system can be actively modulated in order to decrease immunopathology opens new venues for the development of therapies for diseases in which the underlying cause of pathology is immune-mediated.

Chapter 1: General Introduction

1. The immune system

The immune system is comprised of a wide range of molecules and cell types spread along the body surface and strategically placed to detect and rapidly respond to invading pathogens and/or insulting agents. Its importance in maintaining host viability is strikingly demonstrated in the rare cases of natural mutations affecting molecules of the immune system in human subjects, leading to increased susceptibility to infections[1-5] or to the development of autoimmune diseases[6].

The normal course of a protective immune response is often characterized by the concerted action of the innate and adaptive immune system (*see sections 1.1 and 1.2*). The initial steps in this process require activation of the innate immune system through the recognition of evolutionarily conserved molecules expressed by microorganisms, termed broadly **P**athogen-**A**ssociated **M**olecular **P**atterns (PAMP), and/or host-derived molecules associated with tissue damage or malfunction, termed broadly **D**anger-**A**ssociated **M**olecular **P**atterns (DAMP). This recognition process occurs through a multitude of germ-line encoded receptors, generally termed **P**attern **R**ecognition **R**eceptors (PRR), and leads to innate immune cell activation.

Upon activation, cells of the innate immune system termed **a**ntigen **p**resenting **c**ells (APC) (*see section 1.1)*, migrate to secondary lymphoid organs, carrying processed antigenic peptides. The recognition of peptides in the context of **m**ajor **h**istocompatibility **c**omplex (MHC) molecules, coupled with co-stimulation and cytokine production by APC, initiates the process of T cell activation. This process encompasses several rounds of proliferation with posterior acquisition of effector function,

characterized by the ability to produce large quantities of cytokines and/or kill target cells upon antigenic re-stimulation. B cells can be directly activated by PRR stimulation alone or in combination with B cell receptor ligation, but normally require help from T cells in order to achieve full differentiation. After activation B cells differentiate into plasma cells and start producing large quantities of antibodies.

Importantly, unlike innate immune cells, T and B cells have their specificities determined by receptors generated randomly through somatic gene rearrangements. This randomness allows the generation of a repertoire of receptors capable of recognizing virtually any antigen, although each lymphocyte caries only a single receptor. This single lymphocyte receptor can recognize a range of antigenic determinants. Therefore, APC and antigens migrate to secondary lymphoid organs in order to increase the likelihood that the rare specific T and B cell clones recognizing the antigen in question will be activated. Once the adaptive immune system is activated it will further instruct innate immune cells with molecular cues, such as cytokines, in order to control or eliminate the harmful insult. After the insult is controlled, the majority of the T and B cells in the antigen-specific pool that underwent massive expansion die, and the ones surviving differentiate into memory cells, able to respond more rapidly, with greater intensity and specificity to subsequent antigenic challenge. The acquisition of immunological memory, i.e. the ability to respond faster and with greater intensity and specificity to a second exposition to the same harmful insult, is a specific characteristic of adaptive immune cells as innate immune cells do not acquire immunological memory after responding to a given pathogen and/or insult. Importantly, all the processes, from

innate immune activation to adaptive immune effector function and memory acquisition, need to be tightly regulated to avoid excessive tissue damage and/or development of autoimmunity (*see sections 1.1, 1.2*).

A more detailed description of the innate and adaptive immune response will be given below.

1.1 Innate immunity

The innate immune system is the host's first line of defense against invading pathogens and/or harmful insults. The cellular components of the innate immune system include myeloid cells, such as macrophages and dendritic cells (DC), neutrophils, mast cells, basophils, and natural killer (NK) cells. More recently, previously uncharacterized cell populations with innate characteristics, and mainly involved in inducing T helper 2 responses (T_H2) (*see section 1.2)*, have been described and termed nuocytes, multi-potent progenitor type-2 (MMP^{type2}), innate type 2 helper cells, and natural helper cells[7]. Innate-like lymphocytes such as $\gamma\delta$ T cells and NKT cells, have lymphocyte characteristics but that respond to stimulation in a time frame that is compatible with innate immune responses. Soluble molecules such as the complement system, pentraxins, and lectins, form the humoral arm of the innate immune system. The anatomical localization of innate immune cells is such that they can survey the surfaces of the host likely to be exposed to pathogens and/or harmful insults, such as the skin[8] and mucosal surfaces[9-11], and induce rapid and powerful inflammatory responses upon activation.

The activation of the innate immune system can be depicted schematically as a process that relies on detection of pathogens and/or insults, with the subsequent activation of intracellular signaling cascades leading to gene expression of effector molecules. These effector molecules will, in turn, act to eliminate the insult through a multitude of mechanisms.

The process of detecting pathogens relies on the recognition of evolutionarily conserved molecular structures that are essential for microorganism survival, such as components of the cell wall or nucleic acids, and, therefore, are unlikely to suffer major modifications without consequent loss of pathogen fitness. These conserved structures are recognized by germ-line encoded receptors expressed in a variety of cell types, broadly termed PRR[12]. Importantly, PRR can also recognize or respond to concentration changes in endogenous molecules produced or released upon cellular stress or damage, i.e. ATP[13], uric acid[14,15], serum amyloid A[16], amyloid-β[17] , endogenous nucleic acids[18-21], and high-mobility group box-1 (HMGB1)[22].

Four families of PRR have been described so far: Toll-like receptor (TLRs), Nucleotide-binding oligomerization domain-like receptors (NLRs), retinoic acid inducible gene I (RIG-I)-like receptors (RLRs), and C-type lectin receptors (CLRs). The cellular localization of these receptors varies. TLRs are expressed at the cell surface and in intracellular endossomal compartments[23], NLRs and RLRs are found in the cytoplasm[24,25], while CLRs are exclusively expressed at the cell surface[26]. There are clear distinctions among these families but, nonetheless, they share a similar overall program of detection, signal transduction and subsequent production of effector molecules.

The signals initiated by PAMP recognition via PRR culminate in the activation of key transcription factors that are primarily responsible for the transcription of effector molecules. Among these transcription factors are nuclear factor kappa B (NF-κB), activating protein-1 (AP-1), nuclear factor of activated T-cells (NFAT) and interferon regulatory factor (IRF) 3 and 7[23-26]. The intensity of the signaling pathways leading to the activation of these transcription factors will dictate the specificity of the resultant response[27]. Importantly, in the case of pathogens, most often more than one PRR will be triggered upon recognition. The overall production of effector molecules will, therefore, depend on the net effect of activation and inhibitory signals received by the cell. As a general principle, PRR stimulation will lead to NF-κB, NFAT, and AP-1 activation that will, in turn, initiate the transcription of proinflammatory cytokines, chemokines and molecules involved in direct pathogen killing such as antimicrobial peptides, nicotinamide adenine dinucleotide phosphate (NADPH) oxidase subunits, and nitric oxide synthase (iNOS). The production of type I interferons will occur through the activation of IRF3 and IRF7[28].

The relative specificity in the response triggered by different PRR relies in great deal on the intermediate signaling molecules used to achieve the final activation of transcription factors. In the TLR family, signaling is dependent on two crucial adaptor molecules, i.e. myeloid differentiation primary response gene 88 (MyD88) and TIR-domain-containing adapter-inducing interferon-β (TRIF). All TLRs signal via MyD88, except TLR3 that uses TRIF exclusively, and only TLR4 uses both adaptors[29]. Other signaling molecules such as MyD88-adaptor-like (Mal)[30-32],

and TRIF-related adaptor molecule (TRAM)[33] are also involved in TLR signaling, and distinct combinations among them upon stimuli generate specific patterns of gene transcription.

CLRs signal through tyrosine-based motifs such as immunoreceptor tyrosine-based activation motifs (ITAM), hemITAM (resembling half of normal ITAM motifs) and immunoreceptor tyrosine-based inhibitory motifs (ITIM). While the latter might work by increasing the threshold for innate cell activation[34-36], the first two activate innate cells. Importantly, not all CLRs have an intracellular domain capable of transducing signal and are, therefore, coupled with adaptors, such as the Fc receptor γ chain, that contain tyrosine-based motifs and are responsible for signal transduction upon PAMP stimulation[26]. The ITAMs and hemITAMs will recruit and activate spleen tyrosine kinase (Syk) and the ITIM will recruit phosphatases, i.e. SHP-1 and SHP-2[26]. Upon Syk activation, recruitment of the adaptor molecule CARD9 normally ensues and leads to the activation of downstream transcription factors, such as NF-κB[37,38].

NLRs form a large family of cytoplasmic receptors that have a particular structure containing a nucleotide-binding domain (NBD) and leucine-rich repeat domain (LRR). NOD-1 and NOD-2 induce the production of proinflammatory cytokines using the adaptor molecule RIP2 to activate NF-κB, and mitochondrial antiviral signaling protein (MAVS) to induce IRF-dependent type I interferon production[24]. Importantly, a subfamily of NLRs named NLRP or NALP, is involved in forming a multiprotein structure termed inflammasome[39]. Signals that induce inflammasome assembly and activation include increased cellular potassium efflux[40], reactive oxygen species (ROS)[41-43] and leakage of

lysosomal contents into the cytoplasm[17,44], i.e. cathepsin B. The activation of inflammatory caspases follows inflammasome assembly and may lead to different outcomes such as the conversion of pro-IL-1β and pro-IL-18 to active forms or cell death[39].

RLRs constitute the smallest family of PRR. It is composed of the cytoplasmic RNA helicases retinoic acid inducible gene 1 (RIG-I), melanoma differentiation associated factor 5 (MDA5), and laboratory of genetics and physiology 2 (LGP2). Unlike the other PRR families, RLRs seem to be restricted in the array of pathogens they recognize, being limited to viral detection, and more specifically, to viral RNA detection[25]. Upon RNA binding, RLRs associate with the adaptor protein MAVS and induce NF-kB-dependent transcription of proinflammatory genes and IRF3 and IRF7-dependent transcription of type I interferons[25]. Some of the characteristics and ligands of the different PRR families are summarized in table 1.1.

To avoid exacerbated inflammation and potential tissue damage, innate immune responses are regulated by a myriad of regulatory mechanisms. Some examples are discussed in further detail below.

Animals deficient for IRAK-M (*Irak-m*$^{-/-}$) have increased intestinal inflammation upon *Salmonella thyphimurium* infection[45] and succumb to influenza infection due to an uncontrolled inflammatory response[46]. Accordingly, *Irak-m*$^{-/-}$ cells present increased NF-kB[45], p38 mitogen-activated protein (MAP) kinase [45,47], c-Jun N-terminal kinase (JNK)[45] and extracellular-signal regulated kinase (ERK) 1/2[45] activation upon stimulation with

PAMP.

Table 1.1. Characteristics of PRR from different families.

PRR	Cellular localization	Ligands	Proximal adaptor molecule
TLR			
TLR2	Plasma membrane	Lipoprotein	MyD88
TLR3	Endolysosome	Double Stranded RNA	TRIF
TLR4	Plasma membrane	LPS	MyD88 and TRIF
TLR5	Plasma membrane	Flagelin	MyD88
TLR7	Endolysosome	Single stranded RNA	MyD88
TLR9	Endolysosome	CpG-DNA	MyD88
TLR10	Endolysosome	Profilin-like molecule	MyD88
NLR			
NOD1	Cytoplasm	γ-D-glutamyl-mesodiaminopimelic acid	RIP2
NOD2	Cytoplasm	muramyl dipeptide	RIP2, MAVS
CLR			
Dectin-1	Plasma membrane	β-Glucan	Syk/CARD9
Dectin-2	Plasma membrane	β-Glucan	Syk/CARD9
Mincle	Plasma membrane	SAP130	Syk/CARD9
DNGR-1	Plasma membrane	Unknown content of dead cells	Syk
RLR			
RIG-I	Cytoplasm	Short double stranded RNA	MAVS
MDA5	Cytoplasm	Long double stranded RNA	MAVS

Note: Adapted from references [23-26,29,39].

The ubiquitin-editing enzyme A20 is an essential and absolutely required regulator of innate immune activation. A20 functions by deubiquitinating or polyubiquitinating key signaling molecules involved in PRR and cytokine receptor signaling pathways, leading to their functional inactivation or degradation by the proteassome[48]. Primarily described as an inhibitor of TNF-mediated apoptosis[49], the ability of A20 to regulate NF-κB activation by modulating several upstream signaling molecules

was later described. A20-deficient mice (*A20*$^{-/-}$) die shortly after birth showing severe multi-organ inflammation, an effect at least partially attributable to uncontrolled NF-κB activation[50]. Subsequently, A20 was shown to modulate signaling by TLRs[51,52], NLRs[53] and RLRs[54] as well. Importantly, A20 expression is induced upon NF-κB activation and, therefore, acts in a negative feedback loop to contain exacerbated activation of the former[48]. Other ubiquitin-editing enzymes such as deubiquitinating enzyme A (DUBA)[55] and CYLD[56,57] have also been shown to act as negative modulators of innate immune activation.

There are several other mechanisms described to limit innate immune cell activation such as, but not limited to, the expression of molecules with RNase activity inducing rapid decay of inflammatory cytokine RNA[58], microRNAs[59], inhibitory receptors[36,60,61], and suppression of innate immune cells by specific subsets of T lymphocytes[62-64]. Of note, heme oxygenase-1 (HO-1) is proposed to be one of the molecules involved in controlling activation of innate immune cells[65]. Data supporting this notion is described in detail in *section 2*. The existence of many diverse systems implicated in controlling excessive inflammation highlights its importance in maintaining host viability. Importantly, one common feature of deregulated innate immune cell activation is the consequent unfettered activation of the adaptive immune compartment[58,60], a process thought to be mainly driven by activated dendritic cells (DC).

DC are innate immune cells with matchless capacity to activate adaptive immune cells, in particular T cells, as demonstrated in the seventies by Steinman and colleagues[66-70].

Later, data using transgenic mice allowing for transient DC depletion confirmed that DC are essential *in vivo* for T cell priming[71-75] and re-stimulation[76,77]. This unique capacity relies on DC's ability to provide T cells with adequate amounts of MHC-peptide complex, costimulation and cytokines, when properly activated by PAMP[78,79].

The cytokines produced by DC during T cell activation play a major role in instructing which sort of T cell response will be generated[80,81]. Notwithstanding their role in initiating adaptive immune responses, DC also play a predominant role in central[82,83] and peripheral immunological tolerance[84-86] (*see section 1.2 and 1.3*). The mechanisms employed by DC to generate and maintain peripheral tolerance are discussed in further detail below.

1.2 Adaptive Immunity

1.2.1 T cell activation

Cells from the adaptive immune system, i.e. T and B lymphocytes, carry a single receptor generated by somatic recombination of defined gene segments. The recombination process occurs randomly, generating a massive diversity in the receptor repertoire and endowing T and B cells with the ability to recognize virtually any antigen. That, *per se*, poses a threat to the organism since these lymphocytes could strongly react with self-antigens and, therefore, cause autoimmunity. In an attempt to avoid self-reactivity, T and B cell repertoires undergo selection processes during development to ensure that a minimal amount of potentially self-reactive lymphocytes mature. These processes

are generically termed “central tolerance” and, although essential to maintain host viability, fall out of the scope of this thesis and will not be described in further detail. The focus will be given to mechanisms inducing effector function on the major T cell subsets, i.e. $CD4^+$ and $CD8^+$, and on mechanisms involved in maintaining immunological tolerance in the periphery and avoiding immunopathology.

Both major T cell subsets, i.e. $CD4^+$ and $CD8^+$, are activated via a similar process that is comprised of signals given to the T cell by the APC. The first signal inducing T cell activation is triggering of the **T c**ell **r**eceptor (TCR) by cognate recognition of antigenic peptides presented by APC, particularly DC, in the context of MHC class I and II molecules, for $CD8^+$ and $CD4^+$ T cells respectively. Together with TCR stimuli, APC will deliver costimulatory signals by engaging several pairs of receptors on the APC and the T cell surface such as CD80/86 and CD28[87,88], 4-IBB and 4-IBBL[89,90], CD70 and CD27[91,92]. The costimulatory signals will convey proliferative, survival and, in some cases, instructive signals to T cells. Cytokines are the third signal provided by APC to T cells. They work as instructive signals that transmit to T cells information regarding the kind of pathogen encountered and, therefore, gear T cells to differentiate into the appropriate effector phenotype[79]. The net effect of available antigen amount, costimulation and instructive cytokines will ultimately lead to the generation of the adequate T cell response.

As described above, cytokines are the distinctive signal required for the differentiation of $CD4^+$ T cells into different effector T_H cell lineages, although some costimulatory molecules have also been reported to provide signals that drive T_H cell differentiation[93,94]. The essential cytokine requirements for the

differentiation of the main T_H cell subsets, i.e. T_H1, T_H2 and T_H17, are well defined. Briefly, T_H1 cells rely on IL-12 signaling for their differentiation[95], T_H2 rely on IL-4[96], and T_H17 relies on TGF-β and IL-6[97,98]. Each of these subsets will produce a determined set of signature cytokines that will mediate their effector function (*see table 1.2*). Importantly, the main cytokines produced by each T_H cell lineage, will reinforce their own phenotype while inhibiting the conversion of naïve cells into any other T_H cell phenotype[80]. Signaling through cytokine receptors will lead to activation of specific **s**ignal **t**ransducers and **a**ctivators of **t**ranscription (STAT) transcription factors. STAT activation, in turn, will lead to expression of lineage specification transcription factors that reinforce T_H lineage commitment, largely through epigenetic modifications of target genes[99]. An overall view of the cytokines and transcription factors involved in T_H cell differentiation can be found on table 1.2.

Table 1.2. Minimal cytokine requirements for T_H cell lineage commitment.

Lineage	Inducer cytokines	Cytokine signal transduction	Lineage transcription factor	Effector cytokines/molecules
T_H1	IL-12	STAT4	T-bet	IFNγ, TNF
T_H2	IL-4	STAT6	GATA-3	IL-4, IL-5, IL-13
T_H17	IL-6+TGF-β	STAT3	RORγT	IL-17, IL-22, IL-21
T_{REG}	TGF-β+IL-2	Smad3/ STAT5	Foxp3	IL-10, TGF-β, CLTA4

Note: Cytokine requirements based on *in vitro* differentiation of naïve T cells in the presence of TCR triggering and costimulation[80].

Importantly, each of the T cell subsets described will be differentiated in specific microenvironments, generated as a

response to signals received by innate immune cells via their PRR. Therefore, upon recognition of PAMP from fungi APC will produce higher amounts of IL-6 and IL-23[37,38] and induce T_H17 responses. On the other hand, Gram-positive bacteria[95] or PAMP from protozoan parasites, such as *Toxoplasma gondii*[100], will induce IL-12 production and the consequent generation of T_H1 cells. In the context of helminth infection IL-4, most probably derived from innate cells[101-103], has been shown to play a predominant role and will orchestrate the development of a T_H2 response.

The requirements of TCR stimulation, costimulation and instructive cytokines are also necessary for $CD8^+$ T cell activation. In the case of $CD8^+$ T cells, antigen is recognized coupled to MHC class I molecules and delivered together with costimulation by APC. It is also possible for $CD8^+$ T cells to become producers of cytokines analogous to those produced by T_H2 and T_H17 cells however, the relevance of these subpopulations is currently poorly understood[104-107]. In fact, the cytokine milieu present during $CD8^+$ T cell activation is thought to influence more dramatically the acquisition of effector *versus* memory potential[108,109]. When fully activated, $CD8^+$ T cells will become IFNγ and TNF producers and will express cytotoxic molecules, i.e. perforin and granzyme B.

Type I IFN and IL-12 are largely produced upon viral infection and, together with IL-2, drive expansion and generation of fully activated short-lived cytotoxic $CD8^+$ T cells expressing IFNγ and granzyme B[110-114]. Importantly, under a high proinflammatory setting the generation of memory $CD8^+$ T cells is impaired[108,109,115]. Presence of IL-21, on the other hand, favors

the generation of memory $CD8^+$ T cells rather than short-lived effector cells, as observed by the abnormal accumulation of memory $CD8^+$ T cells in mice overexpressing IL-21[116] and the inability to control chronic viral infection when IL-21 signaling is disrupted[117-119]. Activation of the mammalian target of rapamycin (mTOR) pathway seems to be critically involved in driving $CD8^+$ T cell differentiation towards an effector *versus* a memory phenotype. IL-12-induced expression of the transcription factor T-bet is blocked by rapamycin with a concomitant increase in expression of the transcription factor Eomesodermin[120]. Importantly, while T-bet promotes effector $CD8^+$ T cell response, Eomesodermin is associated with memory $CD8^+$ T cell generation[121,122].

Complete activation of $CD8^+$ T cells with concomitant acquisition of cytotoxic potential has been shown to depend on $CD4^+$ T cell help in some contexts. Particularly, this seems to be the case when $CD8^+$ T cells are activated in the context of non-immunogenic antigen presentation that is, when there is no previous activation of the innate immune system[123-125]. This notion is supported by reports demonstrating acquisition of full blown effector function by $CD8^+$ T cells during infection in the absence of $CD4^+$ help[126,127]. Nonetheless, $CD4^+$ help seems crucial in the development of $CD8^+$ T cell memory[128-130], possibly by serving as a source of IL-21. However, the necessity of $CD4^+$ help even in the presence of a highly inflammatory milieu might depend on the model being studied. This is illustrated in the case of *Plasmodium* infection where $CD4^+$ help is required to induce full $CD8^+$ T cell activation in liver stage[131] and blood stage[132,133] infection (*see section 4.2*).

1.2.2 Regulation of immune responses by T cells

Regulatory T cells (T_{REG}) are the main cell type involved in regulating immune reactivity in homeostatic conditions. Unlike T_H cells, T_{REG} cells exit the thymus already committed to this lineage, and with a phenotype resembling that of activated/effector T cells[134]. Mice that had their thymus removed shortly after birth, allowing T_H but impeding T_{REG} migration to the periphery, develop autoimmune disease[135]. The master transcription factor implicated in T_{REG} differentiation is forkhead box P3 (Foxp3) and animals and humans deficient in this transcription factor show loss of immunological tolerance and develop severe autoimmunity[136-139]. Importantly, T_{REG} are fundamental throughout life as its conditional ablation in adult animals leads to severe autoimmunity[64].

Many different mechanism(s) have been described via which T_{REG} suppress immune responses. These include inhibition of stable contact formation between DC and naïve T_H cells in the lymph-node[140,141], production of the anti-inflammatory cytokines TGF-β[142,143] and IL-10[144,145], and use of membrane bound molecules such as cytotoxic T lymphocyte antigen-4 (CTLA-4)[146,147]. Most likely, all the mechanisms described above, and possibly others, will act in concert to maintain homeostasis. Importantly, during infections the control of ongoing immune responses to pathogens by T_{REG} needs to be tightly regulated to ensure pathogen clearance and, at the same time, avoid immunopathology[148-151].

Although T_{REG} were at first thought to be exclusively of thymic origin, naïve $CD4^+$ T cells can be differentiated, *in vitro*

and *in vivo,* towards a T_{REG} phenotype. *In vitro*, TCR stimulation with concomitant IL-2 and TGF-β signaling induce naïve $CD4^+$ T cells to express the transcription factor Foxp3 and to acquire suppressive function[152,153]. *In vivo*, DC were shown to be an important cell type in maintaining peripheral tolerance, partially through *de novo* generation and maintenance of T_{REG} in the periphery. Several different mechanisms used by DC to maintain and generate peripheral tolerance have been demonstrated. Non-immunogenic antigen presentation by DC was shown to delete $CD4^{+}$[84] and $CD8^+$ T[85,86] cell clones in the periphery, leading to antigen-specific unresponsiveness. DC were also shown to recirculate into the thymus carrying peripherally acquired antigens and inducing deletion of T cell clones reactive to these antigens[82].

The induction and expansion of T cells with regulatory properties in the periphery by DCs, including IL-10 producing type-1 T regulatory cells (Tr1)[154,155] and T_{REG}[156-159], was also demonstrated. Until recently the differences between thymic derived T_{REG} and peripheral induced T_{REG} cells were very poorly understood. However, in 2010 the transcription co-factor homeodomain-only protein (Hopx) was described as being fundamental for the suppressor function of T_{REG} generated by DC in the periphery, without interfering with the function of thymic-derived T_{REG}[160]. Importantly, a specific DC subpopulation present in the gut was described to be especially tailored to induce T_{REG} via a pathway that involves TGF-β and retinoic acid[161-163]. Most recently, it was demonstrated that in order to avoid T_H cell-mediated autoimmunity both thymic and peripheral T_{REG} are

necessary, presumably because the peripheral conversion of naïve T cells expands the TCR repertoire of T_{REG}[164].

Of note, recent reports have suggested that T_{REG} cells can themselves be subdivided into different lineages capable of suppressing distinct types of immune responses. It was demonstrated that T_{REG} expressing the transcription factor IRF4, involved in T_H2 differentiation, were more efficient in suppressing T_H2 responses[165]. That was also the case for the expression of STAT3 in T_{REG} involved in suppressing T_H17 responses[166], and T-bet in T_{REG} suppressing T_H1 responses[167]. These findings suggest that T_{REG} would be generated or instructed outside the thymus as an immune response begins, and that the cues involved in T_H differentiation could also serve to endow T_{REG} with specific capacity of controlling the T_H response in question.

An interesting feedback loop controlling DC and T_{REG} numbers has been described *in vivo*. Adult mice engineered to express the diphtheria toxin receptor along with Foxp3 show a sharp increase in the number of DC upon T_{REG} ablation[64]. This increase in DC numbers is thought to be partially responsible for the deregulated T_H cell response that followns T_{REG} ablation. It was later demonstrated that the mechanism underscoring the increase in DC numbers relies on the fact that T_{REG} ablation increases the amount of available Flt3L, a cytokine that induces the proliferation of DC precursors in secondary lymphoid organs[168]. Interestingly, loss of DC also induces loss of T_{REG} cells and consequent T cell activation[169]. Conversely, increasing DC numbers also increases the number of T_{REG}, to the extent that limits the development of autoimmune diabetes in autoimmune prone non-obese diabetic (NOD) mice[169]. These findings demonstrate that DC and T_{REG} are engaged into an important

regulatory loop to avoid unregulated immune activation and immunopathology.

Interestingly, not only cells with clear regulatory phenotypes, such as T_{REG} and Tr1 cells are able to restrain immune activation. $CD8^+$ and $CD4^+$ T cells were shown to regulate innate immune activation after PAMP administration, *in vivo* and *in vitro*, in an antigen and T_{REG}-independent manner[62]. Strikingly, effector/memory $CD4^+$ T cells specifically block NLRP1 and NLRP3 activation in macrophages via signaling pathways initiated by ligation of receptors of the TNF family[63].

1.3 Tolerance to infection

In animals, the most studied mechanism to survive infections is resistance. It relies on the ability of the host to prevent disease by diminishing pathogen load. Many mechanisms used by innate and adaptive immunity work by reducing pathogen load and are, therefore, involved in host resistance. Acting in concert with resistance, tolerance to infection encompasses mechanisms that limit the decrease in host health status to a given pathogen load. Tolerance has been well documented and studied in plants, but is still poorly understood in animals[170,171].

Tolerance to a given pathogen is given by the slope of the curve that determines host health status *versus* pathogen load. That is, how much host health is affected by a given pathogen load. The more the host health is affected by a given pathogen load, the more steep is the curve and less tolerant is the host. Host health status can be determined as follows[170,172,173]:

$$H_{HS} = u_{HS} + b_H.I$$

H_{HS}: host health status or fitness

u_{HS}: health status of an uninfected host

b_H: slope of the relationship between H_{HS} and I, or tolerance

I: pathogen load

Given the above, it is possible to conclude that H_{HS} upon infection depends on host's health status when uninfected (U_{HS}) and on how much its health status declines at a given pathogen load during infection ($B_H.I$).

An example of how one can compare tolerance among hosts is shown in figure 1.1. Figure 1.1A shows two genotypes that share the same health status when uninfected. However, upon infection the decline in health status as a function of parasite load is greater in the green genotype, i.e. the slope is steeper, than in the red genotype. In this case the red genotype is more tolerant to infection, by the specific pathogen in question, than the green genotype.

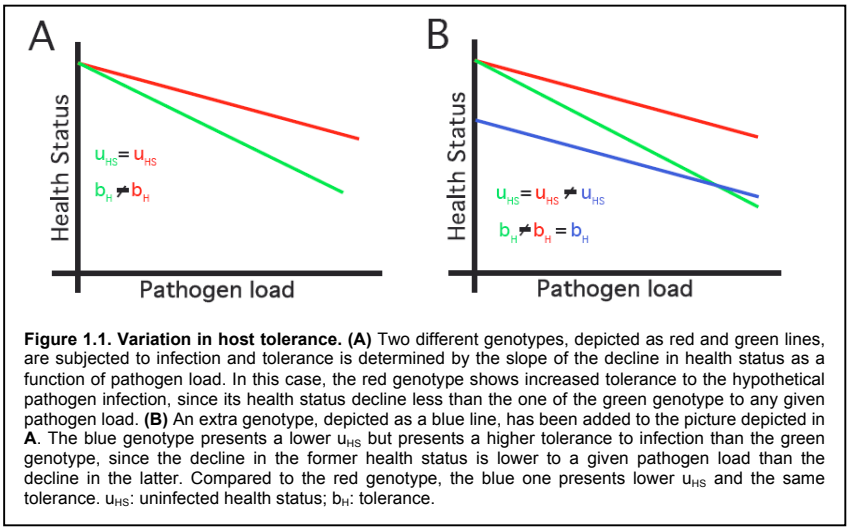

Figure 1.1. Variation in host tolerance. (A) Two different genotypes, depicted as red and green lines, are subjected to infection and tolerance is determined by the slope of the decline in health status as a function of pathogen load. In this case, the red genotype shows increased tolerance to the hypothetical pathogen infection, since its health status decline less than the one of the green genotype to any given pathogen load. **(B)** An extra genotype, depicted as a blue line, has been added to the picture depicted in **A**. The blue genotype presents a lower u_{HS} but presents a higher tolerance to infection than the green genotype, since the decline in the former health status is lower to a given pathogen load than the decline in the latter. Compared to the red genotype, the blue one presents lower u_{HS} and the same tolerance. u_{HS}: uninfected health status; b_H: tolerance.

In figure 1.1B a somewhat more complex scenario is depicted. In this case a third genotype (blue) is added which has an uninfected health status that differs from genotypes red and green. Upon infection, however, the health status decline of the blue genotype follows the same slope as that of the red genotype, which is flatter than the green slope. In this case, although through a great extent of the pathogen load gradient, the total health status of the blue genotype is lower than the green and red, the blue genotype shows increased tolerance as compared to the green genotype and the same tolerance as the red one. The difference in health status observed is given by a lower uninfected health status of the blue genotype.

Intriguingly, some of the mechanisms involved in resistance to infection might also alter tolerance and vice-versa. This was clearly demonstrated by Raberg *et al*[174] when addressing tolerance of different mouse strains to *Plasmodium chabaudi* infection. The authors demonstrated in this study, using the slope of the relationship between health status and parasite load as a measure of tolerance, that different mouse strains have distinct levels of tolerance to *Plasmodium chabaudi* infection. Importantly, mouse strains that had increased tolerance to infection presented decreased resistance, suggesting that these properties negatively regulate each other in this model of infection. However, it is important to underline that this inverse correlation might not be true for the interaction among different pathogens and a single host. In *Drosophila melanogaster* it has been shown that a single mutation can cause variation in resistance and/or tolerance in the same genotype depending on the pathogen used[175].

There is data in the literature suggesting that mechanisms that alter tolerance to infection operate during mouse models of infectious diseases. Nonetheless, this data is frequently generated in studies addressing resistance to infection. Some examples of molecules possibly involved in increasing or decreasing tolerance to infection are given below.

Molecules involved in increasing tolerance to infection can be uncovered by studies where deficiency of such molecules induces a worst disease outcome without changes in parasite load. Lack of IL-10 causes a massive and deleterious inflammatory response in mice infected with *Toxoplasma gondii*, causing premature death of IL-10 deficient mice (*Il-10*$^{-/-}$) animals due to immunopathology, while parasite loads remained unchanged[176]. Furthermore, *Il-10*$^{-/-}$ mice, despite presenting significantly lower parasitemias than wild type animals when infected with *Trypanosoma cruzi*, die earlier due to a shock-like syndrome caused by excessive TNF production[177]. Using a mouse model of malaria infection, it was also shown that mice lacking HO-1 are more susceptible to infection with *Plasmodium berghei* ANKA as compared to WT mice without changes in parasite load[178]. This mechanism seems to operate also to protect mice from non-cerebral forms of severe malaria[179].

On the other hand, some cytokines and PRR can reduce tolerance to infection. This fact is uncovered when deletion of genes encoding such molecules are beneficial to the host without altering pathogen load. In a model of oral infection with *Toxoplasma gondii*, death is accompanied by massive intestinal immunopathology in WT mice. IL-18 deficient mice (*Il-18*$^{-/-}$) are protected from the ensuing immunopathology after infection without changes in parasite load in intestines or liver as

compared to WT mice[180]. Lethal outcomes of dengue virus infection can be avoided by blocking the CLR CLEC5A, thus avoiding unfettered proinflammatory cytokine production and vascular permeability, without changing host's ability to clear viral infection[181]. Lack of inflammasome components was shown to be protective in *Schistosoma mansoni*[182] and *Mycobacterium marinum*[183] infection by diminishing immunopathology associated with infection, not by altering pathogen load.

Although these studies suggest a role for tolerance to infection in determining disease outcome, since they have not been designed to specifically address tolerance to infection, i.e. determining the slope of health status in relation to varying pathogen load, it is difficult to unequivocally conclude that these molecules alter uniquely tolerance instead of, or in addition to, overall health status.

2. Heme Oxygenase-1

Part of section 2 was adapted from *"Immunoregulatory effects of HO-1: How does it work?"* Soares, MP, **Marguti I**, Cunha A, Larsen R, published in *Current Opinion in Pharmacology, August, 2009, volume 9, issue 4, pages 482-489*[65].

2.1 Heme catabolism and its by-products

Heme oxygenases (HO) are heme (iron protoporphyrin IX) catabolizing enzymes. Two isoforms of HO are present in human and mice, heme oxygenase-1 (HO-1, encoded by the *Hmox1* gene) and heme oxygenase-2 (HO-2, encoded by the *Hmox2* gene). A third HO isoform, heme oxygenase-3, is a

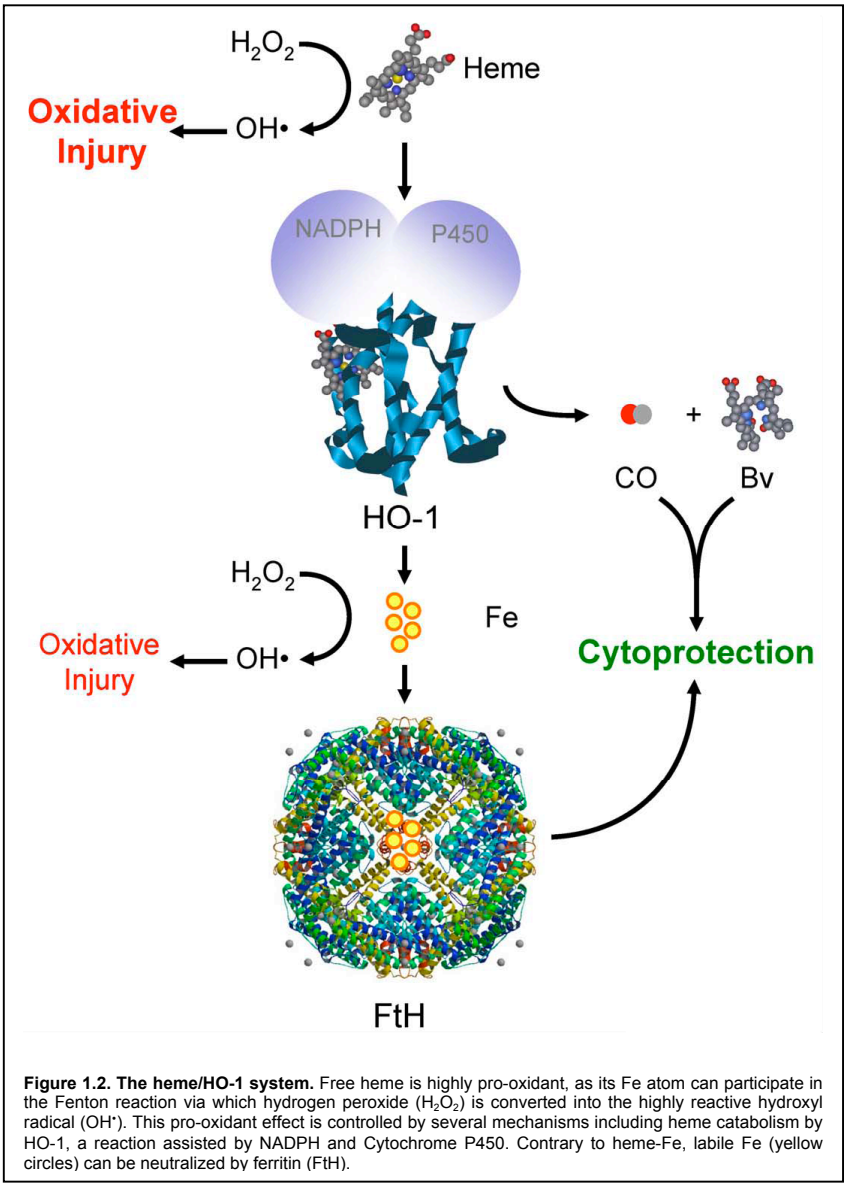

Figure 1.2. The heme/HO-1 system. Free heme is highly pro-oxidant, as its Fe atom can participate in the Fenton reaction via which hydrogen peroxide (H_2O_2) is converted into the highly reactive hydroxyl radical ($OH^{\bullet}$). This pro-oxidant effect is controlled by several mechanisms including heme catabolism by HO-1, a reaction assisted by NADPH and Cytochrome P450. Contrary to heme-Fe, labile Fe (yellow circles) can be neutralized by ferritin (FtH).

pseudogene[184]. Both isoforms, HO-1 and HO-2, are ubiquitously expressed but while HO-2 is expressed constitutively and not upregulated under cellular stress conditions, HO-1 is strongly upregulated under these circumstances. Therefore, HO-1 is termed a stress-responsive enzyme. Its expression is induced by a multitude of different stimuli such as, but not limited to,

oxidative stress, hypoxia, heat shock, cytokines, and TLR ligation[185]. The reaction leading to heme catabolism by HO enzymes opens the protoporphyrin ring leading to the generation of equimolar amounts of carbon monoxide (CO), biliverdin and labile iron (Fe^{2+}) (Figure 1.2). Biliverdin is further converted into the potent anti-oxidant bilirubin by the enzymatic action of biliverdin reductase (BVR), and labile iron is secluded by ferritin multimers preventing its pro-oxidant activity[186].

A major effect of heme catabolism by HO-1 is the avoidance of unfettered oxidative damage generated by heme molecules once they have been uncoupled from hemoproteins. The iron molecule inside the protoporphyrin ring of heme can generate large amounts of hydroxil radicals (HO•) from hydrogen peroxide (H_2O_2), through the Fenton reaction[187]. The extremely reactive HO• can, in turn, cause DNA breaks, lipid peroxidation and protein denaturation[188]. As HO-1 cleaves the protoporphyrin ring, the iron molecule is freed and becomes available to be taken up and stored intracellularly by ferritin molecules, which has its expression increased in response to iron. Ferritin molecules oxidize iron to its ferric (Fe^{3+}) state, thus impairing its pro-oxidant activity, and store the iron inside its cage-like structure[189]. In addition, with the opening of the protoporphyrin ring, biliverdin and subsequently bilirubin, a potent anti-oxidant, are generated, providing further protection against oxidative damage.

The most in depth studied by-product of heme catabolism is CO, and it has been shown to exert several biological effects. CO can inhibit apoptosis[190], avoid unlocking of heme from hemoproteins[178], and regulate inflammatory responses[191].

Several lines of evidence suggest that many of the effects of CO are mediated via the modulation of the p38 MAP kinase pathway. CO can prevent cell death by modulating the p38 MAP kinase pathway[190,192]. The anti-inflammatory effect of CO on macrophages, i.e CO-mediated inhibition of TNF production, is also dependent on p38 MAP kinase [191], and on an initial burst of ROS production by the mitochondria induced by CO[193]. Furthermore, it is proposed that the protective effects of CO rely on its capacity to interact with heme inside hemoproteins preventing their oxidation and release from heme pockets, a process that would render heme pro-oxidant[178,188,194].

Biliverdin/bilirubin also have been demonstrated to induce protection against cell death and inflammation, presumably by their anti-oxidant properties[195]. Cell death mediated by either NO or H_20_2 has been shown to be prevented by bilirubin[196,197]. Biliverdin/bilirubin are also implicated in regulating immune responses, as discussed below (*see section 2.3*). Finally, the labile iron generated by heme catabolism is thought to afford cytoprotection by inducing the expression of ferritin, an iron storage molecule[198]. The iron storage capacity of ferritin also underlies its ability to prevent TNF-mediated cell death. Iron sequestration by ferritin prevents excessive ROS production and sustained JNK activation, therefore preventing cell death in this system[199].

2.2 Regulation of HO-1 expression

Expression of HO-1 is mainly transcriptionally regulated. The *Hmox1* gene contains binding sites for different transcription factors such as NF-E2-related factor-2 (Nrf2), NF-κB, heat shock

factors (HSF), and Activator Protein-1 (AP-1) in its promoter and enhancer regions[200]. The broad array of transcription factors capable of regulating HO-1 expression might explain the induction of HO-1 expression by a variety of stimuli.

Under homeostasis, the transcriptional repressor Bach1 inhibits *Hmox1* transcription by, in conjunction with small Maf proteins, blocking accessibility of transcription factors to *Hmox1* promoter. Both heme and oxidative stress can induce conformational changes in Bach1 leading to its export from the nucleus, ubiquitination and degradation[188]. Concomitantly, ROS can also activate Nrf2. When cells are under normal conditions, Nrf2 is found in the cytoplasm bound to Kelch-like ECH-associating protein 1 (Keap1) that blocks Nrf2 migration to the nucleus and also facilitates Nrf2 polyubiquitination and degradation. Under oxidative stress conditions, alterations in Keap1 key cysteine residues liberate Nrf2 from sequestration in the cytoplasm and degradation. Furthermore, oxidative stress can also modify cysteine residues on Nrf2 nuclear export signals (NES) facilitating its concentration in the nucleus[201]. Of note, environmental stress, such as the ones posed by cigarette smoke and xenobiotics, also leads to Nrf2 activation and transcription of other detoxifying and cytoprotective enzymes besides HO-1[202].

Importantly, HO-1 expression controls the outcome of a variety of pathologic conditions in which uncontrolled immune responses cause significant damage, e.g. ischemia/reperfusion injury[203], graft rejection[204], arteriosclerosis[205], autoimmune neuroinflammation[206], severe sepsis[207], experimental cerebral and severe non-cerebral malaria[178,179]. These observations

suggest that HO-1 expression is key to control of immune responses and/or the resulting immunopathology.

2.3 Immunoregulatory effects of HO-1

The notion that HO-1 is an immunoregulatory molecule is supported by the observation that *Hmox1* deficiency leads, in mice and humans, to the spontaneous development of a chronic inflammatory pathology characterized by increased blood leukocyte count, serum immunoglobulin M (IgM), accumulation of polymorphonuclear (PMN) cells, and monocyte/macrophages in the spleen, as well as in nonlymphoid tissues, and widespread oxidative tissue injury[208-210]. Data supporting the notion that the immunoregulatory effects of HO-1 are exerted via its expression on innate and adaptive immune cells, as well as by its expression in non-lymphoid tissues where it affords cytoprotection against oxidative injury, will be discussed below.

2.3.1 Effects of the heme/HO-1 system on innate immunity

Under homeostasis, heme exists essentially as a prosthetic group in several hemoproteins. However, under pathologic conditions noncovalently bound heme can be released from those hemoproteins[178,194]. The heme produced in this manner can be recognized by TLR4, triggering the production of proinflammatory cytokines by macrophages[211]. Furthermore, heme can induce neutrophil migration and ROS production by directly activating a G-protein-coupled receptor[212] and/or by inducing the production of leukotriene B_4[213]. Although this is the case for *in vitro* experiments and for exogenous administration of

heme, it remains to be established whether this is the case in more physiological settings, since heme can bind to several proteins[194] and lipids[188] in plasma and, therefore, might have its ability to activate TLR4 or G protein-coupled-receptors[212] altered.

Interestingly, the anti-inflammatory effect of immunoregulatory molecules such as IL-10[214] and 15-deoxy-Δ12,14-prostaglandin J2 (15D-PGJ2)[215] on innate immune cells, appears to be exerted via the induction of HO-1 in macrophages. Consistent with a role for HO-1 in dampening inflammatory responses after stimulation of the innate immune system, is the observation that stimulation of *Hmox1*$^{-/-}$splenocytes with LPS resulted in increased production of pro-inflammatory cytokines, as compared to *Hmox1*$^{+/+}$ splenocytes[216]. Importantly, evidence that HO-1 does not control the inflammatory response in macrophages is also available. For instance, peritoneal macrophages isolated from *Hmox1*$^{-/-}$ or *Hmox1*$^{+/+}$ mice have a similar proinflammatory response to LPS *in vitro*[207,209], raising the possibility that HO-1 may differentially affect macrophage populations and/or other immune cells.

Similar to macrophages, neutrophils can 'sense' heme, directly or indirectly, through a yet unidentified G-protein-coupled receptor[212,217]. As such, heme can act as a neutrophil chemoattractant, activating neutrophils to produce reactive oxygen species as well as proinflammatory cytokines[212,217]. Since heme can act as a potent pro-oxidant catalyst via the Fenton chemistry, this latter effect might exacerbate macrophage as well as neutrophil-driven oxidative tissue injury. Therefore, by limiting the availability of heme, HO-1 might inhibit neutrophil chemotaxis and activation, and thus, oxidative tissue injury. This notion is

supported by the observation that *Hmox1* deficiency, in mice and humans, is associated with widespread neutrophil activation and tissue infiltration, as well as with oxidative tissue injury[208-210,218]. In addition, pharmacologic induction of HO-1 inhibits the activity of the $p47^{phox}$, $p67^{phox}$, and $gp91^{phox}$ subunits of NADPH oxidase, thereby reducing the production of reactive oxygen species by activated neutrophils and macrophages[219,220], contributing further to limit oxidative tissue injury.

CO can also modulate TLR signaling. This inhibition can occur via two independent non-exclusive pathways: one that involves enhanced caveolin-1 binding to TLR, and one that is dependent on CO-mediated inhibition of ROS formation by NADPH oxidase. Upon LPS stimulation HO-1 colocalizes with the caveolin-1/TLR4 complex, a process dependent on p38 MAPK activity. Importantly, HO-1-generated CO was shown to enhance caveolin-1 interaction with TLR4, inhibiting downstream signaling and production of pro-inflammatory cytokines[221]. A broader role for CO in inhibiting TLR function has been shown to depend on its ability to decrease ROS formation, via modulation of NADPH oxidase activity, upon TLR 2, 4, 5 and 9, stimulation and consequently inhibition of TLR recruitment (specifically TLR4 recruitment) towards lipid rafts[222]. This data shows that CO generated by HO-1 can interfere with the molecular machinery involved in proximal TLR signaling.

Importantly, there is a large body of evidence suggesting that CO can modulate cytokine production by macrophages. The first description of CO-mediated anti-inflammatory effects in macrophages indicated that through the p38 MAPK signaling pathway CO could decrease the amount of TNF production while increasing IL-10 production by these cells[191]. Furthermore, CO

was shown to induce the production of TGF-β, a potent anti-inflammatory cytokine, by macrophages, through a pathway that involves stabilization of hypoxia-inducible factor-1 α (HIF-1α) via mitochondrial-generated ROS[223]. Generation of ROS by the mitochondria is also involved in CO-mediated upregulation of peroxisome proliferator-activated receptor-γ (PPAR-γ), an event shown to be crucial for the anti-inflammatory effects of CO in macrophages[224]. Most importantly, in an *in vivo* model of LPS-mediated shock, exogenous CO blocks pro-inflammatory cytokine production and promotes survival of mice challenged with a lethal dose of LPS[225].

Mouse immature DC express negligible levels of HO-1, inducing its expression upon activation[226,227]. Intriguingly, rat and human immature DC express HO-1 constitutively, downregulating its expression upon activation[228]. In any case, pharmacologic induction of HO-1 inhibits mouse, rat, and human DC activation and immunogenicity[206,228,229] (Figure 1.3a), an effect mimicked by pharmacologic delivery of CO[229] or biliverdin/bilirubin[230] (Figure 1.3a). This suggests that CO and/or biliverdin/bilirubin mediate the immunosuppressive effects associated with pharmacologic modulation of HO-1 expression in DC (Figure 1.3a). However, the physiological relevance of these observations is somehow questioned by the observation that the pharmacologic modulators of HO-1 used in these studies can exert immunosuppressive effects in DC independently of HO-1[226]. However, if proven correct under physiological circumstances, the effects of HO-1 on DC might impact the generation of adaptive immunity, which, in turn, can explain in part the salutary effect of HO-1 expression in diseases where the

major cause of pathology is immune-mediated.

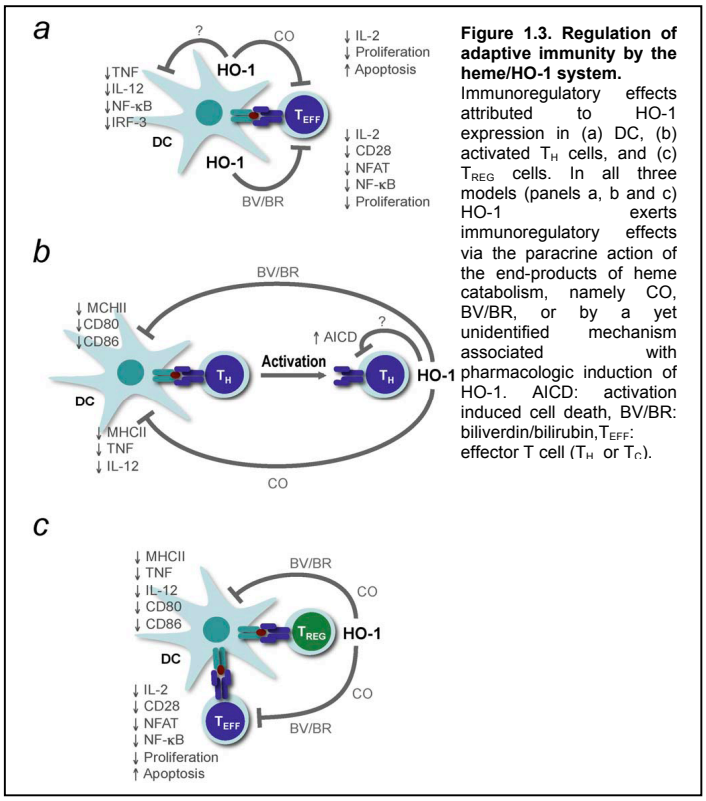

Figure 1.3. Regulation of adaptive immunity by the heme/HO-1 system. Immunoregulatory effects attributed to HO-1 expression in (a) DC, (b) activated T_H cells, and (c) T_{REG} cells. In all three models (panels a, b and c) HO-1 exerts immunoregulatory effects via the paracrine action of the end-products of heme catabolism, namely CO, BV/BR, or by a yet unidentified mechanism associated with pharmacologic induction of HO-1. AICD: activation induced cell death, BV/BR: biliverdin/bilirubin, T_{EFF}: effector T cell (T_H or T_C).

2.3.2 Effects of the heme/HO-1 system on adaptive immunity

Several *in vitro* observations suggest that HO-1 exerts immunoregulatory effects by inhibiting T cell activation, proliferation and/or acquisition of effector function. First, the activation of human $CD4^+$ T cells is associated with a significant induction of HO-1 expression[231] (Figure 1.3b). Second, pharmacologic induction of HO-1 inhibits human $CD4^+$ and $CD8^+$ T cell activation[231]. Third, CO inhibits $CD4^+$ T cell activation[231] and induces apoptosis in Jurkat T cells[232] (Figure 1.3b). Fourth, biliverdin/bilirubin inhibits mouse and human $CD4^+$ T cell activation[230] (Figure 1.3b). In keeping with these observations,

pharmacologic induction of HO-1 *in vivo* can drive activated $CD4^+$ T cells to undergo apoptosis via activation-induced cell death (AICD)[233] (Figure 1.3b), and can promote dominant peripheral T cell tolerance against transplanted organs[234]. This latter effect is mimicked by biliverdin/bilirubin, which suppresses T cell-driven inflammatory pathologies such as the rejection of transplanted organs[230,235] and autoimmune neuroinflammation[43]. The immunoregulatory effects of biliverdin/bilirubin are mediated via inhibition of the transcription factors, NFAT and NF-κB, which suppresses IL-2 production by $CD4^+$ T cells[230,235]. Whether these effects of BV/BR are mediated by its anti-oxidant activity is still unclear, although data suggests that this might not be the case[230]. Of notice, both biliverdin and bilirubin are endogenous ligands for the aryl hydrocarbon receptor (AHR)[236], which can determine the differentiation of $CD4^+$ T cells towards an anti-inflammatory T_{REG} phenotype or a proinflammatory T_H17 effector phenotype[237,238]. Although speculative, it is possible that the immunoregulatory effects of HO-1 might be exerted, to at least some extent, through the production of these endogenous AHR ligands.

More recently, it was shown that HO-1 expression in myeloid lineages has protective effects in a model of autoimmune neuroinflammation. This study shows that lack of HO-1 in the myeloid lineages leads to decreased production of IFN-β, a cytokine that blocks the development of pathogenic IL-17 producing $CD4^+$ T cells. Consequently, animals in which *Hmox1* gene was deleted developed more severe disease. This was the first work published using animals in which the *Hmox1* gene was flanked by *loxP*-sites, and deletion could be achieved in specific

cell populations through the activity of Cre-recombinase. It is important to highlight that in this system the authors did not observe the pathologic features associated with total *Hmox1* deletion, i.e. diminished fertility and progressive inflammatory disease, allowing for a more clear evaluation of the mechanisms responsible for exacerbating disease[239] in the absence of HO-1.

HO-1 has been suggested to exert immunoregulatory effects by modulating T_{REG} cell function[240] (Figure 1.3c), a notion supported by the following set of observations. First, human and mouse T_{REG} cells express HO-1 constitutively[241,242] (Figure 1.3c). Second, pharmacologic inhibition of HO-1 suppresses human T_{REG} cell function *in vitro*[243]. Third, the suppressive activity of *Hmox1*$^{+/+}$ T_{REG} cells is compromised, *in vitro*, by the presence of *Hmox1*$^{-/-}$ DC[244]. This finding, however, was not reproduced when total irradiated splenocytes were used as APCs[242]. While these observations suggest that HO-1 regulates T_{REG} cell function *in vitro*, the finding that T_{REG} cell development as well as peripheral maintenance and function, *in vitro* and *in vivo*, are normal in *Hmox1*$^{-/-}$ mice[242], questions the physiologic relevance of the effects attributed to pharmacologic modulation of HO-1 in T_{REG} cells. Of note, the function of *Hmox1*$^{-/-}$ T_{REG} has not yet been tested in conditions where there is strong innate and adaptive immune activation, such as in an infectious disease model. It would be interesting to address whether the increased production of proinflammatory cytokines by *Hmox1*$^{-/-}$ spleen cells upon stimulation[216] might, somehow, affect T_{REG} function.

A role for HO-1 in controlling antibody responses has not yet been the subject of a profound analysis. Nevertheless, data show that naïve *Hmox1*$^{-/-}$ have increased IgM levels in serum when compared with *Hmox1*$^{+/+}$ mice[216]. More recently, a report

suggests that heme might control B cell differentiation into plasma cells by interacting with the transcriptional repressor Bach2 and inducing its degradation. Bach2 degradation, in turn, leads to increased expression of the transcription factor B lymphocyte-induced maturation protein 1 (Blimp-1), diminished class switch recombination and somatic hypermutation, and increased plasma cell differentiation[245].

2.3.3 Cytoprotective effects of HO-1

Many if not all immune-mediated inflammatory diseases are associated with the production of free radicals, leading to some level of cellular oxidative stress and oxidative tissue injury. If not controlled, oxidative stress can drive cells to undergo necrosis, a form of cell death associated with the release of their intracellular content, including uric acid[246] and HMGB1[22] (Figure 1.4). These intracellular components can be recognized by PRR expressed in innate immune cells, such as macrophages and DC, and thus act as proinflammatory agonists[247]. Given the above, mechanisms regulating cell death/survival in tissues should exert immunoregulatory effects that impact on the outcome of immune-mediated inflammatory diseases[248]. The cytoprotective effect of HO-1might act in such a manner (Figure 1.4).

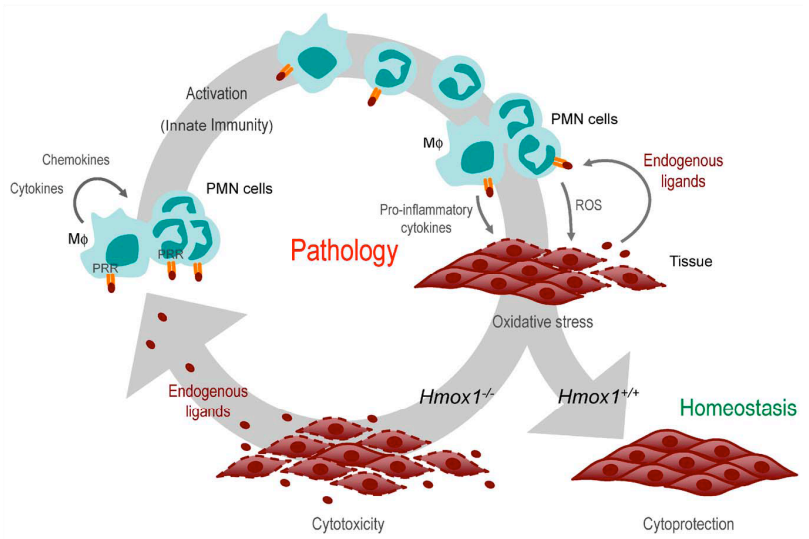

Figure 1.4. Cytoprotective effect of the heme/HO-1 system. Activation of innate immune cells, including Mø and PMN cells is associated with the production of ROS and proinflammatory cytokines, leading to oxidative stress. Expression of HO-1 in response to oxidative stress (i.e. *Hmox1*$^{+/+}$) is cytoprotective and prevents the release of endogenous proinflammatory ligands from injured cells, thus promoting the resolution of inflammation and the return to homeostasis. When expression of HO-1 is impaired (i.e. *Hmox1*$^{-/-}$) oxidative stress leads to widespread programmed cell death resulting in impaired tissue function as well as release of endogenous proinflammatory ligands. By engaging PRR in innate immune cells, endogenous ligands sustain the activation of innate immune cells (inflammation) and exacerbate tissue injury, an effect that might promote the development of immune-mediated inflammatory diseases.

When challenged by a proinflammatory agonist such as LPS, *Hmox1*$^{-/-}$ mice succumb to unfettered oxidative stress, associated with widespread oxidative tissue injury and end-stage multi-organ failure[209,249]. This suggests that HO-1 prevents the pathologic outcome of inflammatory responses by affording cytoprotection against oxidative stress. In subsequent studies, the cytoprotective effect of HO-1 was associated with protection against many other immune-mediated inflammatory diseases[186].

Expression of HO-1, or exposure to the by-products of its enzymatic activity, is cytoprotective against oxidative injury in a wide variety of cells including fibroblasts, vascular endothelial cells, pancreatic β-cells, hepatocytes, kidney epithelial cells,

cardiac myocytes, astrocytes and neurons, among others[185,186,188,250]. This broad cytoprotective effect might account for the equally broad protective effects of HO-1 against the development of vascular diseases, diabetes, liver dysfunction, kidney failure, myocardial infarction as well as diseases of the central nervous system[186].

Presumably, the cytoprotective effect of HO-1 has a dual salutary role in that it sustains tissue/organ function while inhibiting the release of endogenous proinflammatory ligands from injured cells (Figure 1.4). In keeping with this notion, *Hmox1*$^{-/-}$ mice produce high levels of circulating endogenous proinflammatory ligands, for example HMGB1, in response to LPS[251], and cecal ligation and puncture[207], an effect that promotes the development of septic shock[251-253]. Moreover, pharmacologic induction of HO-1 affords tissue cytoprotection and inhibits the production of extracellular HMGB1 in response to LPS[252].

Assuming that tissue cytoprotection contributes to the salutary effects of HO-1, other cytoprotective genes should also prevent the pathogenesis and/or progression of immune-mediated inflammatory diseases. The mechanism underlying the salutary effect of HO-1 against immune-mediated inflammatory diseases is not completely elucidated. However, this might be related to the finding that heme can sensitize tissue cells to undergo programmed cell death, a deleterious effect that should promote the pathogenesis of a number of immune-mediated inflammatory diseases[179,207].

3. Iron metabolism and immunity

Iron is a fundamental trace element for organisms, being implicated in the function of crucial proteins such as cytochrome *c* and hemoglobin[254]. Nonetheless, iron molecules, present or not in heme groups, that are not inside a functional protein moiety can be extremely toxic. As such, iron levels need to be tightly regulated both systemically and intracellularly. Importantly, mammals are not proficient in excreting iron, increasing the relevance of a delicate regulation of systemic iron levels. The regulation of systemic iron levels occurs mainly by controlling dietary iron absorption and mobilization from cellular iron stores, while intracellular iron status is regulated by iron storage and import/export[189].

Recycling iron molecules contained in heme groups supplies the majority of the iron needed by mammals. The daily need for iron is approximately 20 milligrams, while the dietary intake is normally not greater than 1-2 milligrams *per* day[189]. In that context, one of the fundamental roles of heme oxygenases is to recycle iron contained in the protoporphyrin ring of heme. Unlocking iron form the protoporphyrin ring serves at least two functions: *a)* recycle iron present in heme groups of hemoproteins and, *b)* avoid oxidative stress generated by the iron molecules inside heme, by converting it into labile iron able to be stored by ferritin inside cells and transported by transferrin (Tf) in circulation. The former is especially relevant for recycling iron present in hemoglobin once RBC become senescent and/or damaged and are destroyed by macrophages. In fact, about 60% of body iron content in humans is present in hemoglobin heme, further emphasizing the importance of recycling iron from

hemoproteins, especially hemoglobin[189]. The regulation of systemic iron status in mammals is subject to modulation by different stimuli such as anemia, inflammation, hypoxia and changes in erythropoietic rate[255,256].

Intracellularly, iron levels are regulated by two major mechanisms: *a)* storage by ferritin molecules and, *b)* modifying mRNA stability of proteins involved in import/export of cellular iron[256]. Ferritin molecules normally contain the majority of the intracellular iron pool. Ferritin is composed by the assembly of multiple L and H-ferritin chains, encoded by different genes, forming a cage-like structure capable of oxidizing and subsequently store iron molecules in a non-reactive state[189]. On the other hand, ferroportin (FPN) controls cellular iron efflux, and regulation of its levels determines the amount intracellular iron[189]. Interestingly, mRNA from iron transport and storage molecules, e.g. ferritin, transferrin receptor 1 (TfR1), ferroportin, contain, in its 3´ and/or 5´ untranslated regions, iron responsive elements (IREs) that are responsive to iron regulatory proteins (IRPs) that, in turn, respond to iron levels. The interaction between IRPs and IREs can either stabilize or destabilize the mRNA of target molecules and thus regulate intracellular iron availability[257-259].

The master regulator of iron systemic homeostasis is hepcidin. Hepcidin is a hormone that in its active form is composed of 25 amino acids, produced mainly by the liver but also by the heart, hematopoietic cells and the pancreas[260,261]. It controls intra and extracellular iron pools by regulating the expression of FPN in duodenal enterocytes, thus regulating the rate of dietary iron intake, and on macrophages and hepatocytes, regulating the amount of iron stored inside these cells (mainly stored in ferritin molecules) or available in circulation (bound to

Tf)[262]. In situations where there is anemia, iron deficit, hypoxia and/or increased erythropoiesis, hepcidin expression is decreased, allowing increased iron absorption from dietary sources and iron mobilization from cellular stores. The reverse is true in cases of iron excess and inflammation[263].

The fundamental role of hepcidin in iron regulation is demonstrated by the severe iron overload phenotype that occurs when the hepcidin gene is disrupted[264,265] and, on the other hand, by the severe iron deficiency associated with hepcidin overexpression[266,267]. Induction of hepcidin expression is thought to occur by at least two different pathways, one involved in homeostatic hepcidin expression and another involved in the fluctuations in hepcidin levels during inflammation. In homeostasis, hepcidin transcription responds to transferrin (Tf)-bound iron levels. Tf-bound iron is sensed by Tf receptor-1 (TfR1) that, under normal iron levels, is coupled with the hemochromatosis gene (HFE), a non-classical MHCI molecule[268], on the surface of hepatocytes. When serum Tf-bound iron levels increase, its binding to TfR1 dislodges HFE from the complex allowing the association of the latter with the Tf receptor-2 (TfR2). These induced changes initiate hepcidin transcription via a still uncharacterized pathway[256]. An alternative pathway can induce SMAD4-dependent hepcidin transcription via activation of the bone morphogenetic protein (BMP) receptor in complex with its co-receptor hemojuvelin[269,270].

Under inflammatory conditions, hepcidin production is increased in response to IL-6[271]. In such situations, upregulation of hepcidin transcription is mediated via the signal transducing subunit of the IL-6 receptor, gp130. Upon IL-6 binding it induces STAT3 phosphorylation, translocation to the nucleus, binding to

the hepcidin promoter and hepcidin transcription[272-274]. This response is thought to be a defense strategy used by the host to limit the amount of iron in circulation, thus limiting pathogens access to it[275].

Molecularly, hepcidin acts by binding to FPN expressed on membranes of enterocytes, macrophages and hepatocytes, and targeting it for degradation, thus impairing iron export from cells. As FPN is targeted for degradation, these cells become incapable of exporting iron, leading to a decrease in the extracellular iron pool[276]. Given the above, when hepcidin levels are elevated there is a decrease in the expression of FPN and a consequent decrease in extracellular and increase in intracellular iron content. The reverse happens in cases of low hepcidin expression (*see Figure 1.5*).

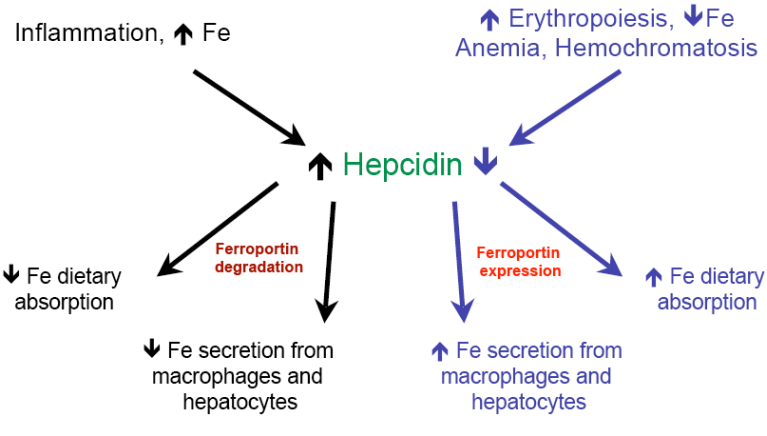

Figure 1.5. Regulation of hepcidin expression. Under homeostasis hepcidin expression is controlled by fluctuation in iron levels. When systemic iron levels are elevated hepcidin levels rise leading to ferroportin degradation and, consequently, to diminished dietary iron intake and reduced mobilization of iron from iron stores. Conversely, when systemic iron levels fall hepcidin expression is decreased leading to stable ferroportin expression and increased dietary iron intake and mobilization from cellular stores. Pathological conditions might also alter hepcidin production. While inflammation increases hepcidin expression, anemia, hemochromatosis and increased erythropoiesis decrease hepcidin levels.

The major protein involved in carrying iron in serum is transferrin (Tf). Tf is mainly produced by the liver and assures, by binding to free iron molecules, that circulating iron in the body is

devoid of its pro-oxidant activity. Tf carries up to two iron molecules and is responsible for carrying it to where it is needed, i.e. the liver for storage or the bone marrow for red blood cell (RBC) generation[255]. The majority of the iron present in the body is used by the erythroid bone marrow in the generation of heme groups to be used in hemoglobin molecules in emerging RBC. The delivery of iron to erythroblasts, nucleated precursors of RBC, is mediated by transferrin that, once bound to TfR1, is taken up by erythroblasts. The Tf-iron/TfR1 complex is internalized and degraded, iron is reduced to its Fe^{2+} form and becomes ready to be used in the confection of new heme groups[255]. Disruption of the TfR1 gene leads to defective erythropoiesis[277,278].

Deregulation of hepcidin production by mutations in hepcidin, TfR2, HFE or hemojuvelin, leads to the development of hemochromatosis a condition characterized by iron overload. In the four cases, hepcidin production is diminished. Mutations in FPN can also lead to a hemochromatosis-like disease. In the latter case, iron overload is found predominantly inside macrophages[262]. The study of the effects of iron status in immune functions greatly benefited from the occurrence of natural mutations causing hemochromatosis, and from the development of mouse models to mimic these pathologies[262].

Iron has been shown to modulate the activation of transcription factors involved in the inflammatory response, such as NF-κB and HIF-1α, in opposing ways. While high iron contents might increase NF-κB activation[279-282], it inhibits HIF-1α by targeting it for degradation[283]. Other signaling molecules, such as JNK[284], and PRR, such as NALP3[43], have been shown to

be regulated by ROS levels and, therefore, might respond to changes in intracellular iron levels, since iron can foster ROS production.

Importantly, the study of animal models of hemochromatosis, especially the model induced by targeted disruption of the hemochromatosis gene (*Hfe*), has provided insight on the molecular mechanisms involved in the regulation of immune responses by intracellular iron levels. *Hfe*-deficient mice (*Hfe*$^{-/-}$) have lower hepcidin production leading to increased FPN expression by cells and, consequently, low intracellular iron level. Macrophages with low intracellular iron content present diminished production of IL-6, TNF and IFN-β upon stimulation via TLR4 and *Salmonella* infection. Importantly, the decreased production of pro-inflammatory cytokines led to decreased intestinal inflammation upon *Salmonella* infection, but also to increased bacterial load[285,286]. Furthermore, administration of compounds able to block hepcidin production recapitulate the protective effects against excessive inflammation seem on *Hfe*$^{-/-}$ animals[285]. The mechanisms responsible for these changes rely on diminished translation of inflammatory genes[286] and on impairment of the TRIF signaling pathway downstream of TLR4[285].

The process of FPN degradation induced by hepcidin can also induce transient suppression of proinflammatory cytokine production by macrophages. FPN degradation is dependent on Janus-kinase 2 (JAK2) activation upon hepcidin binding to FPN and, in some circumstances can lead to STAT3 activation, which induces suppressor of cytokine signaling 3

(SOCS3) transcription and transient suppression of cytokine production[287].

The effects of iron status on the adaptive immune system seems to be related with the need of iron uptake for normal cell proliferation. T and B cell development is impaired in *TfR1*$^{-/-}$ mice[278]. Also, mature human B and T cells proliferate less when stimulated in the presence of anti-TfR1 antibodies[288] indicating that iron uptake is critical for an adequate adaptive response.

4. Sepsis and malaria as models of immune-mediated diseases

Although apparently very distinct conditions, sepsis and malaria, at least in experimental models, share similarities. In both cases, after infection there is an exuberant immune response aiming at eliminating the pathogen(s). Notwithstanding, the pathology observed after infection has as its major causative agents the same immune response that inadvertently targets host tissues causing immunopathology. Some of the mechanisms leading to the frequent lethal outcomes of these two diseases will be discussed below.

4.1 Sepsis

In humans, sepsis is one of the possible facets of systemic inflammatory syndrome (SIRS). SIRS is characterized when individuals present simultaneously at least two of the following symptoms: abnormally high or low body temperature (higher than 38ºC or lower than 36ºC), elevated heart and respiratory rate, and alterations in white blood cell counts. Sepsis

is characterized when SIRS is coupled with infection[289]. In the USA alone it is estimated that around 750.000 sepsis cases occur annually[290,291]. Most important, mortality rates in septic patients are extremely high as demonstrated by a large study involving 11.000 patient from 37 countries where the mortality associated with sepsis was around 50%[292].

The immune system plays a fundamental role in the pathogenesis of sepsis. In fact, in 1972 the idea that an exacerbated host response, and not infection *per se*, was the driving force for pathology was put forward by Lewis Thomas[293]. Curiously, the observation that in cases of human sepsis antibiotics are often used but only with limited effectiveness[294] supports Lewis´ claim.

"Cytokine storm" is the term normally employed to designate the massive generation of proinflammatory mediators, e.g. cytokines, chemokines, lipid mediators, which takes place in the initial phases of sepsis. The characteristic symptoms of sepsis start occurring when the levels of the proinflammatory mediators are high enough to impair physiological processes[295]. In accordance, mice deficient in molecules involved in the inflammatory response[296], i.e NALP3[297], Myd88[298], TLR4[299] and TLR9[300], components of the complement cascade[301,302], TNF receptor 1 and 2[303] and chemokines[304-307], show attenuated severity in animal models of sepsis.

During the initial phase of sepsis there is massive lymphocyte[308] and DC apoptosis[309,310], and interventions aiming at modulating apoptosis have been shown to ameliorate the disease outcome[311]. Death of these critical immune cells is thought to play a role in the "immunoparalysis" observed in late phases of sepsis. This phenomenon is characterized by inability

to control secondary infections after sepsis resolution and is thought to involve, besides depletion of key immune cells, the generation of an overall unresponsive state in the host, possibly as a negative feedback on the previous excessive inflammatory state. Alterations in neutrophil functions[312], decreased production of proinflammatory cytokines such as IL-12, IL-1α and IFNγ[308], increased production of the anti-inflammatory cytokine IL-10[308], and increased numbers of T_{REG} cells leading to T_H cell unresponsiveness[313], are all thought to play a role in "immunoparalysis".

HO-1 and its by-products have been shown to be protective in animal models of sepsis. Biliverdin administration to rats undergoing cecal ligation and puncture (CLP), considered as the gold standard animal model of sepsis[294], ameliorated disease severity, an effect that was associated with expression of reduced amounts of proinflammatory molecules[314]. *Hmox1*$^{-/-}$ mice are more susceptible to CLP[315] and to LPS-mediated shock[251]. In the first case, CO-mediated enhancement of bacteria phagocytosis is proposed as the underlying protective mechanism. This notion is supported by the observations that administration of CO-releasing molecules (CO-RM) and transgenic mice overexpressing HO-1, present lower bacterial load after CLP[315]. In the second report, the protective effects of HO-1 were proposed to work by inhibiting the release of the highly proinflammatory molecule HMGB1[22] after LPS administration. Importantly, the protective effect of HO-1, with concomitant decrease in HMGB1 release, could be mimicked by exogenous biliverdin and CO-RM administration[251]. Notably, HMGB-1 release by dead cells or by activated innate immune

cells[316] has been proposed as a major mediator of the unfettered inflammatory response in sepsis[253,317].

4.2 Malaria

Malaria is caused by infection with *Plasmodium* parasites. Natural infection occurs when infected *Anopheles* mosquitoes bite the host delivering *Plasmodium* infective sporozoites to host's bloodstream. Subsequently, sporozoites travel to the liver and invade hepatocytes, where they replicate generating thousands of merozoites before reentering the bloodstream, ending the liver stage and initiating the blood stage of infection. During the blood stage merozoites will infect RBC and replicate until RBC burst, releasing merozoites into the bloodstream and reinitiating the blood stage infection[318]. Importantly, while the liver stage of infection is asymptomatic, during the blood stage of infection malaria symptoms arise[319,320].

In 2009 the World Health organization reported a total of 225 million cases of malaria infection worldwide, with 781 thousand leading to death (http://www.who.int/malaria/world_malaria_report_2010/en/). The most lethal form of malaria is cerebral malaria (CM), which affects mainly children in Africa and adults in Southeast Asia. CM develops in individuals infected with *Plasmodium falciparum* and is characterized by development of impaired consciousness, seizures and subsequent coma. The mortality associated with CM development is about 20 percent[321,322]. The mechanisms involved in CM development in humans are not well characterized, but are thought to involve parasite sequestration in

brain microvasculature, coupled with production of inflammatory mediators, culminating in dysfunction of the blood brain barrier[322].

A long known observation, first put forward as an hypothesis by Haldane[323], is the fact that hemoglobinopathies affecting hemoglobin production or structure, afford protection against severe forms of malaria[324,325]. These hemoglobinopathies include α^+-thalassemia[326], sickle cell trait (HbAS)[327], hemoglobin C (HbC)[328] and hemoglobin E (HbE)[329].

Several studies have tried to clarify the mechanisms by which protection is conferred to these individuals, and all sorts of mechanisms have been implicated in the protection granted by hemoglobinopathies. These include early removal of infected RBC[330], early acquisition of antibodies against *Plasmodium* proteins[331], improper expression of *Plasmodium falciparum* erythrocyte membrane protein 1 (PfEMP1) on RBC surface presumably leading to reduced adherence of RBC to the microvasculature[332], and decreased parasite multiplication[333]. Most probably more than one mechanism will operate concomitantly, but defining the basis for protection against severe forms of malaria conferred by hemoglobinopathies has proven a difficult assignment.

Animal models resembling CM have been developed in mice and have helped to define mechanisms underlying the development of CM. The mouse model of CM, frequently termed experimental cerebral malaria (ECM), consists of a combination of a specific mouse strain, C57Bl/6, and a specific murine *Plasmodium* strain, *Plasmodium berghei* ANKA (*P. berghei* ANKA). Using this mouse model to dissect the mechanism of ECM development, several lines of evidence showed that, as it

happens in sepsis, the immune response generated by the host is the main driver of ECM pathology.

Several studies have reported that *Plasmodium* can trigger innate immune activation by engaging different PRR. Malarial hemozoin, a polymer of heme molecules produced by the parasite after digestion of hemoglobin inside RBC[334,335], is a potent activator of the innate immune system. Hemozoin, coupled or not with parasite DNA, can activate TLR9 in innate immune cells, particularly DC, inducing the production of proinflammatory cytokines[336-338]. Importantly, interfering with TLR9's ability to recognize *Plasmodium*-derived PAMP prevents ECM development[339]. Although some controversy exists on the exact *Plasmodium*-derived ligand for TLR9 in DC, it seems clear that *Plasmodium*-derived products engage this receptor.

NALP3 has also been reported to be activated by hemozoin and, again, some polemic exists about the actual ligand and molecules involved in NALP3 activation. Nonetheless, three independent studies have shown that NALP3 deficient animals (*Nalp3*$^{-/-}$) have a modest but reproducible survival advantage over WT animals when infected with *Plasmodium berghei* ANKA[340,341] or with *Plasmodium chabaudi adami* DS[342]. It is possible that the *bona fide* NALP3 activator is not hemozoin itself but rather uric acid released by damaged cells[343-345].

The activation of the adaptive immune system during *Plasmodium* infection has been shown to greatly rely on antigen presentation by DC. This is the case for the induction of antigen-specific CD8$^+$ T cells against liver stage *Plasmodium*[71] infection, and for the unregulated adaptive immune activation observed during blood stage infection leading to ECM development[346]. Several lines of evidence suggest that ECM pathology is driven

by a concerted action of $CD4^+$ and $CD8^+$ T cells. First, recombination activating gene-2 deficient mice (*Rag2*$^{-/-}$) or severe combined immune deficient (SCID) mice, both lacking T and B cells, are protected gainst ECM development[132,347]. Second, depletion of $CD4^+$ cells early after infection and $CD8^+$ cells until the first symptoms of ECM appear, can rescue mice from ECM[348]. Third, mice deficient for the chemokines CXCL9 and CXCL10, or the chemokine receptors CCR5 and CXCR3, have impaired $CD8^+$ T cell activation and/or recruitment to the brain after *Plasmodium* infection and are protected from ECM development [349-351]. Fourth, expression of the cytotoxic molecules perforin and granzyme B by $CD8^+$ T cells is essential for ECM development[352,353]. Fifth, increasing T_{REG} numbers during infection protects mice against disease, concomitant with reduced $CD4^+$ and $CD8^+$ T cell responses[354]. An interesting finding regarding the role of T cells in promoting ECM development is that they increase parasite sequestration in the microvasculature, a feature that is thought to be essential for disease development[347,355,356]. The exact mechanisms responsible for increased microvasculature sequestration are not fully elucidated yet.

Of note, HO-1 has been shown to be protective against ECM[178] and non-cerebral forms of severe malaria[179] by related mechanisms that involve controlling heme levels. The protective effect on ECM is thought to rely on HO-1-derived CO binding to hemoglobin released after RBC lyses. This process would avoid heme release from hemoglobin, hindering heme's deleterious effects[178]. In the case of severe non-cerebral malaria, HO-1 is thought to protect in two ways: *a)* by cleaving heme molecules and avoiding their pro-apoptotic effects on hepatocytes when in

conjunction with proinflammatory agonists such as TNF, and *b)* by acting as an antioxidant molecule[179]. Interestingly, HO-1 seems to act, via CO and biliverdin, as a major anti-inflammatory molecule during *Plasmodium* liver infection, allowing for parasite replication and establishment of blood stage infection[357]. These findings suggest that during the liver stage of *Plasmodium* infection, HO-1 expression leads to decreased resistance allowing the establishment of infection and its progression to blood stage.

5. Thesis Aims

Although fundamental to protect hosts against infection, immune responses carry a danger within: the very same mechanisms operating to achieve pathogen clearance are also harmful to host's tissues, leading to immunopathology. Therefore, the occurrence of immunopathology depends on the interplay between at least two compartments: the tissue being damaged and the immune system causing the harm. With that notion in mind, we hypothesized that avoidance of immunopathology might be achieved by mechanisms that operate on tissues and/or on the immune system. The present Thesis aims at achieving a better understanding of the mechanisms operating in these two compartments to counteract immunopathology. To address whether tissue's capacity to sustain homeostasis in face of immune-mediated insult could prevent immunopathology, we assessed the role of the cytoprotective enzyme HO-1 in the outcome of an animal model of sepsis. On the other side of the spectrum, we used an *in vitro* co-culture system to assess whether DC could expand T_{REG} under different experimental conditions, being T_{REG} expansion a putative mechanism operating to avoid unfettered immune activation. Furthermore, by using ECM as a model where pathology is adaptive immune driven, we addressed the role of tissue cytoprotection and immune regulation in the protection afforded by mutations in hemoglobin.

Chapter 2: Expansion of $CD4^+CD25^+Foxp3^+$ T Cells by Bone Marrow-Derived Dendritic Cells

Ivo Marguti[1,2], Guilherme Lopes Yamamoto[2], Thaís Boccia da Costa[2], Luiz Vicente Rizzo[2,3] and Luciana de Deus Vieira de Moraes[1,2]

[1]Instituto Gulbenkian de Ciência, Oeiras, Portugal. [2]Laboratory of Clinical Immunology, Department of Immunology, Biomedical Science Institute, São Paulo University, São Paulo, Brasil. [3] Albert Einstein Jewish Institute for Education and Research, São Paulo, Brasil.

Published in **Immunology 2009, May, 127(1):50-61**.

1. ABSTRACT

Dendritic cells (DCs) are the most important antigen-presenting cells of the immune system and have a crucial role in T-lymphocyte activation and adaptive immunity initiation. However, DCs have also been implicated in maintaining immunological tolerance. In this study, we evaluated changes in the $CD4^+CD25^+Foxp3^+$ T cell population after co-culture of lymph node cells from BALB/c mice with syngeneic bone marrow-derived DCs. Our results showed an increase in $CD4^+CD25^+Foxp3^+$ T cells after co-culture which occurred regardless of the activation state of DCs and the presence of allogeneic apoptotic cells; however, it was greater when DCs were immature and were pulsed with alloantigen. Interestingly, syngeneic apoptotic thymocytes were not as efficient as allogeneic apoptotic cells in expanding the $CD4^+CD25^+Foxp3^+$ T cell population. In all experimental settings, DCs produced high amounts of transforming growth factor (TGF)-β. The presence of allogeneic apoptotic cells induced interleukin (IL)-2 production in immature and mature DC cultures. This cytokine was also detected in the supernatants under all experimental conditions and enhanced when immature DCs were pulsed with the alloantigen. $CD4^+CD25^+Foxp3^+$ T cell expansion during co-culture of lymph node cells with DCs strongly suggests that the presence of alloantigen enhanced the number of regulatory T cells (T_{REG}) *in vitro*. Our data also suggest a role for both TGF-β and IL-2 in the augmentation of the $CD4^+CD25^+Foxp3^+$ population.

2. INTRODUCTION

Dendritic cells (DC) are professional antigen presenting cells with a unique capacity to activate T lymphocytes and induce adaptive immune responses. This capacity, however, is dependent on the activation state of the DC. Upon encounter with pathogens and recognition of "pathogen associated molecular patterns" (PAMP), or under inflammatory environments, DC become activated. The activation process involves several phenotypic and functional changes on DC, including up regulation of co-stimulatory molecules, migration to lymph nodes and production of cytokines, which, acting in concert, will lead to proper T cell activation[1].

Despite its ability to initiate adaptive immune responses, evidences also show that DC play a role in generating T cells with regulatory properties and in maintaining peripheral tolerance. In the steady state, presentation of antigens derived from apoptotic bodies to T lymphocytes leads to tolerance induction[2]. The mechanisms involved are not clear but evidences suggest that DC that have internalized apoptotic bodies remain immature[3-5] and, therefore, are not efficient in inducing effector T cell responses[6-8]. Several other mechanisms have also been implicated in the maintenance of peripheral tolerance. DC treated with interleukin-10 (IL-10) were shown to induce anergy in CD4 and CD8 T cells[9,10]. Further studies have shown that IL-10 treated DC[11], or DC generated from bone marrow precursors in the presence of this cytokine[12], were capable of generating IL-10 producing T cells endowed with regulatory properties. Other studies have also highlighted the ability of DC to delete T cell

clones in the periphery as a way of maintaining tolerance to self[13-15].

Over the last decade regulatory T cells (T_{REG}) have been described as an indispensable cell population in maintaining peripheral tolerance[16]. T_{REG} cells develop in the thymus[17] and are characterized by the expression of CD4, CD25 and the transcription factor Foxp3[18]. In the periphery, one of the requisites for T_{REG} survival is its ability to respond to IL-2[19]. In accordance, mice lacking this cytokine[20] or components of its receptor[21] develop spontaneous autoimmune syndrome. Interestingly, it has been demonstrated that T_{REG} cells can also be generated from naïve T cells in the periphery[22,23]. Recently, the interactions between T_{REG} and DC have been explored in an attempt to elucidate the contribution of the latter to the maintenance of the T_{REG} population in the periphery. Importantly, these studies have shown that T_{REG} can either proliferate or be converted from naïve T $CD4^+$ lymphocytes after interaction with DC[24-30].

Herein we show that immature DC pulsed with allogeneic apoptotic thymocytes were more efficient in expanding $CD4^+CD25^+Foxp3^+$ cells *in vitro* as compared to DC pulsed with syngeneic apoptotic thymocytes. We established an experimental system to better understand the contribution of apoptotic cells in the expansion of the $CD4^+CD25^+Foxp3^+$ population as well as the activation state of dendritic cells in this process. We co-cultured mature or immature bone marrow-derived DC, previously pulsed with apoptotic allogeneic thymocytes, with syngeneic lymph node cells. Our results show that mature and immature DC are capable of expanding $CD4^+CD25^+Foxp3^+$ T cells. Importantly, we observed an enhanced percentage of $CD4^+CD25^+Foxp3^+$ cells in

conditions where immature DC were previously loaded with apoptotic allogeneic cells.

3. RESULTS

3.1 Characterization of bone marrow-derived dendritic cells

Dendritic cells were generated *in vitro* from BALB/c mice bone marrow cells using rmGM-CSF. At the end of the culture period approximately 80% of these cells were $CD11c^{+}CD11b^{+}CD4^{-}CD8^{-}B220^{-}$. Upon stimulation with LPS, DC enhanced the expression of MHC-II and the costimulatory molecules CD80, CD86 and CD40 (Figure 2.1). To evaluate the functional properties of bone marrow-derived DC we tested their capacity to induce allogeneic spleen cells proliferation. Immature or mature DC were cultured with spleen cells from C57Bl/6 mice, and the proliferative response was evaluated. Splenocytes alone were used as control. As shown in Figure 2.2, both immature and mature DC were capable of inducing allogeneic T cell proliferation, with mature DC being more efficient at all time-points analyzed.

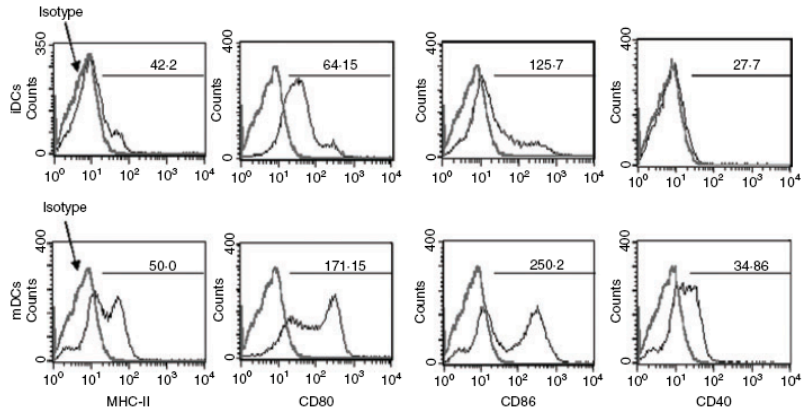

Figure 2.1. Phenotypic analysis of immature dendritic cells (iDC) and mature dendritic cells (mDC). DC were generated from bone marrow cells from BALB/c mice with recombinant murine granulocyte–macrophage colony-stimulating factor (rmGM-CSF). Cells were stimulated with lipopolysaccharide (LPS) or left unstimulated for 24 hr and were labelled with fluorescent antibodies against surface molecules. (-) isotype control; (-) surface marker. The mean fluorescence intensity (MFI) is indicated.

3.2 Phagocytosis of apoptotic thymocytes by dendritic cells

Since we wanted to evaluate the effect of apoptotic cells-derived antigens in the generation of $CD4^+CD25^+Foxp3^+$ T cells we setup a condition in which allogeneic cells would be apoptotic during the incubation period with DC. Thymocytes from C57Bl/6 mice were incubated with dexamethasone for 4 hours, extensively washed and added to DC cultures for 18 hours. Phagocytosis of apoptotic thymocytes by immature and mature DC at different DC:apoptotic cell ratios and at different time-points was evaluated. Data on figure 2.3 show the number of DC that had phagocytosed apoptotic cells after 2 and 4 hours. No differences were observed between immature and mature DC and there was a progressive and modest, but not statistically significant, increase in the phagocytosis rate when apoptotic cells were added in higher numbers.

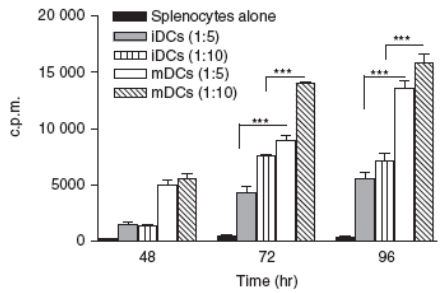

Figure 2.2. Induction of allogeneic splenic cells proliferation by bone marrow-derived dendritic cells (DC). Immature or lipopolysaccharide (LPS)-matured DC from BALB/c mice were co-cultured with total spleen cells from C57Bl/6 mice at different DC:splenocytes ratios (1 : 5 and 1 : 10) for 48, 72 and 96 hr, in a 96-well U-bottom plate. Proliferation was measured by [^{3}H]thymidine incorporation. Data is shown as mean ± standard deviation and are representative of three independent experiments. ***P < 0,001 compared with immature DC. c.p.m., counts per minute; iDC, immature DC; mDC, mature DC.

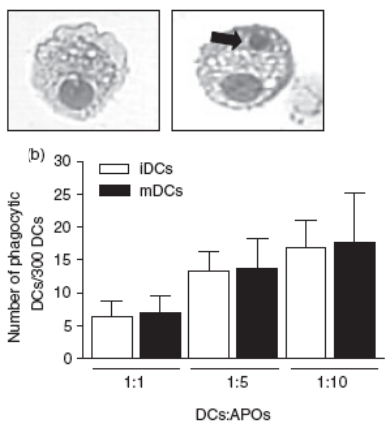

Figure 2.3. Phagocytosis of apoptotic allogeneic thymocytes (APOs) by dendritic cells (DC). Immature DC (iDC) or lipopolysaccharide (LPS)-matured DC (mDC) were incubated with APOs and phagocytosis was evaluated after 2 and 4 hr of incubation. Cells were collected and transferred to glass slides by cytospin and stained with haematoxylin and eosin. Upper panel an iDC (left); an apoptotic thymocyte (arrow) that has been phagocytosed by an iDC (right). In the lower graph results are presented as the mean ± standard deviation of both time-points combined and are representative of three independent experiments.

3.3 Effect of apoptotic cells on dendritic cell maturation

We next evaluated the expression of MHC II and costimulatory molecules, as well as the production of cytokines by DC after incubation with apoptotic allogeneic thymocytes. Mature DC population showed a slightly decrease in the percentage of MHC II^{high} cells upon incubation with apoptotic cells. No changes were observed in the expression of costimulatory molecules (CD80, CD86 and CD40) neither in immature nor in mature DC after incubation with apoptotic cells (Figure 2.4). The production of IL-10, IL-12, TNF-α (Figure 2.5 A) and TGF-® (Figure 2.5 B) by mature DC was not altered in the presence of apoptotic cells. However, the secretion of IL-2 was increased (Figure 2.5 C). Regarding immature DC, all cytokines with the exception of TGF-β were below the detection limit of the assay. The presence of allogeneic apoptotic thymocytes induced only IL-2 production (Figure 2.5 C) and did not modulate the production of TGF-β (Figure 2.5 B). Taken together, this data shows that in our system, allogeneic apoptotic cells have no interference in the maturation state of DC but are able to induce IL-2 production in immature DC and enhance the secretion of this cytokine by mature cells.

3.4 Evaluation of the $CD4^+CD25^+Foxp3^+$ T cell population after co-culture of lymph node cells with DC

Our next step was to study the influence of the maturation state of DC and the presence of apoptotic cells on the expansion of the $CD4^+CD25^+Foxp3^+$ T cell population *in vitro*. We cultured total lymph node cells from BALB/c mice with syngeneic DC that were previously incubated with apoptotic allogeneic thymocytes from C57Bl/6 mice, and evaluated the percentage of $CD4^+CD25^+Foxp3^+$ lymphocytes obtained after co-culture. Under all conditions the $CD4^+CD25^+Foxp3^+$

population was as expanded compared to the population observed in of the lymph nodes from naïve mice (Figure 2.6 A). The maturation

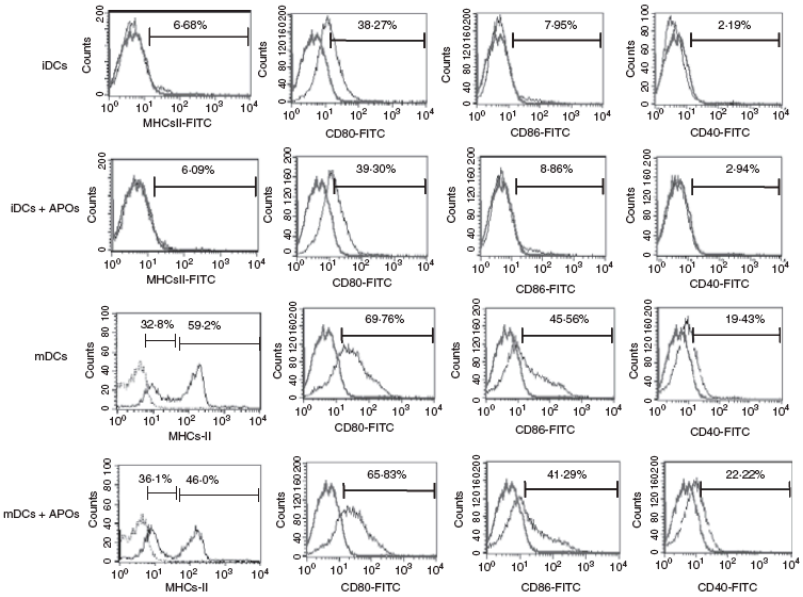

Figure 3.4. Activation phenotype of immature dendritic cells (iDC) or mature dendritic cells (mDC) incubated or not with apoptotic allogeneic thymocytes (APOs). DC were generated from bone marrow cells from BALB/c mice with recombinant murine granulocyte–macrophage colony-stimulating factor (rmGM-CSF), as described in the main text. On day 6, cells were stimulated with lipopolysaccharide (LPS; 1 μg/ml) or left unstimulated for 24 hr. On day 7, iDC and mDC were incubated with APOs for 18 hr. Cells were collected and evaluated for the expression of MHC-II, CD80, CD86 and CD40. Data are representative of three independent experiments.

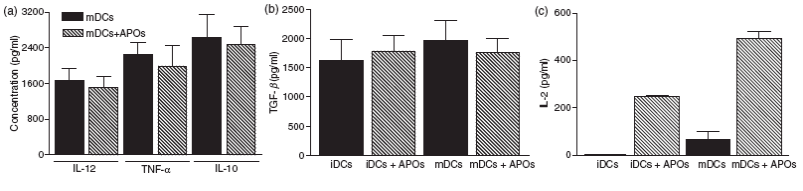

Figure 3.5. Cytokine production by mature dendritic cells (mDC) and immature dendritic cells (iDC) incubated or not with apoptotic allogeneic thymocytes (APOs). DC were generated from bone marrow-derived cells from BALB/c mice treated with rmGM-CSF for 6 days. On day 7, cells ($5x10^5$) were transferred to a 96-well flat-bottom plate and stimulated with lipopolysaccharide (LPS; 1 μg/ml) or left unstimulated in the presence or absence of APOs ($2{,}5x10^6$) for 24 hr. Supernatants were harvested and **(a)** interleukin (IL)-12, tumour necrosis factor (TNF)-α and IL-10, **(b)** transforming growth factor (TGF)-β and **(c)** IL-2 were measured by enzyme-linked immunosorbent assay (ELISA) in triplicate for each experimental condition. Results are presented as mean ± standard deviation and are representative of two independent experiments.

state of DC did not influence the expansion of T_{REG} cells since both immature and mature DC were capable of enhancing the percentages of $CD4^+CD25^+Foxp3^+$ cells (Figure 2.6 B). Interestingly, immature DC

pulsed with apoptotic allogeneic cells lead to increased percentages of T_{REG} cells compared to other experimental conditions, and these cells were suppressive *in vitro* (Figure 2.6 B and D). Apoptotic syngeneic thymocytes were not as efficient as allogeneic thymocytes in inducing T_{REG} cells in immature DC cultures (Figure 2.7 A). We also evaluated IL-2 in the supernatants of DC-lymph node co-cultures in all conditions. Interestingly, IL-2 production was significantly enhanced in the supernatants of iDC cultures that were previously incubated with allogeneic apoptotic cells compared to the other conditions (Figure 2.6 C) as well as compared to apoptotic syngeneic-incubated iDC assays (Figure 2.7 B). This observation indicates a correlation between production of IL-2 and expansion of $CD4^+CD25^+Foxp3^+$ cells.

3.5 Expansion of the $CD4^+CD25^+Foxp3^-$ T cell population in $CD4^+CD25^+$ depleted cultures

In the experiments described previously we have shown that mature and immature DC were efficient in expanding $CD4^+CD25^+Foxp3^+$ cells however, the $CD4^+CD25^+Foxp3^-$ population was not observed. This could be due to efficient T_{REG} suppression of naïve T cells proliferation or to poor antigen presentation. To evaluate these hypotheses we co-cultured immature or mature DC, pulsed or not with apoptotic allogeneic cells, with lymph node cells depleted of $CD4^+CD25^+$ T cells. We were able to obtain a highly purified population, eliminating approximately 98% of the $CD4^+CD25^+$ cells (Figure 2.7 A, right). In all assays we observed expansion of $CD4^+CD25^+Foxp3^+$ and $CD4^+CD25^+Foxp3^-$ T cells and in almost all of them the percentages of both populations were very similar (Figure 2.7 B). Exception was made when lymph node cells were cultured with mature DC loaded with apoptotic thymocytes. In this condition

activated $CD4^+CD25^+Foxp3^-$ T cells showed almost a two-fold expansion when compared with $CD4^+CD25^+Foxp3^+$ cells (Figure 2.7B)

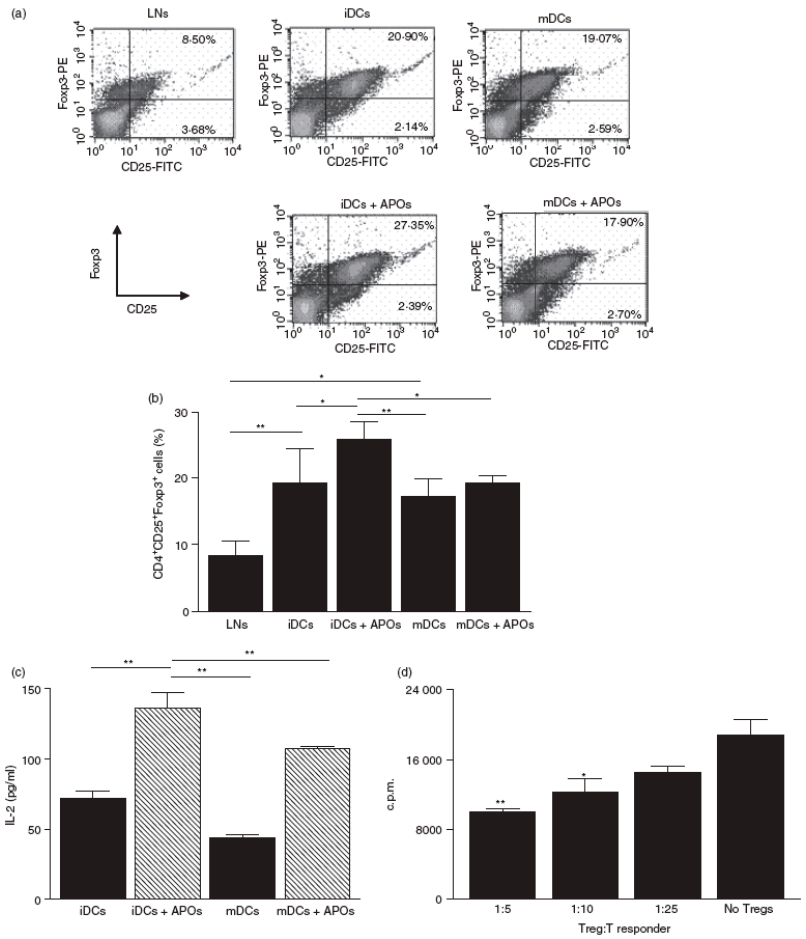

Figure 2.6. Generation of $CD4^+CD25^+Foxp3^+$ cells after co-culture of lymph node cells (LN) from naïve mice with dendritic cells (DC) pulsed or not with apoptotic allogeneic thymocytes (APOs). Mature dendritic cells (mDC) or immature dendritic cells (iDC) were incubated with APOs at a ratio of 1:5 (DC:APOs) for 18 hr. APOs were harvested and DC were co-cultured with syngeneic total lymph node cells for 5 days (1:5 DC:lymph node cell ratio). Cells were collected and labelled with fluorescent antibodies for CD4, CD25 and Foxp3. **(a)** Dot plot and **(b)** bar chart presentations of $CD4^+CD25^+Foxp3^+$ cells (gated on $CD4^+$ cells) are shown. Lymph node cells alone are presented as a control. **(c)** Interleukin (IL)-2 was evaluated in the supernatants by enzyme-linked immunosorbent assay (ELISA). **(d)** $CD4^+CD25^+Foxp3^+$ cells generated in iDC cultures in the presence of APOs were sorted and added to a mixed lymphocyte reaction (MLR) assay ($2{,}5x10^5$ responder cells: $2{,}5x10^5$ stimulator cells at different ratios [T_{REG}:T effector cells] in a 96-well U-bottom plate for 5 days. Proliferation was evaluated by [^{3}H]thymidine incorporation. Data are presented as mean ± standard deviation. In **(b)** *P < 0.05 and **P < 0.01 (LN compared to all groups); in **(c)** **P < 0.01 and in **(d)** *P < 0.05 and **P < 0.01 compared with proliferation in the absence of Tregs. Results regarding the generation of $CD4^+CD25^+Foxp3^+$ cells are representative of four independent experiments and those for the suppressor assay are representative of two independent experiments. c.p.m., counts per minute.

suggesting that these T_{REG} cells might not be able to efficiently control reactive T cell response. Again, the expansion of T_{REG} was increased in immature apoptotic-loaded DC cultures (Fig 2.7 B and C). These results suggest that antigen presentation occurred, and that in our model the presence of $CD4^+CD25^+$ T cells is responsible for suppressing the proliferation of reactive T cells.

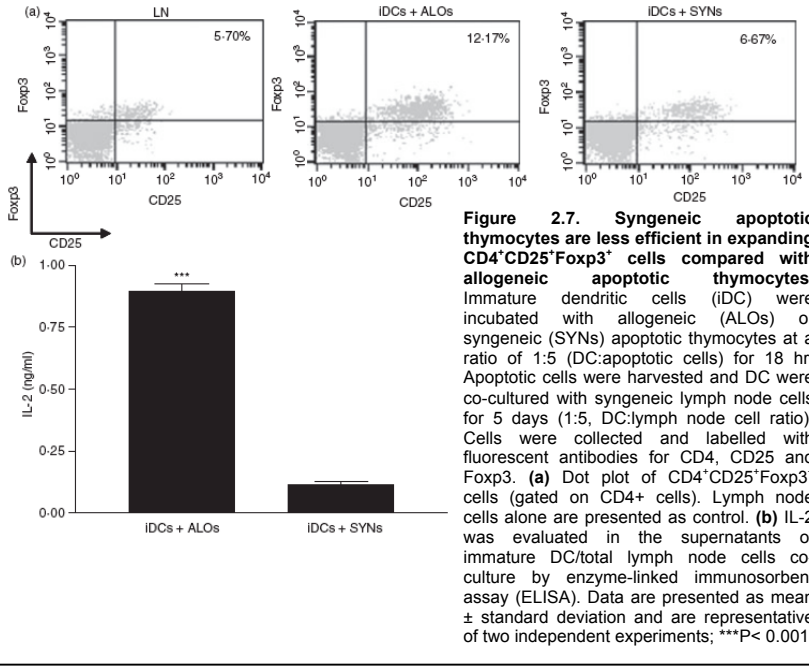

Figure 2.7. Syngeneic apoptotic thymocytes are less efficient in expanding $CD4^+CD25^+Foxp3^+$ cells compared with allogeneic apoptotic thymocytes. Immature dendritic cells (iDC) were incubated with allogeneic (ALOs) or syngeneic (SYNs) apoptotic thymocytes at a ratio of 1:5 (DC:apoptotic cells) for 18 hr. Apoptotic cells were harvested and DC were co-cultured with syngeneic lymph node cells for 5 days (1:5, DC:lymph node cell ratio). Cells were collected and labelled with fluorescent antibodies for CD4, CD25 and Foxp3. **(a)** Dot plot of $CD4^+CD25^+Foxp3^+$ cells (gated on CD4+ cells). Lymph node cells alone are presented as control. **(b)** IL-2 was evaluated in the supernatants of immature DC/total lymph node cells co-culture by enzyme-linked immunosorbent assay (ELISA). Data are presented as mean ± standard deviation and are representative of two independent experiments; ***P< 0.001.

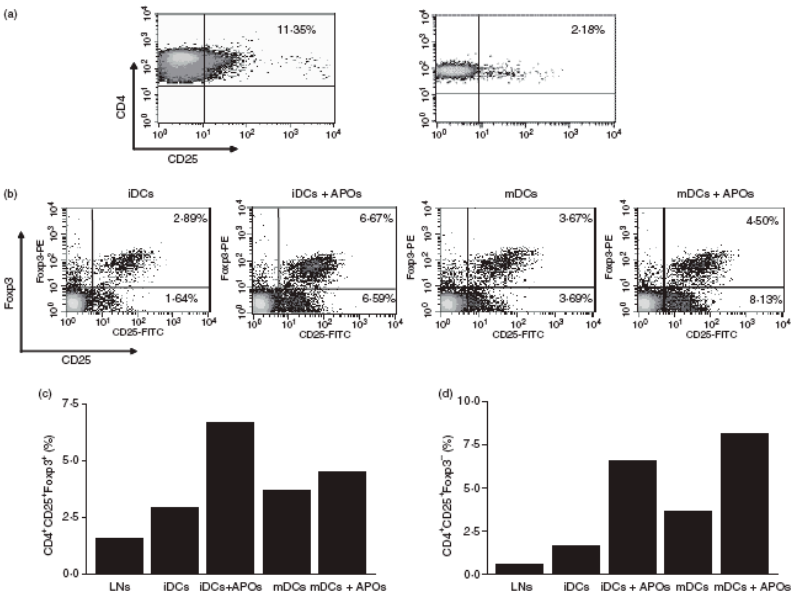

Figure 2.8. Expansion of $CD4^+CD25^+Foxp3^+$ cells from lymph node cells initially depleted of $CD4^+CD25^+$ cells. mDC or iDC were incubated with APOs at a ratio of 1:5 (DC:APOs) for 18 hr. APOs were harvested and DC were co-cultured with syngeneic total lymph node cells (LNs) depleted of $CD4^+CD25^+$ cells for 5 days (1:5, DC:lymph node cell ratio). Cells were collected and labelled with fluorescent antibodies for CD4, CD25 and Foxp3. **(a)** Percentage of $CD4^+CD25^+$ T cells in lymph node cell suspensions before (left) and after (right) depletion. **(b)** dot plot of $CD25^+Foxp3^+$ cells after co-culture in different conditions (gated on $CD4^+$ cells). **(c)** Percentage of $CD4^+CD25^+Foxp3^+$ and **(d)** of $CD4^+CD25^+Foxp3^-$ cells after co-culture with DC. Data are representative of two independent experiments.

4. DISCUSSION

In this study we showed that both immature and mature bone marrow-derived DC are able to promote expansion of the $CD4^+CD25^+Foxp3^+$ T cell population *in vitro*. We also showed that expansion of T_{REG} reached its maximum when immature DC were incubated with allogeneic apoptotic thymocytes, and that T_{REG} generated in this way were suppressive *in vitro*.

The bone marrow-derived DC used in this study showed phenotypic and functional aspects of immature cells. They expressed low levels of co-stimulatory molecules, did not produce proinflammatory cytokines and had a reduced capacity of priming allogeneic T cells. Importantly, when activated with LPS, DC were

efficient in inducing T cell proliferation, enhanced the expression of co-stimulatory molecules and produced proinflammatory cytokines. These results show that the DC population used throughout the study has features of immature DC, and that upon activation with LPS were completely able to mature.

Herein we used a system where non-self antigen is delivered to DC via allogeneic apoptotic thymocytes, and we evaluated the influence of that on T_{REG} expansion. There are some considerations that must be made here about the antigen delivery system used. One of our goals was to evaluate the influence of exogenous antigens on T_{REG} expansion, and assure that immature DC would remain immature during antigen presentation; therefore, we choose to work with allogeneic apoptotic cells. Many studies have shown that apoptotic cells can play an important role in the generation of peripheral tolerance, possibly by maintaining DC in an immature state and/or inducing tolerogenic properties on these cells[36-38]. In fact, in our system the activation status of DC was not altered after contact with allogeneic apoptotic thymocytes. The absence of immunoregulatory effects of apoptotic cells on mature DC in our system might be due to the fact that DC were fully matured when apoptotic cells were added to the culture. In this way, the expected immunomodulatory properties of apoptotic cells would be unable to reverse the activation state of mature DC.

The efficiency of mature DC in expanding $CD4^+CD25^+Foxp3^+$ cells has previously been shown in mouse[33,34] and humans[35]. There is also evidence that induction of T_{REG} proliferation by mature DC is dependent of exogenous IL-2[34]. In our system, exogenous IL-2 was not necessary for expansion of T_{REG} population. In our cultures, IL-2 production by DC occurred after maturation with LPS and when DC were in contact with apoptotic thymocytes. Therefore, it is possible that

contact with apoptotic bodies induces IL-2 production by DC that, in turn, facilitates T_{REG} expansion. Of note, the presence of proinflammatory cytokines, as observed when DC were activated by LPS, seems to decrease T_{REG} expansion, as compared to expansion by immature DC, even in the presence of high IL-2 levels.

Our data also suggests that in the absence of proinflammatory cytokines, the amount of IL-2 might directly affect T_{REG} expansion. In lymph node/DC co-cultures where immature DC had been in contact with allogeneic apoptotic cells, increased IL-2 levels were observed, compared with co-cultures were DC had been in contact with syngeneic apoptotic cells. In the first case, there was also an increased expansion of the T_{REG} population, suggesting that IL-2, in the absence of high levels of proinflammatory cytokines, contributes to T_{REG} expansion. Whether the sources of IL-2 in these cultures were DC or lymph node cells is currently not clear, but it is likely that the presence of non-self antigen induces some degree of T cell activation leading to IL-2 production.

Our results suggest that efficient alloantigen presentation occurs in our system. This notion is supported by the observation of increased percentages of activated T cells ($CD4^+CD25^+Foxp3^-$) when DC were pulsed with allogeneic apoptotic cells, and co-cultured with lymph node cells that had been depleted from $CD4^+CD25^+$ T cells. These observations indicate that DC have captured, processed, and were able to present alloantigens to T cells in our culture conditions.

It is not clear in our system if the expansion of the T_{REG} population is due to $CD4^+CD25^+Foxp3^+$ T cell proliferation after interaction with DC, or due to conversion of naïve $CD4^+CD25^+Foxp3^-$ T cells into $Foxp3^+$ cells, or by a combination of the two mechanisms. We could not unquestionably answer this question, since we had contaminating $CD4^+CD25^+$ T cells still present in our cultures

(approximately 2%). Nonetheless, the sharp decrease in the T_{REG} population when $CD4^+CD25^+$ T cells were depleted prior to co-culture with DC, suggests that expansion of existing $CD4^+CD25^+Foxp3^+$ cells, and not conversion from naïve T cells, plays a major role in increasing T_{REG} population in our system.

Studies have demonstrated that $CD4^+CD25^+Foxp3^+$ cells are more efficiently expanded by mature bone marrow-derived DC, as compared to immature DC[25,26,39]. Our data show that despite the fact that both mature and immature DC expand T_{REG}, presentation of allogeneic peptides in a non-inflammatory environment lead to increased expansion of the T_{REG} population. We were unable to detect production of IL-12 and TNF-α by immature DC, whereas mature cells produced large amounts of these cytokines. Importantly, both mature and immature DC secreted TGF-β and varying amounts of IL-2. These two cytokines have been implicate in homeostasis, proliferation, and *de novo* generation of T_{REG}, in different experimental conditions[22,28,29,41,42]. Despite the enhanced production of pro-inflammatory cytokines by mature DC, the presence of TGF-β and IL-2 might interfere with the activation and/or acquisition of effector function by naïve T cells, while helping T_{REG} maintenance and/or expansion. Overall, these observations indicate that T_{REG} expansion might occur both in non-inflammatory as well as in inflammatory environments, given the presence of IL-2 and TGF-β, and that the presence of pro-inflammatory cytokines might decrease the efficiency of this process.

Our study provides a system that can be used to better comprehend the mechanisms involved in the expansion of the T_{REG} pool by DC. The evaluation of the functional properties of our generated/expanded $CD4^+CD25^+Foxp3^+$ cells *in vivo* is ongoing.

5. METHODS

Mice

Six to ten week-old BALB/c (H-2^d) and C57Bl/6 (H-2^b) female mice were obtained from the Department of Immunology animal facilitiy at the University of São Paulo and kept in microisolator cages under specific-pathogen free conditions. Experiments were performed following the guidelines for animal use and care approved by the Ethics Committee on Animal Research from the Instituto de Ciências Biomédicas of the University of São Paulo.

Generation of Immature dendritic cell

Immature dendritic cells were generated in vitro from bone marrow cells as described by Inaba et al32, with some modifications. In brief, bone marrow cells were removed from the femurs of BALB/c mice and cultured in complete medium (DMEM supplemented with 5% fetal bovine serum (Hyclone, Logan, UT), 10^{-5}M 2-ME (Sigma Chemicals Co, St. Louis, MO, EUA) 2mM L-glutamine, 0.1 mM vitamins, 1mM sodium pyruvate, 0.1 mM non-essential amino-acids and 100μg/ml gentamicine all purchased from Gibco BRL (Rockville, NY)) in a 6-well plate (Sarstedt, Newton, NC, USA) at $2x10^6$ cells/ml in a total volume of 5 ml/well, with 10ng/ml of recombinant murine (rm) GM-CSF for 7 days. rmGM-CSF was renewed on the 4^{th} day of culture. For DC maturation, cells were stimulated for 24 hours with 1μg/mL of LPS on day 6.

Flow cytometry

Cells were incubated with anti-CD16/32 (FcBlock) for 30 minutes at 4^oC in phosphate-buffer saline (PBS) containing 3% fetal calf serum

(FCS), and 0.01% sodium azide (FACS buffer). Cells were labeled with fluorescent antibodies against CD11c (PE), CD11b (FITC), CD8 (FITC), B220 (FITC), MHC-II(I-A^d) (FITC), CD80 (FITC), CD86 (FITC), CD40 (FITC), CD4 (Cy5) and CD25 (FITC) (0.5μg/10^6 cells; all purchased from Pharmingen, BD, San Diego, CA), and incubated for 30 minutes at 4°C. Cells were washed with 1ml of FACS buffer and ressuspended in 300 μl of the same buffer before analysis. For evaluation of Foxp3 expression cells were labeled with anti-CD4 (Cy5) and anti-CD25 (FITC) antibodies and were fixed, permeabilized and labeled with anti-Foxp3 (PE) antibody according to the manufacturer's instructions ("PE anti-mouse/rat Foxp3 Staining Set", eBiosciences, San Diego, CA). Cells were analyzed by flow cytometry using a FACScalibur (BD, San Diego, CA) with a CellQuest software (BD, San Diego, CA).

Cytokine evaluation

Cytokine production by mature and immature DC, pulsed or not with apoptotic cells, was evaluated using the commercial kits OptEIA (BD, San Diego, CA, USA) for IL-12, IL-10 TNF-α and IL-2. For TGF-® evaluation we used the "TGF-®1 E_{MAX} Immunoassay System" (Promega, Madison, WI, USA). After 6 days of culture, DC were harvested from 6-well plates and 5x10^5 cells/well were plated in 96-well plates. DC were left immature or stimulated with LPS (1μg/ml) for 24 hours. 2.5x10^6 apoptotic cells (1:5 DC to apoptotic cells ratio) were added in indicated groups. Supernatants were harvested 24 hours after and stored at -20°C until use. Cytokine measurement was performed according to the manufacturer's instruction.

Induction of apoptosis in thymocytes

Thymuses were obtained from 3 week-old C57Bl/6 female mice. Single cell suspension was prepared and cells were plated in six-well plates at a concentration of 10^7 cells/ml. Cells were treated with 10^{-7}M of dexamethasone and kept in a 37°C, 5% CO_2 incubator for 4 hours. Cells were washed with DMEM and ressupended in complete medium for culture. For evaluation of apoptosis after treatment with dexamethasone, 10^6 cells were washed in HEPES buffer (10 mM HEPES, 150mM NaCl, 5mM KCl, 1mM $MgCl_2$ and 1.8mM $CaCl_2$), ressuspended in the same buffer (100µl) and labeled with Annexin V-FITC for 20 minutes in the dark at room temperature. After the incubation period, 350 µl of HEPES buffer were added to the suspension. Immediately before analysis 40µl of propidium iodide (100 µg/ml) were added. Cells were analyzed by flow cytometry.

Phagocytosis assay

Immature and mature DC ($4x10^4$) were incubated in 1.5ml plastic conical tubes (Eppendorf, Hamburg, Germany) with varying quantities of apoptotic cells in order to obtain 1:1, 1:5 and 1:10 DC:apoptotic cell ratio. Cells were kept in contact for 2 and 4 hours at 37°C, 5% CO_2 atmosphere. After the incubation period the DC were transferred to glass slides by cytospin. The slides were stained using the "Hema 3 Kit" (Biochemical Sciences Inc, Swedesboro, NJ) and the number of DC that had phagocytosed apoptotic cells were determined by optic microscopy.

Allogeneic spleenocytes stimulation by DC

Immature or mature dendritic cells ($5x10^5$) from BALB/c mice were co-cultured with total splenocytes from C57Bl/6 mice at different

responder:stimulator (1:5; 1:10) cell ratios for 5 days in a 96-well U bottom plate. ^{3}H-thymidine (1μCi/well) was added at the last 18 hours. Plates were harvested and ^{3}H-thymidine incorporation was evaluated in counts per minute (cpm).

Dendritic cells and lymph node cell co-culture

Immature or mature DC from BALB/c mice were cultured overnight in complete medium with apoptotic thymocytes from C57Bl/6 animals at a 1:5 ratio (DC: allogeneic cells). After the incubation period allogeneic thymocytes debris were harvested from the culture by washing the cells with DMEM. DC were co-cultured in complete medium with syngeneic lymph node cells at a 1:5 ratio (DC: lymph node cells) for 5 days. At the end of the co-culture period, lymph node cells were harvested with DMEM, washed once and characterized by flow cytometry.

Suppressor assay

Spleens were harvested from BALB/c or C57Bl/6 mice and single cell suspensions were prepared. After red blood cells lysis with NH_4Cl buffer, cells were washed with PBS, ressuspended in complete medium and tested for viability. A number of 2.5 x 10^5 cells from BALB/c mice were co-cultured with 2.5 x 10^5 irradiated cells (3000 rads) from C57Bl/6 in a 96-well round-bottom plate together with different numbers of generated $CD4^+CD25^+$ T cells sorted from immature DC cultures previously incubated with apoptotic allogeneic thymocytes in a total volume of 200μl/well. After 5 days of culture cells were pulsed with ^{3}H-thymidine (1μCi/well; Amersham International, Buckinghamshire, UK) for 18 hours. Cells were harvested and ^{3}H-thymidine uptake was measured using a β-counter.

Depletion of $CD4^+CD25^+$ T cells from lymph node cells suspensions

For the depletion of $CD4^+CD25^+$ T cells from lymph node single cell suspensions we used the "$CD4^+CD25^+$ Regulatory T cell Isolation Kit" (Miltenyi Biotec Inc., Auburn, CA). The depletion was performed following manufacturer's instructions. In all experiments purity obtained was higher than 97% in the population depleted of $CD4^+CD25^+$ T cells.

Statistical analysis

Data were presented as mean values $\pm$ SD. Mann-Whitney's or ANOVA with Tukey's post test were performed using the GraphPad Prism 4.0 software. Data were considered significant for $p<0.05$.

7. ACKNOWLEDGMENTS

I.M. did the majority of experiments, analyzed data and wrote the manuscript; G.L.Y, T.B.C., did experiments; L.D.V.M. and L.V.R. conceived and supervised the project and wrote the manuscript.

8. REFERENCES

1. Guermonprez P, Valladeau J, Zitvogel L, Théry C, Amigorena S. Antigen presentation and T cell stimulation by dendritic cells. *Annu Rev Immunol* 2002; **20:**621-667.
2. Steinman RM, Turley S, Mellman I, Inaba K. The induction of tolerance by DC that have captured apoptotic cells. *J Exp Med*, 2000; **191:** 411-416.
3. Newton PJ, Weller IVD, Katz DR, Chain BM. Autologous apoptotic T cells interact with dendritic cells, but do not affect their surface phenotype or their ability to induce recall immune responses. *Clin Exp Immunol* 2003; **133:** 50-58.
4. Urban BC, Wilcox N, Roberts DJ. A role for CD36 in the regulation of dendritic cell function. *Proc Natl Acad Sci USA* 2001; **98:** 8750-8755.
5. Wang Z, Larregina AT, Shufesky WJ, Perone MJ, Montecalvo A, Zahorchak AF,

Thomson AW, Merelli AE. Use of the inhibitory effect of apoptotic cells on dendritic cells for graft survival via T-cell deletion and regulatory T cells. *Am J Transpl*, 2006, **6:**1297-311.

6. Verbovetski I, Bychkov H, Trahtemberg U et al. Opsonization of apoptotic cells by autologous iC3b facilitates clearance by immature dendritic cells, down-regulates DR and CD86, and upregulates CC chemokine receptor 7. *J Exp Med* 2000; **196:** 1553–1561.
7. Stuart LM, Lucas M, Simpson C, Lamb J, Savill J, Lacy-Hulbert A. Inhibitory effects of apoptotic cell ingestion upon endotoxindriven myeloid dendritic cell maturation. *J Immunol* 2002; **168:**1627–1635.
8. Morelli AE, Larregina AT, Shufesky WJ et al. Internalization of circulating apoptotic cells by splenic marginal zone dendritic cells: Dependence on complement receptors and effect on cytokine production. *Blood* 2003; **101:** 611–620.
9. Steinbrink K, Wolfl M, Jonuleit H, Knop J, Enk AH. Induction of tolerance by IL-10 treated dendritic cells. *J Immunol* 1997**; 159:**4772-80.
10. Steinbrink K, Jonuleit H, Muller G, Schuler G, Knop J, Enk AH. Interluekin-10 treated human dendritic cells induce a melanoma-antigen-specific anergy in CD8 T cells resulting in a failure to lyse tumor cells. *Blood* 1999; **93:**1634-42.
11. Jonuleit H, Schmitt E, Schuler G, Knop J, Enk AH. Induction of interleukin-10 producing, nonproliferanting CD4 T cells with regulatory properties by repetitive stimulation with allogeneic immature human dendritic cells. J Exp Med 2000; **192:**1213-22.
12. Wakkach A, Fournier N, Brun V, Breittmayer JP, Cottrez F, Groux H. Characterization of dendritic cells that induce tolerance and T regulatory 1 cell differentiation in vivo. *Immunity* 2003; **18:**605-17.
13. Liu K, Iyoda T, Saternus M, Kimura Y, Inaba K, Steinman RM. Immune tolerance after delivery of dying cells to dendritic cells in situ. *J Exp Med* 2002; **196:**1091-7.
14. Hawiger D, Inaba K, Dorsett Y, Guo M, Mahnke K, Rivera M, Ravetch JV, Steinman RM, Nussenzweig MC. Dendritic cells induce peripheral T cell unresponsiveness under steady state conditions in vivo. *J Exp Med* 2001**; 194:**769-79.
15. Bonifaz L, Bonnyay D, Mahnke K, Rivera M, Nussenzweig MC, Steinman RM. Efficient targeting of protein antigen to the dendritic cell receptor DEC-205 in the steady state leads to antigen presentation on major histocompatibility complex class I products and peripheral CD8+ T cell tolerance. *J Exp Med* 2002; **196:**1627-38.
16. Sakaguchi S, Ono M, Setoguchi R, Yagi H, Hori S, Fehervari Z, Shimizu J, Takahashi T, Nomura T. Foxp3+ CD25+ CD4+ natural regulatory T cells in dominant self-tolerance and autoimmune disease. *Immunol Rev* 2006; **212:**8-27.
17. Itoh M, Takahashi T, Sakaguchi N, Kuniyasu Y, Shimizu J, otsuka F, Sakaguchi S. Thymus and autoimmunity: production of CD25+CD4+ naturally anergic and suppressive T cells as a key function of the thymus in maintaining immunologic self tolerance. *J Immunol* 1999; **162:**5317-26.

18. Hori S, Nomura T, Sakaguchi S. Control of regulatory T cell development by the transcription factor Foxp3. Science 2003; **299:**1057-61.
19. Fontenot JD, Rasmussen JP, Gavin MA, Rudensky AY. A function for interleukin 2 in Foxp3-expressing regulatory T cells. *Nat Immunol* 2005; **6:**1142-51.
20. Sadlack B, Merz H, Schorle H, Schimpl A, Feller AC, Horak I. Ulcerative colitis like disease in mice with a disrupted interleukin-2 gene. *Cell* 1993; **75:**253-61.
21. Suzuki H, Kundig TM, Furlonger C, Wakeham A, Timms E, Matsuyama T, Schmits R, Simard JJ, Ohashi PS, Griesser H. Deregulated T cell activation and autoimmunity in mice lacking interleukin-2 receptor beta. Science 1995; **268:**1472-6.
22. Mucida D, Kutchukhidze N, Erazo A, Russo M, Lafaille JJ, Curotto de Lafaille MA. Oral tolerance in the absence of naturally occurring Tregs. *J Clin Invest* 2005; **115:**1923-33.
23. Curotto de Lafaille MA, Lino AC, Kutchukhidze N, Lafaille JJ. CD25- T cells generate CD25+Foxp3+ regulatory T cells by peripheral expansion. *J Immunol* 2004; **173:**7259-68.
24. Min WP, Zhou D, Ichim TE, Strejan GH, Xia X, Yang J, Huang X, Garcia B, White D, Dutartre P, Jevnikar AM, Zhong R. Inhibitory feedback loop between tolerogenic dendritic cells and regulatory T cells in transplant tolerance. *J Immunol* 2003; **170:**1304-12.
25. Yamazaki S, Iyoda T, Tarbell K, Olson K, Velinzon K, Inaba K, Steinman RM. Direct expansion of functional CD25+ CD4+ regulatory T cells by antigen-processing dendritic cells. *J Exp Med* 2003; **198:**235-47.
26. Tarbell KV, Yamazaki S, Steinman RM. The interactions of dendritic cells with antigen-specific, regulatory T cells that suppress autoimmunity. *Semin Immunol* 2006; **18:**93-102.
27. Cong Y, Konrad A, Iqbal N, Hatton RD, Weaver CT, Elson CO. Generation of Antigen-Specific, Foxp3-Expressing CD4+ Regulatory T Cells by Inhibition of APC Proteosome Function. *J Immunol* 2005; **174:**2787-95.
28. Kretschmer K, Apostolou I, Hawiger D, Khazaie K, Nussenzweig MC, Von Boehmer H. Inducing and expanding regulatory T cell populations by foreign antigen. *Nat Immunol* 2005; **6:**1219-27.
29. Ochando JC, Homma C, Yang Y, Hidalgo A, Garin A, Tacke F, Angeli V, Li Y, Boros P, Ding Y, Jessberger R, Trinchieri G, Lira SA, Randolph GJ, Bromberg JS. Alloantigen-presenting plasmacytoid dendritic cells mediate tolerance to vascularized grafts. *Nat Immunol* 2006; **7:**652-62.
30. Tarbell KV, Petit L, Zuo X, Toy P, Luo X, Mqadmi A, Yang H, Suthanthiran M, Mojsov S, Steinman RM. Dendritic cell-expanded, islet-specific $CD4^+$ $CD25^+$ $CD62L^+$ regulatory T cells restore normoglycemia in diabetic NOD mice. *J Exp Med* 2007; **204:**191-201.
31. Inaba K, Turley S, Yamaide F et al. Efficient presentation of phagocytosed cellular fragments on the major histocompatibility complex class II products of dendritic cells. *J Exp Med* 1998, **188:** 2163-2173.

32. Inaba K, Inaba M, Romani N, Aya H, Deguchi M, Ikehara S, Muramatsu S, Steinman RM. Generation of large numbers of dendritic cells from mouse bone marrow cultures supplemented with granulocyte/macrophage colony-stimulating factor. *J Exp Med* 1992; **176:** 1693-702.

33. Yamazaki S, Iyoda T, Tarbell K, Olson K, Velinzon K, Inaba K, Steinman RM. Direct expansion of functional CD25+ CD4+ regulatory T cells by antigen-processing dendritic cells. *J Exp Med* 2003; **198:** 235-47

34. Yamazaki S, Patel M, Harper A et al. Effective expansion of alloantigen-specific $Foxp3^+$ $CD25^+$ $CD4^+$ regulatory T cells by dendritic cells during the mixed leukocyte reaction. *PNAS* 2006; **103:** 2753-2763.

35. Banerjee DK, Dhodapkar MV, Matayeva E, Steinman RM, Dhodapkar KM. Expansion of Foxp3high regulatory T cells by human dendritic cells (DC) in vitro and after injection of cytokine-matured DC in myeloma patients *Blood*, 2006 **108:**2655-61.

36. Kleinclauss F, Perruche S, Masson E, de Carvalho Bittencourt M, Biichle S, Remy-Martin JP, Ferrand C, Martin M, Bittard H, Chalopin JM, Seilles E, Tiberghien P, Saas P. Intravenous apoptotic spleen cell infusion induces a TGF-beta-dependent regulatory T-cell expansion. *Cell Death Differ* 2006; **13:**41-52..

37. Wang Z, Larregina AT, Shufesky WJ, Perone MJ, Montecalvo A, Zahorchak AF, Thomson AW, Morelli AE. Use of the inhibitory effect of apoptotic cells on dendritic cells for graft survival via T-cell deletion and regulatory T cells. *Am J Transplant* 2006; **6:**1297-311.

38. Bittencourt MC, Perruche S, Contassot E, Fresnay S, Baron MH, Angonin R, Aubin F, Herve P, Tiberghien P, Saas P. Intravenous injection of apoptotic leukocytes enhances bone marrow engraftment across major histocompatibility barriers. *Blood* 2001; **98:**224-30.

39. Yamazaki S, Patel M, Harper A, Bonito A, Fukuyama H, Pack M, Tarbell KV, Talmor M, Ravetch JV, Inaba K, Steinman RM. Effective expansion of alloantigen-specific Foxp3+ CD25+ CD4+ regulatory T cells by dendritic cells during the mixed leukocyte reaction. *Proc Natl Acad Sci USA* 2006; **103:**2758-63.

40. Marie JC, Letterio JJ, Gavin M, Rudensky AY. TGF-beta1 maintains suppressor function and Foxp3 expression in $CD4^+CD25^+$ regulatory T cells. *J Exp Med* 2005; **201:**1061-7.

41. Luo X, Tarbell KV, Yang H, Pothoven K, Bailey SL, Ding R, Steinman RM, Suthanthiran M. Dendritic cells with TGF-beta1 differentiate naive CD4+CD25- T cells into islet-protective Foxp3+ regulatory T cells+. Proc Natl Acad Sci USA 2007; **104:**2821-2826.

42. Yamazaki S, Bonito AJ, Spisek R, Dhodapkar M, Inaba K, Steinman RM. Dendritic cells are specialized accessory cells along with TGF-β for the differentiation of Foxp3+CD4+ regulatory T cells from peripheral Foxp3- precursors. *Blood* 2007, **110:** 4293-4302

Chapter 3: A Central Role for Free Heme in the Pathogenesis of Severe Sepsis

Rasmus Larsen[1], Raffaella Gozzelino[1], Viktória Jeney[1], László Tokaji[1], Fernando A. Bozza[2,3], André M. Japiassú[2,3], Dolores Bonaparte[1], Moisés Marinho Cavalcante[1], Ângelo Chora[1], Ana Ferreira[1], Ivo Marguti[1], Silvia Cardoso[1], Nuno Sepúlveda[1,4], Ann Smith[5], Miguel P. Soares[1]

[1]Instituto Gulbenkian de Ciência, Oeiras, Portugal. [2]Intensive Care Unit, Instituto de Pesquisa Clínica Evandro Chagas, Fundação Oswaldo Cruz. Rio de Janeiro, Brasil. [3]D´Or Institute for Researh and Education. Rio de Janeiro, Brasil. [4]Center of Statistics and Applications of the University of Lisbon. Lisboa, Portugal.[5]Division of Molecular Biology and Biochemistry, University of Missouri. Kansas City, USA.

Published in **Science Translational Medicine 2010, September, 2(51):51ra71**.

1. ABSTRACT

Low-grade polymicrobial infection induced by cecal ligation and puncture is lethal in heme oxygenase-1–deficient mice (*Hmox1*$^{-/-}$), but not in wild-type (*Hmox1*$^{+/+}$) mice. Here we demonstrate that the protective effect of this heme catabolizing enzyme relies on its ability to prevent tissue damage caused by the circulating free heme released from hemoglobin during infection. Heme administration after low-grade infection in mice promoted tissue damage and severe sepsis. Free heme contributed to the pathogenesis of severe sepsis irrespective of pathogen load, revealing that it compromised host tolerance to infection. Development of lethal forms of severe sepsis after high-grade infection was associated with reduced serum concentrations of the heme sequestering protein hemopexin (HPX), whereas HPX administration after high-grade infection prevented tissue damage and lethality. Finally, the lethal outcome of septic shock in patients was also associated with reduced HPX serum concentrations. We propose that targeting free heme by HPX might be used therapeutically to treat severe sepsis.

2. INTRODUCTION

Severe sepsis is a disease with limited treatment options that kills more than half a million individuals *per* year in the United States alone[1]. Severe sepsis can develop from an unfettered immune response to microbial infection that leads to a systemic refractory drop in blood pressure, disseminated intravascular coagulation, multiple end-stage organ failure, and eventually death[2]. The physiological and molecular mechanisms that underlie the pathogenesis of severe sepsis remain poorly understood[2].

In most cases of microbial infection, the innate and adaptive immune systems allow for pathogen clearance and a return to homeostasis[3]. In some cases, however, this host defense strategy, referred to as resistance to infection[4-6], can lead to irreversible tissue damage and compromise host viability[7]. An alternative host defense strategy, referred to as tolerance to infection[5,6], can limit disease severity irrespective of pathogen load[4-6]. Host genes conferring tolerance to infection include the stress-responsive enzyme heme oxygenase-1 (*Hmox1*), as previously demonstrated for malaria, the disease caused by *Plasmodium* infection[8].

Heme oxygenase-1 (HO-1) acts as the rate-limiting enzyme in the breakdown of heme (Fe protoporphyrin IX; FePPIX) into equimolar amounts of biliverdin, iron (Fe), and carbon monoxide[9]. Induction of HO-1 expression in response to stress caused by microbial infection suppresses the development of severe sepsis in mice[10]. This safeguarding action can act irrespective of pathogen load, relying instead on the cytoprotective effect of HO-1 against the excess free heme

produced via hemolysis during infection.

Free heme induces programmed cell death in response to proinflammatory agonists, as demonstrated for tumor necrosis factor (TNF)[8,11]. We refer to this phenomenon as “heme sensitization” to programmed cell death, because the cytotoxic effect of free heme is revealed only in the presence of other cytotoxic agonists[8,11]. The molecular mechanism underlying the cytotoxic effect of free heme relies on its pro-oxidant activity[8,11], driven by the divalent Fe atom contained within its protoporphyrin IX ring, which can promote the production of free radicals via Fenton chemistry[12].

Given that free heme can cause tissue damage and hence compromise host tolerance to infection, we investigated whether limiting this deleterious effect can be used for therapeutic purposes to enhance host tolerance against microbial infections and prevent the development of severe sepsis.

3. RESULTS

3.1 HO-1 affords host tolerance against polymicrobial infection

Severe sepsis was produced in BALB/c mice by low-grade polymicrobial infection induced by cecal ligation and puncture (CLP). Using quantitative reverse transcription polymerase chain reaction (RT-PCR), we measured the expression of the *Hmox1* gene and found that it was induced in peritoneal infiltrating leukocytes, liver, lung, and kidney at various time points after CLP (Fig 3.1 A). Mortality increased from 13% in wild-type ($Hmox1^{+/+}$) mice to 80% in *Hmox1*-deficient ($Hmox1^{-/-}$)

mice when both were subjected to low-grade CLP (Fig. 3.1 B). Similar results were obtained in BALB/c severe combined immunodeficient (SCID) mice lacking B and T lymphocytes (Fig. 1 B), demonstrating that the protective effect of HO-1 is not dependent on adaptive immunity. The mortality of heterozygous *Hmox1*$^{+/-}$ mice was similar to that of *Hmox1*$^{+/+}$ mice (Fig. 3.1 B). The higher mortality of *Hmox1*$^{-/-}$ *versus Hmox1*$^{+/+}$ mice was not attributable to the surgical procedure per se, as *Hmox1*$^{-/-}$ mice did not succumb to sham laparotomy, which mimicked CLP without polymicrobial infection.

The mortality of *Hmox1*$^{-/-}$ mice after CLP was associated with the development of multiple end-stage organ failure, a hallmark of severe sepsis[2]. Plasma concentrations of aspartate aminotransferase (AST), blood urea nitrogen (BUN), and creatinine phosphokinase (CPK), markers of liver, kidney, and muscle dysfunction, respectively, were significantly increased in infected *Hmox1*$^{-/-}$ *versus Hmox1*$^{+/+}$ mice (Fig. 3.1 C). Liver, kidney, and cardiac damage were confirmed by histological detection of centrolobular necrosis, tubular epithelial necrosis, and myocardial necrosis, respectively (Fig. 3.1 D). This demonstrates that induction of HO-1 expression in response to polymicrobial infection limits tissue damage and the development of severe sepsis.

Exacerbated mortality of *Hmox1*$^{-/-}$ *versus Hmox1*$^{+/+}$ mice did not result from higher pathogen (bacterial) load, as assessed by comparing the number of colony-forming units (CFUs) in the peritoneum and blood (Fig. 3.1 E), as well as in the liver, spleen, kidneys, and lungs (Fig. 3.1 G). *Hmox1*$^{-/-}$ mice also succumbed when challenged with heat-killed bacteria (60% mortality), whereas *Hmox1*$^{+/-}$ and *Hmox1*$^{+/+}$ mice did not (0% mortality) (Fig.

3.1 F). This demonstrates that HO-1 affords tolerance against polymicrobial infection[5,6] independently of its previously reported

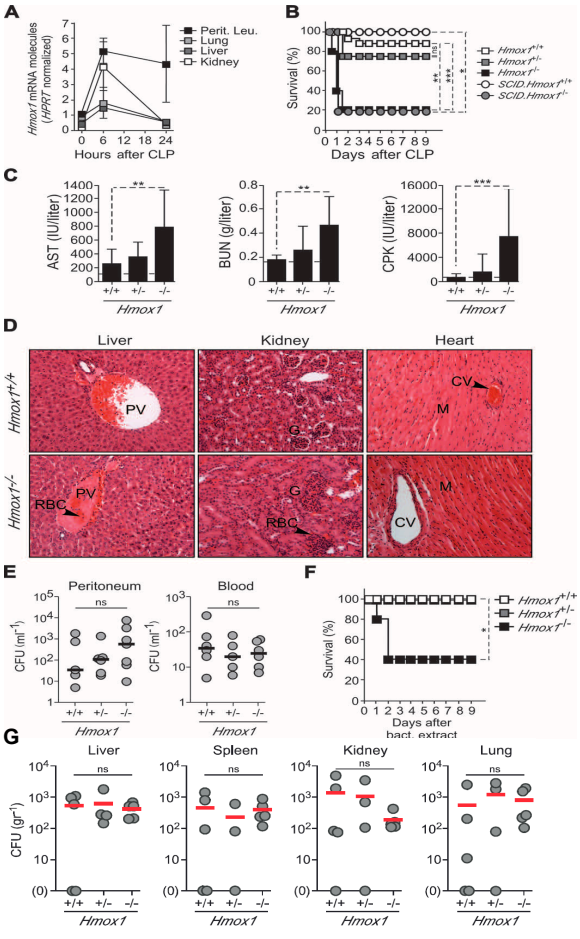

Figure 3.1. HO-1 affords tolerance against polymicrobial infection in mice. (A) *Hmox1* messenger RNA (mRNA) expression in peritoneal leukocytes (Perit.leu.), lung, liver, and kidney after low-grade CLP in BALB/c mice, as determined by quantitative RT-PCR. Data are shown as mean ± SD (n = 3 per group). **(B)** Survival of $Hmox1^{+/+}$ (n=15), $Hmox1^{+/-}$ (n=12), $Hmox1^{-/-}$ (n=10), $SCID.Hmox1^{+/+}$ (n=5), and $SCID.Hmox1^{-/-}$ (n=5) BALB/c mice after low-grade CLP. **(C)** Serological markers of organ injury in $Hmox1^{+/+}$ (n =15 to 17), $Hmox1^{+/-}$ (n=10 to 13), and $Hmox1^{-/-}$ (n=6) BALB/c mice 24 hours after low-grade CLP. Data are shown as mean ± SD. Dashed lines indicate basal plasma concentrations in naïve wild-type BALB/c mice. IU, international units. **(D)** Representative examples of hematoxylin and eosin (H&E)–stained liver, kidney, and heart tissues from $Hmox1^{+/+}$ and $Hmox1^{-/-}$ mice after low-grade CLP. Magnification, x400. Arrows indicate red blood cells (RBCs) associated with vascular congestion and/or thrombosis. CV, coronary vessel; M, myocardium; PV, portal vein; G, glomerulus. **(E)** Bacterial load (CFU) in the peritoneum and blood of mice subjected to low grade CLP (12 hours after CLP). Circles represent individual mice. Bars represent median values. ns, not significant.

(F) Survival of $Hmox1^{+/+}$ (n=7), $Hmox1^{+/-}$ (n=6), and $Hmox1^{-/-}$ (n=5) BALB/c mice after intraperitoneal administration of heat-killed bacteria (Bact.). **(G)** CFU in $Hmox1^{+/+}$(n=5), $Hmox1^{+/-}$ (n=4) and $Hmox1^{-/-}$ (n=5) mice, 12 h after low-grade CLP. Each circle represents an individual mouse and bars indicate mean values. *P < 0.05; **P < 0.01; ***P < 0.001; ns, not significant.

antimicrobial activity[10].

Production of several cytokines involved in the pathogenesis of severe sepsis [for example, TNF, interleukin-6 (IL-6), and IL-10] was similar in $Hmox1^{-/-}$ *versus* $Hmox1^{+/-}$ or $Hmox1^{+/+}$ mice subjected to low-grade CLP (Fig. 3.2, A, D, and G). Likewise, peritoneal or bone marrow–derived

monocytes/macrophages (Mø) from *Hmox1*$^{-/-}$ *versus Hmox1*$^{+/+}$ mice produced similar amounts of IL-6 when exposed *in vitro* to bacterial lipopolysaccharide (LPS) or to live bacteria (Fig. 3.2, E and F), while producing slightly but significantly higher amounts of TNF when exposed to LPS (Fig. 3.2 B) but not to live bacteria (Fig. 3.2 C). Higher production of IL-10 also occurred in *Hmox1*$^{-/-}$ *versus Hmox1*$^{+/+}$ Mø exposed to LPS or to live bacteria (Fig. 3.2, H and I). Because HO-1 regulates the expression of a subset of cytokines, including IL-10 (Fig. 3.2 H and I) in response to bacterial agonists such as LPS (Fig. 3.2 H) or live bacteria (Fig. 3.2 I), we cannot exclude that this effect might contribute to the protective mechanism by which HO-1 suppresses the pathogenesis of severe sepsis.

When exposed to LPS and interferon-γ (IFN-γ), peritoneal Mø from naïve *Hmox1*$^{-/-}$ mice produced slightly but significantly higher amounts of nitric oxide (NO) than did *Hmox1*$^{+/+}$ peritoneal Mø (Fig. 3.2 J). Importantly, NOS2/iNOS expression, the major source of NO in LPS/IFN-γ-activated Mø, was similar in *Hmox1*$^{-/-}$ *vs. Hmox1*$^{+/+}$ peritoneal Mø, suggesting that HO-1 modulates NOS2/iNOS activity but not its level of expression (Fig. 3.2 K). Whether reduced NO production contributes to the protective action of HO-1 remains to be established.

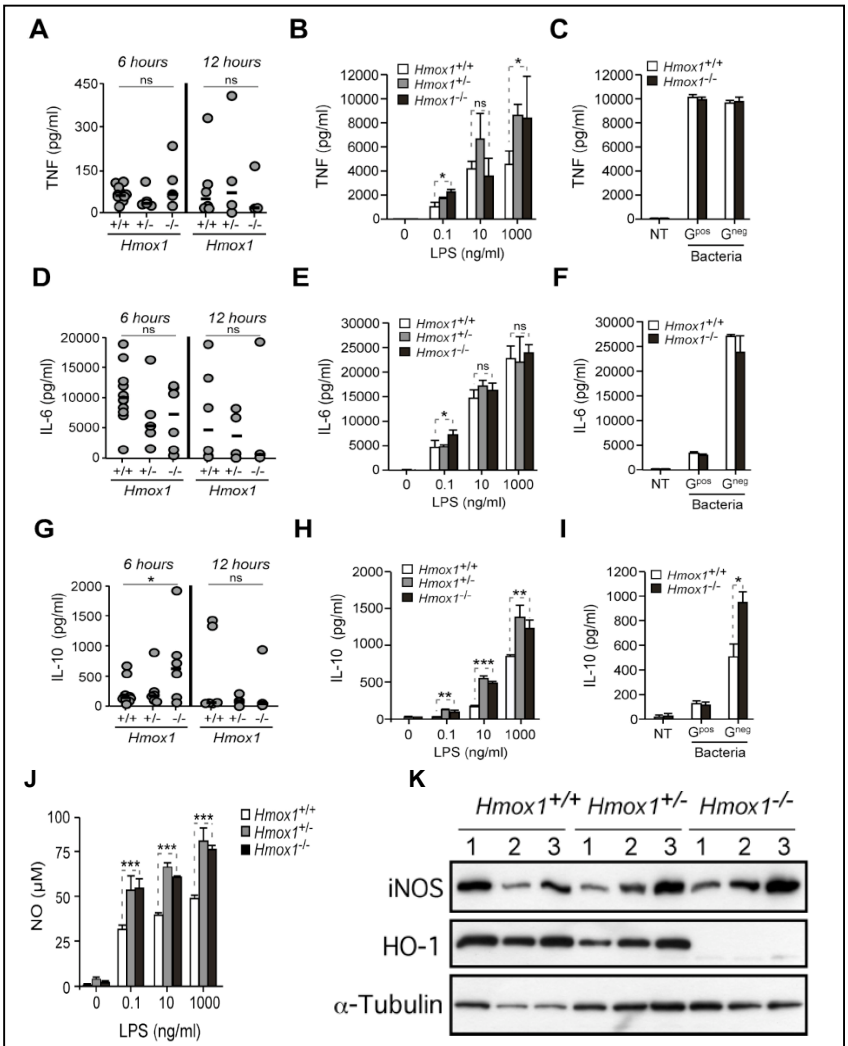

Figure 3.2. HO-1 does not modulate cytokine production in response to CLP. (A) TNF concentrations in peritoneal fluid following low-grade CLP. **(B)** TNF concentrations in supernatants of peritoneal leukocytes stimulated with LPS (6h). **(C)** TNF concentrations in supernatants of bone marrow-derived Mϕ exposed to live Gram positive (G^{pos}; *Enterococcus* subspecies) or Gram negative (G^{ned}; *Escherichia coli*) bacteria (8h). **(D)** IL-6 concentrations in peritoneal fluid following low-grade CLP. **(E)** IL-6 concentrations in supernatants of peritoneal leukocytes stimulated with LPS (24h). **(F)** IL-6 concentrations in supernatants of bone marrow-derived Mϕ exposed to live Gram positive (G^{pos}; *Enterococcus* subspecies) or Gram negative (G^{ned}; *Escherichia coli*) bacteria (8h). **(G)** IL-10 concentrations in peritoneal fluid following low-grade CLP. **(H)** IL-10 concentrations in supernatants of peritoneal leukocytes stimulated with LPS (24h). **(I)** IL-10 concentrations in supernatants of bone marrow-derived Mϕ exposed to live Gram positive (G^{pos}; *Enterococcus* subspecies) or Gram negative (G^{ned}; *Escherichia coli*) bacteria (8h). Cytokine concentrations were quantified by ELISA. Cytokine concentration in peritoneal fluid **(A,D,G)** was measured in *Hmox1*$^{+/+}$ (n=13 at 6h and n=6 at 12h), *Hmox1*$^{+/-}$ (n=6 at 6h and n=4 at 12h) and *Hmox1*$^{-/-}$ (n=6 at 6h and n=3 at 12h) mice. Circles represent individual mice. **(J)** Concentration of nitric oxide (NO) in supernatants of peritoneal leukocytes of naïve *Hmox1*$^{+/+}$ (n=3), *Hmox1*$^{+/-}$ (n=3) and *Hmox1*$^{-/-}$ (n=3) mice and stimulates *in vitro* with bacterial LPS plus IFN-γ (48h). Results are shown as mean±SD from one representative experiment using 3 animals (*p<0.05). **(K)** Inducible nitric oxide synthase (iNOS), HO-1 and α-tubulin were detected by western blot in peritoneal leukocytes from *Hmox1*$^{+/+}$, *Hmox1*$^{+/-}$ or *Hmox1*$^{-/-}$ mice, 12h after low-grade CLP. Numbers indicate individual mice (n=3 *per* genotype). Data in **(B, C, E, F, H,I)** is shown as mean±SD from one representative experiment out of three (*p<0.05).

3.2 HO-1 prevents free heme from eliciting severe sepsis

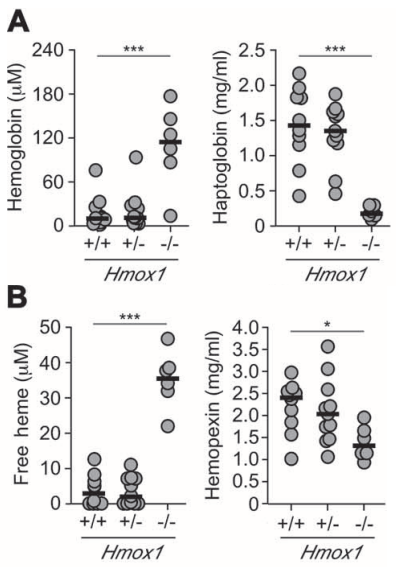

Figure 3.3. Hemoglobin, haptoglobin, heme and hemopexin during sepsis (A) Hemoglobin and haptoglobin plasma concentrations in *Hmox1*$^{+/+}$ (n=10), *Hmox1*$^{+/-}$ (n=11), and *Hmox1*$^{-/-}$ (n=6) BALB/c mice 12 hours after low-grade CLP. **(B)** Free heme and HPX plasma concentrations in *Hmox1*$^{+/+}$ (n=10), *Hmox1*$^{+/-}$ (n=11), and *Hmox1*$^{-/-}$ (n=6) BALB/c mice, 12 hours after low-grade CLP. Circles represent individual mice. Bars represent median values. *P<0.05; **P<0.01; ***P<0.001; ns, not significant.

Free heme, the substrate of HO-1 activity, is cytotoxic to red blood cells and causes hemolysis[13]. This produces cell-free hemoglobin and eventually more free heme[14] (that is, heme not contained within the heme pockets of hemoglobin). This definition of free heme does not preclude the association of heme with other proteins or lipids in a manner that does not control its ability to induce oxidative stress[11]. We asked whether increased mortality of *Hmox1*$^{-/-}$ mice subjected to polymicrobial infection was associated with increased hemolysis, as well as with the accumulation of cell-free hemoglobin and/or free heme in plasma[11]. When subjected to low-grade CLP, *Hmox1*$^{-/-}$ mice, but not *Hmox1*$^{+/+}$ mice, accumulated extracellular hemoglobin (Fig. 3.3 A) and free heme in plasma (Fig. 3.3 B), whereas plasma concentrations of the hemoglobin-binding protein haptoglobin[15] (Fig. 3.3 A) and the heme-binding protein hemopexin (HPX)[16] were decreased (Fig. 3.3 B).

We then asked whether accumulation of free heme in plasma contributes to the pathogenesis of severe sepsis. Heme

administration to wild-type (*Hmox1*$^{+/+}$) mice subjected to low-grade CLP led to severe sepsis (77% mortality) (Fig. 3.4 A), characterized by multiple end stage organ failure, as revealed serologically by increased AST, BUN, and CPK plasma concentrations (Fig. 3.4 B). Organ damage was confirmed histologically (Fig. 3.4 C). Heme administration to naïve wild-type (*Hmox1*$^{+/+}$) mice, although not lethal *per se* (0% mortality), elicited kidney, but not liver or cardiac, damage (Fig. 3.4 B). Heme administration was also not lethal in mice subjected to sham laparotomy (0% mortality). Moreover, "iron-free" protoporphyrin IX failed to cause organ damage or to precipitate severe sepsis when administered to mice subjected to low-grade CLP (0% mortality) (Fig. 3.4 A). These observations demonstrate that free heme can precipitate the onset of severe sepsis in mice subjected to an otherwise benign (nonlethal) polymicrobial infection. They also reveal that the kidney is particularly vulnerable to the damaging effects of free heme.

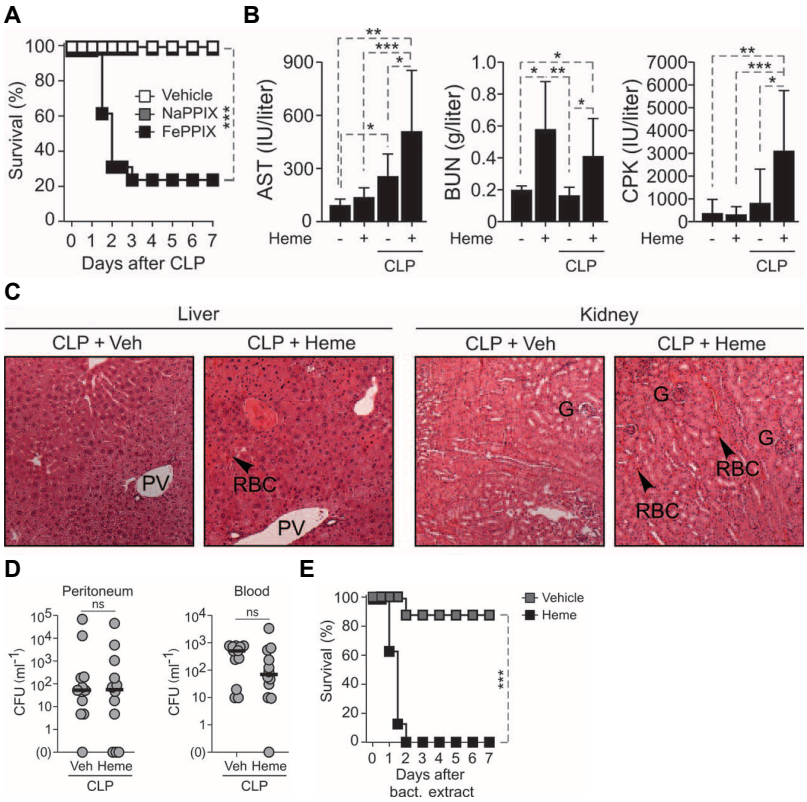

Figure 3.4. Heme precipitates the development of severe sepsis (A) Survival of *Hmox1*$^{+/+}$ BALB/c mice after low-grade CLP. When indicated, mice received vehicle (n = 6), protoporphyrin IX (NaPPIX; n = 8), or heme (FePPIX; n = 13). Protoporphyrins were administered (15 mg/kg i.p.) at 2, 12, and 24 hours after CLP. Dotted line shows statistical comparison of vehicle and FePPIX-treated animals. **(B)** Measurement of serum AST, BUN, and CPK. Mice were treated as in **(A)**, and serum biochemistry was analyzed 24 hours after low-grade CLP. Data are shown as mean ± SD (eight to nine mice per group). IU, international units. **(C)** Representative examples of H&E staining (magnification, x400) of tissue samples taken 24 hours after low-grade CLP from mice that received heme described as in **(A)**. Arrows indicate red blood cells (RBC). PV, portal vein; G, glomerulus. Samples are representative results of three mice in each group. **(F)** Bacterial load in the peritoneum and blood of mice (n = 12 per group) treated as described in **(A)**, 12 to 24 hours after CLP. Veh, vehicle; Heme, FePPIX. **(G)** Survival of BALB/c wild-type (*Hmox1*$^{+/+}$) mice after intraperitoneal administration of a sublethal bolus of heat-killed bacteria (*E. coli*) followed by heme administration as in **(A)** (eight mice per group). Circles represent individual mice. Bars represent median values. *P < 0.05; **P < 0.01; ***P < 0.001; ns, not significant.

The number of CFUs in the peritoneum and blood was similar in mice subjected to low-grade CLP whether or not they received heme thereafter (Fig. 3.4 D). This demonstrated that the ability of free heme to precipitate severe sepsis in mice (Fig. 3.4 A) was not associated with increased pathogen load (Fig. 3.4 D), thus revealing that free heme compromised host tolerance

against polymicrobial infection. This notion was strongly supported by the observation that administration of free heme to wild-type (*Hmox1*$^{+/+}$) mice subjected to a sublethal dose of heat-killed bacteria led to 100% mortality, as compared to 12.5% mortality in control mice receiving vehicle (Fig. 3.4 E).

We then asked whether the deleterious effect of free heme could be attributed to its previously described action on polymorphonuclear (PMN) cells[17]. The numbers of peritoneal-infiltrating $CD45^+CD11b^+GR1^+$ PMN cells in *Hmox1*$^{-/-}$ mice subjected to low-grade CLP were two to threefold higher than those in *Hmox1*$^{+/-}$ and *Hmox1*$^{+/+}$ mice (Figs. 3.5 and 3.6, A and B). This was not the case for peritoneal natural killer (NK), T, or B cells (Fig. 3.6, C to E). Expression of the phagocytic NADPH (reduced form of nicotinamide adenine dinucleotide phosphate) oxidase $gp91^{phox}$ in peritoneal infiltrating leukocytes was also higher in *Hmox1*$^{-/-}$ *versus Hmox1*$^{+/+}$ mice (Fig. 3.5 B). This effect was attributed to the increased numbers of PMN cells in *Hmox1*$^{-/-}$ *versus Hmox1*$^{+/+}$ mice and was associated with enhanced oxidative activity in peritoneal leukocytes from *Hmox1*$^{-/-}$ mice relative to *Hmox1*$^{+/+}$ mice (Fig. 3.5, D). Whereas heme administration to naïve *Hmox1*$^{+/+}$ mice can elicit peritoneal PMN cell infiltration (Fig. 3.5 E)[17], this effect was negligible when heme was administered to mice subjected to low-grade CLP (Fig. 3.5 E). Although these data suggest that heme-driven PMN cell activation does not play a major role in the pathogenesis of severe sepsis, we cannot exclude that other putative effects of free heme on PMN cells, such as degranulation, might act in a detrimental manner to promote the pathogenesis of severe sepsis.

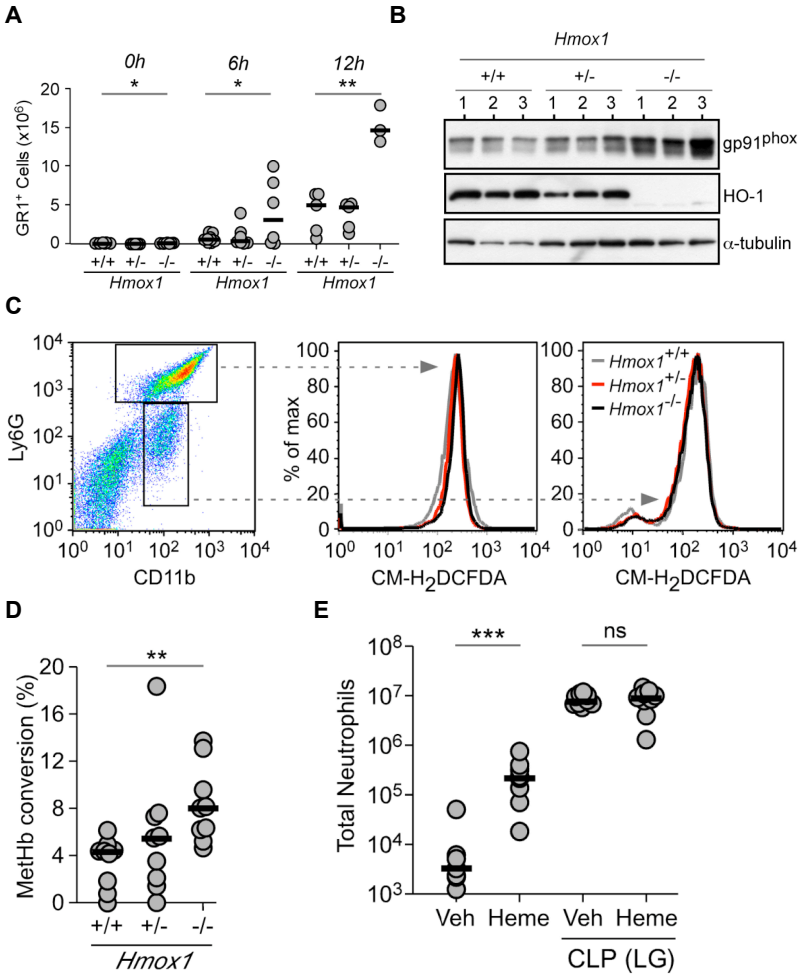

Figure 3.5. HO-1 modulates PMN cell activation in response to CLP. **(A)** Number of peritoneal PMN ($GR1^{high}$) cells in naïve BALB/c mice (0h) *vs.* BALB/c mice subjected to low-grade CLP (6h and 12h). Circles represent individual mice and bars are median values for each genotype. *Hmox1*$^{+/+}$ (n=7 at 0h, n=13 at 6h and n=5 at 12h), *Hmox1*$^{+/-}$ (n=5 at 0h, n=6 at 6h and n=5 at 12h) and *Hmox1*$^{-/-}$ (n=7 at 0h, n=6 at 6h and n=3 at 12h). Data for each time point was compared by regression analysis across genotypes. **(B)** Expression of the NADPH oxidase $gp91^{phox}$ subunit, HO-1 and ⟨-tubulin, determined by western blotting in whole cell extracts from peritoneal leukocytes from *Hmox1*$^{+/+}$(n=3), *Hmox1*$^{+/-}$ (n=3) and *Hmox1*$^{-/-}$ (n=3) mice subjected to low-grade CLP (12h). Numbers indicate individual mice. **(C)** Representative plots and histograms for free radical production in peritoneal infiltrating PMN cells ($CD11b^{+}Ly6G^{high}$) and Mø ($CD11b^{+}Ly6G^{low}$) from *Hmox1*$^{+/+}$ (n=4), *Hmox1*$^{+/-}$ (n=4) or *Hmox1*$^{-/-}$ (n=5), 12h after low-grade CLP. Free radicals were detected using the broad-spectrum probe CM-H_2DCFDA. **(D)** *In vitro* conversion of purified hemoglobin (Fe[II]) into met-hemoglobin (Fe[III]), determined spectrophotometrically after co-incubation of purified hemoglobin (Fe[II]) with peritoneal infiltrating leukocytes (3-5.10^6 cells) isolated from *Hmox1*$^{+/+}$, *Hmox1*$^{+/-}$ or *Hmox1*$^{-/-}$ mice 12h after low-grade CLP. Circles represent data obtained with cells isolated from individual mice and bars are median values for each genotype (n=9 per genotype). A regression model was used to compare data across genotypes. **(E)** Number of peritoneal infiltrating PMN ($GR1^{high}$) cells in BALB/c mice receiving heme (80 nM, i.p.) or vehicle (PBS) and subjected or not to low-grade CLP. Peritoneal infiltrates were collected 16h post-CLP. Notice that while the production of free radicals was similar in PMN cells and Mø from *Hmox1*$^{-/-}$ *vs.* *Hmox1*$^{+/+}$ mice **(C)** the net "oxidative power" of peritoneal infiltrating leukocytes was significantly higher in *Hmox1*$^{-/-}$ *vs.* *Hmox1*$^{+/+}$ mice, as assessed *in vitro* by the oxidation of purified hemoglobin **(D)**. Rather than a consequence of increased free radical production in a per-cell basis, this pro-oxidant effect was due to the relative increase in the proportion of peritoneal infiltrating PMN cells, i.e. ~75% vs. 55%, in *Hmox1*$^{-/-}$ *vs.* *Hmox1*$^{+/+}$ mice, respectively. ANOVA and t-tests were applied to compare different treatment conditions using Bonferroni correction for pairwise comparisons. *P<0.05; **P<0.01; ***P<0.001; ns: non-significant.

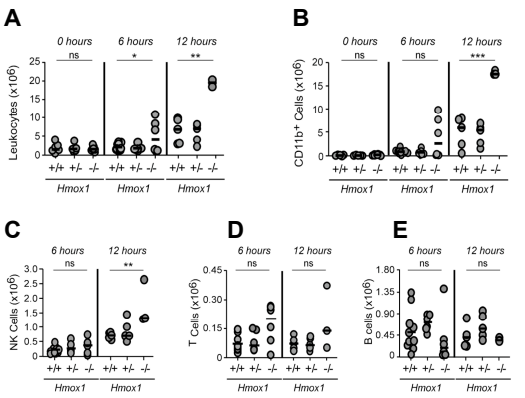

Figure 3.6. Infiltrating leukocytes following CLP. Number of (**A**) peritoneal leukocytes, (**B**) CD11b+ (PMN and Mø), (**C**) NK cells, (**D**) T cells and (**E**) B cells were quantified by flow cytometry, before (0h) and after (6h and 12h) low grade CLP in *Hmox1*$^{+/+}$ (n=7 at 0h, n=13 at 6h and n=5 at 12h), *Hmox1*$^{+/-}$ (n=5 at 0h, n=6 at 6h and n=5 at 12h) and *Hmox1*$^{-/-}$ (n=7 at 0h, n=6 at 6h and n=3 at 12h) mice. Circles represent individual animals. Bars represent median values in each genotype. A regression analysis was performed to describe CD11b^{+}, NK, and B-cell data. T-cell samples did not follow a Normal distribution and was analyzed by Kruskal-Wallis and Mann-Whitney tests. *P<0.05; **P<0.01; ***P<0.001; n: non-significant.

3.3 Free heme is a critical component in the pathogenesis of severe sepsis

When subjected to high-grade CLP (>90% mortality) (Fig. 3.8 A), wild-type (*Hmox1*$^{+/+}$) mice displayed abnormal red blood cell morphology

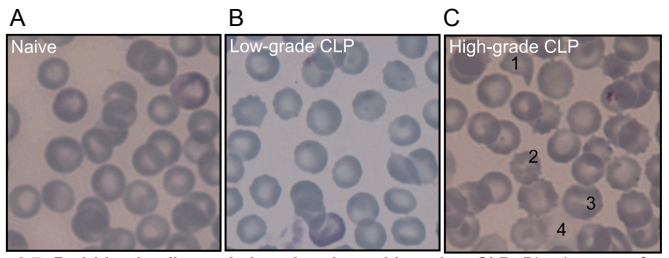

Figure 3.7. Red blood cell morphology in mice subjected to CLP. Blood smears from (**A**) naïve BALB/c mice, (**B**) BALB/c mice 48 h after low-grade CLP or (**C**) BALB/c mice 48 h after high-grade CLP (Giemsa staining, 1000x). Note the appearance of schistocytes (1), acanthocytes (2) and stomatocytes (3) as well as "ghost" cells (4), indicative of disseminated intravascular coagulation and hemolysis.

(poikilocytosis) (Fig. 3.7).

This was associated with the accumulation of cell-free hemoglobin in plasma (Fig. 3.8 B), compared to mice subjected to low-grade CLP (<20% mortality) (Fig. 3.8, A and B). Moreover, there was a decrease in haptoglobin plasma concentrations in *Hmox1*$^{+/+}$ mice subjected to high-grade CLP compared to mice subjected to low-grade CLP (Fig. 3.8 C), confirming that hemolysis occurs in response to high-grade but not low-grade infection. Similarly, the concentration of free heme in plasma

increased (Fig. 3.8 D), whereas HPX plasma concentration decreased (Fig. 3.8 E), in mice subjected to high-grade relative to low-grade CLP.

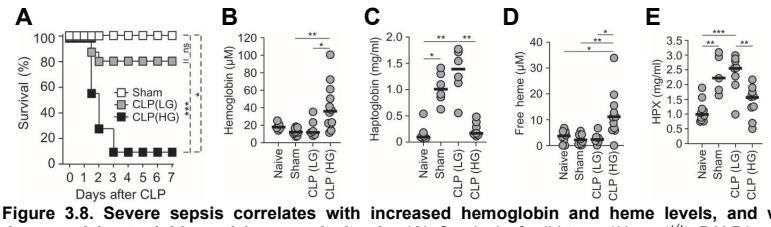

Figure 3.8. Severe sepsis correlates with increased hemoglobin and heme levels, and with decreased haptoglobin and hemopexin levels. (A) Survival of wild-type (*Hmox1*$^{+/+}$) BALB/c mice subjected to "sham" laparotomy (n = 3), low-grade (LG) (n = 15) CLP, or high-grade (HG) (n = 11) CLP. **(B to E)** Hemoglobin **(B)**, haptoglobin **(C)**, free heme **(D)**, and HPX **(E)** plasma concentrations in naïve (n = 6 to 8) mice or 12 hours after sham laparotomy (n = 10), LG CLP (n = 6), or HG CLP (n = 11 to 12). Circles represent individual mice. Bars represent median values. *P < 0.05; **P < 0.01; ***P < 0.001; ns, not significant.

Given that mortality in response to polymicrobial infection is associated with high concentrations of free heme and low concentrations of HPX in plasma, we hypothesized that one might be able to prevent the onset of severe sepsis by restoring HPX plasma concentration, so that HPX is available to neutralize the rising amounts of free heme. Administration of purified HPX to wild-type (*Hmox1*$^{+/+}$) mice subjected to high grade CLP reduced the mortality level to 22%, compared to 86 and 69% in control mice that received phosphate-buffered saline (PBS) (the HPX vehicle) or immunoglobulin G (IgG), respectively (Fig. 3.9 A). The protective effect of HPX was associated with the return of liver, kidney, and cardiac function to homeostatic levels, as assessed by AST, BUN, and CPK plasma concentrations, respectively (Fig. 3.9 B), and as confirmed histologically (Fig. 3.9 C). In contrast, control mice that received a non–heme-binding protein (IgG) after high-grade CLP succumbed to liver, cardiac, and kidney failure, as assessed by AST, BUN, and CPK plasma concentrations, respectively (Fig. 3.9 B).

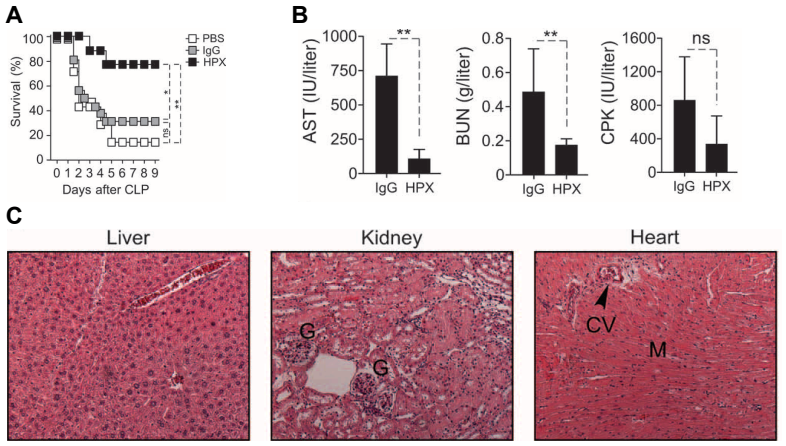

Figure 3.9. Free heme promotes the pathogenesis of severe sepsis. (A) Survival of *Hmox1*$^{+/+}$ BALB/c mice subjected to high-grade CLP. Mice received purified rabbit HPX (50mg/kg i.p.; n = 9), purified rabbit polyclonal IgG (50 mg/kg i.p.; n = 16), or vehicle (i.p., PBS; n = 7) at 2, 12, 24, and 36 hours after CLP. **(B)** Serological markers of organ injury in mice treated as in **(A)**. Measurements were made in serum from IgG-treated mice at the time of death (36 hours) and in HPX-treated mice at the end of the experiment (day 11). Results shown are the mean ± SD (n=5 to 6 mice per group). **(C)** Representative H&E staining (magnification, x400) in mice treated as in **(A)**. Samples are representative of three mice. CV, coronary vessel; G, glomerulus. M, myocardium. Samples are representative results of three mice in each group. HPX-treated mice in **(B)** and **(C)** were analyzed 11 days after CLP. Control IgG-treated mice in **(B)** and **(C)** were analyzed 24 to 36 hours after CLP (time of death). *P < 0.05; **P < 0.01; ***P < 0.001; ns, not significant.

3.4 Free heme elicits programmed cell death

We have previously shown that free heme can promote programmed cell death in response to TNF[8]. We asked whether this effect is extended to other agonists involved in the pathogenesis of severe sepsis. Because hepatic failure is a central component of severe sepsis, we tested whether free heme induces oxidative stress and TNF-mediated programmed cell death in primary mouse hepatocytes *in vitro*. When exposed to free heme, hepatocytes did not produce significant amounts of intracellular free radicals, as assessed by flow cytometry with a broad free radical probe (Fig. 3.10 A). However, when exposed to free heme and TNF (Fig. 3.10 A)[8] or free heme plus Fas cross-linking (which activates the Fas signaling transduction pathway), hepatocytes produced large amounts of intracellular free radicals (Fig. 3.10 A). This effect was not observed when hepatocytes

were exposed to free heme and oxidizing agents such as hydrogen peroxide (H_2O_2) or peroxynitrite ($ONOO^-$), which are sufficient to cause free radical accumulation in hepatocytes (Fig. 3.10 A). Primary hepatocytes did not undergo programmed cell death when exposed to TNF, Fas cross-linking, H_2O_2, or $ONOO^-$ (Fig. 3.10 B)[8], whereas programmed cell death was readily induced in cells treated with free heme first and then TNF, Fas cross-linking, H_2O_2, or $ONOO^-$ (Fig. 3.10 B). These observations suggest that the redox activity of the heme Fe atom underlies its cytotoxicity, presumably by catalyzing the production of free radicals through Fenton chemistry[12]. Consistent with this hypothesis, the antioxidant N-acetyl-cysteine (NAC) protected hepatocytes from programmed cell death in the presence of free heme and TNF, Fas ligand, H_2O_2, or $ONOO^-$ (Fig. 3.10 B). These observations reveal that the pathological effects of free heme, namely, its ability to synergize with other cytotoxic agonists to cause tissue damage, can be extended to a variety of agonists other than TNF[11], including some previously implicated in the pathogenesis of severe sepsis.

Transduction of hepatocytes with a recombinant adenovirus (Rec.Ad.) that expresses HO-1 (Fig. 3.10 D) was protective against programmed cell death in the presence of free heme and TNF, Fas cross-linking, H_2O_2, or $ONOO^-$, when compared with control hepatocytes transduced with a Rec.Ad. that expresses LacZ (Fig. 3.10 C). We have previously shown that the cytoprotective effect of HO-1 is associated with inhibition of free radical production[8], suggesting that HO-1 acts as an antioxidant to suppress the cytotoxic effects of free heme[8].

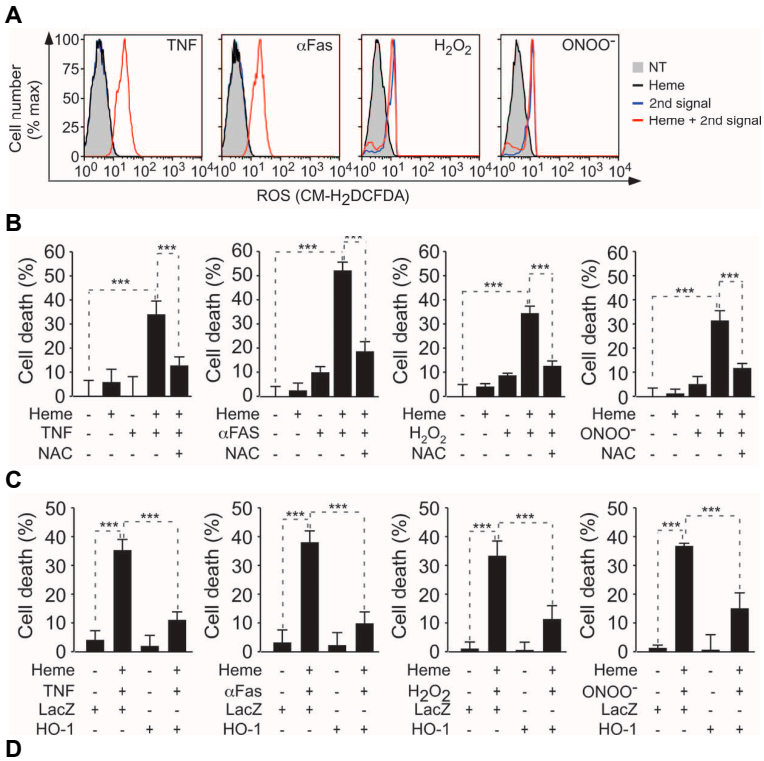

Figure 3.10. The oxidative effect of free heme sensitizes hepatocytes to programmed cell death. (A) Primary BALB/c hepatocytes were either left untreated (NT) or exposed to heme (5 μM, 1 hour) plus mouse recombinant TNF (5 ng/ml, for 16 hours), antibody against Fas (0.5 mg/ml, for 4 hours), H_2O_2 (125 mM, for 8 hours), or the $ONOO^-$ donor SIN-1 (100 mM, for 24 hours). Production of free radicals was determined by flow cytometry with CM-H_2DCFDA. 2nd signal refers to TNF, antibody against Fas, H_2O_2, or $ONOO^-$, as specified for each panel. **(B)** Percentage of cell death in primary hepatocytes treated as in **(A)**. When indicated (+), hepatocytes were pretreated with the antioxidant NAC (10 mM, for 4 hours). Cell viability was determined by crystal violet staining. **(C)** Percentage of cell death in primary hepatocytes treated as in **(A)**. When indicated (+), hepatocytes were transduced with a LacZ- or *Hmox1*-encoding Rec.Ad. Cell viability was determined as in **(B)**. Data are representative of three independent experiments with hepatocytes isolated from different mice. Bars indicate mean ± SD of n = 5 to 6 independent samples per group. *P < 0.05; **P < 0.01; ***P < 0.001.

3.5 Heme triggers HMGB1 release *in vitro* and *in vivo*

We reasoned that the cytotoxic effect of free heme might precipitate severe sepsis by eliciting tissue damage *per se*, as well as by promoting the release of high mobility group box 1 (HMGB1), an endogenous proinflammatory ligand[18] involved in the pathogenesis of severe sepsis[19] and previously linked to HO-1[20]. In untreated primary hepatocytes, HMGB1 expression was

mainly restricted to the nucleus (Fig. 3.11 A). However, when hepatocytes were exposed *in vitro* to free heme plus TNF, HMGB1 was translocated from the nucleus to the cytoplasm (Fig. 3.11 A) and released extracellularly (Fig. 3.11 B). This was not the case when hepatocytes were exposed to either free heme or TNF alone (Fig. 3.11, A and B). Extracellular HMGB1 release was suppressed by the antioxidant NAC (Fig. 3.11 C), as well as by HO-1 overexpression (Fig. 3.11 D). These observations reveal that the oxidative effect of free heme promotes HMGB1 release from hepatocytes, an effect suppressed by HO-1.

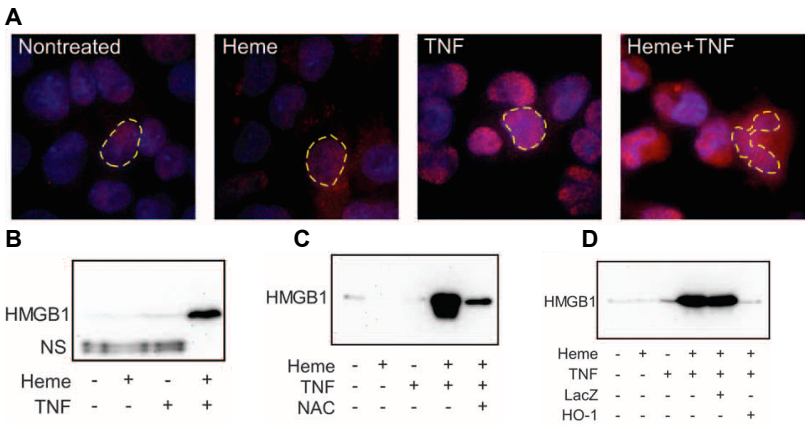

Figure 3.11. Free heme triggers the release of HMGB1 from hepatocytes *in vitro*. (A) HMGB1 (red) and DNA (blue) in mouse Hepa1-6 hepatocytes exposed to vehicle (Non treated), free heme (40 μM, for 1 hour), TNF (50 ng/ml, for 3 hours), or heme (40 μM, for 1 hour) plus TNF (50 ng/ml, for 3 hours). Magnification, x400. Images are representative of three independent experiments. One nucleus per field is outlined (dotted line). **(B)** HMGB1 was measured by Western immunoblotting of proteins in the supernatants of primary mouse (BALB/c) hepatocytes that were exposed to heme (5 μM, for 1 hour) and TNF (5 ng/ml, for 16 hours) in culture. A representative result from two independent experiments is shown. NS, nonspecific band. **(C)** HMGB1 was measured by Western immunoblotting of proteins in the supernatants of mouse Hepa1-6 hepatocytes exposed to heme and TNF as described in **(A)**. When indicated, cells were pretreated with the antioxidant NAC (10 mM; for 4 hours). A representative result from two independent experiments is shown. **(D)** HMGB1 was measured by Western immunoblotting of proteins in the supernatants of mouse Hepa1-6 hepatocytes treated with heme and TNF as in **(A)** and either transduced or not transduced with LacZ or *Hmox1* Rec.Ad. Blots are representative of two independent experiments.

Next, we asked whether HO-1 would prevent HMGB1 release from damaged tissue *in vivo*[18], as suggested in previous studies[20]. In *Hmox1*$^{-/-}$ mice subjected to low-grade CLP there was translocation of HMGB1 into the cytoplasm, as assessed in the liver and kidney (Fig. 3.12 C), whereas translocation was less

pronounced in wild-type (*Hmox1*$^{+/+}$) mice (Fig. 3.12 C). This effect was associated with the systemic release of HMGB1 into the peritoneum and plasma of *Hmox1*$^{-/-}$ relative to *Hmox1*$^{+/+}$ mice (Fig. 3.12, A and B). The relative amount of peritoneal or plasma IgG was unchanged in *Hmox1*$^{-/-}$ *versus* *Hmox1*$^{+/+}$ mice (Fig. 3.12, A and B).

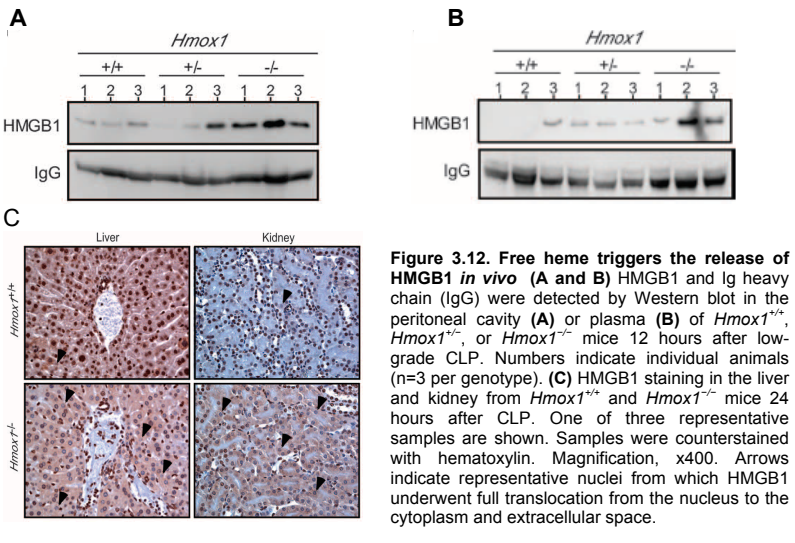

Figure 3.12. Free heme triggers the release of HMGB1 *in vivo* (A and B) HMGB1 and Ig heavy chain (IgG) were detected by Western blot in the peritoneal cavity **(A)** or plasma **(B)** of *Hmox1*$^{+/+}$, *Hmox1*$^{+/-}$, or *Hmox1*$^{-/-}$ mice 12 hours after low-grade CLP. Numbers indicate individual animals (n=3 per genotype). **(C)** HMGB1 staining in the liver and kidney from *Hmox1*$^{+/+}$ and *Hmox1*$^{-/-}$ mice 24 hours after CLP. One of three representative samples are shown. Samples were counterstained with hematoxylin. Magnification, x400. Arrows indicate representative nuclei from which HMGB1 underwent full translocation from the nucleus to the cytoplasm and extracellular space.

3.6 HPX neutralizes the cytotoxic effect of free heme

We next sought to determine whether HPX, which binds tightly to heme (Kd <1 pM) in a manner that dampens its pro-oxidant activity[21], can also prevent heme-induced tissue damage (Fig. 3.9, A to C)[16]. The ability of free heme to sensitize hepatocytes *in vitro* such that they produced high amounts of free radicals in response to TNF was inhibited when heme was bound to HPX (Fig. 3.13 A). Moreover, the ability of free heme to sensitize hepatocytes to undergo programmed cell death in response to TNF was also inhibited once heme was bound to HPX (Fig. 3.13 B). Similar results were obtained with primary human hepatocytes in that HPX prevented heme sensitization to

programmed cell death in response to TNF (Fig. 3.13 C). Accordingly, HPX-bound heme also failed to promote HMGB1 release from primary mouse hepatocytes *in vitro* (Fig. 3.13 D). Similarly, HPX-bound heme also failed to promote HMGB1 release from primary human hepatocytes in response to TNF (Fig. 3.13 E). The increased molecular weight of the cell-free HMGB1 released from primary human hepatocytes is most likely attributed to posttranslational HMGB1 modifications, such as phosphorylation. Together, these observations suggest that HPX suppresses the cytotoxic effects of free heme in both mouse and human hepatocytes.

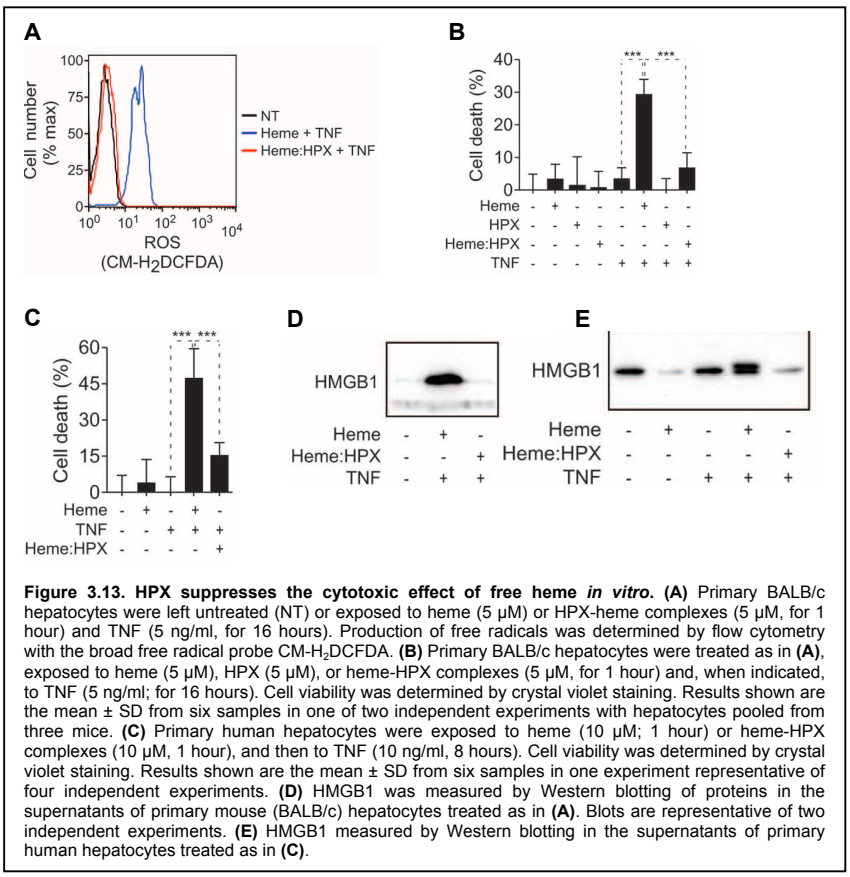

Figure 3.13. HPX suppresses the cytotoxic effect of free heme *in vitro*. (A) Primary BALB/c hepatocytes were left untreated (NT) or exposed to heme (5 μM) or HPX-heme complexes (5 μM, for 1 hour) and TNF (5 ng/ml, for 16 hours). Production of free radicals was determined by flow cytometry with the broad free radical probe CM-H_2DCFDA. **(B)** Primary BALB/c hepatocytes were treated as in **(A)**, exposed to heme (5 μM), HPX (5 μM), or heme-HPX complexes (5 μM, for 1 hour) and, when indicated, to TNF (5 ng/ml; for 16 hours). Cell viability was determined by crystal violet staining. Results shown are the mean ± SD from six samples in one of two independent experiments with hepatocytes pooled from three mice. **(C)** Primary human hepatocytes were exposed to heme (10 μM; 1 hour) or heme-HPX complexes (10 μM, 1 hour), and then to TNF (10 ng/ml, 8 hours). Cell viability was determined by crystal violet staining. Results shown are the mean ± SD from six samples in one experiment representative of four independent experiments. **(D)** HMGB1 was measured by Western blotting of proteins in the supernatants of primary mouse (BALB/c) hepatocytes treated as in **(A)**. Blots are representative of two independent experiments. **(E)** HMGB1 measured by Western blotting in the supernatants of primary human hepatocytes treated as in **(C)**.

3.7 Low HPX serum concentration is associated with organ dysfunction and fatal outcome in septic shock patients

Given that HPX plasma concentration is reduced in mice that succumb to severe sepsis (Fig. 3.8 E), we asked whether this would also be the case in patients that succumb to septic shock[22]. In a cohort of 52 patients (table 3.1), HPX serum concentration within 48 hours of presentation with septic shock was positively associated with patient survival time (Fig. 3.14 A). That is, patients with lower HPX serum concentrations succumbed at earlier time points compared to patients with higher HPX serum concentrations (Fig. 3.14 A). This observation allowed us to extrapolate the probability of survival/mortality as a function of HPX serum concentration (Fig. 3.14 B), in keeping with the observation that HPX serum concentration within 48 hours of septic shock diagnosis was higher in patients that survived septic shock compared to nonsurvivors (Fig. 3.14 C). Finally, there was an inverse correlation between HPX serum concentration and severity of organ dysfunction, as defined by the sequential organ failure assessment (SOFA) score[23] (table 3.2). Overall, these observations support the notion that HPX serum concentration defines the extent of tissue damage (organ dysfunction) and hence the outcome of septic shock in humans.

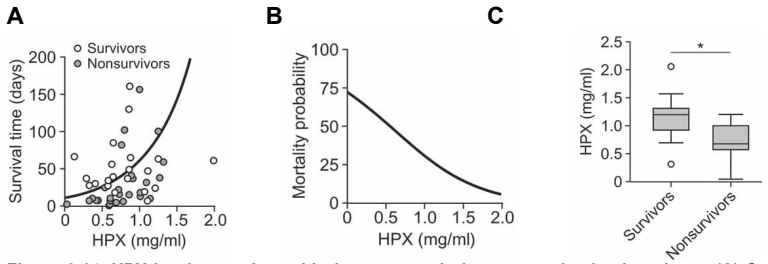

Figure 3.14. HPX levels correlate with the outcome in human septic shock patients. (A) Survival time (see Materials and Methods) of patients developing septic shock *versus* prediction of best-fitted model. The solid line refers to the expected median survival time as a function of HPX serum concentration at the time of septic shock diagnosis, predicted by the best model for survival time (based on lognormal distribution). Gray circles represent individuals that succumbed during hospitalization (nonsurvivors). White circles represent individuals that survived septic shock and left the hospital at the times indicated. $P < 0.05$ for the respective effect. **(B)** Expected mortality probability at day 28, plotted as a function of HPX serum concentration at the time of septic shock diagnosis, predicted by the best model for survival time (based on lognormal distribution). **(C)** Box plot representation of HPX serum concentration at the time of septic shock diagnosis in a cohort of 52 patients, including survivors (n = 34) and nonsurvivors (n=18).Data represent mean [interquartile range (IQR), 25 to 75%]. *P< 0.05.

	N=52	%
Age (years)	**69 (51-82)**	**-**
Gender (female/male)	**24/28**	**46/54**
Surgical admission	**37**	**71**
SAPS II score (points)	**52.5 (45-60)**	**-**
SOFA score on day 1 (points)	**9 (6-11)**	**17**
Positive microbiological cultures	**34**	**65**
28-day mortality	**18**	**35**
Hospital morality	**28**	**54**

Table 3.1: Characteristics of septic shock patients. Severity of organ dysfunction was defined using the Sequential Organ Failure Assessment (SOFA) score. Ranges are indicated between brackets.

Days	Survivors	Nonsurvivors
1	**-0.33 (p=0.26)**	**-0.41 (p=0.08)**
2	**-0.40 (p=0.20)**	**-0.13 (p=0.61)**
3	**-0.10 (p=0.75)**	**-0.58 (p=0.048)**
5	**-0.63 (p=0.051)**	**-0.93 (p=0.002)**
7	**-0.63 (p=0.051)**	**-0.58 (p=0.08)**

Table 3.2: Correlations between HPX serum concentration and SOFA. The correlations are based on Spearman coefficient calculated between HPX and SOFA at the days indicated. P-values are given in parentheses.

4. DISCUSSION

An infected host has two distinct evolutionarily conserved defense strategies that limit disease severity. The best characterized of these two strategies relies on the capacity of the host immune system to contain and reduce its pathogen load. This defense strategy is referred to as host resistance to infection[6]. The other defense strategy acts irrespective of pathogen load and relies instead on limiting tissue damage caused directly or indirectly by the pathogen and/or by the immune response elicited by that pathogen. This defense strategy, referred to as host tolerance to infection[6], has long been recognized in plants[5], but only more recently in flies[6] and mice[24].

Blood-borne pathogens can cause hemolysis[25] and hence lead to accumulation of extracellular hemoglobin in circulation. Oxidation of cell-free hemoglobin can be highly deleterious to the host in at least three ways. First, it can exacerbate inflammation[26]. Second, it can release heme (Figs. 3.3, A and B, and 3.8 D)[14], a putative source of iron that can promote microbial growth[27]. Third, as shown herein, free heme can be highly cytotoxic in the presence of proinflammatory agonists (Fig. 3.10 B)[11], causing irreversible tissue damage and organ failure (Fig. 3.4, B and C), the hallmarks of severe sepsis[2].

That heme-driven tissue damage can contribute to the pathogenesis of severe sepsis is suggested by four independent lines of evidence. First, exacerbated mortality of *Hmox1*$^{-/-}$ mice subjected to microbial infection (Fig. 3.1B) correlated with the accumulation of free heme in the plasma (Fig. 3.3 B). Second, administration of free heme to wild-type (*Hmox1*$^{+/+}$) mice

subjected to low-grade (nonlethal) microbial infection was sufficient to elicit a lethal form of severe sepsis (Fig. 3.4 E). Third, free heme accumulated in the plasma of wild-type (*Hmox1*$^{+/+}$) mice subjected to high-grade (lethal), but not low-grade, microbial infection (Fig. 3.8 D). Fourth, sequestration of free heme by HPX suppressed the development of severe sepsis in wild-type (*Hmox1*$^{+/+}$) mice subjected to high-grade microbial infection (Fig. 3.9).

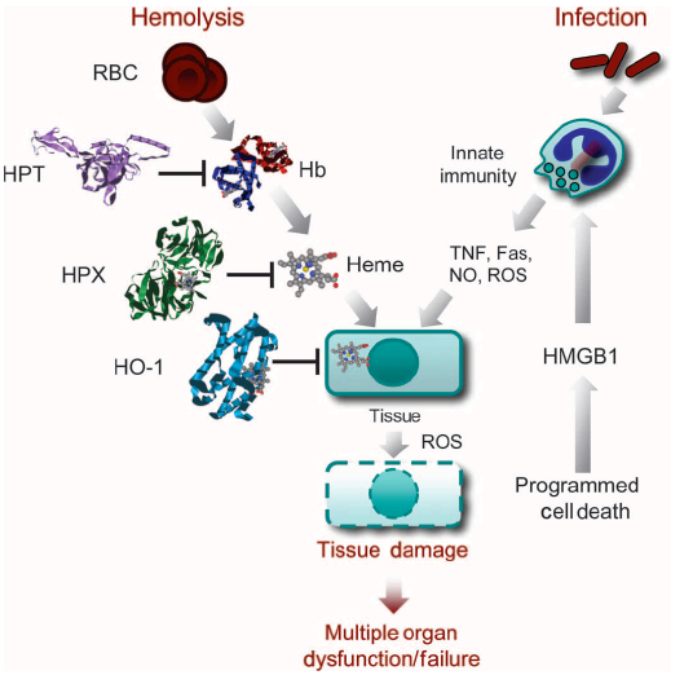

Figure 3.15. Role of free heme in the pathogenesis of severe sepsis. The pathogenesis of severe sepsis is associated with hemolysis, which involves the release of hemoglobin (Hb) from red blood cells (RBC). Oxidation of cell-free Hb leads to the release of its prosthetic heme groups. This pathological event can be prevented by the acute-phase protein haptoglobin (HPT), whereas free heme can be captured by the acute-phase protein HPX. Once the concentration of HPT and/or HPX in serum decreases below a certain threshold level, free heme accumulates in plasma and can sensitize cells in parenchymal tissues to undergo programmed cell death in response to a variety of proinflammatory agonists. This leads to the release of endogenous proinflammatory ligands from damaged tissues, for example, HMGB1. Expression of the stress-responsive enzyme HO-1 in parenchymal cells affords cytoprotection against free heme, thus suppressing tissue damage and ultimately multiple-organ dysfunction/failure.

There are a number of cytoprotective mechanisms against the deleterious effects of free heme[8,11,16,28]. These include the plasma protein HPX, which binds free heme and neutralizes

its oxidative (Fig. 3.13 A) and hence cytotoxic (Fig. 3.13, B and C) effects[16] (Fig. 3.15). As shown, the lethal outcome of severe sepsis in mice (Fig. 3.8 E) and septic shock in humans is associated with decreased concentration of circulating HPX (Fig. 3.14 A). Therefore, we reasoned that administration of exogenous HPX might be used therapeutically to increase tolerance to infection and hence prevent the development of severe sepsis in mice, which we found to be the case (Fig. 3.9, A to C). It is likely that a similar approach will translate into the treatment of severe sepsis in humans, given the observation that low concentrations of circulating HPX are associated with septic shock lethality in humans as well (Fig. 3.14, A to C). One cannot exclude at this point that in addition to preventing the cytotoxic effects of free heme, HPX[29] might exert anti-inflammatory effects that contribute to its protective effect.

The salutary effect of HPX most probably requires the expression of HO-1 to catabolize HPX-bound heme (Fig. 3.15). This would explain why, despite the presence of HPX, HO-1–deficient (*Hmox1*$^{-/-}$) mice are highly susceptible to immune-mediated inflammatory diseases[30], including endotoxic shock[31] and polymicrobial infection[10] (Fig. 3.1 B), in which lack of adequate HPX-bound heme catabolism leads to irreversible tissue damage, end-stage organ dysfunction, and eventually to death[32,33].

The protective effect of HO-1 against polymicrobial infection has previously been attributed to the antimicrobial activity of carbon monoxide[10], one of the end products of heme catabolism carried out by HO-1[9]. This would suggest that HO-1 affords some level of resistance against polymicrobial infection. Two independent lines of evidence support the notion that HO-1

also affords tolerance against polymicrobial infection: first, mice that can induce the expression of HO-1 (*Hmox1*$^{+/+}$) in response to polymicrobial infection (Fig. 3.1 A) survive (Fig. 3.1 B) when subjected to the same pathogen load (Fig. 3.1 E) that kills *Hmox1*$^{-/-}$ mice (Fig. 3.1 B). Second, *Hmox1*$^{-/-}$ but not *Hmox1*$^{+/+}$ mice succumb to death even when challenged with heat-killed bacteria (Fig. 3.1 F)[31,33]. These observations provide mechanistic evidence for the proposed protective effect of HO-1 expression in the outcome of severe sepsis and septic shock[34].

The mechanism by which HO-1 affords tolerance against microbial infections relies to a large extent on its ability to suppress the deleterious effect of free heme (Fig. 3.10, A and B) produced during the course of infection (Figs. 3.8 D and 3.15). This notion is strongly supported by the observation that HO-1 protected mouse cells from the cytotoxic effects of free heme (Fig. 3.10 C), and should prevent irreversible tissue damage, multiple organ dysfunction, and host death (Fig. 3.1, C and D). Because this protective effect of HO-1 does not interfere with pathogen load (Fig. 3.1 E), we conclude that HO-1 promotes, whereas extracellular heme compromises, host tolerance to polymicrobial infection.

The findings from the studies reported here potentially can be translated into several clinical applications for monitoring and treatment of sepsis. In the clinical setting, monitoring the patients' levels of circulating heme and/or HPX might be used to predict the likelihood of a fatal outcome in each case of severe sepsis (Fig. 3.16 B). In addition, the development of strategies that mitigate the deleterious effects of free heme might also be used therapeutically to prevent the all-too-common lethal outcome of severe sepsis.

5. METHODS

Mice and genotyping

BALB/c, BALB/c.SCID, BALB/c.*Hmox1*$^{+/-}$, and BALB/c.SCID.*Hmox1*$^{+/-}$ mice were maintained under specific pathogen-free conditions according to the Animal Care Committee of the Instituto Gulbenkian de Ciência. All animal protocols were approved by the "Direcção Geral de Veterinária" of the Portuguese government. BALB/c.*Hmox1*$^{+/-}$ mice were generated originally by S. F. Yet (Pulmonary and Critical Care Division, Brigham and Women's Hospital, Boston, MA) by disruption of exon 3 in the Hmox1 locus[35]. Mice were backcrossed 10 times into the BALB/c background. Heterozygous (*Hmox1*$^{+/-}$) breeding pairs yield ~8% viable and otherwise healthy *Hmox1*$^{-/-}$ mice[35]. Littermate *Hmox1*$^{-/+}$ and *Hmox1*$^{+/+}$ mice were used as controls. Mice were genotyped by PCR. Briefly, a 400–base-pair (bp) PCR product spanning the 5′ flanking region of the neomycin complementary DNA (cDNA) in the *Hmox1* locus was amplified from genomic DNA with the following primers: 5′-TCTTGACGAGTTCTTCTGAG-3′ and 5′-ACGAAGTGACGCCATCTGT-3′ [35]. For the endogenous *Hmox1* locus, 5′-GGTGACAGAAGAGGCTAAG-3′ and 5′-CTGTAACTCCACCTCCAAC-3′ primers were used to amplify a 456-bp product. PCRs were repeated at least two times before experiments were performed and were carried out after experiments to confirm genotypes.

Cell culture

Primary mouse peritoneal leukocytes were obtained by peritoneal lavage with ice-cold apyrogen PBS (Sigma). Briefly,

leukocytes were washed in PBS and resuspended in RPMI 1640 Glutamax I (Gibco) supplemented with 5% fetal bovine serum, penicillin (50 U/ml), and streptomycin (50 mg/ml) (Life Technologies). For cytokine measurements, cells ($2.5x10^4$) were plated in flat-bottom 96-well microtiter plates (Techno Plastic Products AG) (100 µl, 2 hours, 37°C); nonadherent cells were removed, and adherent cells, that is, Mø, were activated with bacterial LPS (Sigma, Escherichia coli serotype 0127:B8) for 6 or 24 hours. Bone marrow cells were incubated for 6 days in RPMI 1640 Glutamax I (Gibco), 10% fetal calf serum, 30% L929 supernatant [as macrophage colony-stimulating factor (M-CSF) source]. The bone marrow-derived macrophages (BMDMs) were seeded (16 hours) in six-well plates ($3x10^5$ cells per well) in RPMI, 3.3% FCS, and 5% L929 supernatant. BMDMs were incubated with live Gram-positive (*Enterococcus* subsp. isolated from mouse intestine) or Gram-negative (*E. coli* DH5a) bacteria (8 hours), after which cell culture supernatant was collected and centrifuged (5 min, 1200 rpm, 4°C) to remove cells and bacteria (5 min, 10.000 rpm, 4°C). Cell-free supernatants were stored at −80°C until use. Hepa1-6 cells (C57BL/6 mouse hepatoma; American Type Culture Collection) were seeded in DMEM (Invitrogen), 10% FCS, penicillin, and streptomycin (20 U/ml, Invitrogen). All cells were incubated at 37°C, 95% humidity, and 5% CO2.

Protoporphyrins

Heme (iron protoporphyrin; FePPIX; Frontier Scientific) and protoporphyrin IX (protoporphyrin IX disodium salt; NaPPIX; Frontier Scientific) were dissolved in 0.2 M HCl, and pH was adjusted to 7.4 with sterile 0.2 M NaOH.

Primary hepatocytes

Primary mouse hepatocytes were isolated as described[36]. Briefly, livers from naïve BALB/c mice were perfused through the portal vein (5 ml/min, 10 min, 37°C) with liver perfusion medium (Invitrogen), and the tissue was disrupted. Cells were filtered (100 μm), washed (William's E medium; 4% FCS) (Invitrogen), pelleted (100g, 30s, 20°C), and resuspended (William's E medium, 4% FCS). Hepatocytes were isolated in a Percoll gradient (1.06/1.08/1.12 g/ml; 750g, 20 min, 20°C) (GE Healthcare), resuspended (William's E medium; 4% FCS), centrifuged (2x200g, 10 min, 4°C), resuspended (William's E medium; 4% FCS), and seeded onto gelatin (0.2%)–coated plates. The medium was replaced after 4 hours, and experiments were performed 24 to 48 hours thereafter. Primary human hepatocytes were cultured in hepatocytes culture medium as detailed by the supplier (Lonza).

Heme sensitization assays

Hepatocytes were seeded and exposed to heme (5 mM, 1 hour) in Hanks' Balanced Salt Solution (Invitrogen) without serum to avoid potential heme scavenging by serum proteins, as described[8]. Subsequently, hepatocytes were washed (PBS) and challenged in Dulbecco's modified Eagle's medium, 10% FCS (Hepa1-6), or 4% FCS (primary hepatocytes), with human recombinant TNF (5 to 40 ng/ml, 3 to 16 hours; R&D Systems), Fas ligand (Jo2 antibody against CD95, 0.5 mg/ml, 4 hours; BD Biosciences), H_2O_2 (125 mM, 8 hours; Sigma), or 3-morpholinosydnonimine (SIN-1; 100 mM, 24 hours; Sigma). Cell viability was assessed by crystal violet assay, as described[37].

Heme (FePPIX; Frontier Scientific) was dissolved in sterile 0.2 M NaOH at alkaline pH and adjusted to pH 7.4 with sterile 0.2 M HCl. Iron-free protoporphyrin (NaPPIX, Frontier Scientific) was dissolved in sterile 0.2 M HCl at acidic pH, and pH was adjusted to 7.4 with sterile 0.2 M NaOH. Aliquots were stored at −80°C until use.

Cytokines and NO measurements

TNF, IL-6 and IL-10 were quantified by enzyme-linked immunosorbent assay (ELISA) according to the manufacturer's instructions (Becton Dickinson). NO was measured with a Griess colorimetric assay[38].

CLP

CLP was performed as described elsewhere[39,40]. Briefly, mice were anesthetized [ketamine (120 mg/kg)/xylazine (16 mg/kg) (i.p.)]. Under sterile conditions, a 1-cm incision was made parallel to the midline, and the cecum was exteriorized and ligated (sterile 3-0 Mersilk sutures; Ethicon) immediately distal to the ileocecal valve (reducing the lumen by 50 to 60% for low-grade CLP and 80 to 90% for high-grade CLP). The cecum was punctured once with a 23-gauge needle (low-grade CLP) or twice with a 21-gauge needle (high-grade CLP) and its content was extruded by applying pressure and reinserted into the abdominal cavity. The peritoneal wall was sutured with sterile 3-0 Dafilon sutures (Braun) and the skin was closed with a surgical staple (Autoclip 9 mm; Becton Dickinson). A single dose of saline was injected subcutaneously (1 ml per animal) for fluid resuscitation. After the surgical procedure, animals were maintained at 37°C (30 min) and received antibiotics intraperitoneally

(imipenemcilastatin, Tienam, MSD; 0.5 mg per animal) 2 hours after the surgical procedure and every 12 hours during 72 hours.

Colony-forming units

Peritoneal fluid was obtained by peritoneal lavage with 5 ml of sterile PBS (Sigma). Organs were weighed and homogenized under sterile conditions in 0.5 ml of PBS with Dounce tissue grinders (Sigma). Serial dilutions of blood, peritoneal lavage, and homogenized organs were immediately plated on Trypticase Soy Agar II plates supplemented with 5% Sheep Blood (Becton Dickinson). CFUs were counted after 24 hours of incubation at 37°C.

cDNA synthesis and LightCycler analysis

Total RNA was extracted with RNeasy Protect Mini Kit (Qiagen) and reverse-transcribed (SuperScriptII RNase H^- reverse transcriptase; Invitrogen) with random hexamer primers (Invitrogen) as follows: 70°C for 10min, 37°C for 50 min, and 95°C for 5min (RoboCycler Stratagene). HO-1 primers are 5′-TCTCAGGGGGTCAGGTC-3′ (forward) and 5′-GGAGCGGTGTCTGGGATG-3′ (reverse). The reaction was carried out with 1 μl of cDNA and 3 pmol of each primer, 2 mM MgCl2, and 1X FastStartDNASYBR Green I mix (Roche). The thermal cycler program was composed of 1 cycle at 95°C for 10min, 45 cycles at 95°C for 15s, 58°C for 5s, and 72°C for 16s, with transition rates of 20°C/s. PCR products were quantified by LightCycler Real-Time quantitative PCR software (Roche). Cycle numbers in the log-linear phase were plotted against the logarithm of template DNA. External standardization was

performed with full-length HO-1 cDNA. Hypoxanthine-guanine phosphoribosyl-transferase (HPRT) was used to normalize cDNA levels[41].

Flow cytometry

Leukocytes were washed and blocked in calcium- and magnesium-free PBS containing 2% FCS (v/v). After incubation (30min, 4°C) with fluorochrome-conjugated monoclonal antibodies directed against CD11b (clone M1/70), IAd (clone AMS-32.1), GR1 (clone RB6-8C5), Ly6G (clone 1A8), CD49b (clone DX5), α/β TCR (clone H57-597), or CD19 (clone 1D3) (BD Biosciences, Pharmingen), cells were washed twice with PBS and 2% FCS (v/v) and acquired in a FACScan or FACSCalibur with CellQuest software (BD Biosciences). Dead cells were excluded from the analysis with propidium iodide. Analysis was done with FlowJo software (Tree Star Inc.). Cellular free radical generation was determined by incubating cells (10 mM, 15 min, 37°C, 95% humidity, 5%CO2) with the broad free radical probe 5-(and 6)-chloromethyl-2′7′-dichlorodihydrofluoscein diacetate acetyl ester (CM-H_2DCFDA; Molecular Probes).

Immunofluorescence

Hepa1-6 cells, seeded and treated (as described above) on glass cover slips (Paul Marienfeld GmbH & Co.), were fixed (4% paraformaldehyde, 30 min), permeabilized (0.1% Triton X-100, 20 min), blocked (PBS, 10% goat serum, 20 min), and incubated overnight at 4°C with rabbit antibody against human HMGB1 (Abcam, ab18256; 0.5 mg/ml) or control rabbit IgG (Sigma) in PBS and 10% goat serum. Alexa 568–conjugated

goat antibody against rabbit IgG (5 mg/ml; Invitrogen) was used as secondary antibody. Nuclear DNA was stained with Hoechst 33342 (10 mg/ml, PBS, 20 min; Invitrogen), and cells were mounted in Vectashield (Vector Laboratories). Images were captured with a fluorescence microscope (Leica, DMRA2) equipped with UV light and Evolution MP 5.0 Color Camera (Media Cybernetics). Images were analyzed with ImageJ software (National Institutes of Health).

Histology and immunohistology

Tissue samples were processed and stained essentially as described[42]. HMGB1 was detected in paraffin-embedded, formalin-fixed sections (5 μm) after microwave antigen retrieval [0.01 M citrate buffer (pH 6.0) 20 min] with rabbit antibody against human HMGB1 (Becton Dickinson, 556528) (0.5 mg/ml, 4°C, overnight). Rabbit IgG was detected with biotin-conjugated donkey antibody against rabbit secondary antiserum (1:1000; Jackson Immunoresearch) and streptavidin conjugated horseradish peroxidase amplification kit (Vectastain Elite ABCKit, Vector Labs). Signal was revealed with 3,3′-diaminobenzidine (DAB). Sections were counterstained with Harris hematoxylin. Negative controls were performed by omitting the primary antibody or with a nonspecific rabbit polyclonal antibody. Images were obtained and analyzed as described above.

Serum biochemistry

Blood was collected in tubes with heparin after cardiac puncture, centrifuged (2x5 min, 1600g). AST, BUN, and CPK were measured according to the protocols of the International Federation of Clinical Chemistry, as described[43-45], by

spectrophotometric analysis (modular DP; Roche-Hitachi, Echevarne Laboratories). Plasma HPX and haptoglobin were determined by ELISA (Life Diagnostics). Plasma hemoglobin was determined by spectroscopy at a wavelength of 577 nm (I577). Total plasma heme was measured with the 3,3′,5,5′ tetramethylbenzidine (TMB) peroxidase assay (BD Biosciences) at I655. Purified hemoglobin was used as standard for plasma hemoglobin and heme measurements. Blood smears were fixed in methanol and stained with Giemsa stain, and images were obtained and analyzed as described above.

HPX

Intact apo-HPX was isolated from rabbit serum as described[46]. Purified HPX binds heme as assessed by absorbance and circular dichroism spectroscopy of the apoprotein or the oxidized and reduced heme-HPX complexes; the concentration of the protein and equimolar heme binding were quantified with published procedures and extinction coefficients[47]. Neither the apo-HPX nor the heme-HPX complex is toxic for cells in vitro even at high concentrations[48]. Mice received purified HPX (50 mg/kg i.p.) at 2, 12, 24, and 36 hours after CLP.

Western blotting

Proteins were prepared and subjected to electrophoresis essentially as described before[49]. For HMGB1 detection in peritoneal fluid and in serum, samples were ultrafiltered with Centricon 100 columns (Millipore) and precipitated with trichloroacetic acid (TCA), washed twice in acetone, dried, dissolved in urea (8 M), and added to SDS–polyacrylamide gel

electrophoresis (SDS-PAGE) loading buffer. Primary hepatocyte and Hepa1-6 culture supernatants were concentrated on Vivaspin 500 columns (10-kD molecular mass cutoff; Vivascience AG) resulting in up to ~10-fold concentration. HMGB1 was detected with polyclonal antibody (Abcam, ab18256; 0.1 mg/ml). HO-1 was detected with a rabbit polyclonal antibody against human HO-1 (1:2.500; SPA-895, StressGen). Monoclonal antibodies were used to detect α-tubulin (T9026, 1:5.000 dilution; Sigma) and inducible NO synthase (Becton Dickinson). Primary antibodies were detected with horseradish peroxidase–conjugated donkey antibody against rabbit, goat antibody against mouse, or rabbit antibody against mouse IgG secondary antibodies (Pierce, Rockford). Peroxidase activity was visualized with the SuperSignal chemiluminescent detection kit (Pierce) according to the manufacturer's instructions and stored in the form of photoradiographs (BiomaxTMMS, Eastman Kodak) or with the Image Station 440CF (Kodak). Digital images were obtained with an image scanner equipped with Adobe Photoshop software.

Septic shock patients

We analyzed the plasma concentration of HPX in 52 patients undergoing septic shock, as defined by the American College of Chest Physicians (ACCP)–Society of Critical Care Medicine (SCCM) consensus criteria[22]. Patients were treated according to standard recommendations[50], including aggressive fluid resuscitation, broad-spectrum antibiotic therapy over the first 24 hours, vasoactive agents, and at least one intravenous dose of hydrocortisone. Blood samples were collected on the first,

second, third, fifth, and seventh day after septic shock diagnosis. Blood was collected on ice between 1000 and 1200 hours with an arterial line or a peripheral vein, and plasma was collected by centrifugation (800g, 15 min, 4°C), aliquoted, and stored (−70°C) until analysis. Organ dysfunction was defined by the SOFA score on the basis of daily measurements[23]. The outcome analyzed was 28th-day hospital mortality. The study protocol was approved by the institutional review board of each participating center (University Hospital of Federal University of Rio de Janeiro, Hospital Quinta D'Or, Casa de Saúde São José, Rio de Janeiro, Brazil). All patients, or their legal surrogates, gave written informed consent before any study-related procedures.

Statistical analysis

The comparison of two independent samples was assessed by the Student's t test and the Mann-Whitney test for Gaussian and non- Gaussian distributed samples, respectively. To compare more than two samples, we performed analysis of variance (ANOVA) or Kruskal-Wallis tests for Gaussian and non-Gaussian distributed samples, respectively. Comparison of different survival curves for the variously treated animals was done by the nonparametric log-rank test. For pairwise comparisons, the Bonferroni correction was used to ensure the overall significance level. Regression models were applied to describe genotype-based data, and statistical significance presented throughout the paper refers to additive effects. Kolmogorov-Smirnov and Shapiro-Wilk tests were performed to assess the normality of the samples under analysis. Regression models were applied to describe genotype-based data. In all data sets, the following model equation was applied: $Y = a + b\ x$

genotype + *c x heterozygote*, where *Y* denotes the variable under analysis, with logarithmic transformation when appropriate; *a* is the baseline referring to the *Hmox1*$^{-/-}$ mean; *b* is the mean effect of adding a *Hmox1*$^{+/+}$ allele in the genotype (additive effect); *c* is the deviation of heterozygote mean from a single additive effect; genotype is an explanatory variable denoting the genotype coded as 0, 1, and 2 (0, 1, 2 *Hmox1*$^{+/+}$ alleles, respectively); and *Hmox1*$^{+/-}$ is the binary variable indicating the heterozygote genotype. Model validation was done by a thorough residual analysis, which included testing normality of the residuals and visual inspection of any trend in the residuals across genotypes. Statistical significance refers to additive effects in the regression analysis. Kolmogorov-Smirnov and Shapiro-Wilk tests were performed to infer whether data could come from normal distributions. All statistical tests were done at 5% significance level with InStat and R software[51]. For human data, a survival analysis was performed with the package available in the R software[51]. For each patient, survival time was computed by the difference between the time of patient inclusion in the intensive care unit and the respective closing date of the hospital record. Patients that left hospital after treatment were considered as right-censored observations for the respective survival time. Because the survival time could be approximated by a lognormal distribution, several survival regression models based on such probability distributions were fitted to the data. HPX was included in the models as an explanatory variable with either the first or the last time point measure available for a patient. The statistical significance of this explanatory variable in the models was assessed by the traditional z-score tests. A correlation analysis between SOFA score and HPX at different time points was also

performed with Spearman's coefficient.

6. ACKNOWLEDGMENTS

We thank S. F. Yet (Pulmonary and Critical Care Division, Brigham and Women's Hospital) for providing *Hmox1* breeding pairs from which *Hmox1*$^{-/-}$ mice were derived; E. Tolosano (University of Torino, Torino, Italy) for critical review of the manuscript; S. Rebelo (Instituto Gulbenkian de Ciência) for invaluable help in breeding the *Hmox1*$^{-/-}$ mice; K. Rish, R. Lovelace, and R. Helston (University of Missouri) for technical expertise in the HPX isolation and characterization; and T. Davis (University of Missouri) for heme-HPX preparation. **Funding:** This work was supported by Fundação para a Ciência e Tecnologia (Portugal) grants SFRH/BPD/25436/2005 and PTDC/BIO/70815/2006 (to R.L.); SFRH/BPD/44256/2008 (to R.G.); SFRH/BD/11816/2003 (to L.T.); SFRH/BD/3106/2000 (to A.C.); SFRH/BPD/21707/2005 and PTDC/SAU MII/71140/ 2006 (to A.F.); SFHR/BD/33218/2007 (to I.M.); POCTI/SAU MNO/56066/ 2004, POCTI/BIA-BCM/56829/2004, PTDC/BIA-BCM/101311/2008, and PTDC/SAU-FCF/100762/2008 (to M.P.S.); as well as GEMI Fund Linde Healthcare (to M.P.S.), the European Community, Sixth Framework grant LSH-2005-1.2.5-1 (to M.P.S.), and Marie Curie FP7-PEOPLE-2007-2-1-IEF, GASMALARIA (to V.J.). A.S. is supported by research incentive funds from the University of Missouri at Kansas City, MO, USA. F.A.B. is a research scholar supported by Conselho Nacional de Desenvolvimento Científico e Tecnológico and FAPERJ, Brazil. **Author contributions:** R.L. performed most of the experimental work with help from A.F. and S.C. R.G. performed the

experiments defining the cytotoxic effect of free heme. V.J. performed the experiments establishing heme and hemoglobin concentrations in plasma. A.C. and I.M. performed flow cytometry analysis. F.A.B. and A.M.J. conduced the clinical study with septic shock patients. M.M.C. and D.B. set up the CLP model in the laboratory. A.S. supplied the purified HPX and heme-HPX, gave critical advise on its use, and contributed to writing of the manuscript. M.P.S. formulated the hypothesis that free heme might play pivotal roles in the pathogenesis of severe sepsis, designed the experimental approach, and wrote the manuscript with help from R.L. R.L. and R.G. contributed to the study design. All authors read and approved the manuscript.

7. REFERENCES

1. Martin, G.S., Mannino, D.M., Eaton, S. & Moss, M. The epidemiology of sepsis in the United States from 1979 through 2000. *N Engl J Med* **348**, 1546-1554 (2003).
2. Cohen, J. The immunopathogenesis of sepsis. *Nature* **420**, 885-891 (2002).
3. Medzhitov, R. Origin and physiological roles of inflammation. *Nature* **454**, 428-435 (2008).
4. Read, A.F., Graham, A.L. & Raberg, L. Animal defenses against infectious agents: is damage control more important than pathogen control. *PLoS Biol* **6**, e4 (2008).
5. Schafer, J. Tolerance to plant disease. *Annu Rev Phytopathol* **9**, 235-252 (1971).
6. Schneider, D.S. & Ayres, J.S. Two ways to survive infection: what resistance and tolerance can teach us about treating infectious diseases. *Nat Rev Immunol* **8**, 889-895 (2008).
7. Medzhitov, R. Damage control in host-pathogen interactions. *Proc Natl Acad Sci U S A* **106**, 15525-15526 (2009).
8. Seixas, E.*, et al.* Heme oxygenase-1 affords protection against noncerebral forms of severe malaria. *Proc Natl Acad Sci U S A* **106**, 15837-15842 (2009).
9. Tenhunen, R., Marver, H.S. & Schmid, R. The enzymatic conversion of heme to bilirubin by microsomal heme oxygenase. *Proc Natl Acad Sci U S A* **61**, 748-755 (1968).
10. Chung, S.W., Liu, X., Macias, A.A., Baron, R.M. & Perrella, M.A. Heme oxygenase-1-derived carbon monoxide enhances the host defense response to microbial sepsis in mice. *J Clin Invest* **118**, 239-247 (2008).
11. Gozzelino, R., Jeney, V. & Soares, M.P. Mechanisms of cell protection by heme oxygenase-1. *Annu Rev Pharmacol Toxicol* **50**, 323-354 (2010).
12. Fenton, H.J.H. Oxidation of tartaric acid in presence of iron. *J. Chem. Soc. Trans.* **65**, 899-910 (1894).
13. Chou, A.C. & Fitch, C.D. Mechanism of hemolysis induced by ferriprotoporphyrin IX. *J Clin Invest* **68**, 672-677 (1981).

14. Pamplona, A.*, et al.* Heme oxygenase-1 and carbon monoxide suppress the pathogenesis of experimental cerebral malaria. *Nat Med* **13**, 703-710 (2007).
15. Nielsen, M.J. & Moestrup, S.K. Receptor targeting of hemoglobin mediated by the haptoglobins: roles beyond heme scavenging. *Blood* **114**, 764-771 (2009).
16. Tolosano, E., Fagoonee, S., Morello, N., Vinchi, F. & Fiorito, V. Heme scavenging and the other facets of hemopexin. *Antioxid Redox Signal* **12**, 305-320 (2010).
17. Porto, B.N.*, et al.* Heme induces neutrophil migration and reactive oxygen species generation through signaling pathways characteristic of chemotactic receptors. *J Biol Chem* **282**, 24430-24436 (2007).
18. Rock, K.L. & Kono, H. The inflammatory response to cell death. *Annu Rev Pathol* **3**, 99-126 (2008).
19. Wang, H.*, et al.* HMG-1 as a late mediator of endotoxin lethality in mice. *Science* **285**, 248-251 (1999).
20. Takamiya, R.*, et al.* High-mobility group box 1 contributes to lethality of endotoxemia in heme oxygenase-1-deficient mice. *Am J Respir Cell Mol Biol* **41**, 129-135 (2009).
21. Gutteridge, J.M. & Smith, A. Antioxidant protection by haemopexin of haem-stimulated lipid peroxidation. *Biochem J* **256**, 861-865 (1988).
22. Bone, R.C.*, et al.* Definitions for sepsis and organ failure and guidelines for the use of innovative therapies in sepsis. The ACCP/SCCM Consensus Conference Committee. American College of Chest Physicians/Society of Critical Care Medicine. *Chest* **101**, 1644-1655 (1992).
23. Moreno, R.*, et al.* The use of maximum SOFA score to quantify organ dysfunction/failure in intensive care. Results of a prospective, multicentre study. Working Group on Sepsis related Problems of the ESICM. *Intensive Care Med* **25**, 686-696 (1999).
24. Raberg, L., Sim, D. & Read, A.F. Disentangling genetic variation for resistance and tolerance to infectious diseases in animals. *Science* **318**, 812-814 (2007).
25. Bhakdi, S.*, et al.* Staphylococcal alpha-toxin, streptolysin-O, and Escherichia coli hemolysin: prototypes of pore-forming bacterial cytolysins. *Arch Microbiol* **165**, 73-79 (1996).
26. Silva, G.*, et al.* Oxidized hemoglobin is an endogenous proinflammatory agonist that targets vascular endothelial cells. *J Biol Chem* **284**, 29582-29595 (2009).
27. Bullen, J., Griffiths, E., Rogers, H. & Ward, G. Sepsis: the critical role of iron. *Microbes Infect* **2**, 409-415 (2000).
28. Ferreira, A., Balla, J., Jeney, V., Balla, G. & Soares, M.P. A central role for free heme in the pathogenesis of severe malaria: the missing link? *J Mol Med* **86**, 1097-1111 (2008).
29. Liang, X.*, et al.* Hemopexin down-regulates LPS-induced proinflammatory cytokines from macrophages. *J Leukoc Biol* **86**, 229-235 (2009).
30. Soares, M.P. & Bach, F.H. Heme oxygenase-1: from biology to therapeutic potential. *Trends Mol Med* **15**, 50-58 (2009).
31. Poss, K.D. & Tonegawa, S. Reduced stress defense in heme oxygenase 1-deficient cells. *Proc Natl Acad Sci U S A* **94**, 10925-10930 (1997).
32. Tracz, M.J.*, et al.* Deficiency of heme oxygenase-1 impairs renal hemodynamics and exaggerates systemic inflammatory responses to renal ischemia. *Kidney Int* **72**, 1073-1080 (2007).
33. Wiesel, P.*, et al.* Endotoxin-induced mortality is related to increased oxidative stress and end-organ dysfunction, not refractory hypotension, in heme oxygenase-1-deficient mice. *Circulation* **102**, 3015-3022 (2000).
34. Takaki, S.*, et al.* Beneficial effects of the heme oxygenase-1/carbon monoxide system in patients with severe sepsis/septic shock. *Intensive Care Med* **36**, 42-48 (2010).
35. Yet, S.F.*, et al.* Hypoxia induces severe right ventricular dilatation and infarction in heme oxygenase-1 null mice. *J Clin Invest* **103**, R23-29 (1999).
36. Goncalves, L.A., Vigario, A.M. & Penha-Goncalves, C. Improved isolation of murine hepatocytes for in vitro malaria liver stage studies. *Malar J* **6**, 169 (2007).

37. Soares, M.P.*, et al.* Heme oxygenase-1 modulates the expression of adhesion molecules associated with endothelial cell activation. *J Immunol* **172**, 3553-3563 (2004).
38. Griess, J.P. On a new series of bodies in which nitrogen is substituted for hydrogen. *Philos. Trans. R. Soc. Lond.* **154**, 667-731 (1864).
39. Wichterman, K.A., Baue, A.E. & Chaudry, I.H. Sepsis and septic shock--a review of laboratory models and a proposal. *J Surg Res* **29**, 189-201 (1980).
40. McMasters, K.M. & Cheadle, W.G. Regulation of macrophage TNF alpha, IL-1 beta, and Ia (I-A alpha) mRNA expression during peritonitis is site dependent. *J Surg Res* **54**, 426-430 (1993).
41. McDaid, J.*, et al.* Heme oxygenase-1 modulates the allo-immune response by promoting activation-induced cell death of T cells. *FASEB J* **19**, 458-460 (2005).
42. Sato, K.*, et al.* Carbon monoxide generated by heme oxygenase-1 suppresses the rejection of mouse-to-rat cardiac transplants. *J Immunol* **166**, 4185-4194 (2001).
43. Bergmeyer, H.U., Horder, M. & Rej, R. International Federation of Clinical Chemistry (IFCC) Scientific Committee, Analytical Section: approved recommendation (1985) on IFCC methods for the measurement of catalytic concentration of enzymes. Part 2. IFCC method for aspartate aminotransferase (L-aspartate: 2-oxoglutarate aminotransferase, EC 2.6.1.1). *J Clin Chem Clin Biochem* **24**, 497-510 (1986).
44. Bergmeyer, H.U., Horder, M. & Rej, R. International Federation of Clinical Chemistry (IFCC) Scientific Committee, Analytical Section: approved recommendation (1985) on IFCC methods for the measurement of catalytic concentration of enzymes. Part 3. IFCC method for alanine aminotransferase (L-alanine: 2-oxoglutarate aminotransferase, EC 2.6.1.2). *J Clin Chem Clin Biochem* **24**, 481-495 (1986).
45. Horder, M., Elser, R.C., Gerhardt, W., Mathieu, M. & Sampson, E.J. International Federation of Clinical Chemistry, Scientific Division Committee on Enzymes: approved recommendation on IFCC methods for the measurement of catalytic concentration of enzymes. Part 7. IFCC method for creatine kinase (ATP: creatine N-phosphotransferase, EC 2.7.3.2). *Eur J Clin Chem Clin Biochem* **29**, 435-456 (1991).
46. Smith, A. & Morgan, W.T. Transport of heme by hemopexin to the liver: evidence for receptor-mediated uptake. *Biochem Biophys Res Commun* **84**, 151-157 (1978).
47. Eskew, J.D., Vanacore, R.M., Sung, L., Morales, P.J. & Smith, A. Cellular protection mechanisms against extracellular heme. heme-hemopexin, but not free heme, activates the N-terminal c-jun kinase. *J Biol Chem* **274**, 638-648 (1999).
48. Li, R.C.*, et al.* Heme-hemopexin complex attenuates neuronal cell death and stroke damage. *J Cereb Blood Flow Metab* **29**, 953-964 (2009).
49. Silva, G., Cunha, A., Gregoire, I.P., Seldon, M.P. & Soares, M.P. The antiapoptotic effect of heme oxygenase-1 in endothelial cells involves the degradation of p38 alpha MAPK isoform. *J Immunol* **177**, 1894-1903 (2006).
50. Dellinger, R.P.*, et al.* Surviving Sepsis Campaign guidelines for management of severe sepsis and septic shock. *Crit Care Med* **32**, 858-873 (2004).
51. http://www.r-project.org.

Chapter 4: Sickle Hemoglobin Confers Tolerance to *Plasmodium* Infection

Ana Ferreira[1],Ivo Marguti[1], Ingo Bechman[2,3], Viktória Jeney[1], Ângelo Chora[1], Nuno R. Palha[1], Sofia Rebelo[1], Annie Henri[4,5,6], Yves Beuzard[4,5,6], Miguel Soares[1]

[1]Instituto Gulbenkian de Ciência, Oeiras, Portugal. [2]Institute of Anatomy, University of Leipzig. Leipzig, Germany. [3]Dr. Senckenbergische Anatomie, Institute for Clinical Neuroanatomy, Johann Wolfgang Goethe-University. Frankfurt/Main, Germany. [4]Institut Universitaire d´Hematologie, Université Paris 7, France. [5]CEA, Institute of Emerging Diseases and Innovative Therapies. Fontenay-aux-Roses, France. [6]INSERM U962 and University Paris Sud 11, France.

Published in **Cell 2011, April, 145(3):398-409**.

1. ABSTRACT

Sickle human hemoglobin (Hb) confers a survival advantage to individuals living in endemic areas of malaria, the disease caused by *Plasmodium* infection. As demonstrated hereby, mice expressing sickle Hb do not succumb to experimental cerebral malaria (ECM). This protective effect is exerted irrespectively of parasite load, revealing that sickle Hb confers host tolerance to *Plasmodium* infection. Sickle Hb induces the expression of heme oxygenase-1 (HO-1) in hematopoietic cells, via a mechanism involving the transcription factor NF-E2-related factor 2 (Nrf2). Carbon monoxide (CO), a byproduct of heme catabolism by HO-1, prevents further accumulation of circulating free heme after *Plasmodium* infection, suppressing the pathogenesis of ECM. Moreover, sickle Hb inhibits activation and/or expansion of pathogenic $CD8^+$ T cells recognizing antigens expressed by *Plasmodium*, an immunoregulatory effect that does not involve Nrf2 and/or HO-1. Our findings provide insight into molecular mechanisms via which sickle Hb confers host tolerance to severe forms of malaria.

2. INTRODUCTION

Several point mutations in the β-chain of human Hb, e.g. HbS ($^{\beta}$6Glu->Val)[1,2] , HbC ($^{\beta}$6Glu->Lys)[3] and HbE ($^{\beta}$26Glu>Lys)[4], can confer a survival advantage to *Plasmodium* (*P*.) infection[5]. When present in the homozygous form, some of these mutations, e.g. HbS, become pathologic causing hemolytic anemia, leading to accumulation of high levels of cell-free Hb and heme in plasma[6]. Individuals carrying the HbS mutation in the heterozygous form, i.e. the A/S sickle cell trait, also accumulate low (nonpathologic) levels of heme in plasma[7] and are protected against malaria[1,5,8,9].

Once released from Hb, a phenomenon favored in the case of HbS[10], free heme becomes cytotoxic[11-13]. This deleterious effect is countered by the expression of heme oxygenase-1 (HO-1, encoded by the *Hmox1* gene)[11,13,14], a stress responsive enzyme that catabolizes free heme into biliverdin, iron and carbon monoxide (CO)[15]. HO-1 expression is induced by free heme, through a mechanism that involves the ubiquitination-degradation of Kelch-like ECH-associated protein 1 (Keap1)[16], a cytoplasmic repressor of the transcription factor NF-E2-related factor-2 (Nrf2)[17]. Upon nuclear translocation, Nrf2 binds to the stress-responsive elements in the *Hmox1* promoter[18], a regulatory mechanism that plays a central role in the control of *Hmox1* expression in response to heme[16].

HO-1 is protective against a wide variety of immune-mediated inflammatory diseases[19,20] including experimental cerebral malaria (ECM)[21], a lethal neuroinflammatory syndrome that develops in *P. berghei* ANKA infected C57BL/6 mice and

that mimics some of the pathologic features of human cerebral malaria (CM)[22]. This protective effect is mediated by CO, which binds cell-free Hb and inhibits its oxidation, thus preventing heme release from oxidized Hb[10] and hence the pathogenesis of ECM[21]. Given that expression of HO-1[23,24] and production of CO[25] are induced in individuals carrying the HbS mutation we hypothesized that this might explain why individuals carrying the A/S sickle cell trait have a survival advantage against malaria[2,8,26]. We provide evidence demonstrating that this is the case.

3. RESULTS

3.1 Sickle Hb Confers a Survival Advantage against Malaria in Mice

Inoculation of C57BL/6 mice (Hb^{wt}) with *P. berghei* ANKA infected red blood cells (RBC) led within 6 to 12 days to the development of clinical signs of ECM (Figure 4.1 A). Incidence of ECM was significantly reduced in hemizygous C57BL/6 Hb^{SAD} mice (Figure 4.1 A) expressing a β-chain of human Hb carrying the $^{\beta}$6Glu->Val (Hb**S**) mutation as well as two additional mutations, $^{\beta}$23Ala->Ile (**A**ntilles^{23I}) and $^{\beta}$121Asp->Gln (D-Punjab^{121Q}), known to enhance HbS polymerization in humans and mice[27]. Naive Hb^{SAD} mice present a very mild sickle cell syndrome, which does not lead to anemia[28] (Table 4.1) similar to the asymptomatic human A/S sickle cell trait that affords protection against malaria[1,8,9]. Hb^{SAD} mice that did not develop ECM, succumbed 20-25 days postinfection from hyperparasitemia-induced anemia (data not shown), a condition unrelated to ECM[29].

When infected with *P. berghei* ANKA, C57BL/6.Sv/129 $Hb^{A/a}$ mice expressing normal human Hb as well as endogenous mouse Hb[30] developed clinical signs of ECM and succumbed 6 to 12 days after infection (Figure 4.1 G). Littermate control C57BL/6.Sv/129 $Hb^{a/a}$ mice, expressing only the endogenous mouse Hb developed ECM but with lower incidence, as compared to $Hb^{A/a}$ mice (Figure 4.1 G). This suggests that normal human Hb might promote, rather than prevent, the pathogenesis of ECM in C57BL/6.Sv/129 mice. While the reason for this is not clear, it is possible that human Hb alters mouse RBC physiology in a manner that would promote the development of ECM. However, this effect becomes negligible as C57BL/6.Sv/129 mice are backcrossed into the C57BL/6 genetic background (Figure 4.1 J), in which ECM incidence is higher than 95% (Figure 4.1 A). Given that Hb^{SAD} suppresses the pathogenesis of ECM in C57BL/6 mice and that the deleterious effect of normal human Hb becomes negligible under this genetic background, it is reasonable to infer that the protective effect of Hb^{SAD} is attributable to the mutations in the human β-globin chain rather than to human Hb *per se*.

Hb^{SAD} mice that did not succumb within 6–12 days postinfection also did not develop the pathologic hallmarks of ECM, including blood brain barrier (BBB) disruption (Figure 4.1 B), perivascular RBC accumulation in brain (Figure 4.1 B) and brain edema (Figure 4.1 C). These pathologic features were present in Hb^{wt} (Figures 4.1 B and C) and $Hb^{A/a}$ mice, i.e. brain edema (Figure 4.1 H). Given that BBB disruption and brain edema occur in *P. berghei* ANKA infected C57BL/6 mice via a $CD8^+$ T cell-dependent mechanism[29,31], we asked whether the

protective effect of Hb^{SAD} against ECM was associated with

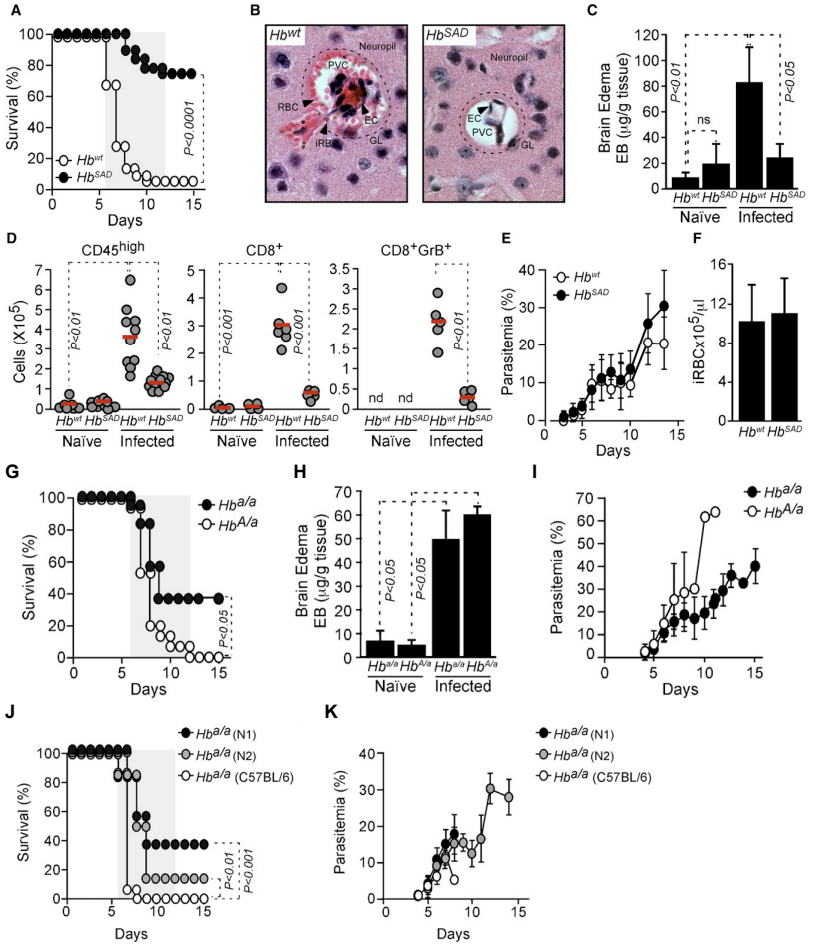

Figure 4.1. Hb^{SAD} Prevents ECM Onset. (A) Survival of *P. berghei* ANKA infected Hb^{wt} (n = 91) and Hb^{SAD} (n = 76) mice (10 independent experiments with survival advantage p < 0.05). Grey shading: expected time of ECM. **(B)** Representative H&E stained microvessel in the BBB of infected Hb^{wt} and Hb^{SAD} mice, at ECM onset in Hb^{wt} mice (n = 3/group). EC: endothelial cell; PVC: perivascular compartment; GL: glia limitans (dotted line); RBC: red blood cells; iRBC: infected RBC. Magnification: 100x. **(C)** Mean brain edema in naïve *versus* infected Hb^{wt} and Hb^{SAD} mice ± standard deviation (n=4/group), at the time of ECM onset in Hb^{wt} mice. ns: not significant. **(D)** Brain leukocyte sequestration in naïve *versus* infected Hb^{wt} and Hb^{SAD} mice, at the time of ECM onset in Hb^{wt} mice. Dots represent single mice (n = 4 -14/ group). Red lines represent mean values. nd: not determined. **(E)** Mean percentage of infected RBC in Hb^{wt} and Hb^{SAD} mice ± standard deviation. Same mice as in **(A)**. **(F)** Mean number of infected RBC in Hb^{wt} (n=7) and Hb^{SAD} (n=9) mice ± standard deviation at the time of ECM onset in Hb^{wt} mice. **(G)** Survival of *P. berghei* ANKA infected $Hb^{A/a}$ (n=15) and littermate control $Hb^{a/a}$ (n=19) mice (3 independent experiments with survival advantage P<0.05). **(H)** Brain edema was measured by Evans blue (EB) accumulation in brains ± standard deviation (n=3-4/group), at the time of ECM onset in $Hb^{A/a}$ mice. **(I)** Mean percentage of infected RBC ± standard deviation, same mice as in **(G)**. Notice that the $Hb^{A/a}$ and $Hb^{a/a}$ mice used in these experiments are in a mixed C57BL/6.SV129 genetic background, produced by breeding $Hb^{A/a}$ mice. **(J)** Survival of *P. berghei* ANKA infected $Hb^{a/a}$ mice under different genetic backgrounds, i.e. $Hb^{a/a}$ N1 (n=19), $Hb^{a/a}$ N2 (n=7) and $Hb^{a/a}$ C57BL/6 (n=15) mice (data pooled from 4 independent experiments). **(K)** Mean percentage of infected RBC in the same mice as in **(J)**. Grey shading indicates expected time of ECM. Notice that expression of a nonmutated β-chain of human Hb in the $Hb^{A/a}$ mice does not protect against ECM, as compared to littermate control $Hb^{a/a}$ mice. This supports the notion that protection of Hb^{SAD} mice against ECM is afforded by the mutations of β-chain of human Hb and not by the β-chain of human Hb itself.

inhibition of $CD8^+$ T cell sequestration in the brain. The number of $CD45^{high}$ leukocytes and $CD8^+$ T cells, including granzyme B-positive (GrB^+) $CD8^+$ T cells, was reduced in *P. berghei* ANKA infected Hb^{SAD}, as compared to Hb^{wt} mice at ECM onset (Figure 4.1 D). When infected with *P. berghei* ANKA, Hb^{wt} mice also developed severe lung injury and a mild form of liver injury (Figure 4.2) with no apparent injury to the kidneys or to the heart (data not shown). The extent of lung and liver injury was reduced in *P. berghei* ANKA infected Hb^{SAD} *versus* Hb^{wt} mice (Figure 4.2).

3.2 Sickle Hb Confers Tolerance to *Plasmodium* Infection in Mice

Protection of Hb^{SAD} mice against ECM was not associated with reduction of pathogen load, as assessed by the percentage of infected RBC, i.e., parasitemia (Figure 4.1 E) as well as by the number of circulating infected RBC (Figure 4.1 F) *versus* control Hb^{wt} (Figures 4.1 E and F) or $Hb^{A/a}$ mice (Figures 4.1 I K). While the protective effect of the human sickle cell trait against malaria has been associated with decreased pathogen load[2,8,26], there are several instances where this does not appear to be the case[32-34], which is in keeping with the observation that Hb^{SAD} confers protection against ECM without interfering with pathogen load. These observations suggest that mutations in the β-chain of human Hb, such as those in Hb^{SAD} can afford tolerance to *Plasmodium* infection, a host defense strategy that limits disease severity by preventing tissue damage, without targeting the pathogen. This contrasts to resistance to infection, the well-recognized host defense strategy that limits disease severity by decreasing pathogen load[35,36].

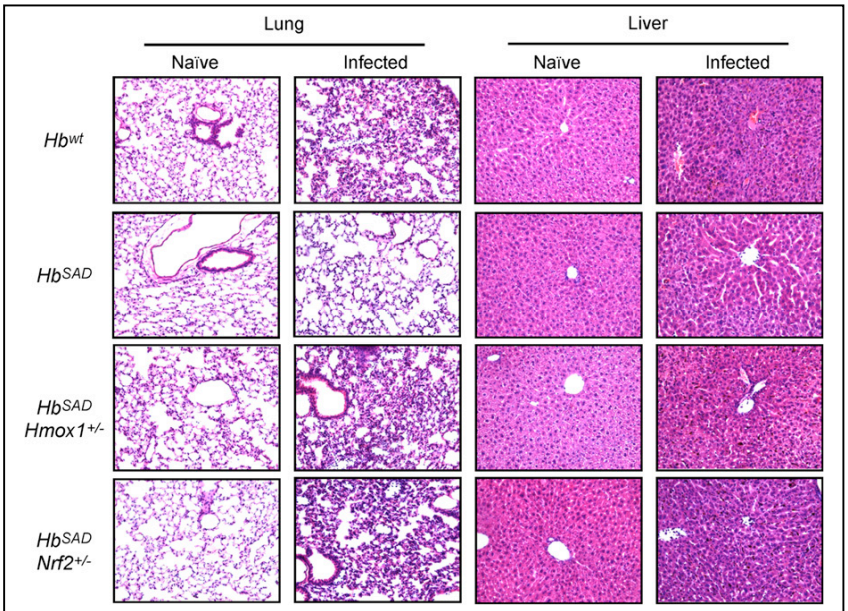

Figure 4.2. *Hb*^{SAD} Affords Protection Against Lung and Liver Injury Via a Mechanism Involving HO-1 and Nrf2. Paraffin sections stained with standard hematoxylin/eosin staining. Naïve *Hb*^{wt}, *Hb*^{SAD}, *Hb*^{SAD}*Hmox1*$^{+/-}$ and *Hb*^{SAD}*Nrf2*$^{+/-}$ mice exhibit normal lungs and livers that were indistinguishable from each other. Infection with *P. berghei* ANKA in *Hb*^{wt} mice was associated with the development of interstitial pneumonia and RBC extravasation as well as iron deposits, prominent in the liver. The latter can also be seen in *P. berghei* ANKA infected *Hb*^{SAD} mice, albeit to a lesser extent. Lungs of *P. berghei* ANKA infected *Hb*^{SAD} were only mildly affected, as compared to those of *Hb*^{wt} mice. The protective effect of *Hb*^{SAD} was lost in *Hb*^{SAD}*Hmox1*$^{+/-}$ and *Hb*^{SAD}*Nrf2*$^{+/-}$ mice. That is, *Hb*^{SAD}*Hmox1*$^{+/-}$ and *Hb*^{SAD}*Nrf2*$^{+/-}$ showed massive pneumonia as well as iron deposits in the liver when infected with *P. berghei* ANKA.

Parasite sequestration was similar in *Hb*^{wt}, *Hb*^{SAD}*Hmox1*$^{+/+}$, and *Hb*^{SAD}*Hmox1*$^{+/-}$ mice, as assessed using a transgenic luciferase-*P. berghei* ANKA strain (Figure 4.3). This supports further the notion that induction of HO-1 by sickle Hb confers host tolerance to *Plasmodium* infection.

3.3 Sickle Hb Induces the Expression of HO-1 that Confers Tolerance to *Plasmodium* Infection

Humans and rodents carrying the HbS mutation express high levels of HO-1 in the hematopoietic compartment[23,24]. Consistent with this, naive *Hb*^{SAD} mice express high levels of *Hmox1* mRNA in bone marrow and peripheral blood cells, as

compared to naïve Hb^{wt} mice (Figure 4.4 A). Naive Hb^{SAD} mice

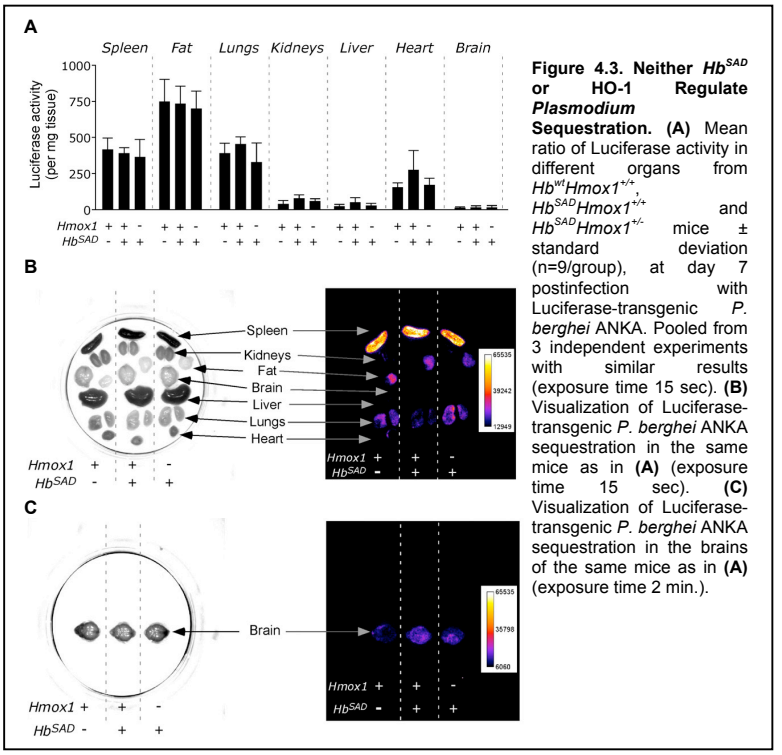

Figure 4.3. Neither Hb^{SAD} or HO-1 Regulate *Plasmodium* Sequestration. (A) Mean ratio of Luciferase activity in different organs from $Hb^{wt}Hmox1^{+/+}$, $Hb^{SAD}Hmox1^{+/+}$ and $Hb^{SAD}Hmox1^{+/-}$ mice ± standard deviation (n=9/group), at day 7 postinfection with Luciferase-transgenic *P. berghei* ANKA. Pooled from 3 independent experiments with similar results (exposure time 15 sec). **(B)** Visualization of Luciferase-transgenic *P. berghei* ANKA sequestration in the same mice as in **(A)** (exposure time 15 sec). **(C)** Visualization of Luciferase-transgenic *P. berghei* ANKA sequestration in the brains of the same mice as in **(A)** (exposure time 2 min.).

also expressed higher levels of *Hmox1* mRNA in the kidneys (Figure 4.4 G), which is consistent with the chronic development of kidney injury in these mice, revealed clinically upon aging[37]. Hb^{SAD} mice expressed similar levels of *Hmox1* mRNA in the liver, heart, lung and spleen (Figure 4.4 G), as compared to Hb^{wt} mice. $Hb^{A/a}$ mice expressed similar levels of *Hmox1* mRNA in the bone marrow and peripheral blood *versus* littermate control $Hb^{a/a}$ mice (Figure 4.4 I), demonstrating that expression of a β^S related variant but not a normal β-globin chain is required to induce *Hmox1* expression.

Given that HO-1 is protective against severe forms of malaria in mice[12,21], we asked whether its induction in Hb^{SAD} mice (Figure 4.4 A) is required to suppress the development of ECM

(Figure 4.1 A). Deletion of one *Hmox1* allele (*Hmox1*$^{+/-}$) reduced *Hmox1* mRNA expression in bone marrow and whole blood leukocytes of *Hb*^{SAD} mice (Figure 4.4 H), without causing overt postnatal lethality (Table 4.2 A). When challenged by *P. berghei* ANKA infection, *Hb*^{SAD}*Hmox1*$^{+/-}$ mice succumbed to ECM (Figure 4.4 B), with concomitant development of BBB disruption (Figure 4.4 C), brain edema (Figure 4.4 D) and sequestration of CD45^{high} leukocytes (data not shown), CD8^{+} T cells and activated GrB^{+}CD8^{+} T cells in the brain (Figure 4.4 E).

The protective effect of *Hb*^{SAD} against lung and liver injury, associated with *P. berghei* ANKA infection, was lost in *Hb*^{SAD}*Hmox1*$^{+/-}$ mice (Figure 4.2). This was not associated with increased parasite load (Figure 4.4 F).

Pharmacologic inhibition of HO activity by zinc protoporphyrin IX (ZnPPIX) (Figures 4.5 A and B), increased ECM incidence in *Hb*^{SAD} mice *versus* vehicle-treated controls (Figure 4.5 C). This effect was not associated with modulation of parasitemia (Figure 4.5 D), suggesting that heme catabolism by HO-1 confers tolerance to *Plasmodium* infection in *Hb*^{SAD} mice.

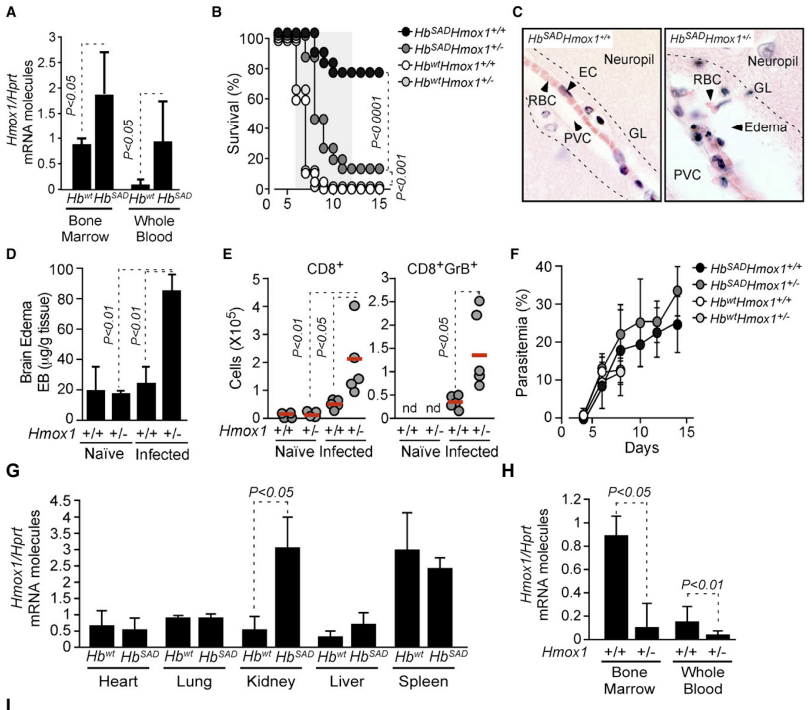

Figure 4.4. HO-1 Mediates the Protective Effect of *Hb*^{SAD} Against ECM (A) Mean ratio of *Hmox1 versus* hypoxanthine-guanine phosphoribosyltransferase (*Hprt*) mRNA molecules in naïve *Hb*^{wt} and *Hb*^{SAD} mice ± standard deviation (n=4/group). **(B)** Survival of *P. berghei* ANKA infected *Hb*^{wt}*Hmox1*$^{+/+}$ (n=19), *Hb*^{SAD}*Hmox1*$^{+/+}$ (n =13), *Hb*^{wt}*Hmox1*$^{+/-}$ (n =15) and *Hb*^{SAD}*Hmox1*$^{+/-}$ (n = 15) mice (three independent experiments; survival advantage p<0.05). Grey shading: expected time of ECM. **(C)** Representative H&E stained micro-vessel in the brain of infected *Hb*^{SAD}*Hmox1*$^{+/+}$ and *Hb*^{SAD}*Hmox1*$^{+/-}$ mice, at ECM onset in *Hb*^{SAD}*Hmox1*$^{+/-}$ mice (n=3/group). EC: endothelial cells; PVC: perivascular compartment; GL: glia limitans (dotted line); RBC: red blood cells. Magnification: 100x. **(D)** Mean brain edema in naïve *versus* infected *Hb*^{SAD}*Hmox1*$^{+/+}$ and *Hb*^{SAD}*Hmox1*$^{+/-}$ mice, at ECM onset in *Hb*^{SAD}*Hmox1*$^{+/-}$ mice ± standard deviation (n=3-4/group). **(E)** CD8^{+} T cells and activated GrB^{+}CD8^{+} T cells in brains of naïve *versus* infected *Hb*^{SAD}*Hmox1*$^{+/+}$ and *Hb*^{SAD}*Hmox1*$^{+/-}$ mice, at the time of ECM onset in *Hb*^{SAD}*Hmox1*$^{+/-}$ mice. Dots represent single mice (n = 4–5/group). Red lines represent mean values. nd: not determined. **(F)** Mean percentage of infected RBC (parasitemia) in the same mice as in **(B)**. **(G)** Mean ratio of *Hmox1 versus* hypoxanthine-guanine phosphoribosyltransferase (*Hprt*) mRNA molecules in different organs of naïve *Hb*^{wt} and *Hb*^{SAD} mice ± standard deviation (n=4/group), **(H)** bone marrow and peripheral blood leukocytes of naïve *Hb*^{SAD}*Hmox1*$^{+/+}$ and *Hb*^{SAD}*Hmox1*$^{+/-}$ mice ± standard deviation (n=4). **(I)** bone marrow and peripheral blood leukocytes of naïve *Hb*$^{A/a}$ and *Hb*$^{a/a}$ mice ± standard deviation (n=4) Notice in **(I)** the lack of up-regulation of *Hmox1* mRNA expression in *Hb*$^{A/a}$ *versus* *Hb*$^{a/a}$ mice. Notice in **(H)** the significant decrease in the levels of *Hmox1* mRNA expression in *Hb*^{SAD} mice with only one (*Hmox1*$^{+/-}$) *versus* two (*Hmox1*$^{+/+}$) functional *Hmox1* alleles.

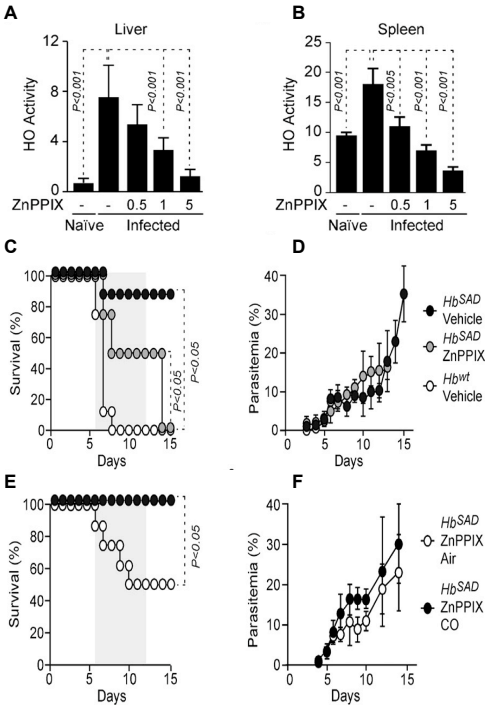

Figure 4.5. Pharmacologic Inhibition of HO Activity Negates the Protective Effect of Sickle Hb Against ECM. HO activity was measured in **(A)** liver and **(B)** spleen of naïve or *P. berghei* ANKA infected Hb^{wt} mice receiving the HO enzymatic inhibitor ZnPPIX (mg/kg bw, every 12 hours from day 2 pre-infection to day 7 postinfection) or vehicle (-). Results are shown as mean percentage of HO enzymatic activity (pmol bilirubin/mg protein/h) ± standard deviation (n=5 mice/group). **(C)** Survival of *P. berghei* ANKA infected Hb^{SAD} mice receiving vehicle (n=8) or ZnPPIX (5mg/kg bw) as in **(A)** and **(B)** (n=8). Vehicle-treated *P. berghei* ANKA infected Hb^{wt} mice were used as controls (n=8). Results shown were pooled from 2 independent experiments with similar results. **(D)** Mean percentage of infected RBC (parasitemia) in infected Hb^{SAD} mice receiving vehicle (n=8) or ZnPPIX (n=8) and in vehicle-treated Hb^{wt} mice (n=8) ± standard deviation. **(E)** Survival of *P. berghei* ANKA infected Hb^{SAD} mice receiving ZnPPIX as in **(A)** and **(B)** and exposed to air (n=8) or CO (250 ppm, 4-7 days postinfection) (n=8). Results shown were pooled from 2 independent experiments with similar results. **(F)** Mean percentage of infected RBC (parasitemia) in the same mice as **(E)**. Grey shadings in panels **(C)** and **(E)** indicate the expected time of ECM.

3.4 Induction of HO-1 by Sickle Hb Inhibits the Production Of Chemokines Involved in the Pathogenesis of ECM

Several chemokines can contribute to the pathogenesis of ECM and presumably to that of human CM[22,29,38]. Expression of mRNA encoding *Ccl2* (*Mcp-1*), *Ccl3* (*MIP1*α), *Ccl5* (*Rantes*), and *Cxcl10* (*Ip-10*) were decreased in the brain of Hb^{SAD} mice that did not develop ECM *versus* Hb^{wt} mice that succumbed to ECM (Figure 4.6 A). This inhibitory effect involved HO-1, since expression of mRNA encoding these chemokines was increased in the brain of infected $Hb^{SAD}Hmox1^{+/-}$ *versus* $Hb^{SAD}Hmox1^{+/+}$ (Figure 4.6 A). The involvement of CXCL10/IP-10 in the pathogenesis of ECM[38] suggests that its inhibition might contribute functionally to the protective effect of Hb^{SAD} against

ECM. Expression of mRNAs encoding other chemokines, such as *Cxcl11* (*Ip-9*) or the chemokine receptors *Ccr2* and *Cxcr3* was also inhibited by Hb^{SAD} but in a manner that was not impaired in $Hb^{SAD}Hmox1^{+/-}$ *versus* $Hb^{SAD}Hmox1^{+/+}$ mice (Figure 4.6 B). This suggests that the inhibitory effect of Hb^{SAD} over the expression of these genes, probably does not involve HO-1. Expression of mRNA encoding the chemokine *Ccl19* (*MIP-3*β) and the chemokines receptor *Ccr7* was not modulated by Hb^{SAD} and/or did not involve HO-1 (Figure 4.6 C). This was also the case for several other genes previously involved or not in the pathogenesis of ECM (Figure 4.6 D to G). Of note is the HO-1 independent marked suppression of cytokines and molecules mainly produced by innate immune cells such as NOS2, IL-1β, IL-6 and TNF, as well as perforin, FasL, GrB, IFNγ and CTLA4, markers of $CD4^+$ and $CD8^+$ T cell activation and/or effector function. This finding suggests that Hb^{SAD} exerts immunosuppressive effects that are independent of HO-1 expression.

3.5 Sickle Hb Confers Tolerance to *Plasmodium* Infection via HO-1 Expression in Hematopoietic Cells

We performed syngenic bone marrow transplants from $Hb^{SAD}Hmox1^{+/+}$ or $Hb^{SAD}Hmox1^{+/-}$ mice into lethally irradiated $Hb^{wt}Hmox1^{+/+}$ or $Hb^{wt}Hmox1^{+/-}$ mice to generate chimeric Hb^{SAD} mice in which one *Hmox1* allele is deleted in the hematopoietic ($Hb^{SAD}Hmox1^{+/-} \rightarrow Hb^{wt}Hmox1^{+/+}$) or nonhematopoietic ($Hb^{SAD}Hmox1^{+/+} \rightarrow Hb^{wt}Hmox1^{+/-}$) compartment. Chimeric Hb^{SAD} mice carrying two functional *Hmox1* alleles in the hematopoietic and in the nonhematopoietic compartments ($Hb^{SAD}Hmox1^{+/+} \rightarrow$

Hb^{wt}*Hmox1*$^{+/+}$) did not succumb to ECM (Figure 4.7 A) or develop brain edema (Figure 4.7 B) in response to *P. berghei* ANKA infection. Control chimeric mice in which the bone marrow of *Hb*^{wt}*Hmox1*$^{+/+}$ mice was transferred into lethally irradiated *Hb*^{SAD}*Hmox1*$^{+/+}$ mice, develop ECM (Figure 4.7 A) and brain edema (Figure 4.7 B), confirming that cells derived from the hematopoietic compartment confer the protective effect of *Hb*^{SAD}. Chimeric *Hb*^{SAD} mice carrying a single functional *Hmox1* allele in hematopoietic cells (*Hb*^{SAD}*Hmox1*$^{+/-}$→*Hb*^{wt}*Hmox1*$^{+/+}$) succumbed to ECM (Figure 4.7 A), developing brain edema (Figure 4.7 B). The reverse was not true in that deletion of a single *Hmox1* allele in nonhematopoietic cells (*Hb*^{SAD}*Hmox1*$^{+/+}$→*Hb*^{wt}*Hmox1*$^{+/-}$) did not impair the protective effect of *Hb*^{SAD} against ECM (Figure 4.7 A), confirmed by lack of brain edema (Figure 4.7 B). Similar results were obtained when transferring bone marrows from *Hb*^{SAD}*Hmox1*$^{+/+}$ or *Hb*^{SAD}*Hmox1*$^{+/-}$ mice into *Hb*^{SAD}*Hmox1*$^{+/+}$ or *Hb*^{SAD}*Hmox1*$^{+/-}$ mice (Figure 4.7 D to F). Lethality after day 12 postinfection (Figure 4.7 A) was most probably due to the development of a ‘‘composite disease’’ in which high levels of parasitemia (>20%) synergize with sickle human Hb to cause death, without overt clinical or pathological signs of ECM. These observations reveal that the protective effect of *Hb*^{SAD} requires the induction of HO-1 expression in hematopoietic cells, consistent with the observed induction of HO-1 expression in blood and bone marrow cells of naïve *Hb*^{SAD} mice (Figure 4.4 A). The protective effect of HO-1 expression in the hematopoietic compartment was not associated with modulation of pathogen load (Figure 4.7 C and F), confirming that HO-1 affords tolerance to *Plasmodium* infection.

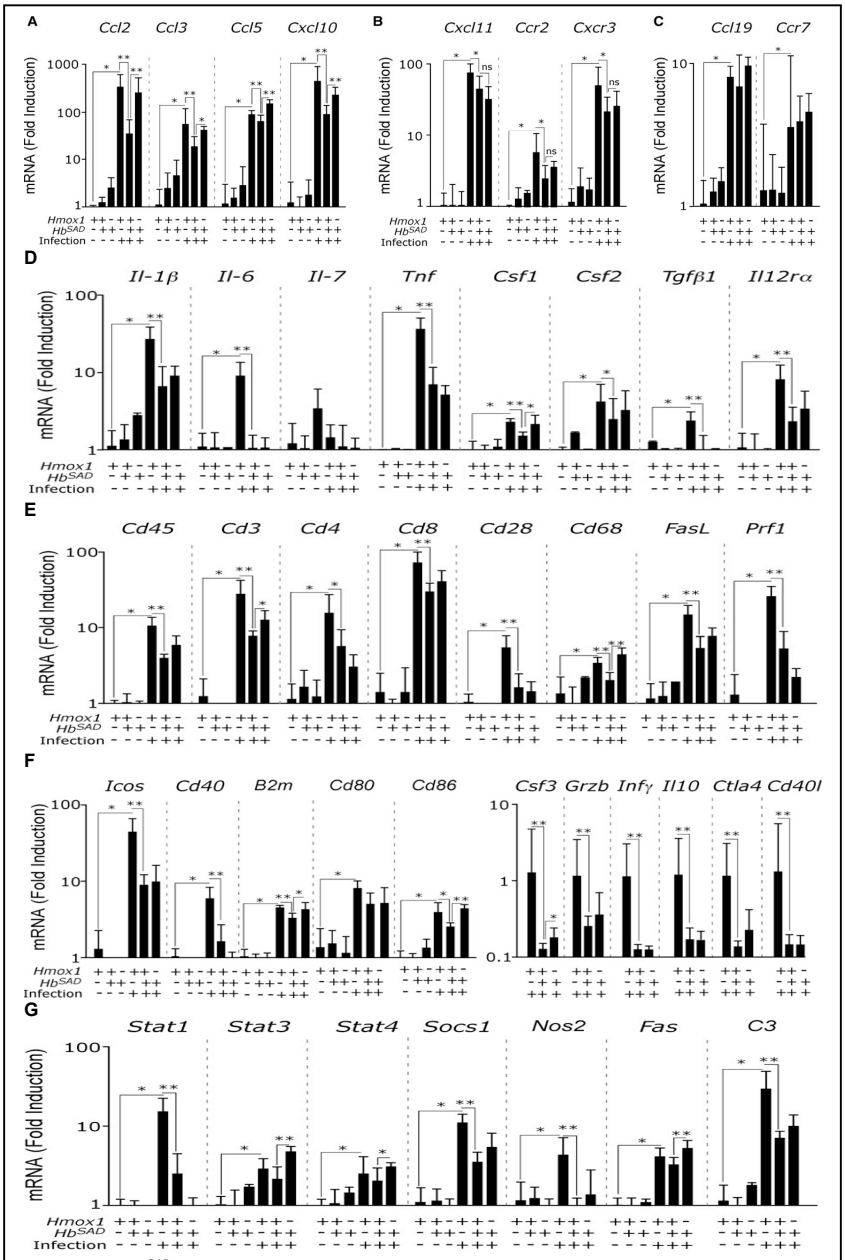

Figure 4.6. *Hb^{SAD}* Inhibits Proinflammatory Molecules Expression in the Brain. (A, B and C) Quantification of mRNA encoding chemokines and chemokine receptors in the brains of naïve (-) and *P. berghei* ANKA infected (+) mice carrying one (-) or two (+) functional *Hmox1* alleles and expressing (+) *Hb^{SAD}* or not (-). Results are shown as mean fold induction over naïve *Hb^{wt}Hmox1$^{+/+}$* mice ± standard deviation (n = 4-8/group), analyzed at ECM onset in *Hb^{wt}* or *Hb^{SAD}Hmox1$^{+/-}$* control groups. **(A)** Genes inhibited by *Hb^{SAD}* under the control of HO-1. **(B)** Genes inhibited by *Hb^{SAD}*, presumably not under the control of HO-1. **(C)** Genes not regulated by *Hb^{SAD}*. **(D)** cytokines, **(E)** molecules expressed by leukocytes, **(F and G)** co-stimulatory molecules, T cell effector molecules, signaling molecules. Notice that inhibition of proinflammatory gene expression in *P. berghei* ANKA infected *Hb^{SAD} versus Hb^{wt}* mice is similar whether the *Hb^{SAD}* mice have one (-) or two (+) functional *Hmox1* alleles. *p < 0.05; **p < 0.01; ns P > 0.05.

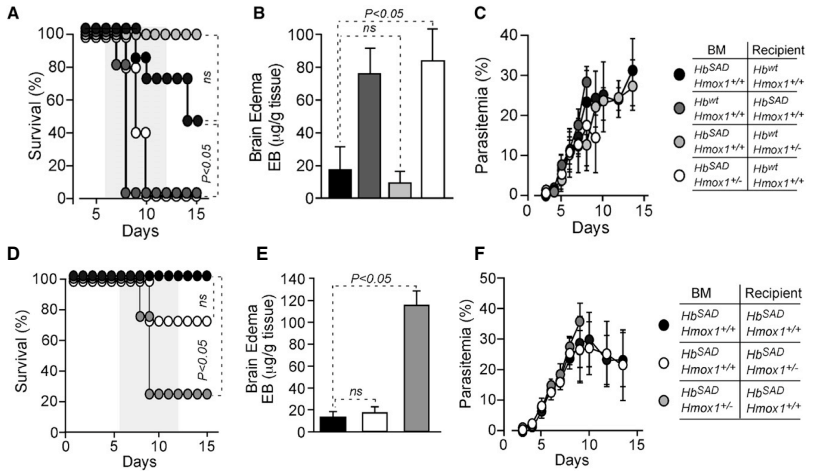

Figure 4.7. The Protective Effect of Sickle Hb Against ECM Involves the Expression of HO-1 in Hematopoietic Cells (A) Survival of *P. berghei* ANKA infected chimeric mice resulting from the adoptive transfer of bone marrow from $Hb^{SAD}Hmox1^{+/+}$ mice into $Hb^{wt}Hmox1^{+/+}$ recipients (n = 6); from $Hb^{wt}Hmox1^{+/+}$ mice into $Hb^{SAD}Hmox1^{+/+}$ recipients (n = 5); from $Hb^{SAD}Hmox1^{+/+}$ mice into $Hb^{wt}Hmox1^{+/-}$ recipients (n = 8) and from $Hb^{SAD}Hmox1^{+/-}$ into $Hb^{wt}Hmox1^{+/+}$ recipients (n = 7). Recipients were lethally irradiated before the adoptive transfer. Grey shading indicates expected time of ECM. Pooled from four independent experiments. **(B)** Mean brain edema ± standard deviation (n = 3/group) in chimeric mice, produced as in **(A)**. **(C)** Mean percentage of infected RBC in chimeric mice ± standard deviation, same mice as in **(A)**. **(D)** Survival of *P. berghei* ANKA infected chimeric Hb^{SAD} mice resulting from the adoptive transfer of bone marrows from $Hb^{SAD}Hmox1^{+/+}$ mice into $Hb^{SAD}Hmox1^{+/+}$ recipients (n=6); from $Hb^{SAD}Hmox1^{+/+}$ mice into $Hb^{SAD}Hmox1^{+/-}$ recipients (n=7) and from $Hb^{SAD}Hmox1^{+/-}$ mice into $Hb^{SAD}Hmox1^{+/+}$ recipients (n=8). Results shown were pooled from 5 independent experiments. **(E)** Brain edema was measured by Evans blue (EB) accumulation in brains of chimeric mice, produced as in **(D)**. Results are shown as mean ± standard deviation (n=3/group). **(F)** Mean percentage of infected RBC in chimeric mice, produced as in **(D)**. Results are shown as mean ± standard deviation. Same mice as in **(D)**.

3.6 Sickle Hb Inhibits the Activation/Expansion of CD8+ T Cells Recognizing Antigens Expressed by *Plasmodium*

The number of splenic $CD8^+$ T cells recognizing specifically a MHC I-restricted epitope derived from glycoprotein B ($gB_{498-505}$) of herpes simplex virus-1 expressed by transgenic *P. berghei* ANKA[39] was reduced in Hb^{SAD} *versus* Hb^{wt} mice, as assessed five days after infection (Figure 4.8 A and C). The number of splenic GrB^+CD8^+ T cells was also reduced in Hb^{SAD} *versus* Hb^{wt} mice five days after infection (Figure 4.8 B and D). This reveals that Hb^{SAD} prevents overt expansion of pathogenic

$CD8^+$ T cells, an effect that should contribute to the protective effect of Hb^{SAD} against ECM[31,39]. We then asked whether this immunoregulatory effect of Hb^{SAD} involved the expression of HO-1. The number of $gB_{498-505}$-specific $CD8^+$ T cells and GrB^+CD8^+ T cells was not different in the spleen of $Hb^{SAD}Hmox1^{+/-}$ *versus* $Hb^{SAD}Hmox1^{+/+}$ mice five days after infection (Figures 4.8 A to D). This suggests that Hb^{SAD} controls the activation and/or expansion of splenic $CD8^+$ T cells, via a mechanism that probably does not involve HO-1.

3.7 Sickle Hb Induces HO-1 Expression via a Mechanism Involving Nrf2

Given that Nrf2 plays a central role in the transcriptional regulation of HO-1 expression[17] we asked whether induction of HO-1 expression in whole blood leukocytes of naïve Hb^{SAD} mice (Figure 4.4 A) involved this transcription factor. Deletion of one Nrf2 allele in Hb^{SAD} mice ($Hb^{SAD}Nrf2^{+/-}$) was sufficient to reduce the level of *Hmox1* mRNA expression in whole blood leukocytes, to those of naïve $Hb^{wt}Nrf2^{+/+}$ mice (Figure 4.9 A). This suggests that sickle Hb induces *Hmox1* transcription and expression via a mechanism involving Nrf2. Incidence of ECM increased significantly in *P. berghei* ANKA infected $Hb^{SAD}Nrf2^{+/-}$ *versus* $Hb^{SAD}Nrf2^{+/+}$ mice (Figure 4.9 B), confirmed by the development of brain edema (Figure 4.9 C). A similar effect was observed in a limited number of Hb^{SAD} mice in which both Nrf2 alleles were functionally deleted, i.e. $Hb^{SAD}Nrf2^{-/-}$ mice (n=5; 20% survival). It should be noted that deletion of both Nrf2 alleles in Hb^{SAD} mice lead to overt postnatal lethality (Table 4.2 B). Loss of protection against ECM in $Hb^{SAD}Nrf2^{+/-}$ *versus* $Hb^{SAD}Nrf2^{+/+}$ mice was not associated with a regain of $CD8^+$ T cell activation and/or

expansion in the spleen, as assessed five days after infection (Figure 4.10 A to D).

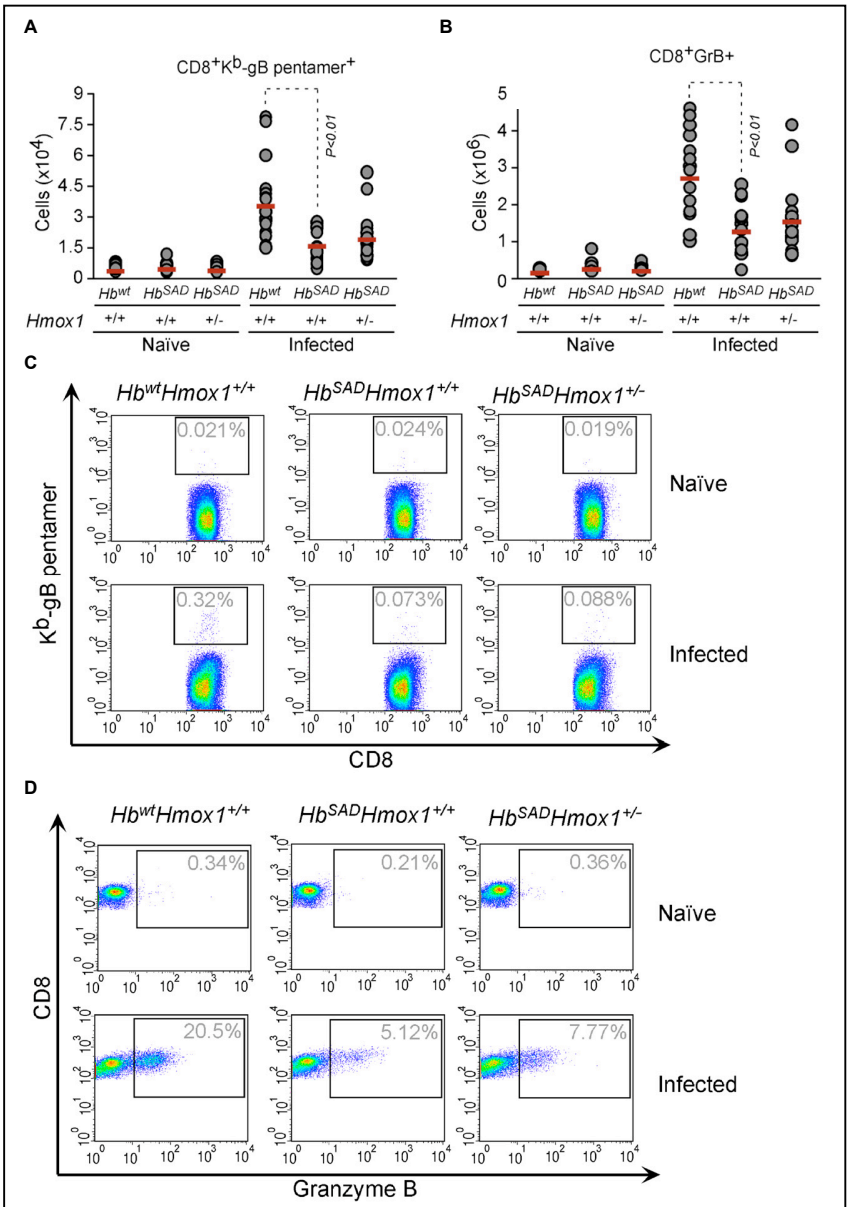

Figure 4.8. The Immunoregulatory Effect of Sickle Hb Does not Depend on Expression of HO-1. **(A)** Number of splenic CD8$^+$ T cells specific for $gB_{498\text{-}505}$ in *Hb^{wt}Hmox1$^{+/+}$*, *Hb^{SAD}Hmox1$^{+/+}$* and *Hb^{SAD}Hmox1$^{+/-}$* naïve mice or 5 days after *P. berghei* ANKA infection. **(B)** Number of splenic CD8$^+$GrB$^+$ T in the same mice as in **(A)**. Circles in **(A)** and **(B)** represent single mice and red lines mean values (n=10 and n=16 in naïve and infected groups, respectively), data pooled from 4 independent experiments with similar results. **(C)** Representative flow cytometry dot plots of CD8$^+$ T cells specific for the *P. berghei* ANKA encoded MHC I-restricted epitope derived from glycoprotein B of herpes simplex virus-1 ($gB_{498\text{-}505}$) in the spleen of *Hb^{wt}Hmox1$^{+/+}$*, *Hb^{SAD}Hmox1$^{+/+}$* and *Hb^{SAD}Hmox1$^{+/+}$* mice not infected or 5 days after *P. berghei* ANKA infection **(D)** Representative flow cytometry dot plots of CD8$^+$GrB$^+$ T cells, in the spleen of *Hb^{wt}Hmox1$^{+/+}$*, *Hb^{SAD}Hmox1$^{+/+}$* and *Hb^{SAD}Hmox1$^{+/+}$* mice not infected or 5 days after *P. berghei* ANKA infection. Numbers in gray indicate the percentage of cells inside the gates.

This suggests that the immunoregulatory effect of *Hb*^{SAD} probably does not involve Nrf2 (Figure 4.10 A to D), which is consistent with the observation that this effect also does not seem to involve HO-1, a gene regulated by *Hb*^{SAD} via Nrf2.

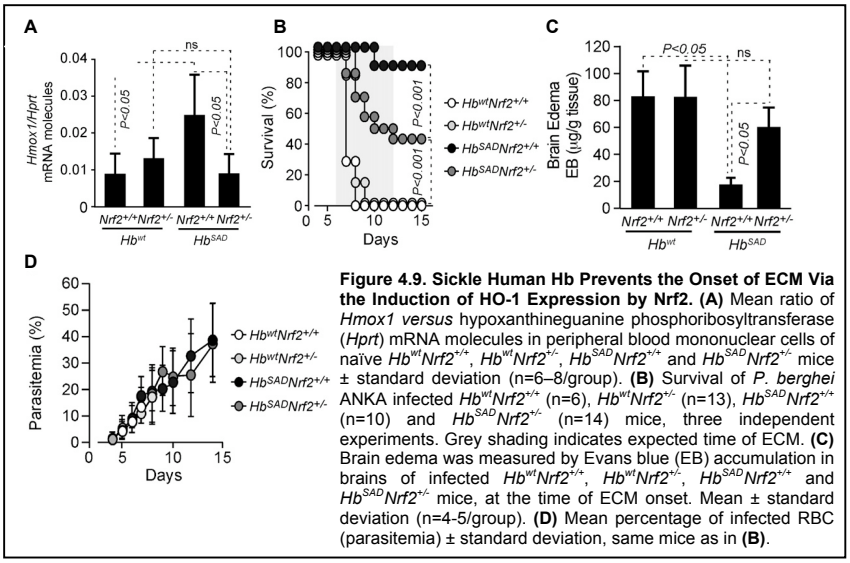

Figure 4.9. Sickle Human Hb Prevents the Onset of ECM Via the Induction of HO-1 Expression by Nrf2. (A) Mean ratio of *Hmox1 versus* hypoxanthineguanine phosphoribosyltransferase (*Hprt*) mRNA molecules in peripheral blood mononuclear cells of naïve *Hb*^{wt}*Nrf2*$^{+/+}$, *Hb*^{wt}*Nrf2*$^{+/-}$, *Hb*^{SAD}*Nrf2*$^{+/+}$ and *Hb*^{SAD}*Nrf2*$^{+/-}$ mice ± standard deviation (n=6–8/group). **(B)** Survival of *P. berghei* ANKA infected *Hb*^{wt}*Nrf2*$^{+/+}$ (n=6), *Hb*^{wt}*Nrf2*$^{+/-}$ (n=13), *Hb*^{SAD}*Nrf2*$^{+/+}$ (n=10) and *Hb*^{SAD}*Nrf2*$^{+/-}$ (n=14) mice, three independent experiments. Grey shading indicates expected time of ECM. **(C)** Brain edema was measured by Evans blue (EB) accumulation in brains of infected *Hb*^{wt}*Nrf2*$^{+/+}$, *Hb*^{wt}*Nrf2*$^{+/-}$, *Hb*^{SAD}*Nrf2*$^{+/+}$ and *Hb*^{SAD}*Nrf2*$^{+/-}$ mice, at the time of ECM onset. Mean ± standard deviation (n=4-5/group). **(D)** Mean percentage of infected RBC (parasitemia) ± standard deviation, same mice as in **(B)**.

The protective effect of *Hb*^{SAD} against lung and liver injury associated to *P. berghei* ANKA infection was lost in *Hb*^{SAD}*Nrf2*$^{+/-}$ *versus Hb*^{SAD}*Nrf2*$^{+/+}$ mice (Figure 4.2). This was not associated with increased parasite load in *Hb*^{SAD}*Nrf2*$^{+/-}$ *versus Hb*^{SAD}*Nrf2*$^{+/+}$ mice (Figure 4.9 D), which is consistent with the notion that induction of HO-1 expression by Nrf2 confers tolerance to *Plasmodium* infection.

3.8 Sickle Hb Confers Tolerance to *Plasmodium* Infection via a Mechanism Involving CO Produced through Heme Catabolism by HO-1

Consistent with similar observations in individuals carrying the HbS mutation in the homozygous[6] or heterozygous[7] form, naïve *Hb*^{SAD} mice had higher concentration of free heme in

plasma, as compared to age-matched control naïve Hb^{wt} mice (Figure 4.11 A). Herein, free heme is defined as heme molecules not contained within the heme pockets of hemoglobin. When pre-exposed *in vitro* to low levels of free heme cells are protected against a subsequent heme challenge[11]. We asked whether free heme would exert a similar protective effect *in vivo*. Administration of free heme to Hb^{wt} mice prior to *P. berghei* ANKA infection suppressed ECM incidence, as compared to vehicle-treated Hb^{wt} mice (Figure 4.11 B).

The protective effect of heme was dose-dependent, with higher dosage leading to (1) increased HO-1 expression in whole blood cells (Figure 4.13 A) and spleen (Figure 4.13 B) and to a lesser extent in the bone marrow (Figure 4.13 C) and (2) suppression of ECM (Figure 4.13 D). This protective effect was not associated with modulation of parasitemia (Figure 4.13 D), suggesting that low concentration of free heme in the plasma of naïve Hb^{SAD} mice (Figure 4.11 A) can confer tolerance to *Plasmodium* infection.

We asked whether accumulation of low levels of free heme in Hb^{SAD} contributes to the immunoregulatory effect exerted by Hb^{SAD} on $CD8^+$ T cells (Figures 4.8 A to D). Administration of free heme to Hb^{wt} mice, prior to infection with transgenic *P. berghei* ANKA expressing $gB_{498\text{-}505}$, reduced the number of splenic $gB_{498\text{-}505}$-specific $CD8^+$ T cells (Figures 4.14 A and C) as well as GrB^+CD8^+ T cells, as compared to vehicle treated Hb^{wt} mice five days after infection (Figures 4.14 B and D). This supports further the notion that the protective effect of Hb^{SAD} against ECM is mediated, to a large extent, via the accumulation of low levels of circulating free heme.

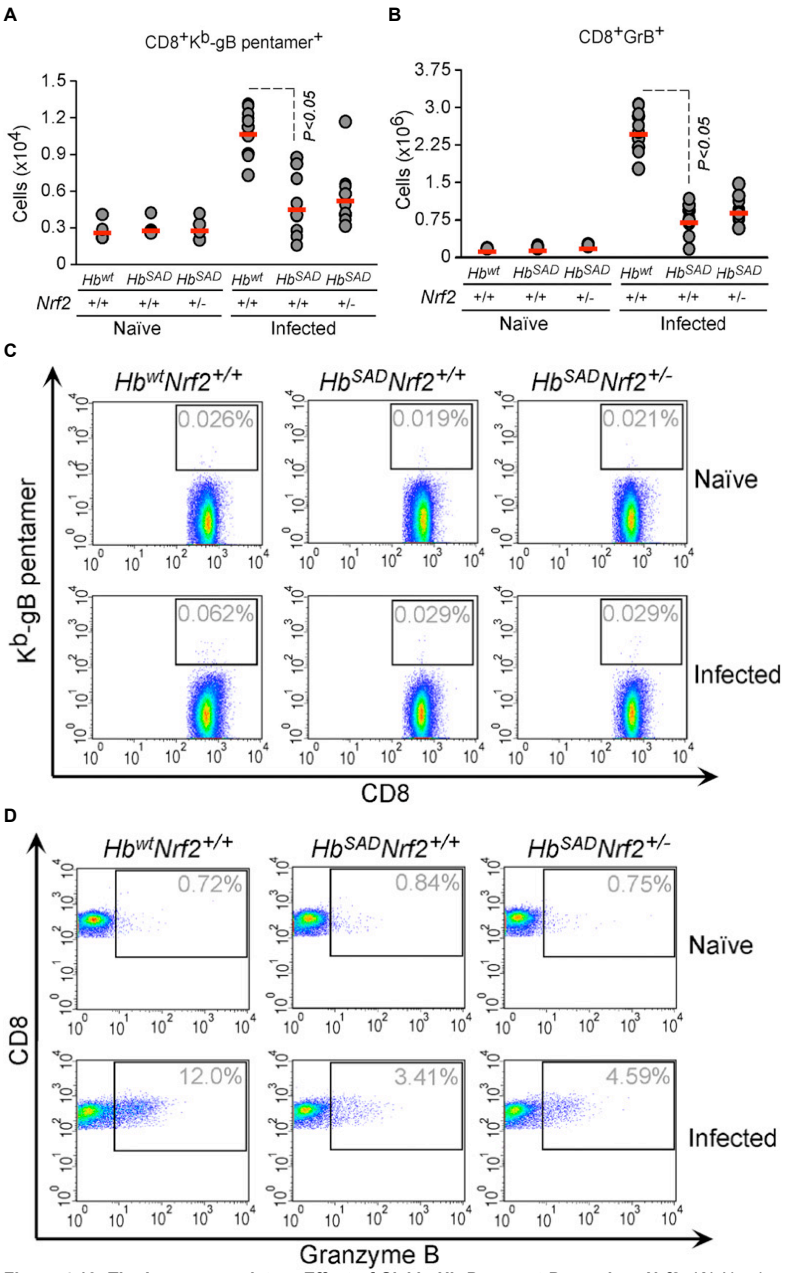

Figure 4.10. The Immunoregulatory Effect of Sickle Hb Does not Depend on Nrf2. (A) Number of $CD8^+$ T cells specific for the *P. berghei* ANKA-encoded MHC I restricted epitope derived from glycoprotein B of herpes simplex virus-1 ($gB_{498-505}$), in the spleen of $Hb^{wt}Nrf2^{+/+}$, $Hb^{SAD}Nrf2^{+/+}$ and $Hb^{SAD}Nrf2^{+/-}$ mice not-infected (naïve) or 5 days after *P. berghei* ANKA infection. **(B)** Number of splenic $CD8^+GrB^+$ T cells in the same mice as in **(A)**. **(C)** Representative flow cytometry dot plots of splenic $CD8^+$ T cells recognizing the $gB_{498-505}$ epitope in the same mice as in **(A)**. **(D)** Representative flow cytometry dot plots of splenic $CD8^+GrB^+$ T cells in the same mice as in **(A)**. Circles in **(A)** and **(B)** represent single mice and red lines mean values (n=4 and n=10 in noninfected and infected groups, respectively), pooled from 2 independent experiments with similar results. Numbers in gray **(C)** and **(D)** indicate the percentage of cells inside the gates.

Plasma free heme concentration increased significantly

following *P. berghei* ANKA infection in Hb^{wt} mice (Figure 4.11 A), an effect we have previously shown to contribute in a critical manner to the pathogenesis of ECM[14,21]. Albeit less pronounced this increase was also observed in Hb^{SAD} mice (Figure 4.11 A). When challenged with free heme after infection, Hb^{SAD} succumbed to ECM (Figure 4.11 C), confirmed by the occurrence of brain edema (Figure 4.11 D). This reveals that free heme has a dual effect in the control of ECM onset, being protective when present at slightly above normal concentration before infection (Figure 4.11 B) while highly pathogenic when present at higher levels after infection (Figure 4.11 C). Free heme did not interfere with pathogen load (Figures 4.13 E and F), revealing that when present at slightly above normal concentration before infection free heme promotes tolerance to malaria, while impairing tolerance to malaria when present at higher concentrations after infection. Heme administration at the same dosage and schedule to naïve Hb^{wt} or Hb^{SAD} mice did not result in lethality (data not shown). When applied via inhalation to wild type mice, CO suppresses the pathogenesis of ECM via a mechanism that relies on the inhibition of heme release from Hb[21]. We asked whether the protective effect of Hb^{SAD} against ECM was mediated via this mechanism. Inhaled CO suppressed the incidence of ECM in $Hb^{SAD}Hmox1^{+/-}$ mice (Figure 4.11 E), confirmed by the lack of brain edema (Figure 4.11 F). A similar protective effect was observed when CO was applied to *P. berghei* infected Hb^{SAD} mice treated with the enzymatic HO inhibitor ZnPPIX (Figures 4.5 E and F).

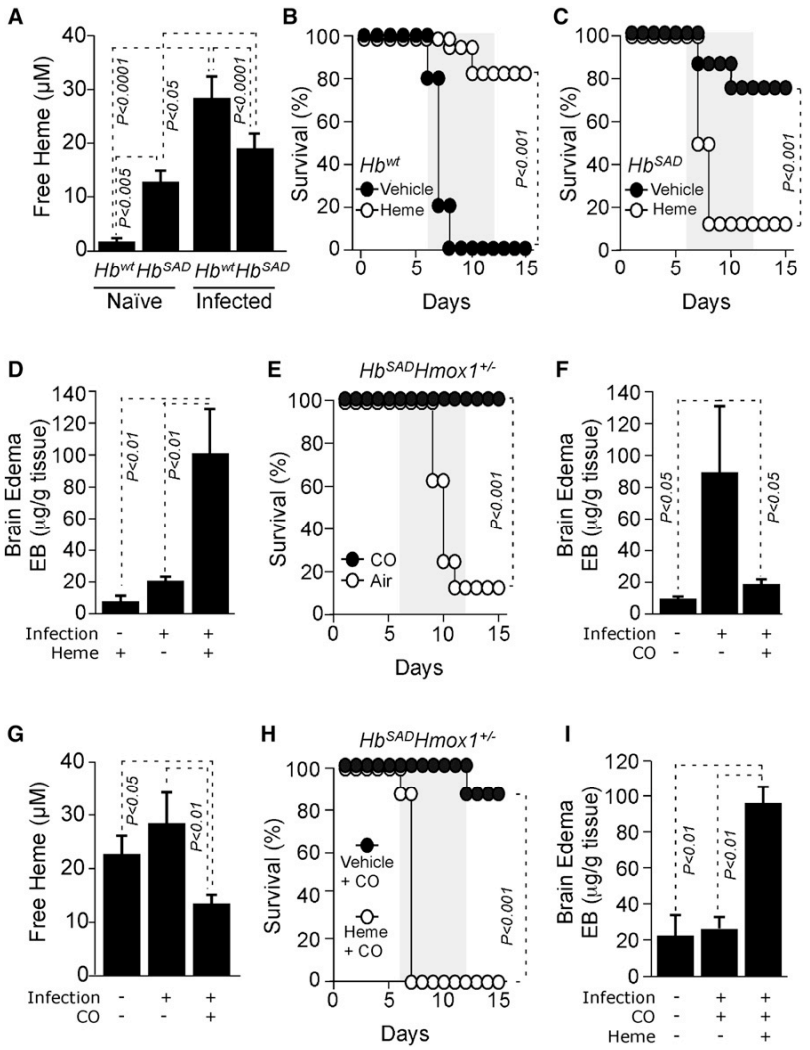

Figure 4.11. Hb^{SAD} Inhibits Free Heme Accumulation Via the Production of CO. (A) Mean plasma free heme concentration in naïve *versus P. berghei* ANKA infected Hb^{wt} and Hb^{SAD} mice at ECM onset in Hb^{wt} mice ± standard deviation (n=4–15/group). **(B)** Survival of infected Hb^{wt} mice receiving vehicle (n=25) or heme (35–40 mg/kg, every 48 hr, day 2 preinfection to 4 postinfection) (n=17). Pooled from four independent experiments, with similar results. **(C)** Survival of infected Hb^{SAD} mice receiving vehicle (n=8) or heme (20 mg/kg, every 12 hr, day 4–7 postinfection) (n=8). Pooled from two independent experiments, with similar results. **(D)** Mean brain edema in Hb^{SAD} mice treated as in **(C)** at ECM onset in heme-treated Hb^{SAD} mice ± standard deviation (n=4/group). **(E)** Survival of infected $Hb^{SAD}Hmox1^{+/-}$ mice exposed to air (n=8) or CO (250 ppm, days 4-7 post infection) (n=12). Pooled from three independent experiments, with similar results. **(F)** Mean brain edema in $Hb^{SAD}Hmox1^{+/-}$ mice treated as in **(E)**, at ECM onset in air-treated mice ± standard deviation (n=3–4/group). **(G)** Mean free heme in plasma of $Hb^{SAD}Hmox1^{+/-}$ mice treated as in **(E)** ± standard deviation (n=4–6/group). **(H)** Survival of infected $Hb^{SAD}Hmox1^{+/-}$ mice exposed to CO (250ppm; days 4–7 postinfection) and receiving vehicle (n=8) or heme (20 mg/kg, every 12 hr, days 4–7 postinfection) (n=8). Pooled from two independent experiments, with similar results. **(I)** Mean brain edema in $Hb^{SAD}Hmox1^{+/-}$ mice treated as in **(H)**, at ECM onset in heme-treated mice ± standard deviation (n=3–4/group). Grey shading in **(B, C, E, and H)** indicates expected time of ECM.

CO did not modulate parasitemia (Figures 4.12 B and C).

Instead, its protective effect was associated with reduction of plasma free heme concentration, below that of naïve *Hb*^{SAD}*Hmox1*$^{+/-}$ mice (Figure 4.11 G). Administration of free heme to infected *Hb*^{SAD}*Hmox1*$^{+/-}$ mice abrogated the protective effect of CO, restoring ECM incidence (Figure 4.11 H), confirmed by brain edema (Figure 4.11 I). Heme was not toxic when administered at the same dosage and schedule to naïve *Hb*^{SAD}*Hmox1*$^{+/-}$ mice receiving CO, i.e. 0% mortality. These observations demonstrate that sickle Hb suppresses the onset of ECM via the induction of HO-1 and the production of CO, which inhibits the accumulation of free heme thus affording tolerance to *Plasmodium* infection (Figure 4.15).

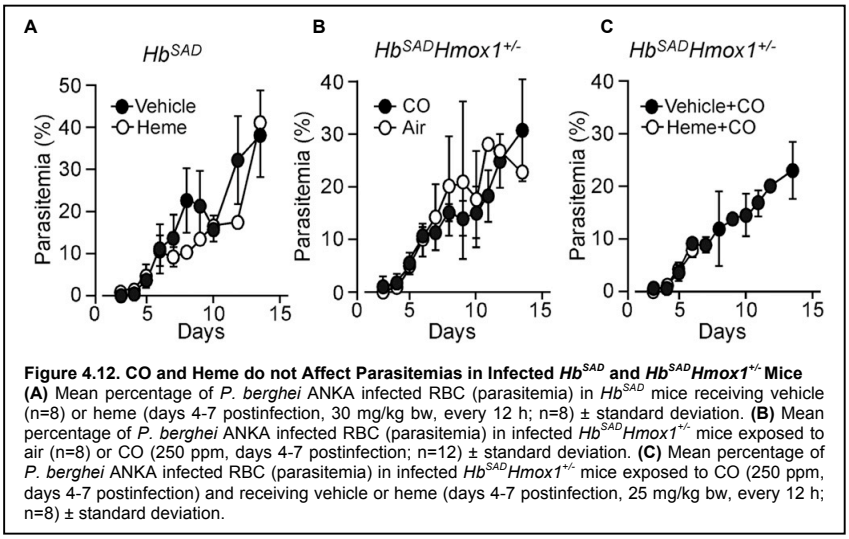

Figure 4.12. CO and Heme do not Affect Parasitemias in Infected *Hb*^{SAD} and *Hb*^{SAD}*Hmox1*$^{+/-}$ Mice
(A) Mean percentage of *P. berghei* ANKA infected RBC (parasitemia) in *Hb*^{SAD} mice receiving vehicle (n=8) or heme (days 4-7 postinfection, 30 mg/kg bw, every 12 h; n=8) ± standard deviation. **(B)** Mean percentage of *P. berghei* ANKA infected RBC (parasitemia) in infected *Hb*^{SAD}*Hmox1*$^{+/-}$ mice exposed to air (n=8) or CO (250 ppm, days 4-7 postinfection; n=12) ± standard deviation. **(C)** Mean percentage of *P. berghei* ANKA infected RBC (parasitemia) in infected *Hb*^{SAD}*Hmox1*$^{+/-}$ mice exposed to CO (250 ppm, days 4-7 postinfection) and receiving vehicle or heme (days 4-7 postinfection, 25 mg/kg bw, every 12 h; n=8) ± standard deviation.

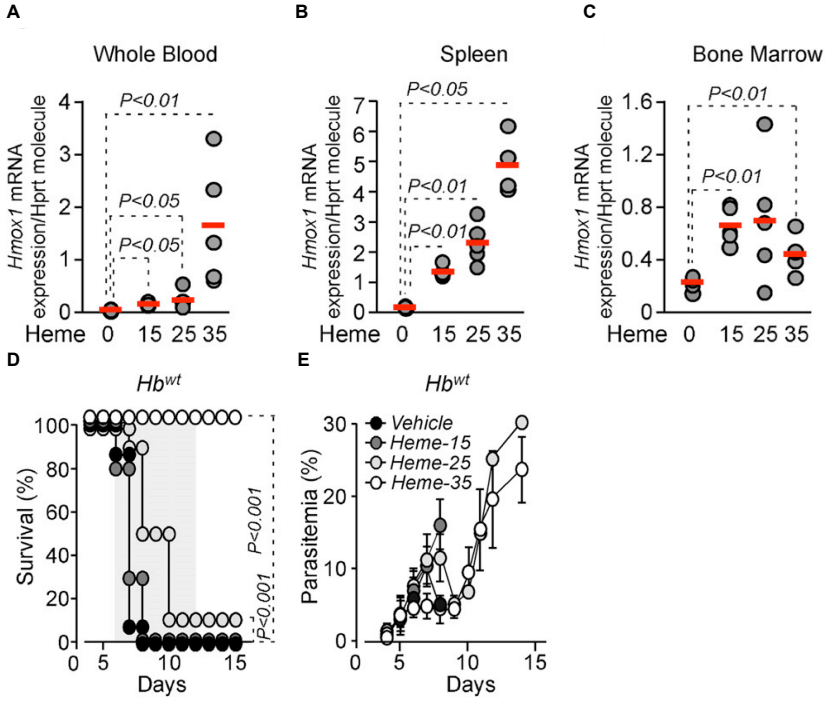

Figure 4.13. Heme Regulates HO-1 Expression and Confers Tolerance to Plasmodium Infection Via CO. *Hmox1* mRNA was measured by qRT-PCR in the **(A)** whole blood **(B)** spleen and **(C)** bone marrow of *Hb*^{wt} mice 12 hours after receiving heme at the dosage indicated (mg/kg bw; i.p.). Circles represent single mice and red lines mean values (n=4-5/group), **(D)** Survival and **(E)** mean percentage ± standard deviation of *P. berghei* ANKA infected RBC (parasitemia) in *Hb*^{wt} mice receiving vehicle (n=15) or heme (mg/kg bw, every 48h, from day 2 pre-infection to 4 postinfection; n=9-10/group). Results shown were pooled from three independent experiments, with similar results.

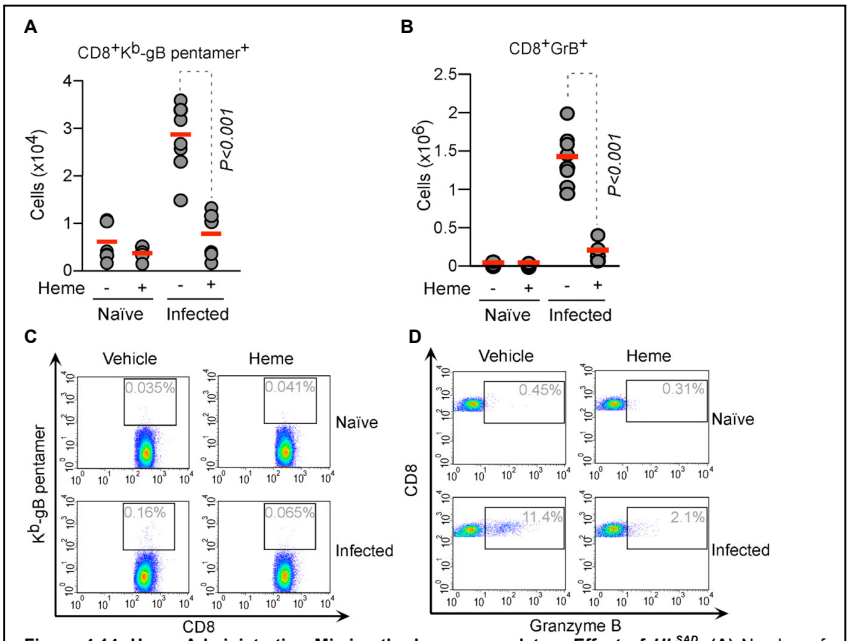

Figure 4.14. Heme Administration Mimics the Immunoregulatory Effect of *Hb^{SAD}*. (A) Number of CD8$^+$ T cells specific for the *P. berghei* ANKA-encoded MHC I-restricted epitope derived from glycoprotein B of herpes simplex virus-1 ($gB_{498-505}$), in the spleen of naïve or infected with *P. berghei* ANKA *Hb^{wt}* mice (5 days postinfection). *Hb^{wt}* received (+) or not (-) heme (35 mg/kg, i.p., every 48h, from day 2 pre-infection to 4 postinfection). **(B)** Number of splenic CD8$^+$GrB$^+$ T cells in the same mice as in **(A). (C)** Representative flow cytometry dot plots of splenic CD8$^+$ T cells recognizing the $gB_{498-505}$ epitope in the same mice as in **(A)**. **(D)** Representative flow cytometry dot plots of splenic CD8$^+$GrB$^+$ T cells in the same mice as in **(C)**. Circles in **(A)** and **(B)** represent single mice and red lines mean values (n=6-8/group), pooled from 2 independent experiments with similar results. Numbers in gray (**C** and **D**) indicate the percentage of cells inside the gates.

4. DISCUSSION

The protective effect of sickle human Hb against malaria is thought to rely on the reduction of parasite load[2,8,26], implying that sickle human Hb affords resistance[35,36] to *Plasmodium* infection. Consistent with this notion, sickle human Hb decreases RBC permissiveness to *Plasmodium* invasion and growth[40,41] while increasing phagocytosis of infected RBC, as assessed *ex vivo*[42]. Whether these effects account for the protective effect of sickle human Hb *in vivo* remained to be established. We used a well-established mouse model of malaria allowing for genetic manipulation of the host, to test *in vivo* the relative contribution of host specific genes to the protective effect of sickle Hb against

Plasmodium infection. For technical and ethical reasons these studies can only be performed in rodent models of malaria.

As demonstrated hereby, sickle Hb affords protection against *Plasmodium* infection in mice (Figure 4.1 A and Figure 4.4), a finding consistent with previous reports using different mouse and *Plasmodium* strains[43,44]. This survival advantage occurs irrespectively of parasite load (Figures 4.1 E and 1F) and is not associated with modulation of parasite sequestering in different organs (Figure 4.3), revealing that sickle human Hb confers tolerance[35,36] to *Plasmodium* infection. This is consistent with our recent observation that heme catabolism by HO-1 also suppresses development of multiple organ dysfunction associated with the pathogenesis of severe sepsis in mice[45], a lethal outcome of polymicrobial infection that resembles, in some aspects, severe malaria[46]. Since the survival advantage conferred by HbS against malaria in human populations can occur without overt decrease of parasite load[32-34], tolerance to *Plasmodium* infection might also operate in individuals expressing sickle Hb.

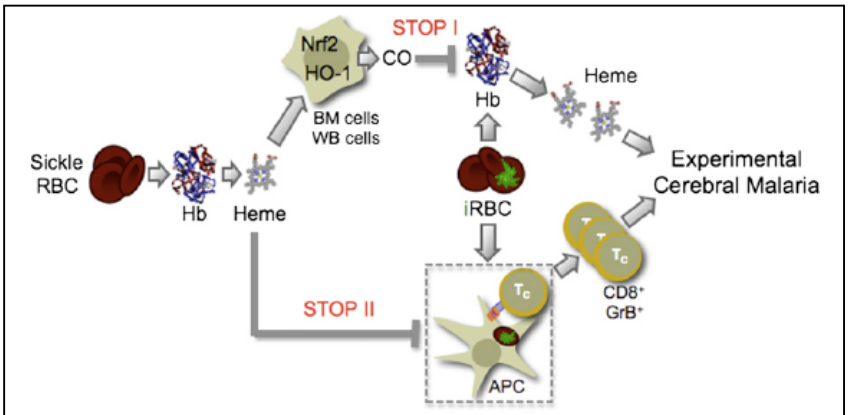

Figure 4.15. Protective Effect of Sickle Hb against ECM. Release of Hb from sickle RBC leads to chronic accumulation of cell-free Hb and release of its heme prosthetic groups. Free heme induces HO-1 expression in bone marrow (BM) and white blood (WB) cells, via a mechanism involving Nrf2. Heme catabolism by HO-1 produces CO that prevents (STOP I) further heme release from the cell-free Hb after *Plasmodium* infection, suppressing the pathogenesis of ECM. Moreover, sickle human Hb exerts an immunoregulatory effect that appears to act independently of Nrf2 and/or HO-1 and that inhibits (STOP II) cytotoxic GrB^+CD8^+ T cells (T_C) activation and expansion. APC: Antigen presenting cell.

We provide evidence for the existence of a specific molecular mechanism via which sickle human Hb confers tolerance to *Plasmodium* infection. When expressed at nonpathological levels in mice, sickle Hb leads to the accumulation of low concentrations of free heme in plasma (Figure 4.11 A). The same is true for individuals carrying the sickle cell trait[7], which affords protection against malaria[1,5,8,9]. Presumably, this is due to the higher rate of heme release from sickle *versus* normal human Hb[10]. In the absence of overt inflammation, free heme induces HO-1 expression without causing cytotoxicity[11,13]. Presumably, this explains how sickle human Hb induces the expression of HO-1 in human[24] and mouse (Figure 4.4 A) peripheral blood mononuclear cells as well as in human endothelial cells[47,48]. Expression of HO-1 prevents the cytotoxic effects of free heme[11,13], hence limiting the pathological outcome of sickle cell anemia in mice[23].

The mechanism via which sickle Hb induces the expression of HO-1 *in vivo* involves Nrf2 (Figure 4.9 A), a transcription factor previously shown to regulate *Hmox1* expression[16,17]. Induction of HO-1 via Nrf2 affords protection against malaria in Hb^{SAD} mice expressing sickle Hb (Figure 4.4 A and B, Figure 4.9 A and B). This protective effect occurs irrespectively of parasite load (Figure 4.4 F and Figure 4.9 D) or parasite sequestration in different organs (Figure 4.3), revealing that sickle human Hb affords tolerance to *Plasmodium* infection via the Nrf2/HO-1 system.

The protective effect of HO-1 against sickle cell anemia[23] and against malaria is mediated by the same end product of heme catabolism, namely CO (Figures 4.11 E and F). This gasotransmitter inhibits Hb oxidation and subsequently heme

release from Hb[10] (Figure 4.11 G), thus preventing free heme from participating in the pathogenesis of ECM (Figures 4.11 H and I)[21] (Figure 4.15). However, CO might have additional protective effects that contribute to prevent the lethal outcome of *Plasmodium* infection[14].

Other end-products of heme catabolism by HO-1, such as labile iron, might also contribute to the protective effect conferred by sickle Hb against malaria. While cytotoxic *per se*, labile iron induces the expression of ferritin H chain (FtH)[49,50], which confers cytoprotection against free heme *in vitro*[11].

The pathogenesis of ECM relies on a ‘‘multiple hit’’ system in which free heme synergizes with other cytotoxic agonists, e.g. pathogenic $CD8^+$ T cells, to trigger disease onset[14,21]. While sickle Hb suppresses both, accumulation of pathogenic free heme (Figure 4.11 A) and activation and/or expansion of pathogenic $CD8^+$ T cells (Figure 4.8), it appears to do so via different mechanisms. Namely, it inhibits the accumulation of free heme after infection, via the HO-1/CO system (Figures 4.11 A and G) while restraining the activation and/or expansion of pathogenic $CD8^+$ T cells (Figure 4.8), via a mechanism that does not seem to involve HO-1 (Figure 4.8) or Nrf2 (Figure 4.10). This latter effect is in keeping with the likely immunoregulatory basis of the protective effect of sickle cell trait against severe malaria in human populations[51]. While the immunoregulatory effect of sickle Hb appears to be driven by free heme (Figure 4.14) its molecular mechanism acts via a signal transduction pathway that remains to be established and that might target antigen presenting cells, e.g. dendritic cells, and/or $CD8^+$ T cells.

It is possible that chronic hemolysis, associated with

oxidation of cell-free Hb and production of circulating free heme, acts as a general protective mechanism against severe forms of malaria in human populations. This would contribute to explain the survival advantage conferred by a variety of RBC mutations against *P. falciparum* infection. In keeping with this notion, many of these RBC mutations can induce hemolysis (spontaneously or upon oxidative challenge) associated with the accumulation of circulating free heme[7]. Some of these also afford protection against CM as illustrated for HbC[3,26], glucose 6 phosphate dihydrogenase (G6PD) deficiency in males[52], β or α-thalassemia that confer protection mainly against severe anemia caused by *P. falciparum* infection[26] as well as other RBC cytoskeleton or membrane protein defects[5]. The notion that chronic hemolysis might be protective *per se* against severe forms of malaria is strongly supported by the observation that heme administration to naïve mice, is sufficient *per se* to elicit a protective response (Figure 4.11 B and Figure 4.14), relying, presumably on the induction of the Nrf2/ HO-1 system. This is however, difficult to prove because the same Nrf2/HO-1 system provides protection against the pathological outcome of some of these RBC mutations, as demonstrated for sickle cell disease[23].

In conclusion, we suggest that induction of the Nrf2/HO-1 system associated with sickle cell trait and probably with other often clinically silent genetic RBC defects might provide a general protective mechanism against *Plasmodium* infection in human populations. We propose that modulation of the Nrf2/HO-1 system might be used therapeutically to treat severe forms of malaria and in particular CM.

5. Tables

Table 4.1. Hematological parameters of *Hb^{WT}Hmox1$^{+/+}$* *Hb^{SAD}Hmox1$^{+/+}$*, *Hb^{SAD}Hmox1$^{+/+}$* mice.

	Non-infected		
	Hb^{wt}	**Hb^{SAD} *Hmox1$^{+/+}$***	**Hb^{SAD} *Hmox1$^{+/-}$***
RBC (10^{6}/ml)	**8.24±0.4**	**8.04±0.3**	**8.06±0.3**
Hb (g/dl)	**12.7±0.7**	**12.3±0.8**	**12.2±0.5**
Hemtocrit (%)	**34.2±1.9**	**32.0±1.4**	**32.1±1.0**
MCV (fl)	**41.5±1.3**	**39.9±0.8**	**39.8±0.9**
MCHC (%)	**37.1±1.0**	**38.5±2.1**	**38.1±1.1**
Leukocytes (x10^{3}/µl)	**9.03±3.5**	**13.85±2.4**	**12.27±3.8**
Neutrophils (x10^{3}/µl)	**1.81±1.3**	**2.06±0.9**	**2.76±1.6**
Lymphocytes (x10^{3}/µl)	**6.0±1.6**	**10.81±1.5**	**12.01±3.37**
Monocytes (x10^{3}/µl)	**0.96±0.4**	**1.14±0.4**	**1.33±0.06**
Eosinophils (x10^{3}/µl)	**0.27±0.27**	**0.24±0.22**	**0.36±0.34**
Basophils/µl	**76.3±91.2**	**55.0±86.2**	**13.8±38.9**
Platelets (x10^{3}/µl)	**0.47±0.18**	**0.56±0.1**	**0.80±0.09**

Table 4.2. Increased mortality in Hb^{SAD} mice carrying two deleted alleles of *Hmox1* and *Nrf2*

A

Hb^{SAD} *Hmox1*$^{+/-}$ x Hb^{WT}*Hmox1*$^{+/-}$

$Hb^{SAD}Hmox1^{+/+}$	$Hb^{SAD}Hmox1^{+/-}$	$Hb^{SAD}Hmox1^{-/-}$
N=148	N=320	N=1
10.9%	23.56%	0.07%
$Hb^{WT}Hmox1^{+/+}$	$Hb^{WT}Hmox1^{+/-}$	$Hb^{WT}Hmox1^{-/-}$
N=293	N=575	N=21
21.28%	42.34%	1.55%

Note: $Hb^{SAD}Hmox1^{-/-}$ *vs* $Hb^{WT}Hmox1^{-/-}$: p<0.00001

B

$Hb^{SAD}Nrf2^{+/-}$ x $Hb^{WT}Nrf2^{+/-}$

$Hb^{SAD}Nrf2^{+/+}$	$Hb^{SAD}Nrf2^{+/-}$	$Hb^{SAD}Nrf2^{-/-}$
N=58	N=93	N=7
9.93%	15.92%	1.2%
$Hb^{WT}Nrf2^{+/+}$	$Hb^{WT}Nrf2^{+/-}$	$Hb^{WT}Nrf2^{-/-}$
N=99	N=247	N=80
16.95%	43.29%	13.7%

Note: $Hb^{SAD}Nrf2^{-/-}$ *vs* $Hb^{WT}Nrf2^{-/-}$: p<0.00001

6. METHODS

Mice

C57BL/6 *Hmox1*$^{+/-}$ mice were provided by Shaw-Fang Yet (Brigham and Women's Hospital, Boston)[53]. C57BL/6 *Nrf2*$^{-/-}$ mice were obtained from the RIKEN BioResource Center (Koyadai, Tsukuba, Ibaraki, Japan)[54]. C57BL/6 *Hb*^{SAD} mice (expressing 19% *Hb*^{SAD}, i.e. $a^{H}{}_{2}\beta_{2}{}^{SAD}$) were provided originally by Annie Henri (INSERM U733 IUH Hôpital Saint-Louis, Paris)[27]. The transgenic *Hb*^{SAD} mice used in this study are hemizygotes for a cluster of human genes including one copy the Hb β SAD gene and two copies of α gene[28]. The insertion site of this cluster in the mouse genome was not determined. The human α globin chains represent about 50% of the total α chain content, while the β SAD chain is only 19% of the total β chains. These human chains are not expressed in addition to the mouse globin chains but at their expense. The ratio of α/β globin chain synthesis remains normal. The relative excess in human α globin chains (compared to the β SAD chains) form functional human α/β mouse hybrid Hb. The Hb content in RBC remains normal (Table 1). The various blood counts are in the normal range (Table 1). However, SAD RBC exhibit a slight dehydration, which revealed by an increase in the intracellular Hb concentration (MCHC) (Table 1). This is expected from the presence of *Hb*^{SAD} (loss of 3 negative charges and an increased isoelectric charge). This modest modification is also seen in HbC heterozygote state in human and it plays a role in the S/C syndrome when associated with the S determinant in compound heterozygote. While hemizygous *Hb*^{SAD} can develop typical complications of sickle cell disease,

e.g. generalized congestion and microvascular occlusions, occasionally with thrombosis and infarctions of lung, kidneys, penis and myocardium these occur only when *Hb*^{SAD} mice are exposed to hypoxia or upon extensive aging, i.e. 38-75 weeks[28]. *Hb*^{SAD} neonates exhibit transient anemia at delivery, related to hemolysis caused by *Hb*^{SAD} polymerization, most probably due to transient hypoxia associated with late fetal development and delivery. Hb values in *Hb*^{SAD} mice return to normal levels shortly after weaning[27]. *Hb*^{SAD} mice used in the experiments described hereby were under the age of 18 weeks presenting no overt hematological changes (Table 1) or complications of sickle cell disease. *Hb*^{SAD}*Hmox1*$^{+/-}$ and *Hb*^{SAD}*Nrf2*$^{+/-}$ mice were generated from *Hb*^{SAD}*Hmox1*$^{+/-}$ x *Hb*^{wt} *Hmox1*$^{+/-}$ or *Hb*^{SAD}*Nrf2*$^{+/-}$ x *Hb*^{wt}*Nrf2*$^{+/-}$ breeding, respectively (Table 2). C57BL/6.Sv129 *Hb*$^{A/A}$ mice, a knock-in mouse model expressing exclusively human Hb without the endogenous mouse Hb were provided originally by Tim Townes (University of Alabama at Birmingham, USA)[30]. *Hb*$^{A/A}$ mice present normal RBC morphology and hematologic parameters[30]. Breeding of the *Hb*$^{A/A}$ with C57BL/6 *Hb*^{wt} mice (or C57BL/6 *Hb*$^{a/a}$) resulted in the production of *Hb*$^{A/a}$ mice, expressing only one copy of the human Hb chains (Hb^{A}) and one copy of the endogenous mouse Hb chains (Hb^{a}). Interbreeding of *Hb*$^{A/a}$ mice produced, among other genotypes, *Hb*$^{A/a}$ mice and littermate control *Hb*$^{a/a}$ mice expressing only the endogenous alleles of the mouse Hb chains. Both genotypes, i.e. *Hb*$^{A/a}$ and *Hb*$^{a/a}$ mice, presented regular Hb levels, 11.0 ± 0.5 and 12.1 ± 0.9 (g/dl), respectively; hematocrit, 40.1 ± 2.5 and 41.8 ± 2.6 (%), respectively and RBC counts, 8.6 ± 0.5 and 8.3 ± 0.6 (x10^{6}/mL), respectively, but decreased levels of Mean Cell Hemoglobin content (MCHC), 27.5 ± 2.0 and 28.8 ± 1.4 (g/dl), respectively.

Mice were genotyped by PCR (*Hmox1* and *Nrf2*) and isoelectric focusing (Hb), as described elsewhere[21,27]. Experimental protocols were approved by the ''Instituto Gulbenkian de Ciência animal care committee'' and by the ''Direcção Geral de Veterenária (DGV)'' of the Portuguese Ministry of Agriculture, Rural Development and Fisheries (License 018831-2010-09-03).

Bone Marrow Chimeras

Bone Marrow chimeras were generated in $Hmox1^{+/+}$, $Hmox1^{+/-}$ mice expressing or not the Hb^{SAD} allele (8-10 weeks). Mice (recipients) were lethally irradiated (900 rad, 2.35 minutes, 137Cs source) (Gammacell 2000, Mølsgaard Medical, Denmark) and reconstituted 4 hours thereafter with 10^6 total bone marrow cells from $Hmox1^{+/+}$, $Hmox1^{+/-}$ expressing or not the Hb^{SAD} allele (6 weeks). Chimerism was assessed 8-10 weeks thereafter by RT-PCR, as described[12]. Flow cytometry was used to assess percent and total number of circulating cells in reconstituted mice as compared to control nonchimeric mice.

Parasites, Infection, and Disease Assessment

Mice were infected by intraperitoneal (i.p.) inoculation of 10^5 RBCs infected with (GFP)-*P. berghei* ANKA[21], GFP-Luciferase *P. berghei* ANKA (MR4-866) or a (GFP)-*P. berghei* transgenic parasite expressing different MHC II and MHC I restricted epitopes including the MHC I-restricted epitope derived from glycoprotein B of herpes simplex virus-1 ($gB_{498-505}$)[39], provided originally by William R. Heath (Walter and Eliza Hall, Melbourne, Victoria, Australia). Drug-resistant *P. berghei* ANKA transfectants were selected using Pyrimethamine (10 mg/ml in drinking water). Parasitemias were determined by flow

cytometry[21]. Infected mice were monitored twice daily for clinical symptoms of ECM including hemi- or paraplegia, head deviation, tendency to roll-over on stimulation, ataxia and convulsions. All experiments were performed in mice sacrificed under CO_2 and perfused with PBS, at the time of ECM in control mice.

Visualization and Quantification of Luciferase Activity *P. berghei* ANKA Infected Mice

Luciferase activity was visualized by imaging of dissected tissues using an electron multiplying-charge-coupled device (EM-CCD) photon-counting camera (ImagEM, Hamamatsu). Mice received d-Luciferin (i.p.) in PBS (100 mg/kg of body weight; Promega) at day 7 postinfection, at the time of ECM onset. Mice were sacrificed and perfused with PBS 5 min thereafter. Organs were dissected, placed in a Petri dish and exposed (5–120s). Imaging quantification was performed with ImageJ software and is expressed arbitrary units per mg of tissue.

Protoporphyrins

Iron-protoporphyrin IX (FePPIX; heme) and zinc-protoporphyrin IX (ZnPPIX) were dissolved in 0.2 M NaOH, neutralized (pH 7.4) with 0.2 M HCl and administered (i.p.), as described[21].

HO-1 Activity

Spleen and liver were harvested and snap frozen in liquid nitrogen. Tissue samples were homogenized in 3mL of homogenizing buffer (200 mM KH_2PO_4, 135 mM KCl, 0.1 mM EDTA, [pH 7.4]), and sonicated at 4ºC. The supernatant was transferred to ultracentrifuge tubes and 5mL of homogenizing

buffer was added, followed by an ultracentrifugation (100.000g, 4ºC, 1h, Beckman L7-35 Ultracentrifuge, 70 Ti rotor). The microsomal pellet was resuspended in 320 ml of HO activity buffer (100 mM KH_2PO_4, 2 mM $MgCl_2$, [pH 7.4]). Samples were sonicated again, centrifuged and the supernatant was used to determine HO activity using rat liver cytosol (as a source of biliverdin reductase, 2 mg/assay), hemin (20 mM), glucose 6-phosphate (2 mM), glucose 6-phosphate dehydrogenase (0.2 U/reaction) and NADPH (0.8 mM) (400 µl 37ºC, 1 hr). Bilirubin was extracted (1 ml of chloroform; vortexing 3x for 10 sec.). After centrifugation optical densities at λ=464 nm and λ=530 nm of the organic phase were determined and HO activity was calculated as pmol bilirubin formed/mg of tissue/hour.

CO treatment

Mice were placed in a gastight 60 L capacity chamber and exposed continuously between days 4-7 postinfection to CO at a flow rate of ~12 L/min (final concentration of 250 parts per million; ppm), as described[21,55]. CO concentration was monitored using a CO analyzer (Interscan Corporation, Chatsworth).

Histology

Brains were harvested, when clinical signs of ECM were noticed in control mice. Tissue was fixed in buffered 4% (vol/vol) paraformaldehyde and histological analysis was performed on perfusion-fixed tissues.

BBB Permeability

Mice were injected intravenously (i.v.) with 0.1 ml of 2%

Evans Blue (Sigma) when clinical symptoms of ECM were noticed in control mice. Mice were sacrificed 1h thereafter. Brains were weighted and placed in formamide (Merck) (37ºC, 48h) to extract Evans Blue dye. Absorbance was measured at λ=620 nm (Spectronic Unicam, Heλios β). Evans Blue concentration was calculated from a standard curve of Evans Blue and is expressed as mg of Evans Blue *per* g of brain tissue[21].

Analyzes of splenic CD8$^+$ T cell activation

Single cell suspensions were obtained from spleen of naïve mice or five days after infection with a transgenic *P. berghei* ANKA strain encoding the MHC I-restricted epitope derived from the glycoprotein B of herpes simplex virus-1 ($gB_{498-505}$)[39]. For intracellular granzyme B staining splenocytes ($1x10^6$) were re-stimulated *in vitro* (5 hours, 37ºC) with 100ng/ml of phorbol 12-myristate 13-acetate (Sigma), 500ng/ml Ionomycin (Calbiochem) in the presence of 10mg/ml brefeldin A (Epicenter Technologies). Fc receptors were blocked using anti-FcγIII/II (2.4G2) receptor antibody (produced in house) and cells were stained with anti-CD8 antibody (YTS169.4 clone, produced in house). Cells were fixed (2% paraformaldehyde in PBS, 30 min, RT) and permeabilized (0,5% saponin in PBS 2% FCS, 10 min, RT) prior to the addition of anti-granzyme B antibody (16G6 clone, eBioscience) in 0,5% saponin in PBS 2% FCS (30 min, RT). For the analyzes of CD8$^+$ T cells recognizing the MHC I-restricted epitope $gB_{498-505}$ (SSIEFARL) from glycoprotein B of herpes simplex virus-1, splenocytes ($2x10^6$) were stained with R-phycoerythrin-conjugated H-2K^b-$gB_{498–505}$ pentamer (ProImmune) according to manufacturer instructions prior to staining with anti-

CD19 (MB19-1, eBioscience) and anti-CD8 antibodies. H-2K^{b}-gB$_{498–505}$ pentamer positive cells were determined as CD19^{-} CD8^{+}H-2K^{b}-gB$_{498–505}$$^{+}$. Data were acquired using FACSCalibur (BD Bioscience) and CyAn ADP (Dako Cytomation) and analyzed using FlowJo software (Tree Star Inc.). Dead cells were excluded from analysis based on propidium iodide staining.

Leukocyte Brain Infiltration

Leukocytes were isolated from the brain of *P. berghei* ANKA infected mice when clinical symptoms of ECM were detectable in control groups. Mice were perfused with PBS *in toto*, brains were collected, homogenized, digested (30 min, 37ºC) in Hanks-balanced salt solution (HBSS; Life Technologies) supplemented with 0.2 mg/ml collagenase VIII (Sigma-Aldrich), strained (100 µm) (Becton Dickinson) and centrifuged (1200 g; 10 min). Brain leukocyte infiltration was quantified by flow cytometry[21].

Quantitative Real-Time Reverse Transcription PCR

Mice were sacrificed at the day of ECM onset in *Hb*^{wt} mice. RNA was isolated from brain, liver, kidney, heart, bone marrow, spleen and lungs using Trizol Reagent (Invitrogen, Life technologies) and RNeasy Plus Mini Kit (Quiagen), according to manufacturers recommendation. RNeasy Protect Animal Blood Kit (Quiagen) was used for the extraction of RNA from whole blood. cDNA was synthesized as described[21]. *Hmox1* mRNA was quantified by qRT-PCR (Roche System) as described[21]. TaqMan Gene Signature Mouse Immune Array (Applied Biosystems) was used to quantify all other mRNAs (7900HT ABI system), according to manufacturers´ recommendations.

Serum Biochemistry

Blood was collected in heparinized tubes by cardiac puncture, centrifuged (2x5min, 1600g). Hematograms were measured by focused flow technology (Hemavet Multispecies Hematology System, HV950FS, Drew Scientific Inc., CDVET Lab, Centro Diagnóstico Veterinário, Lisboa, Portugal). Plasma Hb was determined by spectroscopy at λ=577. Total plasma heme was measured using the 3,3´, 5,5´ tetramethylbenzidine (TMB) peroxidase assay (BD Biosciences), at λ=655 nm. Purified Hb was used as standard for plasma Hb and heme measurements.

Statistical Analysis

Nonparametric Mann-Whitney *U* test was used to assess statistical significance between averages in different samples in which $n<5$. In samples with $n=5$ or $n>5$ the unpaired Student's *t*-test for unequal variances was used. Normal distributions were confirmed using the Kolmogorov-Smirnov test. Significant differences in survival were evaluated by the generation of Kaplan-Meier plots and by performing log-rank analysis for all experiments in which survival was assessed as an end-point. Statistical analysis for the progeny-expected ratios was performed using Pearson's chi-squared tests. *P<0.05 or **P<0.01 were considered statistically significant.

7. Acknowledgments

We thank Ruslan Medzhitov for intellectual support and

encouragement by means of many insightful discussions, Thiago Carvalho (Instituto Gulbenkian de Ciência) and Rui Costa Fundação Champalimaud as well as Marcelo Bozza (Universidade Federal do Rio De Janeiro), Robert P. Hebbel and Gregory Vercellotti (University of Minnesota, USA) for critical review of the manuscript, Nuno Sepúlveda for support in statistical analysis, Tim M. Townes and Tom M. Ryan (University of Alabama at Birmingham) for providing the HbA/A mice. Sílvia Cardoso and Matteo Villa for mouse breeding and genotyping. This work was supported by ''Fundac¸ a˜o para a Cieˆncia e a Tecnologia'', Portugal grants PTDC/SAU-MII/71140/2006 and SFRH/BPD/21707/2005 (AF), SFHR/BD/33218/2007 (IM), PTDC/SAU-MII/71140/2006, PTDC/BIABCM/ 101311/2008, PTDC/SAU-FCF/100762/2008, GEMI Fund Linde Healthcare, European Community and LSH-2005-1.2.5-1 (MPS), FP7-PEOPLE-2007-2-1-IEF (VJ). I.B. is supported by the DFG, BMBF, Dr. Senckenberg-Stiftung, Kassel-Stiftung and Messer-Stiftung, Germany. Annie Henri is supported by INSERM and Yves Beuzard by Paris VII University, Commissariat a` l'E´ nergie Atomique and Agence Nationale de la Recherche Scientifique, France.

Author contribution: A.F. contributed to study design, performed and/or contributed critically to all experiments, analyzed data and was assisted to do so by NRP. A.C. performed experiments and analysis of leukocyte infiltration and generation of bone marrow chimeric animals with A.F. I.M.: performed experiments and interpreted data revealing the immunoregulatory effect of sickle hemoglobin with A.F. I.B. provided expert analysis, advice and teaching on immunopathology. V.J. determined free heme concentrations in

plasma and quantified HO activity. S.R. generated and maintained all mouse colonies used. A.H. provided the HbSAD mice. YB provided mentorship and advise on sickle cell mouse model. M.P.S. formulated the original hypothesis, drove most of the study design, analyzed and provided mentorship. The manuscript was written by M.P.S. with assistance from A.F. and Y.B.

8. References

1. Jallow, M.*, et al.* Genome-wide and fine-resolution association analysis of malaria in West Africa. *Nat Genet* **41**, 657-665 (2009).
2. Williams, T.N.*, et al.* Sickle cell trait and the risk of Plasmodium falciparum malaria and other childhood diseases. *J Infect Dis* **192**, 178-186 (2005).
3. Modiano, D.*, et al.* Haemoglobin C protects against clinical Plasmodium falciparum malaria. *Nature* **414**, 305-308 (2001).
4. Hutagalung, R.*, et al.* Influence of hemoglobin E trait on the severity of Falciparum malaria. *J Infect Dis* **179**, 283-286 (1999).
5. Williams, T.N. Human red blood cell polymorphisms and malaria. *Curr Opin Microbiol* **9**, 388-394 (2006).
6. Reiter, C.D.*, et al.* Cell-free hemoglobin limits nitric oxide bioavailability in sickle-cell disease. *Nat Med* **8**, 1383-1389 (2002).
7. Muller-Eberhard, U., Javid, J., Liem, H.H., Hanstein, A. & Hanna, M. Plasma concentrations of hemopexin, haptoglobin and heme in patients with various hemolytic diseases. *Blood* **32**, 811-815 (1968).
8. Allison, A.C. Protection afforded by sickle-cell trait against subtertian malareal infection. *Br Med J* **1**, 290-294 (1954).
9. Beet, E.A. Sickle cell disease in Northern Rhodesia. *East Afr Med J* **24**, 212-222 (1947).
10. Hebbel, R.P., Morgan, W.T., Eaton, J.W. & Hedlund, B.E. Accelerated autoxidation and heme loss due to instability of sickle hemoglobin. *Proc Natl Acad Sci U S A* **85**, 237-241 (1988).
11. Balla, G.*, et al.* Ferritin: a cytoprotective antioxidant strategem of endothelium. *J Biol Chem* **267**, 18148-18153 (1992).
12. Seixas, E.*, et al.* Heme oxygenase-1 affords protection against noncerebral forms of severe malaria. *Proc Natl Acad Sci U S A* **106**, 15837-15842 (2009).
13. Gozzelino, R., Jeney, V. & Soares, M.P. Mechanisms of cell protection by heme oxygenase-1. *Annu Rev Pharmacol Toxicol* **50**, 323-354 (2010).
14. Ferreira, A., Balla, J., Jeney, V., Balla, G. & Soares, M.P. A central role for free heme in the pathogenesis of severe malaria: the missing link? *J Mol Med* **86**, 1097-1111 (2008).
15. Tenhunen, R., Marver, H.S. & Schmid, R. The enzymatic conversion of heme to bilirubin by microsomal heme oxygenase. *Proc Natl Acad Sci U S A* **61**, 748-755 (1968).
16. Kensler, T.W., Wakabayashi, N. & Biswal, S. Cell survival responses to environmental stresses via the Keap1-Nrf2-ARE pathway. *Annu Rev Pharmacol Toxicol* **47**, 89-116 (2007).
17. Alam, J.*, et al.* Nrf2, a Cap'n'Collar transcription factor, regulates induction of the heme oxygenase-1 gene. *J Biol Chem* **274**, 26071-26078 (1999).

18. Ogawa, K., *et al.* Heme mediates derepression of Maf recognition element through direct binding to transcription repressor Bach1. *EMBO J* **20**, 2835-2843 (2001).
19. Nath, K.A., *et al.* Induction of heme oxygenase is a rapid, protective response in rhabdomyolysis in the rat. *J Clin Invest* **90**, 267-270 (1992).
20. Soares, M.P. & Bach, F.H. Heme oxygenase-1: from biology to therapeutic potential. *Trends Mol Med* **15**, 50-58 (2009).
21. Pamplona, A., *et al.* Heme oxygenase-1 and carbon monoxide suppress the pathogenesis of experimental cerebral malaria. *Nat Med* **13**, 703-710 (2007).
22. Mishra, S.K. & Newton, C.R. Diagnosis and management of the neurological complications of falciparum malaria. *Nat Rev Neurol* **5**, 189-198 (2009).
23. Belcher, J.D., *et al.* Heme oxygenase-1 is a modulator of inflammation and vaso-occlusion in transgenic sickle mice. *J Clin Invest* **116**, 808-816 (2006).
24. Jison, M.L., *et al.* Blood mononuclear cell gene expression profiles characterize the oxidant, hemolytic, and inflammatory stress of sickle cell disease. *Blood* **104**, 270-280 (2004).
25. Sears, D.A., Udden, M.M. & Thomas, L.J. Carboxyhemoglobin levels in patients with sickle-cell anemia: relationship to hemolytic and vasoocclusive severity. *Am J Med Sci* **322**, 345-348 (2001).
26. May, J., *et al.* Hemoglobin variants and disease manifestations in severe falciparum malaria. *JAMA* **297**, 2220-2226 (2007).
27. Trudel, M., *et al.* Towards a transgenic mouse model of sickle cell disease: hemoglobin SAD. *EMBO J* **10**, 3157-3165 (1991).
28. Trudel, M., *et al.* Sickle cell disease of transgenic SAD mice. *Blood* **84**, 3189-3197 (1994).
29. Schofield, L. & Grau, G.E. Immunological processes in malaria pathogenesis. *Nat Rev Immunol* **5**, 722-735 (2005).
30. Wu, L.C., *et al.* Correction of sickle cell disease by homologous recombination in embryonic stem cells. *Blood* **108**, 1183-1188 (2006).
31. Belnoue, E., *et al.* On the pathogenic role of brain-sequestered alphabeta CD8+ T cells in experimental cerebral malaria. *J Immunol* **169**, 6369-6375 (2002).
32. Crompton, P.D., *et al.* Sickle cell trait is associated with a delayed onset of malaria: implications for time-to-event analysis in clinical studies of malaria. *J Infect Dis* **198**, 1265-1275 (2008).
33. Livincstone, F.B. Malaria and human polymorphisms. *Annu Rev Genet* **5**, 33-64 (1971).
34. Motulsky, A.G., Vandepitte, J. & Fraser, G.R. Population genetic studies in the Congo. I. Glucose-6-phosphate dehydrogenase deficiency, hemoglobin S, and malaria. *Am J Hum Genet* **18**, 514-537 (1966).
35. Raberg, L., Sim, D. & Read, A.F. Disentangling genetic variation for resistance and tolerance to infectious diseases in animals. *Science* **318**, 812-814 (2007).
36. Schneider, D.S. & Ayres, J.S. Two ways to survive infection: what resistance and tolerance can teach us about treating infectious diseases. *Nat Rev Immunol* **8**, 889-895 (2008).
37. Sabaa, N., *et al.* Endothelin receptor antagonism prevents hypoxia-induced mortality and morbidity in a mouse model of sickle-cell disease. *J Clin Invest* **118**, 1924-1933 (2008).
38. Campanella, G.S., *et al.* Chemokine receptor CXCR3 and its ligands CXCL9 and CXCL10 are required for the development of murine cerebral malaria. *Proc Natl Acad Sci U S A* **105**, 4814-4819 (2008).
39. Lundie, R.J., *et al.* Blood-stage Plasmodium infection induces CD8+ T lymphocytes to parasite-expressed antigens, largely regulated by CD8alpha+ dendritic cells. *Proc Natl Acad Sci U S A* **105**, 14509-14514 (2008).
40. Friedman, M.J. Erythrocytic mechanism of sickle cell resistance to malaria. *Proc Natl Acad Sci U S A* **75**, 1994-1997 (1978).
41. Pasvol, G., Weatherall, D.J. & Wilson, R.J. Cellular mechanism for the protective effect of haemoglobin S against P. falciparum malaria. *Nature* **274**, 701-703 (1978).
42. Ayi, K., Turrini, F., Piga, A. & Arese, P. Enhanced phagocytosis of ring-parasitized mutant erythrocytes: a common mechanism that may explain

protection against falciparum malaria in sickle trait and beta-thalassemia trait. *Blood* **104**, 3364-3371 (2004).
43. Hood, A.T., Fabry, M.E., Costantini, F., Nagel, R.L. & Shear, H.L. Protection from lethal malaria in transgenic mice expressing sickle hemoglobin. *Blood* **87**, 1600-1603 (1996).
44. Shear, H.L.*, et al.* Transgenic mice expressing human sickle hemoglobin are partially resistant to rodent malaria. *Blood* **81**, 222-226 (1993).
45. Larsen, R.*, et al.* A central role for free heme in the pathogenesis of severe sepsis. *Sci Transl Med* **2**, 51ra71 (2010).
46. Clark, I.A., Alleva, L.M., Mills, A.C. & Cowden, W.B. Pathogenesis of malaria and clinically similar conditions. *Clin Microbiol Rev* **17**, 509-539, (2004).
47. Bains, S.K.*, et al.* Human sickle cell blood modulates endothelial heme oxygenase activity: effects on vascular adhesion and reactivity. *Arterioscler Thromb Vasc Biol* **30**, 305-312 (2010).
48. Nath, K.A.*, et al.* Oxidative stress and induction of heme oxygenase-1 in the kidney in sickle cell disease. *Am J Pathol* **158**, 893-903 (2001).
49. Berberat, P.O.*, et al.* Heavy chain ferritin acts as an antiapoptotic gene that protects livers from ischemia reperfusion injury. *FASEB J* **17**, 1724-1726 (2003).
50. Eisenstein, R.S., Garcia-Mayol, D., Pettingell, W. & Munro, H.N. Regulation of ferritin and heme oxygenase synthesis in rat fibroblasts by different forms of iron. *Proc Natl Acad Sci U S A* **88**, 688-692 (1991).
51. Williams, T.N.*, et al.* An immune basis for malaria protection by the sickle cell trait. *PLoS Med* **2**, e128 (2005).
52. Guindo, A., Fairhurst, R.M., Doumbo, O.K., Wellems, T.E. & Diallo, D.A. X-linked G6PD deficiency protects hemizygous males but not heterozygous females against severe malaria. *PLoS Med* **4**, e66 (2007).
53. Yet, S.F.*, et al.* Hypoxia induces severe right ventricular dilatation and infarction in heme oxygenase-1 null mice. *J Clin Invest* **103**, R23-29 (1999).
54. Itoh, K.*, et al.* An Nrf2/small Maf heterodimer mediates the induction of phase II detoxifying enzyme genes through antioxidant response elements. *Biochem Biophys Res Commun* **236**, 313-322 (1997).
55. Sato, K.*, et al.* Carbon monoxide generated by heme oxygenase-1 suppresses the rejection of mouse-to-rat cardiac transplants. *J Immunol* **166**, 4185-4194 (2001).

Chapter 5: General Discussion

An inexorable side effect of immune responses is the generation of immune-mediated tissue damage. The very same mechanisms used by innate and adaptive immune cells to control infectious agents also affect host cells, leading to varying degrees of immunopathology. An immune response able to control the deleterious effects of pathogen overgrowth and, at the same time, preserve host tissue integrity could be regarded as the perfect immune response. Nonetheless, tissues should not be seen as passive bystanders as immunopathology ensues, as they can and do engage genetic programs devoted to dealing with harmful insults by augmenting tissue resilience to immune-mediated damage. In this thesis data supporting a role for the immune system and tissues in avoiding immunopathology is presented. First, it is demonstrated that DC efficiently expand T_{REG}, a major cell population involved in preventing immunopathology (*see chapter 2*). Second, it is demonstrated that HO-1 expression affords protection against development of severe sepsis by decreasing overall tissue damage (*see chapter 3*). Third, it is demonstrated that protection conferred by Hb^{SAD} against ECM development in mice depends on a composite effect of increased expression of HO-1, and on an immunoregulatory effect leading to diminished immune activation (*see chapter 4*).

The importance of T_{REG} in maintaining immune tolerance and avoiding autoimmunity has long been known[6]. Importantly, T_{REG} also play a fundamental role in controlling immunopathology associated with immune responses against non-self antigens, such as allografts[358] and infectious agents[359]. These findings imply that a pool of non-self antigen-specific T_{REG} is present in the naïve host and/or that naïve $CD4^+$ T cells become T_{REG} upon

encounter with foreign antigen. Herein we provide evidence that the T_{REG} pool specific for non-self antigens, namely alloantigens, can be expanded *in vitro* when in contact with DC regardless of DC activation state (*see chapter 2*). Most importantly, T_{REG} expanded in such conditions are able to suppress T cell proliferation *in vitro* and immunopathology *in vivo*[360].

The capacity of DC to stimulate T_{REG} cells expansion during an immune response might be determinant in preventing immunopathology by maintaining an ideal ratio between effector T cells and T_{REG}, allowing the immune system to act towards the elimination of the harmful insult while, at the same time, preventing immunopathology. It is possible that the expansion of these two T cell compartments follows different kinetics allowing for a powerful initial T cell response, followed by a wave of regulation provided by expanded T_{REG}. The possibility of T_{REG} expansion by DCs uncovers a mechanism via which the immune system might control the development of immunopathology through interactions among its own cells, regardless of the tissue being affected.

On the opposite extreme of the control of immunopathology via interactions solely among immune cells, is the notion that tissues being damaged can modulate their capacity to withstand injury. Genes involved in limiting immunopathology by increasing tissue resilience to damage are often called cytoprotective genes, and *Hmox1* is thought to be a prototypic gene involved in preventing immunopathology via this mechanism (*see chapter 1, section 2*). Herein, data providing evidence that *Hmox1* expression has salutary effects on the development of severe sepsis serves as an example of such a mechanism.

By controlling heme levels, *Hmox1* expression prevents tissue damage caused by the concerted cytotoxic action of heme and inflammatory agonists such as those elicited by CLP (*see chapter 3*). The absence of apparent excessive immune activation or increased bacterial load in *Hmox1*$^{-/-}$ mice undergoing CLP, suggest that lethality observed in these animals derives from an inability of organs to sustain normal function under severe inflammatory conditions. Most probably, organ dysfunction occurs as a result of massive cell death induced by high heme levels in conjunction with proinflammatory agonists (*see chapter 3*). Furthermore, the salutary effect of hemopexin administration to *Hmox1*$^{+/+}$ mice undergoing severe CLP, as a mean to scavenge heme from circulation, strongly supports the notion that heme triggers widespread tissue damage ultimately leading to death.

These findings evoke the concept of tolerance to infection as the mechanism via which *Hmox1* expression limits death caused by disproportionate immunopathology (*see chapter 1, section 1.3 and chapter 3*). Notwithstanding the findings that *Hmox1*$^{-/-}$ mice present increased organ dysfunction leading ultimately to death, and the fact that scavenging heme from circulation by hemopexin administration protects *Hmox1*$^{+/+}$ from death after severe CLP, the conclusion that tolerance to infection is involved in these phenotypes requires a more stringent analysis. The reasons for this are discussed below.

The conclusion that *Hmox1* confers tolerance to infection can only be taken if one accepts that the uninfected health status ($\mathbf{u}_{HS}$, as defined in *chapter 1, section 1.3*) of naïve *Hmox1*$^{+/+}$ and *Hmox1*$^{-/-}$ mice is equal (*see figure 5.1 A*), an assumption that is challenged by several lines of evidence. First, *Hmox1*$^{-/-}$ mice

present severe splenomegaly[208,242] and increased white blood cell counts[208], suggesting that these animals are under a constitutive inflammatory state, a notion further supported by the finding that monocytes/macrophages in liver and kidney of naïve *Hmox1*$^{-/-}$ express TNF constitutively[222]. Second, *Hmox1*$^{-/-}$ present progressive wasting disease and anemia[208]. Third, progressive oxidative damage of organs affected by CLP is observed in naïve *Hmox1*$^{-/-}$ mice, as evidenced by increased protein carbonylation and lipid peroxidation in liver and kidneys[208] with concomitantly increased serum ferritin levels, a finding indicative of liver damage[189]. Fourth, naive *Hmox1*$^{-/-}$ mice develop inflammatory infiltration in the liver[239]. Fifth, heme administration to naïve *Hmox1*$^{+/+}$ causes profound kidney damage (*see chapter 3, figure 4B*) that, *per se*, lowers the uninfected health status ($\mathbf{u}_{HS}$) of the host subjected to CLP. Therefore, it is possible that the direct comparison between *Hmox1*$^{+/+}$ *versus Hmox1*$^{-/-}$ mice disregards differences in the uninfected health status. This oversight might lead to an inaccurate measurement of tolerance to infection (*see figure 5.1 B)*. It remains as a possibility that differences in $\mathbf{u}_{HS}$ occur concomitantly with differences in tolerance to infection. In this scenario, *Hmox1*$^{-/-}$ animals would present both lower $\mathbf{u}_{HS}$ and decreased tolerance to infection (*see figure 5.1 C)*. Further studies will be necessary to determine whether this is the case.

To obtain a better assessment of tolerance to infection and what is the role played by *Hmox1* in this process, it would be fundamental to use mice where *Hmox1* could be deleted shortly before infection, thus avoiding the deleterious effects of prolonged lack of *Hmox1* expression. This could be easily achieved with available tools, namely by making use of mice where the *Hmox1* gene has been flanked by *loxP*-sites crossed

with mice carrying a transgene that would lead to Cre-recombinase expression and activity upon exogenous stimulus. In fact, mice with myeloid-specific ablation of *Hmox1* show no signs of the pathologies associated with total *Hmox1* deletion[239], further supporting the notion that the use of strategies where *Hmox1* deletion is controlled might be extremely informative in the study of its role in tolerance to infection.

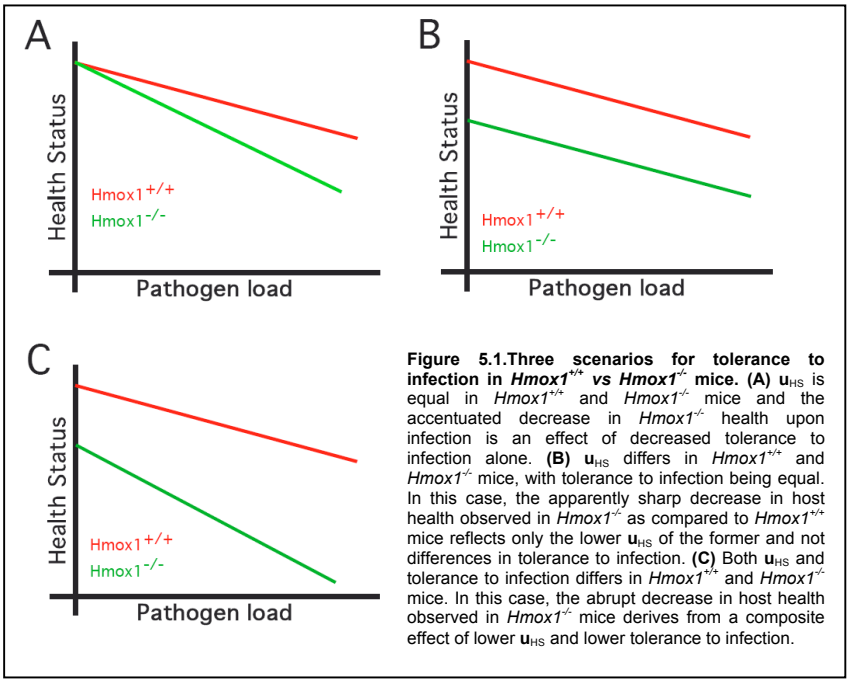

Figure 5.1.Three scenarios for tolerance to infection in *Hmox1*$^{+/+}$ *vs* *Hmox1*$^{-/-}$ mice. (A) $\mathbf{u}_{HS}$ is equal in *Hmox1*$^{+/+}$ and *Hmox1*$^{-/-}$ mice and the accentuated decrease in *Hmox1*$^{-/-}$ health upon infection is an effect of decreased tolerance to infection alone. **(B)** $\mathbf{u}_{HS}$ differs in *Hmox1*$^{+/+}$ and *Hmox1*$^{-/-}$ mice, with tolerance to infection being equal. In this case, the apparently sharp decrease in host health observed in *Hmox1*$^{-/-}$ as compared to *Hmox1*$^{+/+}$ mice reflects only the lower $\mathbf{u}_{HS}$ of the former and not differences in tolerance to infection. **(C)** Both $\mathbf{u}_{HS}$ and tolerance to infection differs in *Hmox1*$^{+/+}$ and *Hmox1*$^{-/-}$ mice. In this case, the abrupt decrease in host health observed in *Hmox1*$^{-/-}$ mice derives from a composite effect of lower $\mathbf{u}_{HS}$ and lower tolerance to infection.

More likely than not, in cases where hosts are at risk of developing immunopathology, mechanisms involved in constraining immune responses and mechanisms involved in increasing tissue protection will be used concomitantly. The concerted action of both mechanisms seems to work at its best in the case of protection against ECM conferred by *Hb*^{SAD} (*see chapter 4*). In *Hb*^{WT} animals ECM development seems to rely on

a “two hit system”, one being the increased heme levels associated with *Plasmodium* infection, the other being $CD8^+$ T cell-mediated cytotoxicity. Most importantly, these “two hit” seem to be controlled by distinct mechanisms. This is revealed by the fact that Hb^{SAD} animals lacking one functional *Hmox1* or *Nrf2* allele lose the protection associated with Hb^{SAD} expression by regaining increased levels of heme in circulation, while maintaining low levels of $CD8^+$ T cell activation (*see chapter 4*). Nonetheless, it is important to note that this observation might be related to a gene dosage effect. In fact, the immunomodulatory effect of Hb^{SAD} might be lost in the complete absence of *Hmox1* or *Nrf2* expression. Unfortunately, the experimental system used herein does not allow for such analysis to be done (*see chapter 4*).

The expression of Hb^{SAD} limits the increase in circulating heme levels upon *Plasmodium* infection by a mechanism that involves increased expression of *Hmox1* via Nrf2 activation. The occurrence of chronic hemolysis in Hb^{SAD} mice presumably leads to high levels of *Hmox1* expression via the action of the Nrf2 transcription factor. That, in turn, avoids pathological levels of heme to accumulate upon *Plasmodium* infection. Furthermore, increased HO-1 expression and heme catabolism will presumably lead to increased CO production that can act to avoid unlocking of heme from hemoproteins thus limiting heme release. Interestingly, disruption of one allele of *Hmox1* or *Nrf2* abrogates the protection conferred by Hb^{SAD}, by impairing the capacity of these animals to control heme levels upon *Plasmodium* infection. Notably, disruption of one allele of *Hmox1* or *Nrf2* did not affect $CD8^+$ T cell activation impairment in mice carrying Hb^{SAD}. This finding indicates that ablation of one *Hmox1*

or *Nrf2* allele is not sufficient to revert the decreased $CD8^+$ T cell activation phenotype. As noted before, it is possible that a complete ablation of *Hmox1* or *Nrf2* would revert the effect of Hb^{SAD} on $CD8^+$ T cell activation. Nonetheless, alternative explanations for the immunomodulatory effect of Hb^{SAD} are discussed below.

Data obtained from mRNA expression analysis in the brains of Hb^{WT}, Hb^{SAD} and $Hb^{SAD}Hmxo1^{+/-}$ mice, at the time of ECM onset, suggests that innate immune activation is suppressed in Hb^{SAD} and $Hb^{SAD}Hmxo1^{+/-}$ mice (*see chapter 4, figure 6*). mRNA encoding IL-1β, IL-6, TNF, CD40 and inducible nitric oxide synthase (NOS2) enzyme, are all downregulated in the brains of Hb^{SAD} and $Hb^{SAD}Hmxo1^{+/-}$ mice as compared to the levels observed in Hb^{WT} animals. These findings suggest that Hb^{SAD} induces a broad modulation of innate and adaptive immunity that is not reverted in the absence of one functional *Hmox1* allele. Since data indicating impaired innate immune activation derives from mRNA obtained from brains of animals undergoing ECM, it becomes difficult to determine whether this is cause or consequence of diminished $CD8^+$ T cell activation. However, given the pivotal role of innate immune cells in initiating adaptive immune responses, the hypothesis that protection conferred by Hb^{SAD} against ECM relies primarily on innate immune suppression leading to defective adaptive immune activation will be discussed in further detail.

Hb^{SAD} mice have been reported to constitutively express higher levels of erythropoietin (EPO) than WT animals. The elevated EPO levels in Hb^{SAD} mice could, *per se*, account for the immunosuppression observed in these animals. It has been

recently demonstrated that macrophages and DC express EPO receptor[361]. Furthermore, binding of EPO to EPO receptor inhibits macrophage production of the proinflammatory cytokines TNF, IL-6, IL-12p70 and IL-23, an effect linked to suppressed NF-κB activation upon TLR stimulation and *Salmonella* infection[361]. Importantly, EPO signaling exacerbated *Salmonella* infection while controlling colitis, demonstrating the functional relevance of this pathway in restraining immune responses[361].

Deregulation of iron homeostasis during hemoglobinopathies, with consequent alterations in intracellular iron pool, might be a general mechanism implicated in the protection afforded by different kinds of hemoglobinopathies to *Plasmodium* infection. Regulation of iron homeostasis is a systemic response orchestrated in great part by hepcidin, and hemoglobinopathies have been linked to decreased levels of hepcidin in humans and mice[362-365]. Hb^{SAD} mice are likely to present low hepcidin levels. In support of this notion is the observation that Hb^{SAD} mice present increased EPO production, increased erythropoiesis, and hemolysys[367,368], three conditions associated with lower levels of hepcidin[255,366,369]. Low hepcidin leads to increased levels of FPN expression on cells, with consequent depletion of intracellular iron pool. Of note, innate immune cells, specially macrophages, but also DC[370], have been reported to express FPN and, therefore, are subjected to intracellular iron content regulation by hepcidin.

The effect of low intracellular iron in cells of the immune system has been extensively reported[283,371]. Macrophages obtained from animals in which the *Hfe* gene has been disrupted, leading to abnormally low hepcidin expression, produce lower

levels of pro-inflammatory cytokines in response to PAMP stimulation as compared to wild type animals, an effect due to increased FPN expression in macrophages and consequent intracellular iron depletion[286]. These effects can be attributed to at least two different molecular mechanisms: *a)* inhibition of cytokine translation[286] and *b)* inhibition of TLR signaling[285]. Since the development of adaptive immunity is normally preceded by a strong activation of the innate immune system, it is possible that decreased intracellular iron levels might impair the ability of innate immune cells to induce a full-blown adaptive immune response. Therefore, the diminished $CD8^+$ T cell activation observed in mice carrying Hb^{SAD} might be a consequence of the diminished hepcidin levels, leading to lower intracellular iron on innate immune cells. Importantly, the immunomodulatory effect of low intracellular iron would fine-tune the immune response against *Plasmodium*, allowing parasitemia control while limiting immunopathology.

In fact, expansion and acquisition of effector functions by short-lived effector $CD8^+$ T cells, has been reported to rely on a strong inflammatory response during the activation phase[81]. Therefore, the failure of $CD8^+$ T cells in Hb^{SAD} mice to achieve complete expansion and effector differentiation is consistent with the hypothesis of a less inflammatory milieu during their activation. Curiously, the observation that a milder inflammatory environment favors formation of memory $CD8^+$ T cells[372], brings about the hypothesis that besides partially dampening detrimental $CD8^+$ T cell response, Hb^{SAD} might increase generation of memory $CD8^+$ T cells which could provide long-term protection against subsequent *Plasmodium* infections.

Indeed, the mechanism described above would predict that in the bone marrow chimeras analyzed (*see chapter 4, Figure 7*), diminished $CD8^+$ T cell activation should be observed whenever Hb^{SAD} or $Hb^{SAD}Hmox1^{+/-}$ bone marrow cells were transferred. The presence of Hb^{SAD} bone marrow would lead to decreased hepcidin production, as a consequence of increased EPO levels, erythropoiesis, and hemolysis, associated with the presence of Hb^{SAD} carrying RBC. In this setting, animals receiving $Hb^{SAD}Hmox1^{+/-}$ bone marrow cells would succumb to ECM due solely to the limited capacity of their bone marrow-derived cells to catabolize heme.

Furthermore, a less inflammatory state, generated by control of innate immunity activation in Hb^{SAD} mice, could provide a more favorable environment for T_{REG} expansion (*see chapter 2*). Inducing T_{REG} expansion during ECM can prevent disease, via a mechanism that rely on $Foxp3^+$ cells-mediated control of T cell activation[354]. Therefore, the less inflammatory environment generated in Hb^{SAD} mice upon *Plasmodium* infection, could lead not only to the generation of non-pathological $CD8^+$ T cell response, but also to an increase in the T_{REG} compartment, adding a further layer of protection against ECM development (*see figure 5.2*).

Of note, African children with sickle-cell anemia present higher risk of developing bacteraemia[373], an observation consistent with impairment in mounting protective immune responses. Furthermore, although some controversy exists in the literature[374], African children with iron deficiency, a condition leading to diminished hepcidin expression, presented lower incidence of clinical malaria[375,376], while iron supplementation has

been associated with increased incidence of severe malaria[377,378,379].

Heme administration during specific periods of time also leads to marked suppression of $CD8^+$ T cell activation (*see chapter 4, Figure 13*). However, the mechanisms responsible for this effect remain obscure, since there is no data indicating whether it is dependent or not on the HO-1/Nrf2 system. Nonetheless, it is possible that, contrary to what might occur in Hb^{SAD} mice, after heme injection the sharp increase in iron concentration leads to a burst in hepcidin production culminating in FPN degradation and a transient decrease in inflammatory cytokine production. In fact, an acute increase in body iron concentration leads to a decreased inflammatory response upon LPS challenge. This effect is dependent on hepcidin and JAK2/STAT3 induced upregulation of SOCS3 transcription[287]. Therefore, it is plausible that chronic decreased hepcidin production and acute increased hepcidin production direct inflammatory responses towards the same outcome, that is, decreased innate immune activation leading to reduced adaptive immune response.

While speculative at this point, the link between deregulated iron homeostasis in Hb^{SAD} mice and the observed suppression of $CD8^+$ T cell response in these animals is a mechanism worth exploring in the effort to determine the molecular basis underlying Hb^{SAD}-mediated immunoregulation. Importantly, hepcidin-dependent regulation of immune responses might also occur in other hemoglobinopathies where hemolysis occurs, leading to protection against the development of severe forms of malaria. Indeed, the role of hepcidin in protecting against *Plasmodium* infection has begun to be addressed. It has

recently been reported that hepcidin is responsible for blocking secondary *Plasmodium* infection, in a host with an ongoing *Plasmodium* infection. This blockade occurs by inhibition of *Plasmodium* growth during the liver stage of infection[380]. This data suggests that hepcidin might play a role in resistance against *Plasmodium* infection in the liver stage of the disease. Furthermore, the possibility of manipulating iron homeostasis in humans by using iron-chelating therapy or iron supplementation might open new therapeutical possibilities for controlling immunopathology mediated by *Plasmodium* infection.

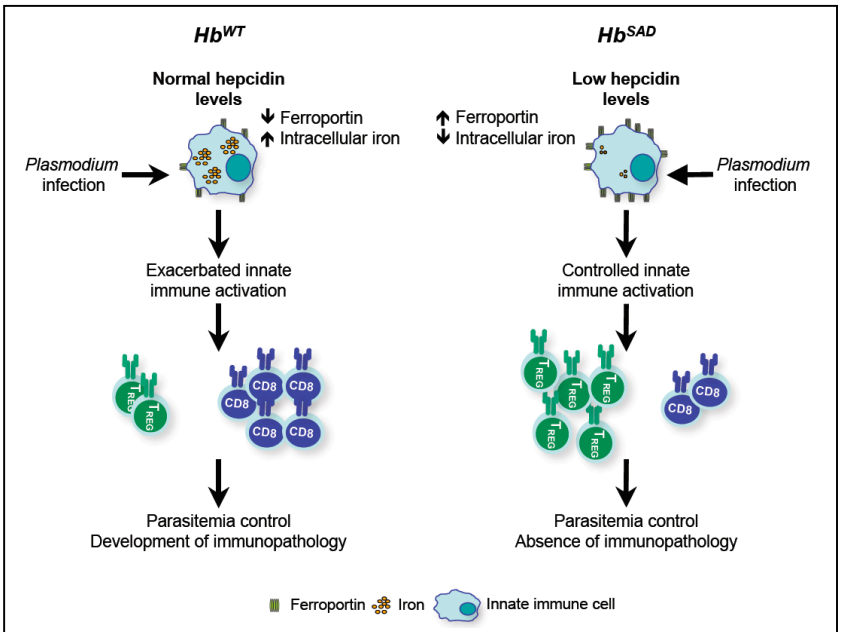

Figure 5.2. Model for hepcidin control of immunopathology in *Hb*^{SAD} mice. *Hb*^{WT} mice, present hepcidin levels that prevent high expression of ferroportin, which in turn maintains the level of intracelular iron in innate immune cells in a normal range. In *Hb*^{SAD} mice, low hepcidin levels sustain high expression of ferroportin, leading to low intracellular iron levels in innate immune cells. Upon *Plasmodium* infection differences in intracellular iron content in innate immune cells determine the magnitude of the innate immune responses that, in turn, determines whether the adaptive immune response will or not be pathological. *Hb*^{WT} mice present an exacerbated innate immune response leading to an adaptive immune response that is capable of controlling parasitemia, but that also causes immunopathology. On the other hand, *Hb*^{SAD} mice present a more controlled innate immune activation, leading to an adaptive immune response that is still capable of controlling parasitemia, but that does not cause immunopathology. In the model presented herein, intracellular iron levels, by controling innate immune activation, determines whether a pathological adaptive immune response is generated or not.

In the present thesis data exploring two different strategies employed by hosts to decrease the deleterious effects of immunopathology have been analyzed. Namely, mechanisms via which the damaging potential of the immune system is restrained, by T_{REG} expansion (*see chapter 2*) and decreased $CD8^+$ T cell response (*see chapter 4*), and mechanisms via which tissue resilience to immune-mediated damage is increased, by reducing heme availability under highly inflammatory conditions (*see chapter 3 and 4*), have been addressed. The body of work presented here suggests that by altering either or both mechanisms it is possible to shift disease outcome towards a more favorable result to the host. Furthermore, it highlights the complexity of mechanisms involved in the pathological outcomes of immune-mediated inflammatory diseases and opens new possibilities in the quest for therapies targeting disorders where the main deleterious effects are consequence of immunopathology.

References

1. Buckley, R.H. Molecular defects in human severe combined immunodeficiency and approaches to immune reconstitution. *Annu Rev Immunol* **22**, 625-655 (2004).
2. Conley, M.E.*, et al.* Primary B cell immunodeficiencies: comparisons and contrasts. *Annu Rev Immunol* **27**, 199-227 (2009).
3. Glocker, E.O.*, et al.* A homozygous CARD9 mutation in a family with susceptibility to fungal infections. *N Engl J Med* **361**, 1727-1735 (2009).
4. Hugot, J.P.*, et al.* Association of NOD2 leucine-rich repeat variants with susceptibility to Crohn's disease. *Nature* **411**, 599-603 (2001).
5. Ogura, Y.*, et al.* A frameshift mutation in NOD2 associated with susceptibility to Crohn's disease. *Nature* **411**, 603-606 (2001).
6. Sakaguchi, S. Naturally arising CD4+ regulatory t cells for immunologic self-tolerance and negative control of immune responses. *Annu Rev Immunol* **22**, 531-562 (2004).
7. Saenz, S.A., Noti, M. & Artis, D. Innate immune cell populations function as initiators and effectors in Th2 cytokine responses. *Trends Immunol* **31**, 407-413 (2010).
8. Chu, C.C., Di Meglio, P. & Nestle, F.O. Harnessing dendritic cells in inflammatory skin diseases. *Semin Immunol* **23**, 28-41 (2011).
9. Ryu, J.H., Kim, C.H. & Yoon, J.H. Innate immune responses of the airway epithelium. *Mol Cells* **30**, 173-183 (2010).
10. Cerf-Bensussan, N. & Gaboriau-Routhiau, V. The immune system and the gut microbiota: friends or foes? *Nat Rev Immunol* **10**, 735-744 (2010).
11. Smith, P.D.*, et al.* Intestinal macrophages and response to microbial encroachment. *Mucosal Immunol* **4**, 31-42 (2011).
12. Medzhitov, R. Recognition of microorganisms and activation of the immune response. *Nature* **449**, 819-826 (2007).
13. Qu, Y., Franchi, L., Nunez, G. & Dubyak, G.R. Nonclassical IL-1 beta secretion stimulated by P2X7 receptors is dependent on inflammasome activation and correlated with exosome release in murine macrophages. *J Immunol* **179**, 1913-1925 (2007).
14. Gasse, P.*, et al.* Uric acid is a danger signal activating NALP3 inflammasome in lung injury inflammation and fibrosis. *Am J Respir Crit Care Med* **179**, 903-913 (2009).
15. Martinon, F., Petrilli, V., Mayor, A., Tardivel, A. & Tschopp, J. Gout-associated uric acid crystals activate the NALP3 inflammasome. *Nature* **440**, 237-241 (2006).
16. Ather, J.L.*, et al.* Serum Amyloid A Activates the NLRP3 Inflammasome and Promotes Th17 Allergic Asthma in Mice. *J Immunol* **187**, 64-73 (2011).
17. Halle, A.*, et al.* The NALP3 inflammasome is involved in the innate immune response to amyloid-beta. *Nat Immunol* **9**, 857-865 (2008).
18. Tian, J.*, et al.* Toll-like receptor 9-dependent activation by DNA-containing immune complexes is mediated by HMGB1 and RAGE. *Nat Immunol* **8**, 487-496 (2007).
19. Yanai, H.*, et al.* HMGB proteins function as universal sentinels for nucleic-acid-mediated innate immune responses. *Nature* **462**, 99-103 (2009).
20. Ganguly, D.*, et al.* Self-RNA-antimicrobial peptide complexes activate human dendritic cells through TLR7 and TLR8. *J Exp Med* **206**, 1983-1994 (2009).
21. Lande, R.*, et al.* Plasmacytoid dendritic cells sense self-DNA coupled with antimicrobial peptide. *Nature* **449**, 564-569 (2007).
22. Scaffidi, P., Misteli, T. & Bianchi, M.E. Release of chromatin protein HMGB1 by necrotic cells triggers inflammation. *Nature* **418**, 191-195 (2002).
23. Kawai, T. & Akira, S. Toll-like Receptors and Their Crosstalk with Other Innate Receptors in Infection and Immunity. *Immunity* **34**, 637-650 (2011).
24. Elinav, E., Strowig, T., Henao-Mejia, J. & Flavell, R.A. Regulation of the Antimicrobial Response by NLR Proteins. *Immunity* **34**, 665-679 (2011).

25. Loo, Y.M. & Gale, M., Jr. Immune Signaling by RIG-I-like Receptors. *Immunity* **34**, 680-692 (2011).
26. Osorio, F. & Reis, E.S.C. Myeloid C-type Lectin Receptors in Pathogen Recognition and Host Defense. *Immunity* **34**, 651-664 (2011).
27. Nish, S. & Medzhitov, R. Host defense pathways: role of redundancy and compensation in infectious disease phenotypes. *Immunity* **34**, 629-636 (2011).
28. Tamura, T., Yanai, H., Savitsky, D. & Taniguchi, T. The IRF family transcription factors in immunity and oncogenesis. *Annu Rev Immunol* **26**, 535-584 (2008).
29. Takeuchi, O. & Akira, S. Pattern recognition receptors and inflammation. *Cell* **140**, 805-820 (2010).
30. Fitzgerald, K.A.*, et al.* Mal (MyD88-adapter-like) is required for Toll-like receptor-4 signal transduction. *Nature* **413**, 78-83 (2001).
31. Horng, T., Barton, G.M. & Medzhitov, R. TIRAP: an adapter molecule in the Toll signaling pathway. *Nat Immunol* **2**, 835-841 (2001).
32. Horng, T., Barton, G.M., Flavell, R.A. & Medzhitov, R. The adaptor molecule TIRAP provides signalling specificity for Toll-like receptors. *Nature* **420**, 329-333 (2002).
33. Yamamoto, M.*, et al.* TRAM is specifically involved in the Toll-like receptor 4-mediated MyD88-independent signaling pathway. *Nat Immunol* **4**, 1144-1150 (2003).
34. Meyer-Wentrup, F.*, et al.* Targeting DCIR on human plasmacytoid dendritic cells results in antigen presentation and inhibits IFN-alpha production. *Blood* **111**, 4245-4253 (2008).
35. Meyer-Wentrup, F.*, et al.* DCIR is endocytosed into human dendritic cells and inhibits TLR8-mediated cytokine production. *J Leukoc Biol* **85**, 518-525 (2009).
36. Fujikado, N.*, et al.* Dcir deficiency causes development of autoimmune diseases in mice due to excess expansion of dendritic cells. *Nat Med* **14**, 176-180 (2008).
37. LeibundGut-Landmann, S.*, et al.* Syk- and CARD9-dependent coupling of innate immunity to the induction of T helper cells that produce interleukin 17. *Nat Immunol* **8**, 630-638 (2007).
38. Robinson, M.J.*, et al.* Dectin-2 is a Syk-coupled pattern recognition receptor crucial for Th17 responses to fungal infection. *J Exp Med* **206**, 2037-2051 (2009).
39. Schroder, K. & Tschopp, J. The inflammasomes. *Cell* **140**, 821-832 (2010).
40. Petrilli, V.*, et al.* Activation of the NALP3 inflammasome is triggered by low intracellular potassium concentration. *Cell Death Differ* **14**, 1583-1589 (2007).
41. Tattoli, I.*, et al.* NLRX1 is a mitochondrial NOD-like receptor that amplifies NF-kappaB and JNK pathways by inducing reactive oxygen species production. *EMBO Rep* **9**, 293-300 (2008).
42. Cruz, C.M.*, et al.* ATP activates a reactive oxygen species-dependent oxidative stress response and secretion of proinflammatory cytokines in macrophages. *J Biol Chem* **282**, 2871-2879 (2007).
43. Zhou, R., Tardivel, A., Thorens, B., Choi, I. & Tschopp, J. Thioredoxin-interacting protein links oxidative stress to inflammasome activation. *Nat Immunol* **11**, 136-140 (2010).
44. Hornung, V.*, et al.* Silica crystals and aluminum salts activate the NALP3 inflammasome through phagosomal destabilization. *Nat Immunol* **9**, 847-856 (2008).
45. Kobayashi, K.*, et al.* IRAK-M is a negative regulator of Toll-like receptor signaling. *Cell* **110**, 191-202 (2002).
46. Seki, M.*, et al.* Critical role of IL-1 receptor-associated kinase-M in regulating chemokine-dependent deleterious inflammation in murine influenza pneumonia. *J Immunol* **184**, 1410-1418 (2010).
47. Su, J., Xie, Q., Wilson, I. & Li, L. Differential regulation and role of interleukin-1 receptor associated kinase-M in innate immunity signaling. *Cell Signal* **19**, 1596-1601 (2007).
48. Coornaert, B., Carpentier, I. & Beyaert, R. A20: central gatekeeper in inflammation and immunity. *J Biol Chem* **284**, 8217-8221 (2009).

49. Opipari, A.W., Jr., Hu, H.M., Yabkowitz, R. & Dixit, V.M. The A20 zinc finger protein protects cells from tumor necrosis factor cytotoxicity. *J Biol Chem* **267**, 12424-12427 (1992).
50. Lee, E.G.*, et al.* Failure to regulate TNF-induced NF-kappaB and cell death responses in A20-deficient mice. *Science* **289**, 2350-2354 (2000).
51. Boone, D.L.*, et al.* The ubiquitin-modifying enzyme A20 is required for termination of Toll-like receptor responses. *Nat Immunol* **5**, 1052-1060 (2004).
52. Turer, E.E.*, et al.* Homeostatic MyD88-dependent signals cause lethal inflamMation in the absence of A20. *J Exp Med* **205**, 451-464 (2008).
53. Hitotsumatsu, O.*, et al.* The ubiquitin-editing enzyme A20 restricts nucleotide-binding oligomerization domain containing 2-triggered signals. *Immunity* **28**, 381-390 (2008).
54. Lin, R.*, et al.* Negative regulation of the retinoic acid-inducible gene I-induced antiviral state by the ubiquitin-editing protein A20. *J Biol Chem* **281**, 2095-2103 (2006).
55. Kayagaki, N.*, et al.* DUBA: a deubiquitinase that regulates type I interferon production. *Science* **318**, 1628-1632 (2007).
56. Trompouki, E.*, et al.* CYLD is a deubiquitinating enzyme that negatively regulates NF-kappaB activation by TNFR family members. *Nature* **424**, 793-796 (2003).
57. Kovalenko, A.*, et al.* The tumour suppressor CYLD negatively regulates NF-kappaB signalling by deubiquitination. *Nature* **424**, 801-805 (2003).
58. Matsushita, K.*, et al.* Zc3h12a is an RNase essential for controlling immune responses by regulating mRNA decay. *Nature* **458**, 1185-1190 (2009).
59. O'Neill, L.A., Sheedy, F.J. & McCoy, C.E. MicroRNAs: the fine-tuners of Toll-like receptor signalling. *Nat Rev Immunol* **11**, 163-175 (2011).
60. Rothlin, C.V., Ghosh, S., Zuniga, E.I., Oldstone, M.B. & Lemke, G. TAM receptors are pleiotropic inhibitors of the innate immune response. *Cell* **131**, 1124-1136 (2007).
61. Lu, Q. & Lemke, G. Homeostatic regulation of the immune system by receptor tyrosine kinases of the Tyro 3 family. *Science* **293**, 306-311 (2001).
62. Kim, K.D.*, et al.* Adaptive immune cells temper initial innate responses. *Nat Med* **13**, 1248-1252 (2007).
63. Guarda, G.*, et al.* T cells dampen innate immune responses through inhibition of NLRP1 and NLRP3 inflammasomes. *Nature* **460**, 269-273 (2009).
64. Kim, J.M., Rasmussen, J.P. & Rudensky, A.Y. Regulatory T cells prevent catastrophic autoimmunity throughout the lifespan of mice. *Nat Immunol* **8**, 191-197 (2007).
65. Soares, M.P., Marguti, I., Cunha, A. & Larsen, R. Immunoregulatory effects of HO-1: how does it work? *Curr Opin Pharmacol* **9**, 482-489 (2009).
66. Steinman, R.M. & Cohn, Z.A. Identification of a novel cell type in peripheral lymphoid organs of mice. I. Morphology, quantitation, tissue distribution. *J Exp Med* **137**, 1142-1162 (1973).
67. Steinman, R.M. & Cohn, Z.A. Identification of a novel cell type in peripheral lymphoid organs of mice. II. Functional properties in vitro. *J Exp Med* **139**, 380-397 (1974).
68. Steinman, R.M., Lustig, D.S. & Cohn, Z.A. Identification of a novel cell type in peripheral lymphoid organs of mice. 3. Functional properties in vivo. *J Exp Med* **139**, 1431-1445 (1974).
69. Steinman, R.M., Adams, J.C. & Cohn, Z.A. Identification of a novel cell type in peripheral lymphoid organs of mice. IV. Identification and distribution in mouse spleen. *J Exp Med* **141**, 804-820 (1975).
70. Steinman, R.M. & Witmer, M.D. Lymphoid dendritic cells are potent stimulators of the primary mixed leukocyte reaction in mice. *Proc Natl Acad Sci U S A* **75**, 5132-5136 (1978).
71. Jung, S.*, et al.* In vivo depletion of CD11c+ dendritic cells abrogates priming of CD8+ T cells by exogenous cell-associated antigens. *Immunity* **17**, 211-220 (2002).
72. Tian, T., Woodworth, J., Skold, M. & Behar, S.M. In vivo depletion of CD11c+ cells delays the CD4+ T cell response to Mycobacterium tuberculosis and exacerbates the outcome of infection. *J Immunol* **175**, 3268-3272 (2005).

73. Liu, C.H., *et al.* Cutting edge: dendritic cells are essential for in vivo IL-12 production and development of resistance against Toxoplasma gondii infection in mice. *J Immunol* **177**, 31-35 (2006).
74. Zaft, T., Sapoznikov, A., Krauthgamer, R., Littman, D.R. & Jung, S. CD11chigh dendritic cell ablation impairs lymphopenia-driven proliferation of naive and memory CD8+ T cells. *J Immunol* **175**, 6428-6435 (2005).
75. Probst, H.C. & van den Broek, M. Priming of CTLs by lymphocytic choriomeningitis virus depends on dendritic cells. *J Immunol* **174**, 3920-3924 (2005).
76. van Rijt, L.S., *et al.* In vivo depletion of lung CD11c+ dendritic cells during allergen challenge abrogates the characteristic features of asthma. *J Exp Med* **201**, 981-991 (2005).
77. Zammit, D.J., Cauley, L.S., Pham, Q.M. & Lefrancois, L. Dendritic cells maximize the memory CD8 T cell response to infection. *Immunity* **22**, 561-570 (2005).
78. Sporri, R. & Reis e Sousa, C. Inflammatory mediators are insufficient for full dendritic cell activation and promote expansion of CD4+ T cell populations lacking helper function. *Nat Immunol* **6**, 163-170 (2005).
79. Reis e Sousa, C. Dendritic cells in a mature age. *Nat Rev Immunol* **6**, 476-483 (2006).
80. Zhu, J., Yamane, H. & Paul, W.E. Differentiation of effector CD4 T cell populations (*). *Annu Rev Immunol* **28**, 445-489 (2010).
81. Williams, M.A. & Bevan, M.J. Effector and memory CTL differentiation. *Annu Rev Immunol* **25**, 171-192 (2007).
82. Bonasio, R., *et al.* Clonal deletion of thymocytes by circulating dendritic cells homing to the thymus. *Nat Immunol* **7**, 1092-1100 (2006).
83. Ohnmacht, C., *et al.* Constitutive ablation of dendritic cells breaks self-tolerance of CD4 T cells and results in spontaneous fatal autoimmunity. *J Exp Med* **206**, 549-559 (2009).
84. Hawiger, D., *et al.* Dendritic cells induce peripheral T cell unresponsiveness under steady state conditions in vivo. *J Exp Med* **194**, 769-779 (2001).
85. Liu, K., *et al.* Immune tolerance after delivery of dying cells to dendritic cells in situ. *J Exp Med* **196**, 1091-1097 (2002).
86. Bonifaz, L., *et al.* Efficient targeting of protein antigen to the dendritic cell receptor DEC-205 in the steady state leads to antigen presentation on major histocompatibility complex class I products and peripheral CD8+ T cell tolerance. *J Exp Med* **196**, 1627-1638 (2002).
87. Carreno, B.M. & Collins, M. The B7 family of ligands and its receptors: new pathways for costimulation and inhibition of immune responses. *Annu Rev Immunol* **20**, 29-53 (2002).
88. Lenschow, D.J., Walunas, T.L. & Bluestone, J.A. CD28/B7 system of T cell costimulation. *Annu Rev Immunol* **14**, 233-258 (1996).
89. Tan, J.T., Whitmire, J.K., Ahmed, R., Pearson, T.C. & Larsen, C.P. 4-1BB ligand, a member of the TNF family, is important for the generation of antiviral CD8 T cell responses. *J Immunol* **163**, 4859-4868 (1999).
90. Kwon, B.S., *et al.* Immune responses in 4-1BB (CD137)-deficient mice. *J Immunol* **168**, 5483-5490 (2002).
91. Hendriks, J., *et al.* CD27 is required for generation and long-term maintenance of T cell immunity. *Nat Immunol* **1**, 433-440 (2000).
92. Keller, A.M., Schildknecht, A., Xiao, Y., van den Broek, M. & Borst, J. Expression of costimulatory ligand CD70 on steady-state dendritic cells breaks CD8+ T cell tolerance and permits effective immunity. *Immunity* **29**, 934-946 (2008).
93. Soares, H., *et al.* A subset of dendritic cells induces CD4+ T cells to produce IFN-gamma by an IL-12-independent but CD70-dependent mechanism in vivo. *J Exp Med* **204**, 1095-1106 (2007).
94. Ito, T., *et al.* TSLP-activated dendritic cells induce an inflammatory T helper type 2 cell response through OX40 ligand. *J Exp Med* **202**, 1213-1223 (2005).
95. Hsieh, C.S., *et al.* Development of TH1 CD4+ T cells through IL-12 produced by Listeria-induced macrophages. *Science* **260**, 547-549 (1993).

96. Le Gros, G., Ben-Sasson, S.Z., Seder, R., Finkelman, F.D. & Paul, W.E. Generation of interleukin 4 (IL-4)-producing cells in vivo and in vitro: IL-2 and IL-4 are required for in vitro generation of IL-4-producing cells. *J Exp Med* **172**, 921-929 (1990).
97. Veldhoen, M., Hocking, R.J., Atkins, C.J., Locksley, R.M. & Stockinger, B. TGFbeta in the context of an inflammatory cytokine milieu supports de novo differentiation of IL-17-producing T cells. *Immunity* **24**, 179-189 (2006).
98. Zhou, L.*, et al.* IL-6 programs T(H)-17 cell differentiation by promoting sequential engagement of the IL-21 and IL-23 pathways. *Nat Immunol* **8**, 967-974 (2007).
99. Wei, G.*, et al.* Global mapping of H3K4me3 and H3K27me3 reveals specificity and plasticity in lineage fate determination of differentiating CD4+ T cells. *Immunity* **30**, 155-167 (2009).
100. Reis e Sousa, C.*, et al.* In vivo microbial stimulation induces rapid CD40 ligand-independent production of interleukin 12 by dendritic cells and their redistribution to T cell areas. *J Exp Med* **186**, 1819-1829 (1997).
101. Perrigoue, J.G.*, et al.* MHC class II-dependent basophil-CD4+ T cell interactions promote T(H)2 cytokine-dependent immunity. *Nat Immunol* **10**, 697-705 (2009).
102. Saenz, S.A.*, et al.* IL25 elicits a multipotent progenitor cell population that promotes T(H)2 cytokine responses. *Nature* **464**, 1362-1366.
103. Neill, D.R.*, et al.* Nuocytes represent a new innate effector leukocyte that mediates type-2 immunity. *Nature* **464**, 1367-1370.
104. Croft, M., Carter, L., Swain, S.L. & Dutton, R.W. Generation of polarized antigen-specific CD8 effector populations: reciprocal action of interleukin (IL)-4 and IL-12 in promoting type 2 versus type 1 cytokine profiles. *J Exp Med* **180**, 1715-1728 (1994).
105. Sad, S., Marcotte, R. & Mosmann, T.R. Cytokine-induced differentiation of precursor mouse CD8+ T cells into cytotoxic CD8+ T cells secreting Th1 or Th2 cytokines. *Immunity* **2**, 271-279 (1995).
106. Huber, M.*, et al.* A Th17-like developmental process leads to CD8(+) Tc17 cells with reduced cytotoxic activity. *Eur J Immunol* **39**, 1716-1725 (2009).
107. Ciric, B., El-behi, M., Cabrera, R., Zhang, G.X. & Rostami, A. IL-23 drives pathogenic IL-17-producing CD8+ T cells. *J Immunol* **182**, 5296-5305 (2009).
108. Joshi, N.S.*, et al.* Inflammation directs memory precursor and short-lived effector CD8(+) T cell fates via the graded expression of T-bet transcription factor. *Immunity* **27**, 281-295 (2007).
109. Badovinac, V.P., Porter, B.B. & Harty, J.T. CD8+ T cell contraction is controlled by early inflammation. *Nat Immunol* **5**, 809-817 (2004).
110. Curtsinger, J.M., Lins, D.C. & Mescher, M.F. Signal 3 determines tolerance versus full activation of naive CD8 T cells: dissociating proliferation and development of effector function. *J Exp Med* **197**, 1141-1151 (2003).
111. Curtsinger, J.M.*, et al.* Inflammatory cytokines provide a third signal for activation of naive CD4+ and CD8+ T cells. *J Immunol* **162**, 3256-3262 (1999).
112. Curtsinger, J.M., Valenzuela, J.O., Agarwal, P., Lins, D. & Mescher, M.F. Type I IFNs provide a third signal to CD8 T cells to stimulate clonal expansion and differentiation. *J Immunol* **174**, 4465-4469 (2005).
113. Kolumam, G.A., Thomas, S., Thompson, L.J., Sprent, J. & Murali-Krishna, K. Type I interferons act directly on CD8 T cells to allow clonal expansion and memory formation in response to viral infection. *J Exp Med* **202**, 637-650 (2005).
114. Le Bon, A.*, et al.* Direct stimulation of T cells by type I IFN enhances the CD8+ T cell response during cross-priming. *J Immunol* **176**, 4682-4689 (2006).
115. Pearce, E.L. & Shen, H. Generation of CD8 T cell memory is regulated by IL-12. *J Immunol* **179**, 2074-2081 (2007).
116. Allard, E.L.*, et al.* Overexpression of IL-21 promotes massive CD8+ memory T cell accumulation. *Eur J Immunol* **37**, 3069-3077 (2007).
117. Elsaesser, H., Sauer, K. & Brooks, D.G. IL-21 is required to control chronic viral infection. *Science* **324**, 1569-1572 (2009).
118. Frohlich, A.*, et al.* IL-21R on T cells is critical for sustained functionality and control of chronic viral infection. *Science* **324**, 1576-1580 (2009).

119. Yi, J.S., Du, M. & Zajac, A.J. A vital role for interleukin-21 in the control of a chronic viral infection. *Science* **324**, 1572-1576 (2009).
120. Rao, R.R., Li, Q., Odunsi, K. & Shrikant, P.A. The mTOR kinase determines effector versus memory CD8+ T cell fate by regulating the expression of transcription factors T-bet and Eomesodermin. *Immunity* **32**, 67-78 (2010).
121. Intlekofer, A.M.*, et al.* Effector and memory CD8+ T cell fate coupled by T-bet and eomesodermin. *Nat Immunol* **6**, 1236-1244 (2005).
122. Banerjee, A.*, et al.* Cutting edge: The transcription factor eomesodermin enables CD8+ T cells to compete for the memory cell niche. *J Immunol* **185**, 4988-4992 (2010).
123. Bennett, S.R.*, et al.* Help for cytotoxic-T-cell responses is mediated by CD40 signalling. *Nature* **393**, 478-480 (1998).
124. Ridge, J.P., Di Rosa, F. & Matzinger, P. A conditioned dendritic cell can be a temporal bridge between a CD4+ T-helper and a T-killer cell. *Nature* **393**, 474-478 (1998).
125. Schoenberger, S.P., Toes, R.E., van der Voort, E.I., Offringa, R. & Melief, C.J. T-cell help for cytotoxic T lymphocytes is mediated by CD40-CD40L interactions. *Nature* **393**, 480-483 (1998).
126. Rahemtulla, A.*, et al.* Normal development and function of CD8+ cells but markedly decreased helper cell activity in mice lacking CD4. *Nature* **353**, 180-184 (1991).
127. Buller, R.M., Holmes, K.L., Hugin, A., Frederickson, T.N. & Morse, H.C., 3rd. Induction of cytotoxic T-cell responses in vivo in the absence of CD4 helper cells. *Nature* **328**, 77-79 (1987).
128. Janssen, E.M.*, et al.* CD4+ T cells are required for secondary expansion and memory in CD8+ T lymphocytes. *Nature* **421**, 852-856 (2003).
129. Shedlock, D.J. & Shen, H. Requirement for CD4 T cell help in generating functional CD8 T cell memory. *Science* **300**, 337-339 (2003).
130. Sun, J.C. & Bevan, M.J. Defective CD8 T cell memory following acute infection without CD4 T cell help. *Science* **300**, 339-342 (2003).
131. Carvalho, L.H.*, et al.* IL-4-secreting CD4+ T cells are crucial to the development of CD8+ T-cell responses against malaria liver stages. *Nat Med* **8**, 166-170 (2002).
132. Yanez, D.M., Manning, D.D., Cooley, A.J., Weidanz, W.P. & van der Heyde, H.C. Participation of lymphocyte subpopulations in the pathogenesis of experimental murine cerebral malaria. *J Immunol* **157**, 1620-1624 (1996).
133. Hermsen, C., van de Wiel, T., Mommers, E., Sauerwein, R. & Eling, W. Depletion of CD4+ or CD8+ T-cells prevents Plasmodium berghei induced cerebral malaria in end-stage disease. *Parasitology* **114 (Pt 1)**, 7-12 (1997).
134. Sakaguchi, S., Sakaguchi, N., Asano, M., Itoh, M. & Toda, M. Immunologic self-tolerance maintained by activated T cells expressing IL-2 receptor alpha-chains (CD25). Breakdown of a single mechanism of self-tolerance causes various autoimmune diseases. *J Immunol* **155**, 1151-1164 (1995).
135. Itoh, M.*, et al.* Thymus and autoimmunity: production of CD25+CD4+ naturally anergic and suppressive T cells as a key function of the thymus in maintaining immunologic self-tolerance. *J Immunol* **162**, 5317-5326 (1999).
136. Brunkow, M.E.*, et al.* Disruption of a new forkhead/winged-helix protein, scurfin, results in the fatal lymphoproliferative disorder of the scurfy mouse. *Nat Genet* **27**, 68-73 (2001).
137. Wildin, R.S.*, et al.* X-linked neonatal diabetes mellitus, enteropathy and endocrinopathy syndrome is the human equivalent of mouse scurfy. *Nat Genet* **27**, 18-20 (2001).
138. Hori, S., Nomura, T. & Sakaguchi, S. Control of regulatory T cell development by the transcription factor Foxp3. *Science* **299**, 1057-1061 (2003).
139. Fontenot, J.D., Gavin, M.A. & Rudensky, A.Y. Foxp3 programs the development and function of CD4+CD25+ regulatory T cells. *Nat Immunol* **4**, 330-336 (2003).
140. Tadokoro, C.E.*, et al.* Regulatory T cells inhibit stable contacts between CD4+ T cells and dendritic cells in vivo. *J Exp Med* **203**, 505-511 (2006).
141. Tang, Q.*, et al.* Visualizing regulatory T cell control of autoimmune responses in nonobese diabetic mice. *Nat Immunol* **7**, 83-92 (2006).

142. Zhang, X., Izikson, L., Liu, L. & Weiner, H.L. Activation of CD25(+)CD4(+) regulatory T cells by oral antigen administration. *J Immunol* **167**, 4245-4253 (2001).
143. Levings, M.K.*, et al.* Human CD25+CD4+ T suppressor cell clones produce transforming growth factor beta, but not interleukin 10, and are distinct from type 1 T regulatory cells. *J Exp Med* **196**, 1335-1346 (2002).
144. Maloy, K.J.*, et al.* CD4+CD25+ T(R) cells suppress innate immune pathology through cytokine-dependent mechanisms. *J Exp Med* **197**, 111-119 (2003).
145. Rubtsov, Y.P.*, et al.* Regulatory T cell-derived interleukin-10 limits inflammation at environmental interfaces. *Immunity* **28**, 546-558 (2008).
146. Read, S.*, et al.* Blockade of CTLA-4 on CD4+CD25+ regulatory T cells abrogates their function in vivo. *J Immunol* **177**, 4376-4383 (2006).
147. Tang, Q.*, et al.* Distinct roles of CTLA-4 and TGF-beta in CD4+CD25+ regulatory T cell function. *Eur J Immunol* **34**, 2996-3005 (2004).
148. Robertson, S.J. & Hasenkrug, K.J. The role of virus-induced regulatory T cells in immunopathology. *Springer Semin Immunopathol* **28**, 51-62 (2006).
149. Demengeot, J., Zelenay, S., Moraes-Fontes, M.F., Caramalho, I. & Coutinho, A. Regulatory T cells in microbial infection. *Springer Semin Immunopathol* **28**, 41-50 (2006).
150. Wohlfert, E. & Belkaid, Y. Role of endogenous and induced regulatory T cells during infections. *J Clin Immunol* **28**, 707-715 (2008).
151. Belkaid, Y. Regulatory T cells and infection: a dangerous necessity. *Nat Rev Immunol* **7**, 875-888 (2007).
152. Chen, W.*, et al.* Conversion of peripheral CD4+CD25- naive T cells to CD4+CD25+ regulatory T cells by TGF-beta induction of transcription factor Foxp3. *J Exp Med* **198**, 1875-1886 (2003).
153. Fu, S.*, et al.* TGF-beta induces Foxp3 + T-regulatory cells from CD4 + CD25 - precursors. *Am J Transplant* **4**, 1614-1627 (2004).
154. Wakkach, A.*, et al.* Characterization of dendritic cells that induce tolerance and T regulatory 1 cell differentiation in vivo. *Immunity* **18**, 605-617 (2003).
155. Awasthi, A.*, et al.* A dominant function for interleukin 27 in generating interleukin 10-producing anti-inflammatory T cells. *Nat Immunol* **8**, 1380-1389 (2007).
156. Ochando, J.C.*, et al.* Alloantigen-presenting plasmacytoid dendritic cells mediate tolerance to vascularized grafts. *Nat Immunol* **7**, 652-662 (2006).
157. Yamazaki, S.*, et al.* Direct expansion of functional CD25+ CD4+ regulatory T cells by antigen-processing dendritic cells. *J Exp Med* **198**, 235-247 (2003).
158. Tarbell, K.V., Yamazaki, S., Olson, K., Toy, P. & Steinman, R.M. CD25+ CD4+ T cells, expanded with dendritic cells presenting a single autoantigenic peptide, suppress autoimmune diabetes. *J Exp Med* **199**, 1467-1477 (2004).
159. Kretschmer, K.*, et al.* Inducing and expanding regulatory T cell populations by foreign antigen. *Nat Immunol* **6**, 1219-1227 (2005).
160. Hawiger, D., Wan, Y.Y., Eynon, E.E. & Flavell, R.A. The transcription cofactor Hopx is required for regulatory T cell function in dendritic cell-mediated peripheral T cell unresponsiveness. *Nat Immunol* **11**, 962-968 (2010).
161. Mucida, D.*, et al.* Reciprocal TH17 and regulatory T cell differentiation mediated by retinoic acid. *Science* **317**, 256-260 (2007).
162. Sun, C.M.*, et al.* Small intestine lamina propria dendritic cells promote de novo generation of Foxp3 T reg cells via retinoic acid. *J Exp Med* **204**, 1775-1785 (2007).
163. Coombes, J.L.*, et al.* A functionally specialized population of mucosal CD103+ DCs induces Foxp3+ regulatory T cells via a TGF-beta and retinoic acid-dependent mechanism. *J Exp Med* **204**, 1757-1764 (2007).
164. Haribhai, D.*, et al.* A requisite role for induced regulatory T cells in tolerance based on expanding antigen receptor diversity. *Immunity* **35**, 109-122 (2011).
165. Zheng, Y.*, et al.* Regulatory T-cell suppressor program co-opts transcription factor IRF4 to control T(H)2 responses. *Nature* **458**, 351-356 (2009).
166. Chaudhry, A.*, et al.* CD4+ regulatory T cells control TH17 responses in a Stat3-dependent manner. *Science* **326**, 986-991 (2009).

167. Koch, M.A., *et al.* The transcription factor T-bet controls regulatory T cell homeostasis and function during type 1 inflammation. *Nat Immunol* **10**, 595-602 (2009).
168. Liu, K., *et al.* In vivo analysis of dendritic cell development and homeostasis. *Science* **324**, 392-397 (2009).
169. Darrasse-Jeze, G., *et al.* Feedback control of regulatory T cell homeostasis by dendritic cells in vivo. *J Exp Med* **206**, 1853-1862 (2009).
170. Raberg, L., Graham, A.L. & Read, A.F. Decomposing health: tolerance and resistance to parasites in animals. *Philos Trans R Soc Lond B Biol Sci* **364**, 37-49 (2009).
171. Schneider, D.S. & Ayres, J.S. Two ways to survive infection: what resistance and tolerance can teach us about treating infectious diseases. *Nat Rev Immunol* **8**, 889-895 (2008).
172. Simms, E.L. Defining tolerance as a norm of reaction. *Evol Ecol* **14**, 563-570 (2001).
173. Stowe, K.A., Marquis, R.J., Hochwender, C.G. & Simms, E.L. The evolutionary ecology of tolerance to consumer damage. *Annu Rev Ecol Syst* **31**, 565-595 (2000).
174. Raberg, L., Sim, D. & Read, A.F. Disentangling genetic variation for resistance and tolerance to infectious diseases in animals. *Science* **318**, 812-814 (2007).
175. Ayres, J.S. & Schneider, D.S. A signaling protease required for melanization in Drosophila affects resistance and tolerance of infections. *PLoS Biol* **6**, 2764-2773 (2008).
176. Gazzinelli, R.T., *et al.* In the absence of endogenous IL-10, mice acutely infected with Toxoplasma gondii succumb to a lethal immune response dependent on CD4+ T cells and accompanied by overproduction of IL-12, IFN-gamma and TNF-alpha. *J Immunol* **157**, 798-805 (1996).
177. Holscher, C., *et al.* Tumor necrosis factor alpha-mediated toxic shock in Trypanosoma cruzi-infected interleukin 10-deficient mice. *Infect Immun* **68**, 4075-4083 (2000).
178. Pamplona, A., *et al.* Heme oxygenase-1 and carbon monoxide suppress the pathogenesis of experimental cerebral malaria. *Nat Med* **13**, 703-710 (2007).
179. Seixas, E., *et al.* Heme oxygenase-1 affords protection against noncerebral forms of severe malaria. *Proc Natl Acad Sci U S A* **106**, 15837-15842 (2009).
180. Vossenkamper, A., *et al.* Both IL-12 and IL-18 contribute to small intestinal Th1-type immunopathology following oral infection with Toxoplasma gondii, but IL-12 is dominant over IL-18 in parasite control. *Eur J Immunol* **34**, 3197-3207 (2004).
181. Chen, S.T., *et al.* CLEC5A is critical for dengue-virus-induced lethal disease. *Nature* **453**, 672-676 (2008).
182. Ritter, M., *et al.* Schistosoma mansoni triggers Dectin-2, which activates the Nlrp3 inflammasome and alters adaptive immune responses. *Proc Natl Acad Sci U S A* **107**, 20459-20464.
183. Carlsson, F., *et al.* Host-detrimental role of Esx-1-mediated inflammasome activation in mycobacterial infection. *PLoS Pathog* **6**, e1000895.
184. Hayashi, S., *et al.* Characterization of rat heme oxygenase-3 gene. Implication of processed pseudogenes derived from heme oxygenase-2 gene. *Gene* **336**, 241-250 (2004).
185. Otterbein, L.E., Soares, M.P., Yamashita, K. & Bach, F.H. Heme oxygenase-1: unleashing the protective properties of heme. *Trends Immunol* **24**, 449-455 (2003).
186. Soares, M.P. & Bach, F.H. Heme oxygenase-1: from biology to therapeutic potential. *Trends Mol Med* **15**, 50-58 (2009).
187. Fenton, H.J.H. Oxidation of tartaric acid in presence of iron. *J. Chem. Soc. Trans.* **65**, 899-910 (1894).
188. Gozzelino, R., Jeney, V. & Soares, M.P. Mechanisms of cell protection by heme oxygenase-1. *Annu Rev Pharmacol Toxicol* **50**, 323-354 (2010).
189. Ganz, T. & Nemeth, E. Regulation of iron acquisition and iron distribution in mammals. *Biochim Biophys Acta* **1763**, 690-699 (2006).
190. Brouard, S., *et al.* Carbon monoxide generated by heme oxygenase 1 suppresses endothelial cell apoptosis. *J Exp Med* **192**, 1015-1026 (2000).

191. Otterbein, L.E., *et al.* Carbon monoxide has anti-inflammatory effects involving the mitogen-activated protein kinase pathway. *Nat Med* **6**, 422-428 (2000).
192. Silva, G., Cunha, A., Gregoire, I.P., Seldon, M.P. & Soares, M.P. The antiapoptotic effect of heme oxygenase-1 in endothelial cells involves the degradation of p38 alpha MAPK isoform. *J Immunol* **177**, 1894-1903 (2006).
193. Zuckerbraun, B.S., *et al.* Carbon monoxide signals via inhibition of cytochrome c oxidase and generation of mitochondrial reactive oxygen species. *FASEB J* **21**, 1099-1106 (2007).
194. Ferreira, A., Balla, J., Jeney, V., Balla, G. & Soares, M.P. A central role for free heme in the pathogenesis of severe malaria: the missing link? *J Mol Med (Berl)* **86**, 1097-1111 (2008).
195. Stocker, R., Yamamoto, Y., McDonagh, A.F., Glazer, A.N. & Ames, B.N. Bilirubin is an antioxidant of possible physiological importance. *Science* **235**, 1043-1046 (1987).
196. Reiter, T.A., Pang, B., Dedon, P. & Demple, B. Resistance to nitric oxide-induced necrosis in heme oxygenase-1 overexpressing pulmonary epithelial cells associated with decreased lipid peroxidation. *J Biol Chem* **281**, 36603-36612 (2006).
197. Dore, S., *et al.* Bilirubin, formed by activation of heme oxygenase-2, protects neurons against oxidative stress injury. *Proc Natl Acad Sci U S A* **96**, 2445-2450 (1999).
198. Balla, G., *et al.* Ferritin: a cytoprotective antioxidant strategem of endothelium. *J Biol Chem* **267**, 18148-18153 (1992).
199. Pham, C.G., *et al.* Ferritin heavy chain upregulation by NF-kappaB inhibits TNFalpha-induced apoptosis by suppressing reactive oxygen species. *Cell* **119**, 529-542 (2004).
200. Alam, J. & Cook, J.L. How many transcription factors does it take to turn on the heme oxygenase-1 gene? *Am J Respir Cell Mol Biol* **36**, 166-174 (2007).
201. Sykiotis, G.P. & Bohmann, D. Stress-activated cap'n'collar transcription factors in aging and human disease. *Sci Signal* **3**, re3 (2010).
202. Kensler, T.W., Wakabayashi, N. & Biswal, S. Cell survival responses to environmental stresses via the Keap1-Nrf2-ARE pathway. *Annu Rev Pharmacol Toxicol* **47**, 89-116 (2007).
203. Akamatsu, Y., *et al.* Heme oxygenase-1-derived carbon monoxide protects hearts from transplant associated ischemia reperfusion injury. *FASEB J* **18**, 771-772 (2004).
204. Soares, M.P., *et al.* Expression of heme oxygenase-1 can determine cardiac xenograft survival. *Nat Med* **4**, 1073-1077 (1998).
205. Otterbein, L.E., *et al.* Carbon monoxide suppresses arteriosclerotic lesions associated with chronic graft rejection and with balloon injury. *Nat Med* **9**, 183-190 (2003).
206. Chora, A.A., *et al.* Heme oxygenase-1 and carbon monoxide suppress autoimmune neuroinflammation. *J Clin Invest* **117**, 438-447 (2007).
207. Larsen, R., *et al.* A central role for free heme in the pathogenesis of severe sepsis. *Sci Transl Med* **2**, 51ra71 (2010).
208. Poss, K.D. & Tonegawa, S. Heme oxygenase 1 is required for mammalian iron reutilization. *Proc Natl Acad Sci U S A* **94**, 10919-10924 (1997).
209. Poss, K.D. & Tonegawa, S. Reduced stress defense in heme oxygenase 1-deficient cells. *Proc Natl Acad Sci U S A* **94**, 10925-10930 (1997).
210. Yachie, A., *et al.* Oxidative stress causes enhanced endothelial cell injury in human heme oxygenase-1 deficiency. *J Clin Invest* **103**, 129-135 (1999).
211. Figueiredo, R.T., *et al.* Characterization of heme as activator of Toll-like receptor 4. *J Biol Chem* **282**, 20221-20229 (2007).
212. Porto, B.N., *et al.* Heme induces neutrophil migration and reactive oxygen species generation through signaling pathways characteristic of chemotactic receptors. *J Biol Chem* **282**, 24430-24436 (2007).
213. Monteiro, A.P., *et al.* Leukotriene B4 mediates neutrophil migration induced by heme. *J Immunol* **186**, 6562-6567 (2011).
214. Lee, T.S. & Chau, L.Y. Heme oxygenase-1 mediates the anti-inflammatory effect of interleukin-10 in mice. *Nat Med* **8**, 240-246 (2002).

215. Lee, T.S., Tsai, H.L. & Chau, L.Y. Induction of heme oxygenase-1 expression in murine macrophages is essential for the anti-inflammatory effect of low dose 15-deoxy-Delta 12,14-prostaglandin J2. *J Biol Chem* **278**, 19325-19330 (2003).
216. Kapturczak, M.H.*, et al.* Heme oxygenase-1 modulates early inflammatory responses: evidence from the heme oxygenase-1-deficient mouse. *Am J Pathol* **165**, 1045-1053 (2004).
217. Graca-Souza, A.V., Arruda, M.A., de Freitas, M.S., Barja-Fidalgo, C. & Oliveira, P.L. Neutrophil activation by heme: implications for inflammatory processes. *Blood* **99**, 4160-4165 (2002).
218. Wiesel, P.*, et al.* Exacerbation of chronic renovascular hypertension and acute renal failure in heme oxygenase-1-deficient mice. *Circ Res* **88**, 1088-1094 (2001).
219. Taille, C.*, et al.* Induction of heme oxygenase-1 inhibits NAD(P)H oxidase activity by down-regulating cytochrome b558 expression via the reduction of heme availability. *J Biol Chem* **279**, 28681-28688 (2004).
220. Li, X., Schwacha, M.G., Chaudry, I.H. & Choudhry, M.A. Heme oxygenase-1 protects against neutrophil-mediated intestinal damage by down-regulation of neutrophil p47phox and p67phox activity and O2- production in a two-hit model of alcohol intoxication and burn injury. *J Immunol* **180**, 6933-6940 (2008).
221. Wang, X.M., Kim, H.P., Nakahira, K., Ryter, S.W. & Choi, A.M. The heme oxygenase-1/carbon monoxide pathway suppresses TLR4 signaling by regulating the interaction of TLR4 with caveolin-1. *J Immunol* **182**, 3809-3818 (2009).
222. Nakahira, K.*, et al.* Carbon monoxide differentially inhibits TLR signaling pathways by regulating ROS-induced trafficking of TLRs to lipid rafts. *J Exp Med* **203**, 2377-2389 (2006).
223. Chin, B.Y.*, et al.* Hypoxia-inducible factor 1alpha stabilization by carbon monoxide results in cytoprotective preconditioning. *Proc Natl Acad Sci U S A* **104**, 5109-5114 (2007).
224. Bilban, M.*, et al.* Carbon monoxide orchestrates a protective response through PPARgamma. *Immunity* **24**, 601-610 (2006).
225. Morse, D.*, et al.* Suppression of inflammatory cytokine production by carbon monoxide involves the JNK pathway and AP-1. *J Biol Chem* **278**, 36993-36998 (2003).
226. Mashreghi, M.F.*, et al.* Inhibition of dendritic cell maturation and function is independent of heme oxygenase 1 but requires the activation of STAT3. *J Immunol* **180**, 7919-7930 (2008).
227. Nolte, M.A., Leibundgut-Landmann, S., Joffre, O. & Reis e Sousa, C. Dendritic cell quiescence during systemic inflammation driven by LPS stimulation of radioresistant cells in vivo. *J Exp Med* **204**, 1487-1501 (2007).
228. Chauveau, C.*, et al.* Heme oxygenase-1 expression inhibits dendritic cell maturation and proinflammatory function but conserves IL-10 expression. *Blood* **106**, 1694-1702 (2005).
229. Remy, S.*, et al.* Carbon monoxide inhibits TLR-induced dendritic cell immunogenicity. *J Immunol* **182**, 1877-1884 (2009).
230. Liu, Y.*, et al.* Bilirubin possesses powerful immunomodulatory activity and suppresses experimental autoimmune encephalomyelitis. *J Immunol* **181**, 1887-1897 (2008).
231. Pae, H.O.*, et al.* Carbon monoxide produced by heme oxygenase-1 suppresses T cell proliferation via inhibition of IL-2 production. *J Immunol* **172**, 4744-4751 (2004).
232. Song, R.*, et al.* Carbon monoxide promotes Fas/CD95-induced apoptosis in Jurkat cells. *J Biol Chem* **279**, 44327-44334 (2004).
233. McDaid, J.*, et al.* Heme oxygenase-1 modulates the allo-immune response by promoting activation-induced cell death of T cells. *FASEB J* **19**, 458-460 (2005).
234. Yamashita, K.*, et al.* Heme oxygenase-1 is essential for and promotes tolerance to transplanted organs. *FASEB J* **20**, 776-778 (2006).
235. Yamashita, K.*, et al.* Biliverdin, a natural product of heme catabolism, induces tolerance to cardiac allografts. *FASEB J* **18**, 765-767 (2004).

236. Phelan, D., Winter, G.M., Rogers, W.J., Lam, J.C. & Denison, M.S. Activation of the Ah receptor signal transduction pathway by bilirubin and biliverdin. *Arch Biochem Biophys* **357**, 155-163 (1998).
237. Quintana, F.J.*, et al.* Control of T(reg) and T(H)17 cell differentiation by the aryl hydrocarbon receptor. *Nature* **453**, 65-71 (2008).
238. Veldhoen, M.*, et al.* The aryl hydrocarbon receptor links TH17-cell-mediated autoimmunity to environmental toxins. *Nature* **453**, 106-109 (2008).
239. Tzima, S., Victoratos, P., Kranidioti, K., Alexiou, M. & Kollias, G. Myeloid heme oxygenase-1 regulates innate immunity and autoimmunity by modulating IFN-beta production. *J Exp Med* **206**, 1167-1179 (2009).
240. Brusko, T.M., Wasserfall, C.H., Agarwal, A., Kapturczak, M.H. & Atkinson, M.A. An integral role for heme oxygenase-1 and carbon monoxide in maintaining peripheral tolerance by CD4+CD25+ regulatory T cells. *J Immunol* **174**, 5181-5186 (2005).
241. Pae, H.O., Oh, G.S., Choi, B.M., Chae, S.C. & Chung, H.T. Differential expressions of heme oxygenase-1 gene in CD25- and CD25+ subsets of human CD4+ T cells. *Biochem Biophys Res Commun* **306**, 701-705 (2003).
242. Zelenay, S., Chora, A., Soares, M.P. & Demengeot, J. Heme oxygenase-1 is not required for mouse regulatory T cell development and function. *Int Immunol* **19**, 11-18 (2007).
243. Choi, B.M., Pae, H.O., Jeong, Y.R., Kim, Y.M. & Chung, H.T. Critical role of heme oxygenase-1 in Foxp3-mediated immune suppression. *Biochem Biophys Res Commun* **327**, 1066-1071 (2005).
244. George, J.F.*, et al.* Suppression by CD4+CD25+ regulatory T cells is dependent on expression of heme oxygenase-1 in antigen-presenting cells. *Am J Pathol* **173**, 154-160 (2008).
245. Watanabe-Matsui, M.*, et al.* Heme regulates B-cell differentiation, antibody class switch, and heme oxygenase-1 expression in B cells as a ligand of Bach2. *Blood* **117**, 5438-5448 (2011).
246. Shi, Y., Evans, J.E. & Rock, K.L. Molecular identification of a danger signal that alerts the immune system to dying cells. *Nature* **425**, 516-521 (2003).
247. Kono, H. & Rock, K.L. How dying cells alert the immune system to danger. *Nat Rev Immunol* **8**, 279-289 (2008).
248. Matzinger, P. Tolerance, danger, and the extended family. *Annu Rev Immunol* **12**, 991-1045 (1994).
249. Wiesel, P.*, et al.* Endotoxin-induced mortality is related to increased oxidative stress and end-organ dysfunction, not refractory hypotension, in heme oxygenase-1-deficient mice. *Circulation* **102**, 3015-3022 (2000).
250. Kim, H.P., Ryter, S.W. & Choi, A.M. CO as a cellular signaling molecule. *Annu Rev Pharmacol Toxicol* **46**, 411-449 (2006).
251. Takamiya, R.*, et al.* High-mobility group box 1 contributes to lethality of endotoxemia in heme oxygenase-1-deficient mice. *Am J Respir Cell Mol Biol* **41**, 129-135 (2009).
252. Gong, Q.*, et al.* Heme oxygenase-1 upregulation significantly inhibits TNF-alpha and Hmgb1 releasing and attenuates lipopolysaccharide-induced acute lung injury in mice. *Int Immunopharmacol* **8**, 792-798 (2008).
253. Wang, H.*, et al.* HMG-1 as a late mediator of endotoxin lethality in mice. *Science* **285**, 248-251 (1999).
254. Nairz, M., Schroll, A., Sonnweber, T. & Weiss, G. The struggle for iron - a metal at the host-pathogen interface. *Cell Microbiol* **12**, 1691-1702 (2010).
255. Andrews, N.C. Forging a field: the golden age of iron biology. *Blood* **112**, 219-230 (2008).
256. Andrews, N.C. & Schmidt, P.J. Iron homeostasis. *Annu Rev Physiol* **69**, 69-85 (2007).
257. Hentze, M.W.*, et al.* Identification of the iron-responsive element for the translational regulation of human ferritin mRNA. *Science* **238**, 1570-1573 (1987).
258. Casey, J.L., Koeller, D.M., Ramin, V.C., Klausner, R.D. & Harford, J.B. Iron regulation of transferrin receptor mRNA levels requires iron-responsive elements and a rapid turnover determinant in the 3' untranslated region of the mRNA. *EMBO J* **8**, 3693-3699 (1989).

259. Leipuviene, R. & Theil, E.C. The family of iron responsive RNA structures regulated by changes in cellular iron and oxygen. *Cell Mol Life Sci* **64**, 2945-2955 (2007).
260. Ilyin, G.*, et al.* Comparative analysis of mouse hepcidin 1 and 2 genes: evidence for different patterns of expression and co-inducibility during iron overload. *FEBS Lett* **542**, 22-26 (2003).
261. Peyssonnaux, C.*, et al.* TLR4-dependent hepcidin expression by myeloid cells in response to bacterial pathogens. *Blood* **107**, 3727-3732 (2006).
262. Ganz, T. & Nemeth, E. Hepcidin and disorders of iron metabolism. *Annu Rev Med* **62**, 347-360 (2011).
263. Pietrangelo, A. Hepcidin in human iron disorders: therapeutic implications. *J Hepatol* **54**, 173-181 (2011).
264. Viatte, L.*, et al.* Deregulation of proteins involved in iron metabolism in hepcidin-deficient mice. *Blood* **105**, 4861-4864 (2005).
265. Nicolas, G.*, et al.* Lack of hepcidin gene expression and severe tissue iron overload in upstream stimulatory factor 2 (USF2) knockout mice. *Proc Natl Acad Sci U S A* **98**, 8780-8785 (2001).
266. Nicolas, G.*, et al.* Severe iron deficiency anemia in transgenic mice expressing liver hepcidin. *Proc Natl Acad Sci U S A* **99**, 4596-4601 (2002).
267. Roy, C.N.*, et al.* Hepcidin antimicrobial peptide transgenic mice exhibit features of the anemia of inflammation. *Blood* **109**, 4038-4044 (2007).
268. Ehrlich, R. & Lemonnier, F.A. HFE--a novel nonclassical class I molecule that is involved in iron metabolism. *Immunity* **13**, 585-588 (2000).
269. Babitt, J.L.*, et al.* Bone morphogenetic protein signaling by hemojuvelin regulates hepcidin expression. *Nat Genet* **38**, 531-539 (2006).
270. Wang, R.H.*, et al.* A role of SMAD4 in iron metabolism through the positive regulation of hepcidin expression. *Cell Metab* **2**, 399-409 (2005).
271. Nemeth, E.*, et al.* IL-6 mediates hypoferremia of inflammation by inducing the synthesis of the iron regulatory hormone hepcidin. *J Clin Invest* **113**, 1271-1276 (2004).
272. Verga Falzacappa, M.V.*, et al.* STAT3 mediates hepatic hepcidin expression and its inflammatory stimulation. *Blood* **109**, 353-358 (2007).
273. Pietrangelo, A.*, et al.* STAT3 is required for IL-6-gp130-dependent activation of hepcidin in vivo. *Gastroenterology* **132**, 294-300 (2007).
274. Wrighting, D.M. & Andrews, N.C. Interleukin-6 induces hepcidin expression through STAT3. *Blood* **108**, 3204-3209 (2006).
275. Schaible, U.E. & Kaufmann, S.H. Iron and microbial infection. *Nat Rev Microbiol* **2**, 946-953 (2004).
276. Nemeth, E.*, et al.* Hepcidin regulates cellular iron efflux by binding to ferroportin and inducing its internalization. *Science* **306**, 2090-2093 (2004).
277. Levy, J.E., Jin, O., Fujiwara, Y., Kuo, F. & Andrews, N.C. Transferrin receptor is necessary for development of erythrocytes and the nervous system. *Nat Genet* **21**, 396-399 (1999).
278. Ned, R.M., Swat, W. & Andrews, N.C. Transferrin receptor 1 is differentially required in lymphocyte development. *Blood* **102**, 3711-3718 (2003).
279. Seldon, M.P.*, et al.* Heme oxygenase-1 inhibits the expression of adhesion molecules associated with endothelial cell activation via inhibition of NF-kappaB RelA phosphorylation at serine 276. *J Immunol* **179**, 7840-7851 (2007).
280. Soares, M.P.*, et al.* Heme oxygenase-1 modulates the expression of adhesion molecules associated with endothelial cell activation. *J Immunol* **172**, 3553-3563 (2004).
281. Xiong, S.*, et al.* Signaling role of intracellular iron in NF-kappaB activation. *J Biol Chem* **278**, 17646-17654 (2003).
282. She, H.*, et al.* Iron activates NF-kappaB in Kupffer cells. *Am J Physiol Gastrointest Liver Physiol* **283**, G719-726 (2002).
283. Wang, L. & Cherayil, B.J. Ironing out the wrinkles in host defense: interactions between iron homeostasis and innate immunity. *J Innate Immun* **1**, 455-464 (2009).
284. Bubici, C., Papa, S., Pham, C.G., Zazzeroni, F. & Franzoso, G. NF-kappaB and JNK: an intricate affair. *Cell Cycle* **3**, 1524-1529 (2004).

285. Wang, L., *et al.* Selective modulation of TLR4-activated inflammatory responses by altered iron homeostasis in mice. *J Clin Invest* **119**, 3322-3328 (2009).
286. Wang, L., *et al.* Attenuated inflammatory responses in hemochromatosis reveal a role for iron in the regulation of macrophage cytokine translation. *J Immunol* **181**, 2723-2731 (2008).
287. De Domenico, I., *et al.* Hepcidin mediates transcriptional changes that modulate acute cytokine-induced inflammatory responses in mice. *J Clin Invest* **120**, 2395-2405 (2010).
288. Kemp, J.D., *et al.* Inhibition of lymphocyte activation with anti-transferrin receptor Mabs: a comparison of three reagents and further studies of their range of effects and mechanism of action. *Cell Immunol* **122**, 218-230 (1989).
289. Bone, R.C., *et al.* Definitions for sepsis and organ failure and guidelines for the use of innovative therapies in sepsis. The ACCP/SCCM Consensus Conference Committee. American College of Chest Physicians/Society of Critical Care Medicine. *Chest* **101**, 1644-1655 (1992).
290. Angus, D.C., *et al.* Epidemiology of severe sepsis in the United States: analysis of incidence, outcome, and associated costs of care. *Crit Care Med* **29**, 1303-1310 (2001).
291. Martin, G.S., Mannino, D.M., Eaton, S. & Moss, M. The epidemiology of sepsis in the United States from 1979 through 2000. *N Engl J Med* **348**, 1546-1554 (2003).
292. Martin, G., *et al.* The international PROGRESS registry of patients with severe sepsis: drotrecogin alfa (activated) use and patient outcomes. *Crit Care* **13**, R103 (2009).
293. Thomas, L. Germs. *N Engl J Med* **287**, 553-555 (1972).
294. Dejager, L., Pinheiro, I., Dejonckheere, E. & Libert, C. Cecal ligation and puncture: the gold standard model for polymicrobial sepsis? *Trends Microbiol* **19**, 198-208 (2011).
295. Stearns-Kurosawa, D.J., Osuchowski, M.F., Valentine, C., Kurosawa, S. & Remick, D.G. The pathogenesis of sepsis. *Annu Rev Pathol* **6**, 19-48 (2011).
296. Rittirsch, D., Flierl, M.A. & Ward, P.A. Harmful molecular mechanisms in sepsis. *Nat Rev Immunol* **8**, 776-787 (2008).
297. Sutterwala, F.S., *et al.* Critical role for NALP3/CIAS1/Cryopyrin in innate and adaptive immunity through its regulation of caspase-1. *Immunity* **24**, 317-327 (2006).
298. Weighardt, H., *et al.* Cutting edge: myeloid differentiation factor 88 deficiency improves resistance against sepsis caused by polymicrobial infection. *J Immunol* **169**, 2823-2827 (2002).
299. Alves-Filho, J.C., de Freitas, A., Russo, M. & Cunha, F.Q. Toll-like receptor 4 signaling leads to neutrophil migration impairment in polymicrobial sepsis. *Crit Care Med* **34**, 461-470 (2006).
300. Plitas, G., Burt, B.M., Nguyen, H.M., Bamboat, Z.M. & DeMatteo, R.P. Toll-like receptor 9 inhibition reduces mortality in polymicrobial sepsis. *J Exp Med* **205**, 1277-1283 (2008).
301. Czermak, B.J., *et al.* Protective effects of C5a blockade in sepsis. *Nat Med* **5**, 788-792 (1999).
302. Rittirsch, D., *et al.* Functional roles for C5a receptors in sepsis. *Nat Med* **14**, 551-557 (2008).
303. Secher, T., *et al.* Crucial role of TNF receptors 1 and 2 in the control of polymicrobial sepsis. *J Immunol* **182**, 7855-7864 (2009).
304. Calandra, T., *et al.* Protection from septic shock by neutralization of macrophage migration inhibitory factor. *Nat Med* **6**, 164-170 (2000).
305. Ness, T.L., *et al.* CCR1 and CC chemokine ligand 5 interactions exacerbate innate immune responses during sepsis. *J Immunol* **173**, 6938-6948 (2004).
306. Matsukawa, A., *et al.* Absence of CC chemokine receptor 8 enhances innate immunity during septic peritonitis. *FASEB J* **20**, 302-304 (2006).
307. Ness, T.L., Hogaboam, C.M., Strieter, R.M. & Kunkel, S.L. Immunomodulatory role of CXCR2 during experimental septic peritonitis. *J Immunol* **171**, 3775-3784 (2003).
308. Muenzer, J.T., *et al.* Characterization and modulation of the immunosuppressive phase of sepsis. *Infect Immun* **78**, 1582-1592 (2011).

309. Hotchkiss, R.S. & Nicholson, D.W. Apoptosis and caspases regulate death and inflammation in sepsis. *Nat Rev Immunol* **6**, 813-822 (2006).
310. Tinsley, K.W.*, et al.* Sepsis induces apoptosis and profound depletion of splenic interdigitating and follicular dendritic cells. *J Immunol* **171**, 909-914 (2003).
311. Inoue, S.*, et al.* IL-15 prevents apoptosis, reverses innate and adaptive immune dysfunction, and improves survival in sepsis. *J Immunol* **184**, 1401-1409 (2010).
312. Delano, M.J.*, et al.* Sepsis induces early alterations in innate immunity that impact mortality to secondary infection. *J Immunol* **186**, 195-202.
313. Nascimento, D.C.*, et al.* Role of regulatory T cells in long-term immune dysfunction associated with severe sepsis. *Crit Care Med* **38**, 1718-1725.
314. Overhaus, M.*, et al.* Biliverdin protects against polymicrobial sepsis by modulating inflammatory mediators. *Am J Physiol Gastrointest Liver Physiol* **290**, G695-703 (2006).
315. Chung, S.W., Liu, X., Macias, A.A., Baron, R.M. & Perrella, M.A. Heme oxygenase-1-derived carbon monoxide enhances the host defense response to microbial sepsis in mice. *J Clin Invest* **118**, 239-247 (2008).
316. Gardella, S.*, et al.* The nuclear protein HMGB1 is secreted by monocytes via a non-classical, vesicle-mediated secretory pathway. *EMBO Rep* **3**, 995-1001 (2002).
317. Yang, H.*, et al.* Reversing established sepsis with antagonists of endogenous high-mobility group box 1. *Proc Natl Acad Sci U S A* **101**, 296-301 (2004).
318. Haldar, K., Murphy, S.C., Milner, D.A. & Taylor, T.E. Malaria: mechanisms of erythrocytic infection and pathological correlates of severe disease. *Annu Rev Pathol* **2**, 217-249 (2007).
319. Clark, I.A., Alleva, L.M., Mills, A.C. & Cowden, W.B. Pathogenesis of malaria and clinically similar conditions. *Clin Microbiol Rev* **17**, 509-539, table of contents (2004).
320. Clark, I.A. & Cowden, W.B. The pathophysiology of falciparum malaria. *Pharmacol Ther* **99**, 221-260 (2003).
321. Idro, R., Jenkins, N.E. & Newton, C.R. Pathogenesis, clinical features, and neurological outcome of cerebral malaria. *Lancet Neurol* **4**, 827-840 (2005).
322. Idro, R., Marsh, K., John, C.C. & Newton, C.R. Cerebral malaria: mechanisms of brain injury and strategies for improved neurocognitive outcome. *Pediatr Res* **68**, 267-274 (2010).
323. Haldane, J.B.S. The rate of mutation of human genes. *Hereditas* **35**, 267-273 (1949).
324. Lopez, C., Saravia, C., Gomez, A., Hoebeke, J. & Patarroyo, M.A. Mechanisms of genetically-based resistance to malaria. *Gene* **467**, 1-12 (2010).
325. Williams, T.N. Human red blood cell polymorphisms and malaria. *Curr Opin Microbiol* **9**, 388-394 (2006).
326. Mockenhaupt, F.P.*, et al.* Alpha(+)-thalassemia protects African children from severe malaria. *Blood* **104**, 2003-2006 (2004).
327. Williams, T.N.*, et al.* Sickle cell trait and the risk of Plasmodium falciparum malaria and other childhood diseases. *J Infect Dis* **192**, 178-186 (2005).
328. Mockenhaupt, F.P.*, et al.* Hemoglobin C and resistance to severe malaria in Ghanaian children. *J Infect Dis* **190**, 1006-1009 (2004).
329. Hutagalung, R.*, et al.* Influence of hemoglobin E trait on the severity of Falciparum malaria. *J Infect Dis* **179**, 283-286 (1999).
330. Ayi, K., Turrini, F., Piga, A. & Arese, P. Enhanced phagocytosis of ring-parasitized mutant erythrocytes: a common mechanism that may explain protection against falciparum malaria in sickle trait and beta-thalassemia trait. *Blood* **104**, 3364-3371 (2004).
331. Cabrera, G.*, et al.* The sickle cell trait is associated with enhanced immunoglobulin G antibody responses to Plasmodium falciparum variant surface antigens. *J Infect Dis* **191**, 1631-1638 (2005).
332. Fairhurst, R.M.*, et al.* Abnormal display of PfEMP-1 on erythrocytes carrying haemoglobin C may protect against malaria. *Nature* **435**, 1117-1121 (2005).
333. Fairhurst, R.M., Fujioka, H., Hayton, K., Collins, K.F. & Wellems, T.E. Aberrant development of Plasmodium falciparum in hemoglobin CC red cells: implications for the malaria protective effect of the homozygous state. *Blood* **101**, 3309-3315 (2003).

334. Rosenthal, P.J. & Meshnick, S.R. Hemoglobin catabolism and iron utilization by malaria parasites. *Mol Biochem Parasitol* **83**, 131-139 (1996).
335. Pandey, A.V.*, et al.* Hemozoin formation in malaria: a two-step process involving histidine-rich proteins and lipids. *Biochem Biophys Res Commun* **308**, 736-743 (2003).
336. Coban, C.*, et al.* Toll-like receptor 9 mediates innate immune activation by the malaria pigment hemozoin. *J Exp Med* **201**, 19-25 (2005).
337. Parroche, P.*, et al.* Malaria hemozoin is immunologically inert but radically enhances innate responses by presenting malaria DNA to Toll-like receptor 9. *Proc Natl Acad Sci U S A* **104**, 1919-1924 (2007).
338. Coban, C.*, et al.* Immunogenicity of whole-parasite vaccines against Plasmodium falciparum involves malarial hemozoin and host TLR9. *Cell Host Microbe* **7**, 50-61 (2010).
339. Franklin, B.S.*, et al.* Therapeutical targeting of nucleic acid-sensing Toll-like receptors prevents experimental cerebral malaria. *Proc Natl Acad Sci U S A* **108**, 3689-3694 (2011).
340. Reimer, T.*, et al.* Experimental cerebral malaria progresses independently of the Nlrp3 inflammasome. *Eur J Immunol* **40**, 764-769 (2010).
341. Dostert, C.*, et al.* Malarial hemozoin is a Nalp3 inflammasome activating danger signal. *PLoS One* **4**, e6510 (2009).
342. Shio, M.T.*, et al.* Malarial hemozoin activates the NLRP3 inflammasome through Lyn and Syk kinases. *PLoS Pathog* **5**, e1000559 (2009).
343. Griffith, J.W., Sun, T., McIntosh, M.T. & Bucala, R. Pure Hemozoin is inflammatory in vivo and activates the NALP3 inflammasome via release of uric acid. *J Immunol* **183**, 5208-5220 (2009).
344. Orengo, J.M.*, et al.* Plasmodium-induced inflammation by uric acid. *PLoS Pathog* **4**, e1000013 (2008).
345. Orengo, J.M.*, et al.* Uric acid is a mediator of the Plasmodium falciparum-induced inflammatory response. *PLoS One* **4**, e5194 (2009).
346. deWalick, S.*, et al.* Cutting edge: conventional dendritic cells are the critical APC required for the induction of experimental cerebral malaria. *J Immunol* **178**, 6033-6037 (2007).
347. Amante, F.H.*, et al.* Immune-mediated mechanisms of parasite tissue sequestration during experimental cerebral malaria. *J Immunol* **185**, 3632-3642 (2010).
348. Belnoue, E.*, et al.* On the pathogenic role of brain-sequestered alphabeta CD8+ T cells in experimental cerebral malaria. *J Immunol* **169**, 6369-6375 (2002).
349. Belnoue, E.*, et al.* CCR5 deficiency decreases susceptibility to experimental cerebral malaria. *Blood* **101**, 4253-4259 (2003).
350. Campanella, G.S.*, et al.* Chemokine receptor CXCR3 and its ligands CXCL9 and CXCL10 are required for the development of murine cerebral malaria. *Proc Natl Acad Sci U S A* **105**, 4814-4819 (2008).
351. Miu, J.*, et al.* Chemokine gene expression during fatal murine cerebral malaria and protection due to CXCR3 deficiency. *J Immunol* **180**, 1217-1230 (2008).
352. Nitcheu, J.*, et al.* Perforin-dependent brain-infiltrating cytotoxic CD8+ T lymphocytes mediate experimental cerebral malaria pathogenesis. *J Immunol* **170**, 2221-2228 (2003).
353. Haque, A.*, et al.* Granzyme B expression by CD8+ T cells is required for the development of experimental cerebral malaria. *J Immunol* **186**, 6148-6156 (2011).
354. Haque, A.*, et al.* CD4+ natural regulatory T cells prevent experimental cerebral malaria via CTLA-4 when expanded in vivo. *PLoS Pathog* **6**, e1001221 (2010).
355. Claser, C.*, et al.* CD8+ T cells and IFN-gamma mediate the time-dependent accumulation of infected red blood cells in deep organs during experimental cerebral malaria. *PLoS One* **6**, e18720 (2011).
356. Baptista, F.G.*, et al.* Accumulation of Plasmodium berghei-infected red blood cells in the brain is crucial for the development of cerebral malaria in mice. *Infect Immun* **78**, 4033-4039 (2010).
357. Epiphanio, S.*, et al.* Heme oxygenase-1 is an anti-inflammatory host factor that promotes murine plasmodium liver infection. *Cell Host Microbe* **3**, 331-338 (2008).

358. Wieckiewicz, J., Goto, R. & Wood, K.J. T regulatory cells and the control of alloimmunity: from characterisation to clinical application. *Curr Opin Immunol* **22**, 662-668 (2010).
359. Belkaid, Y. & Tarbell, K. Regulatory T cells in the control of host-microorganism interactions (*). *Annu Rev Immunol* **27**, 551-589 (2009).
360. da Costa, T.B., Sardinha, L.R., Larocca, R., Peron, J.P. & Rizzo, L.V. Allogeneic apoptotic thymocyte-stimulated dendritic cells expand functional regulatory T cells. *Immunology* **133**, 123-132 (2010).
361. Nairz, M.*, et al.* Erythropoietin contrastingly affects bacterial infection and experimental colitis by inhibiting nuclear factor-kappaB-inducible immune pathways. *Immunity* **34**, 61-74 (2011).
362. Papanikolaou, G.*, et al.* Hepcidin in iron overload disorders. *Blood* **105**, 4103-4105 (2005).
363. Kearney, S.L.*, et al.* Urinary hepcidin in congenital chronic anemias. *Pediatr Blood Cancer* **48**, 57-63 (2007).
364. Origa, R.*, et al.* Liver iron concentrations and urinary hepcidin in beta-thalassemia. *Haematologica* **92**, 583-588 (2007).
365. Gardenghi, S.*, et al.* Ineffective erythropoiesis in beta-thalassemia is characterized by increased iron absorption mediated by down-regulation of hepcidin and up-regulation of ferroportin. *Blood* **109**, 5027-5035 (2007).
366. Nicolas, G.*, et al.* The gene encoding the iron regulatory peptide hepcidin is regulated by anemia, hypoxia, and inflammation. *J Clin Invest* **110**, 1037-1044 (2002).
367. Trudel, M.*, et al.* Sickle cell disease of transgenic SAD mice. *Blood* **84**, 3189-3197 (1994).
368. Trudel, M.*, et al.* Towards a transgenic mouse model of sickle cell disease: hemoglobin SAD. *EMBO J* **10**, 3157-3165 (1991).
369. Pinto, J.P.*, et al.* Erythropoietin mediates hepcidin expression in hepatocytes through EPOR signaling and regulation of C/EBPalpha. *Blood* **111**, 5727-5733 (2008).
370. Brinkmann, M.*, et al.* Expression of iron transport proteins divalent metal transporter-1, Ferroportin-1, HFE and transferrin receptor-1 in human monocyte-derived dendritic cells. *Cell Biochem Funct* **25**, 287-296 (2007).
371. Cherayil, B.J. Iron and immunity: immunological consequences of iron deficiency and overload. *Arch Immunol Ther Exp (Warsz)* **58**, 407-415 (2010).
372. Cox, M.A., Harrington, L.E. & Zajac, A.J. Cytokines and the inception of CD8 T cell responses. *Trends Immunol* **32**, 180-186 (2011).
373. Williams, T.N.*, et al.* Bacteraemia in Kenyan children with sickle-cell anaemia: a retrospective cohort and case-control study. *Lancet* **374**, 1364-1370 (2009).
374. Menendez, C.*, et al.* Randomised placebo-controlled trial of iron supplementation and malaria chemoprophylaxis for prevention of severe anaemia and malaria in Tanzanian infants. *Lancet* **350**, 844-850 (1997).
375. Nyakeriga, A.M.*, et al.* Iron deficiency and malaria among children living on the coast of Kenya. *J Infect Dis* **190**, 439-447 (2004).
376. Smith, A.W., Hendrickse, R.G., Harrison, C., Hayes, R.J. & Greenwood, B.M. The effects on malaria of treatment of iron-deficiency anaemia with oral iron in Gambian children. *Ann Trop Paediatr* **9**, 17-23 (1989).
377. Sazawal, S.*, et al.* Effects of routine prophylactic supplementation with iron and folic acid on admission to hospital and mortality in preschool children in a high malaria transmission setting: community-based, randomised, placebo-controlled trial. *Lancet* **367**, 133-143 (2006).
378. Oppenheimer, S.J.*, et al.* Iron supplementation increases prevalence and effects of malaria: report on clinical studies in Papua New Guinea. *Trans R Soc Trop Med Hyg* **80**, 603-612 (1986).
379. Prentice, A.M. Iron metabolism, malaria, and other infections: what is all the fuss about? *J Nutr* **138**, 2537-2541 (2008).
380. Portugal, S.*, et al.* Host-mediated regulation of superinfection in malaria. *Nat Med* **17**, 732-737.

Appendix

Appendix: Control of Immunopathology During *Plasmodium* Infection by Hepcidin

Ivo Marguti[1]

[1]Instituto Gulbenkian de Ciência, Oeiras, Portugal.

Manuscript submmited for publication.

1. ABSTRACT

Malaria is a major health problem affecting millions of people annually especially in underdeveloped countries. Mutations causing alterations in hemoglobin production or structure are known to afford protection against the development of severe forms of malaria. Not surprisingly, these hemoglobin disorders are present at high frequency in areas where malaria is endemic, indicating a survival advantage for individuals carrying them. Despite many years of research, the exact mechanisms underlying the protection afforded by hemoglobinopathies against severe forms of malaria have not yet found a definitive answer. One feature of hemoglobinopathies, observed both in humans and mice, is the fact that individuals carrying these disorders express low levels of the hormone hepcidin that plays a major role in iron homeostasis. Hepcidin acts by binding to the iron exporter ferroportin and inducing its degradation. When hepcidin levels are low, ferroportin expression in cells is sustained leading to export of intracellular iron. Importantly, low intracellular iron content may affect activation of innate immune cells leading to diminished production of proinflammatory cytokines. Notably, several lines of evidence support the notion that development of severe forms of malaria is dependent on immune-mediated damage, caused by unfettered immune responses. Herein the hypothesis that hemoglobinopathies afford protection against severe forms of malaria by limiting exacerbated immune activation, via a mechanism that involves low hepcidin expression, is discussed.

2. BACKGROUND

Malaria, caused by infection with *Plasmodium* parasites, constitutes a major health problem. In 2009, the World Health Organization reported a total of 225 million cases of malaria infection worldwide, with 781 thousand leading to death[1]. Natural infection occurs when *Plasmodium* infective sporozoites are delivered to host's bloodstream via infected *Anopheles* mosquitoes bite[2]. The most lethal form of malaria in humans is cerebral malaria (CM), which affects mainly children in Africa and adults in Southeast Asia. CM develops in individuals infected with *Plasmodium falciparum*, and is characterized by development of impaired consciousness, seizures and subsequent coma[3,4].

The use of animal models of *Plasmodium* infection, in which a syndrome similar to cerebral malaria occurs, termed experimental cerebral malaria (ECM), allowed the identification of several components of the immune system as important players in ECM pathology. Hemozoin, a polymer of heme molecules produced by *Plasmodium* after digestion of hemoglobin inside red blood cells [5], coupled or not with DNA, can activate Toll-like receptor 9 (TLR9) and NALP3 in innate immune cells, inducing the production of proinflammatory cytokines [6-9]. Importantly, interfering with *Plasmodium*-mediated TLR9 or NALP3 activation prevents ECM development [9, 10]. Furthermore, several lines of evidence support the notion that exacerbated adaptive immune activation precipitates ECM development. First, recombination activating gene-2 deficient mice (*Rag2*$^{-/-}$) and severe combined immune deficient (SCID) mice, both lacking T and B cells, are protected against ECM development [11, 12]. Second, depletion of $CD4^+$ cells early after infection, and $CD8^+$ cells until the first symptoms of ECM appear, can prevent ECM [13]. Third,

expression of the cytotoxic molecules perforin and granzyme B, by $CD8^+$ T cells, is essential for ECM development [14, 15]. Fifth, induction of regulatory T cells (T_{REG}) expansion during infection protects mice against ECM, concomitantly with a reduced $CD4^+$ and $CD8^+$ T cell response [16]. These data strongly suggest that ECM pathology is mainly driven by an excessive immune response leading to immunopathology and ultimately to death.

A long known observation, first put forward as a hypothesis by Haldane[17], is the fact that hemoglobinopathies, affecting hemoglobin production or structure, afford protection against development of severe forms of malaria in humans. These hemoglobinopathies include thalassemias, sickle cell trait (HbAS), hemoglobin C (HbC) and hemoglobin E (HbE) (*reviewed in*[18,19]). Several studies have tried to clarify the mechanisms by which protection is granted by these alterations in hemoglobin, and multiple mechanisms have been implicated[20-24]. Nonetheless, a definitive mechanism is still missing.

Hemoglobinopathies have been linked to decreased levels of the hormone hepcidin in humans and mice[25-28]. Hepcidin regulates systemic iron homeostasis by controlling dietary iron intake, and mobilization of iron from cellular iron stores, such as macrophages and hepatocytes (*reviewed in*[29,30]). The fundamental role played by hepcidin in iron homeostasis is strikingly demonstrated by the severe iron overload phenotype observed when the hepcidin gene (*Hamp*) is disrupted[31,32] and, on the other hand, by the severe iron deficiency associated with hepcidin overexpression[33,34]. On the molecular level, hepcidin works by binding to the iron transporter ferroportin and inducing its degradation[35]. When hepcidin levels are high, ferroportin degradation limits iron absorption from the diet and iron

mobilization from cellular iron stores. On the other hand, in the case of decreased hepcidin levels, high ferroportin expression leads to increased dietary iron absorption and export from cellular stores. Therefore, in conditions where hepcidin expression is diminished it is expected that macrophages will present lower intracellular iron levels.

The role of iron in controlling immune and inflammatory responses has been addressed in different systems. Adequate levels of intracellular iron are required for proper activation of nuclear factor-κB (NF-κB) in macrophages[36,37]. Accordingly, conditions where the intracellular iron pool is diminished, due to low hepcidin levels, have been associated with impaired immune responses. The hemochromatosis gene (*Hfe*) is involved in regulation of hepcidin expression in homeostasis, and in its absence hepcidin levels are reduced[38] and iron overload is observed, due to increased dietary intake and export from cellular stores[39,40]. *Hfe*-deficient mice (*Hfe*$^{-/-}$) present high levels of ferroportin expression in splenocytes and low intracellular iron levels in peritoneal macrophages[41]. Furthermore, overexpression of ferroportin in a macrophage cell line[41] and iron chelation[42], leads to decreased pro-inflammatory cytokine production. Accordingly, macrophages obtained from *Hfe*$^{-/-}$ animals produce lower amounts of interleukin-6 (IL-6), tumor necrosis factor (TNF) and interferon-β (IFN-β) in response to stimulation via TLR4, and upon *Salmonella typhimurium* infection as compared to WT mice[41,42]. Intestinal inflammation mediated by *Salmonella typhimurium* infection is also reduced in *Hfe*$^{-/-}$ animals[41], and treatment of WT animals with inhibitors of hepcidin expression

leads to decreased T cell-mediated[43] and *Salmonella typhimurium*-induced[42] intestinal inflammation.

Herein it is proposed that decreased hepcidin production, as seen in hemoglobinopathies, leads to intracellular iron depletion in innate immune cells, limiting their inflammatory potential and preventing the generation of pathological immune responses after *Plasmodium* infection.

3. HYPOTHESIS

The association between hemoglobinopathies and decreased hepcidin levels has been reported in humans and mice. In these circumstances, macrophages should have their intracellular iron pool depleted, due to sustained ferroportin expression. Low levels of intracellular iron in macrophages, and possibly other immune cells, decrease their ability to properly activate NF-kB and produce pro-inflammatory cytokines. Therefore, low hepcidin levels, as seen in individuals carrying hemoglobinopathies, would have an immunomodulatory effect by limiting unfettered immune responses upon *Plasmodium* infection. Importantly, the immunomodulatory effect of low intracellular iron would influence the immune response against *Plasmodium* in a way that allows parasitemia control while limits immunopathology.

4. DISCUSSION

The protection afforded by hemoglobinopathies against malaria is not associated with diminished infection rate, but rather to a diminished incidence of severe forms of malaria[19]. Furthermore, in some reports parasite densities are comparable between individuals carrying normal hemoglobin and individuals

with hemoglobinopathies[44-47]. These observations support the notion that the mechanisms via which hemoglobinopathies afford protection against severe forms of malaria are active during ongoing *Plasmodium* infection, and do not depend on decreased parasitemias. Therefore, limiting potentially pathological immune responses against *Plasmodium* could act as one such protective mechanism.

A possible way to control immunopathology during *Plasmodium* infection would be to regulate intracellular iron levels on innate immune cells, thus avoiding unfettered immune activation. In keeping with the notion that intracellular iron levels can regulate immune function, it has been shown that ferroportin overexpression on macrophages leads to increased iron export[48], and reduced pro-inflammatory cytokine production[41]. Accordingly, macrophages obtained from *Hfe*$^{-/-}$ mice have low intracellular iron levels[41] and produce lower levels of pro-inflammatory cytokines as compared to WT mice[42]. Therefore, conditions leading to low intracellular iron levels would be expected to protect against immunopathology during *Plasmodium* infection by preventing immune responses to reach pathological levels.

Hemoglobinopathies[25-28] and iron deficiency[49,50] have been associated with low levels of hepcidin. On the other hand, iron supplementation increase hepcidin expression[51]. Remarkably, while hemoglobinopathies and iron deficiency have been associated with protection against the development of severe forms of malaria in endemic zones[19,52], iron supplementation was shown to increase the likelihood of severe malaria episodes[53]. This data suggests that conditions leading to alterations in hepcidin levels might profoundly impact the outcome of *Plasmodium* infection.

It was recently demonstrated that genetically modified mice carrying mutated human hemoglobin (*Hb*^{SAD}), leading to a mild sickle cell disease phenotype[54,55], are protected from ECM development[24]. The protection is associated with decreased levels of activated *Plasmodium*-specific CD8$^+$ T cells, known to be the effector cells leading to ECM development[13]. The exact mechanism through which CD8$^+$ T cell response is suppressed in these animals is currently unknown, but could be explained by the mechanism proposed above since *Hb*^{SAD} mice, despite showing no signs of anemia, present increased erythropoietin levels and erythropoiesis[55], two conditions that induce a decrease in hepcidin levels[56,57]. Importantly, *Hb*^{SAD} mice, despite diminished CD8$^+$ T cell activation, still retain the capacity to control infection as demonstrated by similar parasitemias as compared to wild type animals[24]. This data reinforces the hypothesis that low intracellular iron could affect the immune response against *Plasmodium*, allowing protective immunity to occur while preventing harmful responses.

The use of experimental models of severe malaria would be of great help in unequivocally determining a role for hepcidin in controlling fatal outcomes of *Plasmodium* infection. Moreover, the thorough study of the role played by hepcidin in animal models of *Plasmodium* infection, could provide valuable insights to the development of new therapeutical strategies to limit severe malaria in humans.

Systematic studies designed to address the levels of hepcidin in patients carrying protective hemoglobinopathies against severe forms of malaria, and its correlation with protection, would be extremely informative. Furthermore, correlating severity of malaria with hepcidin levels in patients

without protective hemoglobinopathies could reveal a more general role for hepcidin in controlling severe malaria. In addition, determining whether hemochromatosis patients, in which hepcidin production is diminished, are protected against severe forms of malaria would give further strength to the hypothesis proposed herein.

5. ACKNOWLEDGEMENTS

The author would like to thank Dr. Virginia de Oliveira Marques, Dr. Thiago Lopes Carvalho (Instituto Gulbenkian de Ciência) and Dr. Jorge Carneiro (Instituto Gulbenkian de Ciência) for critical reading of the manuscript. This work was supported by "*Fundação para a Ciência e a Tecnologia"*, Portugal grant SFHR/BD/33218/2007 to IM.

6. REFERENCES

1. WHO. World Malaria Report 2010. *http://www.who.int/malaria/world_malaria_report_2010/en/* (2010).
2. Haldar, K., Murphy, S.C., Milner, D.A. & Taylor, T.E. Malaria: mechanisms of erythrocytic infection and pathological correlates of severe disease. *Annu Rev Pathol* **2**, 217-249 (2007).
3. Idro, R., Jenkins, N.E. & Newton, C.R. Pathogenesis, clinical features, and neurological outcome of cerebral malaria. *Lancet Neurol* **4**, 827-840 (2005).
4. Idro, R., Marsh, K., John, C.C. & Newton, C.R. Cerebral malaria: mechanisms of brain injury and strategies for improved neurocognitive outcome. *Pediatr Res* **68**, 267-274 (2010).
5. Rosenthal, P.J. & Meshnick, S.R. Hemoglobin catabolism and iron utilization by malaria parasites. *Mol Biochem Parasitol* **83**, 131-139 (1996).
6. Coban, C.*, et al.* Toll-like receptor 9 mediates innate immune activation by the malaria pigment hemozoin. *J Exp Med* **201**, 19-25 (2005).
7. Parroche, P.*, et al.* Malaria hemozoin is immunologically inert but radically enhances innate responses by presenting malaria DNA to Toll-like receptor 9. *Proc Natl Acad Sci U S A* **104**, 1919-1924 (2007).
8. Coban, C.*, et al.* Immunogenicity of whole-parasite vaccines against Plasmodium falciparum involves malarial hemozoin and host TLR9. *Cell Host Microbe* **7**, 50-61 (2010).
9. Dostert, C.*, et al.* Malarial hemozoin is a Nalp3 inflammasome activating danger signal. *PLoS One* **4**, e6510 (2009).
10. Franklin, B.S.*, et al.* Therapeutical targeting of nucleic acid-sensing Toll-like receptors prevents experimental cerebral malaria. *Proc Natl Acad Sci U S A* **108**, 3689-3694 (2011).

11. Yanez, D.M., Manning, D.D., Cooley, A.J., Weidanz, W.P. & van der Heyde, H.C. Participation of lymphocyte subpopulations in the pathogenesis of experimental murine cerebral malaria. *J Immunol* **157**, 1620-1624 (1996).
12. Amante, F.H.*, et al.* Immune-mediated mechanisms of parasite tissue sequestration during experimental cerebral malaria. *J Immunol* **185**, 3632-3642 (2010).
13. Belnoue, E.*, et al.* On the pathogenic role of brain-sequestered alphabeta CD8+ T cells in experimental cerebral malaria. *J Immunol* **169**, 6369-6375 (2002).
14. Nitcheu, J.*, et al.* Perforin-dependent brain-infiltrating cytotoxic CD8+ T lymphocytes mediate experimental cerebral malaria pathogenesis. *J Immunol* **170**, 2221-2228 (2003).
15. Haque, A.*, et al.* Granzyme B expression by CD8+ T cells is required for the development of experimental cerebral malaria. *J Immunol* **186**, 6148-6156 (2011).
16. Haque, A.*, et al.* CD4+ natural regulatory T cells prevent experimental cerebral malaria via CTLA-4 when expanded in vivo. *PLoS Pathog* **6**, e1001221 (2010).
17. Haldane, J.B.S. The rate of mutation of human genes. *Hereditas* **35**, 267-273 (1949).
18. Lopez, C., Saravia, C., Gomez, A., Hoebeke, J. & Patarroyo, M.A. Mechanisms of genetically-based resistance to malaria. *Gene* **467**, 1-12 (2010).
19. Williams, T.N. Human red blood cell polymorphisms and malaria. *Curr Opin Microbiol* **9**, 388-394 (2006).
20. Ayi, K., Turrini, F., Piga, A. & Arese, P. Enhanced phagocytosis of ring-parasitized mutant erythrocytes: a common mechanism that may explain protection against falciparum malaria in sickle trait and beta-thalassemia trait. *Blood* **104**, 3364-3371 (2004).
21. Fairhurst, R.M., Fujioka, H., Hayton, K., Collins, K.F. & Wellems, T.E. Aberrant development of Plasmodium falciparum in hemoglobin CC red cells: implications for the malaria protective effect of the homozygous state. *Blood* **101**, 3309-3315 (2003).
22. Cabrera, G.*, et al.* The sickle cell trait is associated with enhanced immunoglobulin G antibody responses to Plasmodium falciparum variant surface antigens. *J Infect Dis* **191**, 1631-1638 (2005).
23. Fairhurst, R.M.*, et al.* Abnormal display of PfEMP-1 on erythrocytes carrying haemoglobin C may protect against malaria. *Nature* **435**, 1117-1121 (2005).
24. Ferreira, A.*, et al.* Sickle hemoglobin confers tolerance to Plasmodium infection. *Cell* **145**, 398-409 (2011).
25. Papanikolaou, G.*, et al.* Hepcidin in iron overload disorders. *Blood* **105**, 4103-4105 (2005).
26. Kearney, S.L.*, et al.* Urinary hepcidin in congenital chronic anemias. *Pediatr Blood Cancer* **48**, 57-63 (2007).
27. Origa, R.*, et al.* Liver iron concentrations and urinary hepcidin in beta-thalassemia. *Haematologica* **92**, 583-588 (2007).
28. Gardenghi, S.*, et al.* Ineffective erythropoiesis in beta-thalassemia is characterized by increased iron absorption mediated by down-regulation of hepcidin and up-regulation of ferroportin. *Blood* **109**, 5027-5035 (2007).
29. Ganz, T. & Nemeth, E. Hepcidin and disorders of iron metabolism. *Annu Rev Med* **62**, 347-360 (2011).
30. Andrews, N.C. & Schmidt, P.J. Iron homeostasis. *Annu Rev Physiol* **69**, 69-85 (2007).
31. Viatte, L.*, et al.* Deregulation of proteins involved in iron metabolism in hepcidin-deficient mice. *Blood* **105**, 4861-4864 (2005).
32. Nicolas, G.*, et al.* Lack of hepcidin gene expression and severe tissue iron overload in upstream stimulatory factor 2 (USF2) knockout mice. *Proc Natl Acad Sci U S A* **98**, 8780-8785 (2001).
33. Nicolas, G.*, et al.* Severe iron deficiency anemia in transgenic mice expressing liver hepcidin. *Proc Natl Acad Sci U S A* **99**, 4596-4601 (2002).
34. Roy, C.N.*, et al.* Hepcidin antimicrobial peptide transgenic mice exhibit features of the anemia of inflammation. *Blood* **109**, 4038-4044 (2007).
35. Nemeth, E.*, et al.* Hepcidin regulates cellular iron efflux by binding to ferroportin and inducing its internalization. *Science* **306**, 2090-2093 (2004).

36. She, H.*, et al.* Iron activates NF-kappaB in Kupffer cells. *Am J Physiol Gastrointest Liver Physiol* **283**, G719-726 (2002).
37. Xiong, S.*, et al.* Signaling role of intracellular iron in NF-kappaB activation. *J Biol Chem* **278**, 17646-17654 (2003).
38. Ahmad, K.A.*, et al.* Decreased liver hepcidin expression in the Hfe knockout mouse. *Blood Cells Mol Dis* **29**, 361-366 (2002).
39. Bahram, S.*, et al.* Experimental hemochromatosis due to MHC class I HFE deficiency: immune status and iron metabolism. *Proc Natl Acad Sci U S A* **96**, 13312-13317 (1999).
40. Zhou, X.Y.*, et al.* HFE gene knockout produces mouse model of hereditary hemochromatosis. *Proc Natl Acad Sci U S A* **95**, 2492-2497 (1998).
41. Wang, L.*, et al.* Attenuated inflammatory responses in hemochromatosis reveal a role for iron in the regulation of macrophage cytokine translation. *J Immunol* **181**, 2723-2731 (2008).
42. Wang, L.*, et al.* Selective modulation of TLR4-activated inflammatory responses by altered iron homeostasis in mice. *J Clin Invest* **119**, 3322-3328 (2009).
43. Wang, L.*, et al.* The bone morphogenetic protein-hepcidin axis as a therapeutic target in inflammatory bowel disease. *Inflamm Bowel Dis* (2011).
44. Modiano, D.*, et al.* Haemoglobin C protects against clinical Plasmodium falciparum malaria. *Nature* **414**, 305-308 (2001).
45. Mockenhaupt, F.P.*, et al.* Hemoglobin C and resistance to severe malaria in Ghanaian children. *J Infect Dis* **190**, 1006-1009 (2004).
46. Mockenhaupt, F.P.*, et al.* Alpha(+)-thalassemia protects African children from severe malaria. *Blood* **104**, 2003-2006 (2004).
47. Allen, S.J.*, et al.* alpha+-Thalassemia protects children against disease caused by other infections as well as malaria. *Proc Natl Acad Sci U S A* **94**, 14736-14741 (1997).
48. Knutson, M.D., Oukka, M., Koss, L.M., Aydemir, F. & Wessling-Resnick, M. Iron release from macrophages after erythrophagocytosis is up-regulated by ferroportin 1 overexpression and down-regulated by hepcidin. *Proc Natl Acad Sci U S A* **102**, 1324-1328 (2005).
49. Nicolas, G.*, et al.* The gene encoding the iron regulatory peptide hepcidin is regulated by anemia, hypoxia, and inflammation. *J Clin Invest* **110**, 1037-1044 (2002).
50. Weinstein, D.A.*, et al.* Inappropriate expression of hepcidin is associated with iron refractory anemia: implications for the anemia of chronic disease. *Blood* **100**, 3776-3781 (2002).
51. De Domenico, I.*, et al.* Hepcidin mediates transcriptional changes that modulate acute cytokine-induced inflammatory responses in mice. *J Clin Invest* **120**, 2395-2405 (2010).
52. Nyakeriga, A.M.*, et al.* Iron deficiency and malaria among children living on the coast of Kenya. *J Infect Dis* **190**, 439-447 (2004).
53. Sazawal, S.*, et al.* Effects of routine prophylactic supplementation with iron and folic acid on admission to hospital and mortality in preschool children in a high malaria transmission setting: community-based, randomised, placebo-controlled trial. *Lancet* **367**, 133-143 (2006).
54. Trudel, M.*, et al.* Towards a transgenic mouse model of sickle cell disease: hemoglobin SAD. *EMBO J* **10**, 3157-3165 (1991).
55. Trudel, M.*, et al.* Sickle cell disease of transgenic SAD mice. *Blood* **84**, 3189-3197 (1994).
56. Pinto, J.P.*, et al.* Erythropoietin mediates hepcidin expression in hepatocytes through EPOR signaling and regulation of C/EBPalpha. *Blood* **111**, 5727-5733 (2008).
57. Andrews, N.C. Forging a field: the golden age of iron biology. *Blood* **112**, 219-230 (2008).